Biochemiezentrum
der Universität Heidelberg
Direktor Prof. Dr. M. Brunner
AG Prof. Dr. E. Hurt

The Role of Energy Consuming Enzymes in 60S Ribosomal Subunit Assembly

Kumulative Habilitationsschrift
zur Erlangung der *venia legendi*
für das Fach Biochemie
der Medizinischen Fakultät Heidelberg
der Ruprecht-Karls-Universität

vorgelegt von
Dr. Jochen Baßler
2010

Table of Contents

1. Introduction

The ribosome is a highly dynamic and complex molecular machine, which is essential for protein synthesis. It is composed of a small and a large subunit. The prokaryotic small subunit (30S) consists of the 16S rRNA and 21 ribosomal proteins (RP); and its the large subunit (50S) is made up of 23S rRNA, 5S rRNA and 34 RPs. In contrast the eukaryotic subunits are significantly increased in size and complexity (*S. cerevisiae*: 40S [18S rRNA, 33 RPs]; 60S [25S, 5.8S, 5S rRNA, 46 RPs]). These differences allow for additional regulation of translation in eukaryotes and for specific inhibition of prokaryotic ribosomes by antibiotics (Lafontaine and Tollervey, 2001). Although the structure and function of ribosomes are well characterised to date (reviewed in Steitz, 2008; Zaher and Green, 2009), the molecular details of eukaryotic ribosome assembly remain largely elusive. The nuclear biogenesis of ribosomal subunits includes the transcription of rRNA, modification of rRNA (*e.g.* O-methylation, formation of pseudouridines), rRNA folding and assembly with ribosomal proteins. Subsequently, the pre-mature subunits are transported to the cytoplasm, where the final maturation steps take place. These assembly events are coordinated to ensure the correct temporal and spatial order. Additionally, these biogenesis steps are regulated depending on the cellular demands (Warner, 1999). For example, the assembly of ribosomes in rapidly dividing cells, like cancer cells, depends on efficient ribosome biogenesis; whereas, arrested or starving cells halt the synthesis of new ribosomal subunits.

The biogenesis of eukaryotic ribosomes is best studied in the yeast *S. cerevisiae* due to its easy experimental accessibility by genetic, biochemical and cell biological methods. Such as, the tandem affinity purification method (TAP) enabled the purification and characterization of several assembly intermediates, which represent snapshots of pre-ribosomal particles along their maturation path (Fromont-Racine et al., 2003; Granneman and Baserga, 2004; Nissan et al., 2002; Schäfer et al., 2003; Tschochner and Hurt, 2003). These proteomic approaches revealed that approximately 200 non-ribosomal factors and about 75 small nucleolar RNAs (snoRNA) are involved in ribosome assembly (reviewed in Fromont-Racine et al., 2003; Henras et al., 2008). The current challenge is to characterize of the structure of individual factors and entire pre- ribosomal

particles as well as the identification of direct protein-protein and protein-rRNA interactions within these particles.

1.1 The Ribosome Assembly Pathway

1.1.1 Assembly of the Small Subunit

The synthesis of ribosomes starts with the transcription of the 35S rRNA, which is required for the production of both, the small and large subunit (Figure 1). This RNA-polymerase I (Pol I) mediated process presents the major level for the regulation of the rate of ribosome synthesis (reviewed in Martin et al., 2006; Mayer and Grummt, 2006; Moss et al., 2007; Rudra and Warner, 2004; Warner, 1999). During transcription the nascent rRNA is modified by about 75 different small nucleolar ribonucleoprotein particles (snoRNPs), which catalyze 2´-O-ribose methylation of nucleotides and the formation of pseudouridines. These snoRNP complexes are recruited to their substrate via base-pairing between rRNA and snoRNAs, while the associated proteins catalyze the modification reaction. For a more detailed review on rRNA processing see (Fromont-Racine et al., 2003; Henras et al., 2004; Henras et al., 2008; Venema and Tollervey, 1999). The first pre-ribosomal particle that can be isolated is the 90S precursor, which is formed co-transcriptionally by the assembly of small subunit ribosomal proteins (Rps) and non-ribosomal factors with the nascent pre-rRNA. Subsequently, the cleavage at site A2, which occurs predominantly co-transcriptionally (Kos and Tollervey, 2010), separates the early 40S pre-ribosome from the remaining pre-rRNA, which later assembles with ribosomal proteins of the large subunit (Rpl) and non-ribosomal factors to form the earliest pre-60S ribosomal particles (Figure 1, see section 1.1.2, Granneman and Baserga, 2004; Henras et al., 2008).

The co-transcriptional assembly of the 90S particle, the precursor of the 40S subunit, starts with a stepwise modular incorporation of the sub-complexes UTP-A, UTP-B and UTP-C (Krogan et al., 2004; Osheim et al., 2004; Perez-Fernandez et al., 2007). This 90S precursor contains more than 20 non-ribosomal protein factors, the U3 snoRNP, some Rps proteins and the 35S pre-rRNA (Figure 1, 2, Dragon et al., 2002; Grandi et al., 2002). This particle is then converted into

an early 40S pre-ribosome by cleavage of the 35S pre-rRNA at sites A0, A1 and A2 yielding the 20S pre-rRNA. These steps are accompanied with a dramatic change in the composition of the pre-ribosomal particle. Most of the early

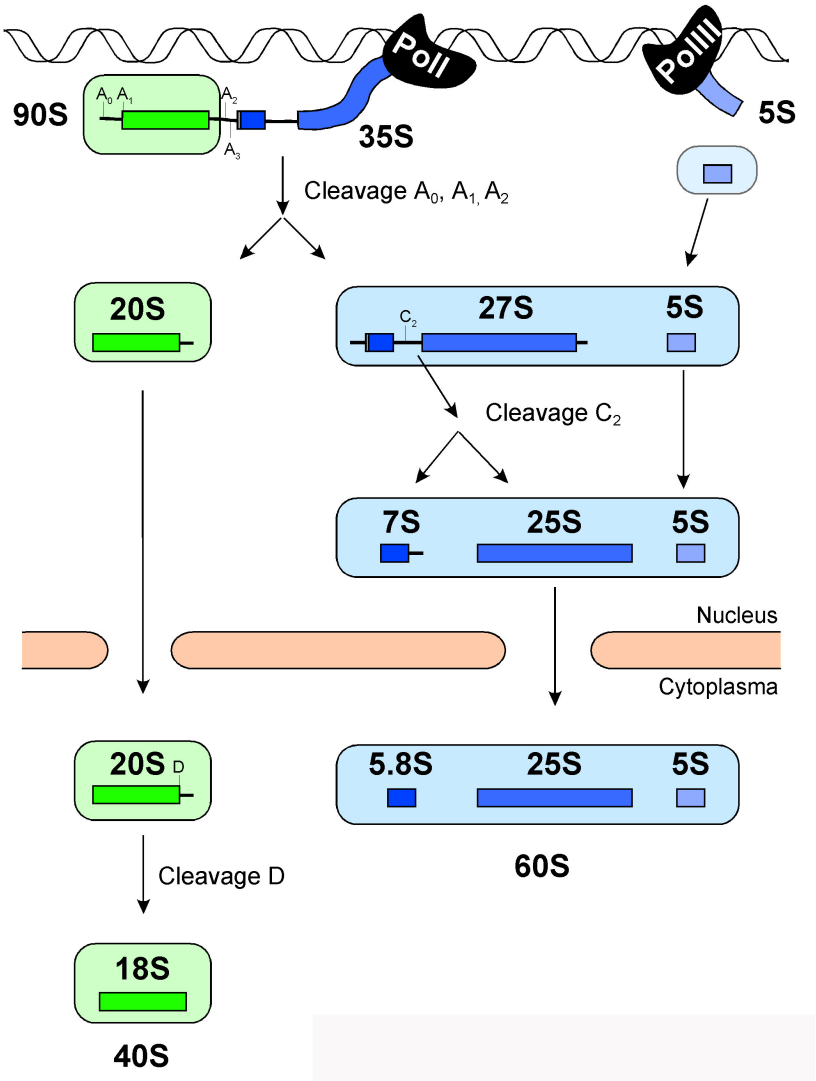

Figure 1: Simplified overview of the major steps in pre-rRNA processing. For a detailed review see Henras et al., 2008. The assembly of both ribosomal subunits starts with the transcription of the mutual 35S rRNA precursor. RNA cleavage at site A2 separates the two branches into the 40S (green) and 60S pre-ribosomes (blue). Within the cytoplasmic 40S precursor particle, the 20S pre-rRNA is cleaved at site D to generate the mature 18S rRNA. Whereas, 27S pre-rRNA, 5S RNA, ribosomal proteins, and non-ribosomal factors form the first precursor of the large subunit. Within pre-60S particles, the 27S pre-rRNA is further processed to generate the mature 5.8S and 25S rRNA.

non-ribosomal factors dissociate and a relatively small set of late biogenesis factors and further Rps proteins are recruited (Schäfer et al., 2006; Schäfer et al., 2003). This pre-40S particle, which already displays the typical 'head', 'platform', and 'body' structural landmarks of mature 40S subunits, but lacks the characteristic 'beak' structure (Schäfer et al., 2006), is rapidly transported out of the nucleolus into the cytoplasm (Figure 2). There the formation of the typical 40S "beak" and the stable association of Rps3 is promoted by Hrr25- mediated phos-

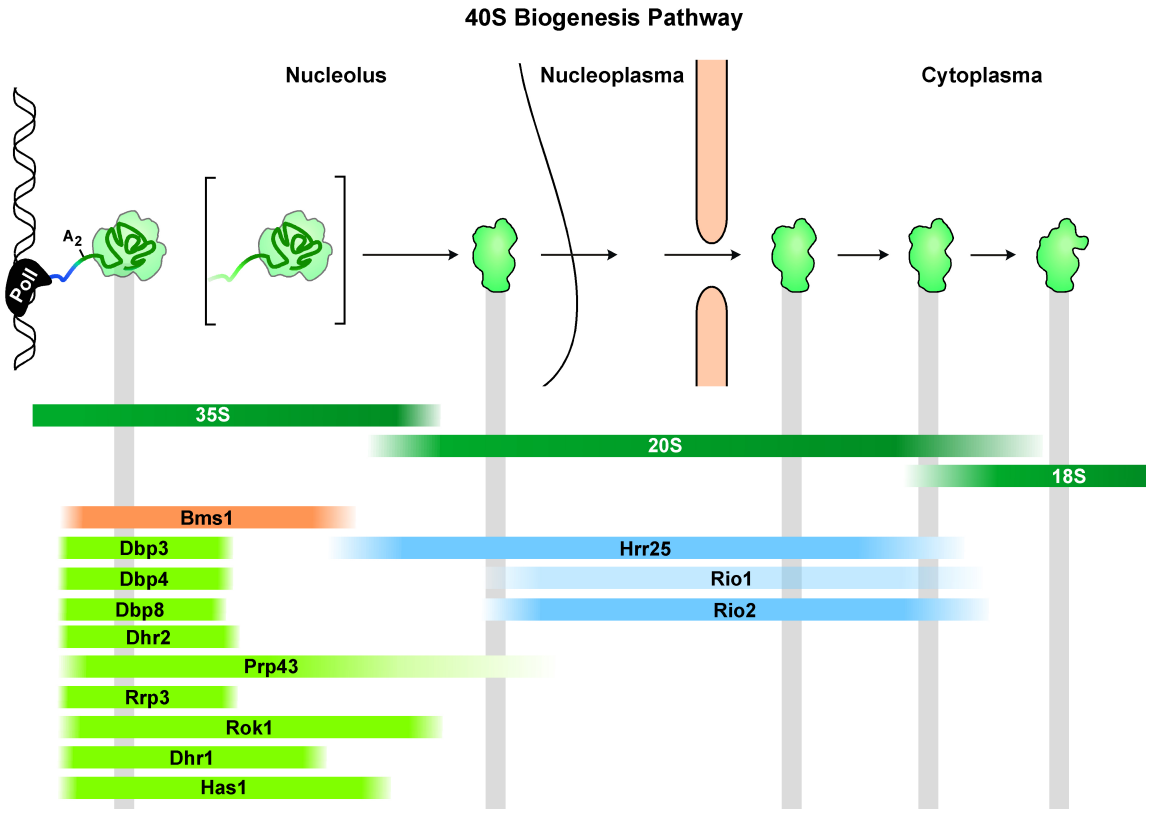

Figure 2: Pre-ribosomal particles along the 40S assembly pathway. The major intermediates of 40S pre-ribosomes, their rRNA components (dark green) and the presence of ATP/GTP consuming enzymes are depicted (DExD/H-box ATPases in green, kinases in light blue, GTPase in orange). The nascent 35S pre-rRNA is modified, folded and assembled to a first precursor of the 40S subunit. The cleavages at site A0, A1, A2, which generate the 20S pre-rRNA, are accompanied by a major exchange of non-ribosomal factors and structural rearrangements. The formation of the "beak" and final 20S processing occurs in the cytoplasm.

phorylation and subsequent de-phosphorylation of the Enp1-Ltv1-Rps3 complex (Schäfer et al., 2006). Finally, the matured 18S rRNA is generated by the cleavage of the 20S pre- rRNA at site D. This step depends on several non-ribosomal factors (*e.g.* Nob1, Rio1, Rio2, Tsr1 and Fap7), as mutation of these factors cause strong cytoplasmic accumulation of the 20S pre-rRNA (Fatica et al., 2003; Gelperin et al., 2001; Granneman et al., 2005; Vanrobays et al., 2003). Recent publications provide further evidence that Nob1, a PIN-domain containing endonuclease (Fatica et al., 2004), catalyzes the D cleavage of the 20S rRNA (Bohnsack et al., 2009; Lamanna and Karbstein, 2009; Pertschy et al., 2009). This 20S>18S rRNA processing step completes the assembly of 40S subunits.

1.1.2 Assembly of the Large Subunit

The first pre-60S particle is generated by rRNA cleavage in the 90S particle at site C2, separating the 40S and 60S pathway. To date, the earliest rather distinct pre-60S particle can be isolated by TAP purification of Ssf1. Such a particle contains a mixture of 27SA and 27SB pre-rRNAs, ribosomal proteins and about 30 non-ribosomal proteins, including diagnostic early factors like Noc1 and Rrp5 (Fatica et al., 2002; Kressler et al., 2008; Ulbrich et al., 2009). However, within this particle no snoRNPs components could be identified, suggesting that an earlier particle may exist. A suitable bait protein to isolate such an earlier particle could be Npa1. The Npa1 purification contains $27SA_2$ pre-rRNA and nearly 40 different non-ribosomal factors, including characteristic early pre-60S factors (*e.g.* Noc1 and Nop4), eight RNA helicases, several snoRNP components and remaining 90S-associated factors (Dez et al., 2004). Moreover, Npa1 was not identified within the Ssf1 particle (Fatica et al., 2002).

The next distinct pre-60S particle is defined by the nucleolar Nsa1 particle (Kressler et al., 2008). This particle contains 5S rRNA, 27SB rRNA, and Noc3 has replaced Noc1 (Bassler et al., 2010; Kressler et al., 2008; Milkereit et al., 2001). Additionally, this nucleolar particle contains the characteristic Ytm1-Erb1-Nop7 subcomplex (Bassler et al., 2010; Miles et al., 2005; Tang et al., 2008), which contributes to 5´ trimming of the 27SA3 pre-rRNA (Sahasranaman et al., 2009).

Interestingly, both the Ssf1 and the Nsa1 particle contain Rpf2, which together with Rrs1 mediate the incorporation of the 5S rRNP complex (5S rRNA and Rpl5) and Rpl11 into pre-ribosomes (Zhang et al., 2007).

The transition from the nucleolus (Nsa1 particle) to the nucleoplasm (Rix1 particle) is characterised by major compositional changes, which are presumably triggered by the Rea1 ATPase (Bassler et al., 2010; Ulbrich et al., 2009). The resulting nuclear Rix1 particle has lost many factors including Spb1, Erb1, Nop2, Puf6, Ebp2, Ytm1, the Noc2-Noc3 subcomplex and the DExD/H-ATPases Dbp10, Drs1, Spb4, Dbp9 and Has1 and has acquired new factors, such as Rea1, the Rix1-Ipi3-Ipi1 subcomplex, Rsa4, the Arx1-Alb1 subcomplex, Sda1, and Nug2 (Figure 3) (Bassler et al., 2010; Kressler et al., 2008). Additionally, the 27SB pre-rRNA has been processed almost completely into 25S and 7S/5.8S rRNAs (Nissan et al., 2002). Studies using electron microscopy (EM) revealed that the Rix1-defined pre-ribosome exhibits a tadpole-like structure (Nissan et al., 2004; Ulbrich et al., 2009). The head is built up by the 60S moiety, whereas the tail of the particle is formed by non-ribosomal factors (Nissan et al., 2004; Ulbrich et al., 2009). The main component of this tail structure is the huge Rea1 AAA-ATPase. ATP hydrolysis by Rea1 promotes the release of Rsa4 and the Rix1-Ipi3-Ipi1 subcomplex, thereby priming the pre-60S particle for its subsequent export towards the cytoplasm (Ulbrich et al., 2009).

After release of Rea1, Rsa4 and the Rix1-Ipi3-Ipi1 subcomplex, export factors like Nmd3, Arx1 and the Mex67-Mtr2 heterodimer are recruited and the particle gains export competence (see also section 1.2). This export competent pre-60S particle can be purified via Arx1-TAP (Bradatsch et al., 2007; Yao et al., 2007). Since Arx1 can be found in the nucleoplasm and cytoplasm, the Arx1 bait protein isolates both, a nuclear and a cytoplasmic pool of the pre-60S particle. Such an Arx1 particle contains more mature 5.8S and less 7S rRNA than the Rix1 particle (B. Bradatsch, B. Pertschy and E.H., unpublished data, Nissan et al., 2002), which is consistent with the finding that the final 7S to 5.8S processing occurs within the cytoplasm (Ansel et al., 2008; Gabel and Ruvkun, 2008; Thomson and Tollervey, 2010).

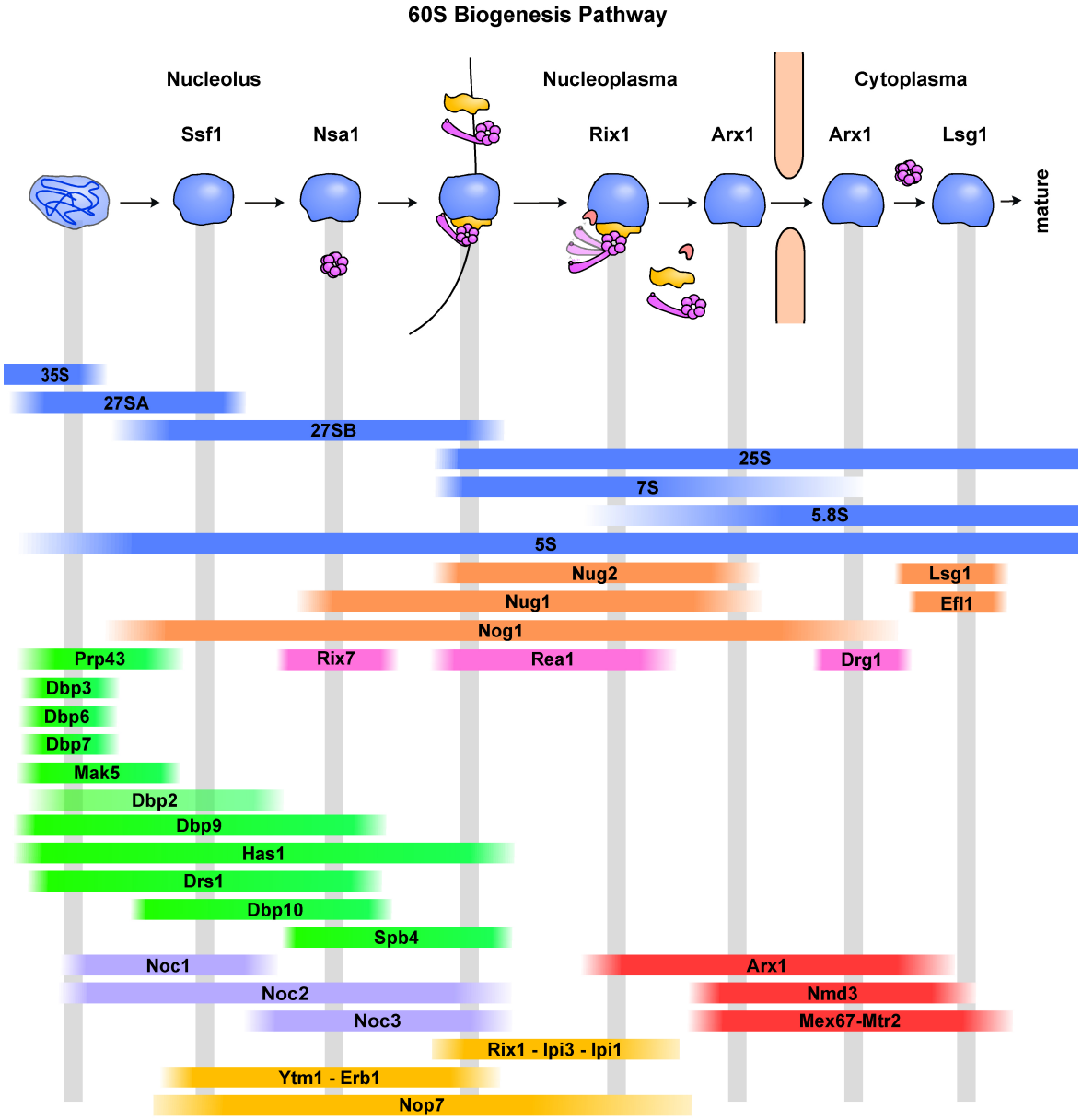

Figure 3: Pre-ribosomal particles along the 60S assembly pathway. The different 60S pre-ribosomes are depicted together with their rRNA content (blue). The presence of ATP/GTP consuming enzymes (GTPases in orange, DExD/H-box ATPases in green, AAA-type ATPases in pink), prominent subcomplexes (purple/yellow), and export factors (red) is shown. Bait proteins purifying the corresponding, distinct particles are indicated on top.

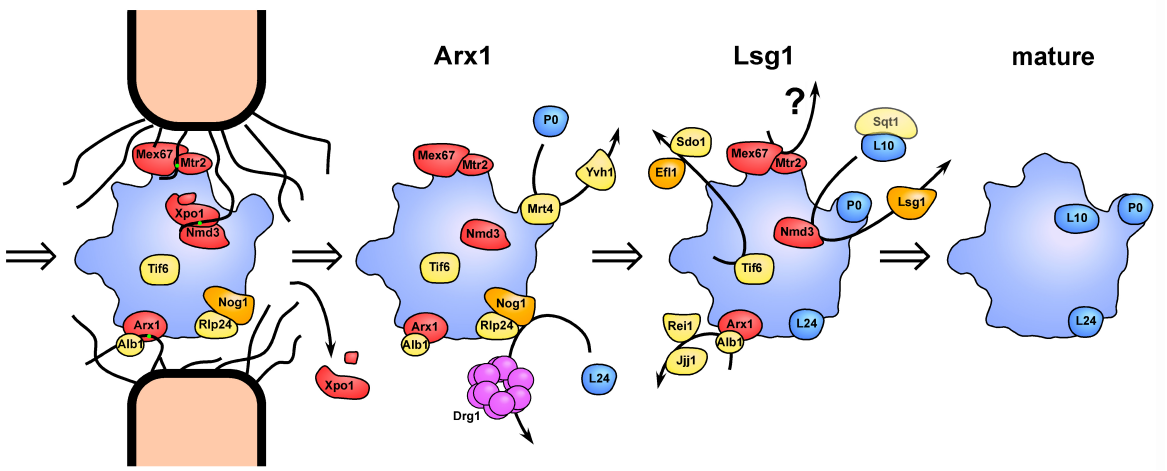

Figure 4: Cytoplasmic release of non-ribosomal factors from the pre-60S particles. Export factors are depicted in red, GTPases in orange, Drg1 AAA-ATPase in pink, and further non-ribosomal factors in yellow. Ribosomal proteins, incorporated into cytoplasmic pre-60S particles, are displayed in blue.

Upon arrival in the cytoplasm, the remaining non-ribosomal factors need to be released and yet missing ribosomal proteins need to be incorporated to gain the translation competent large subunit (Figure 4). Following nuclear export (see section 1.2), the AAA-ATPase Drg1 promotes the release of the GTPase Nog1 and the ribosomal-like protein Rlp24 (Pertschy et al., 2007). Then, the phosphatase Yvh1 facilitates the exchange of Mrt4 for the ribosomal protein Rpp0 (Figure 4) (Kemmler et al., 2009; Lo et al., 2009; Rodriguez-Mateos et al., 2009a; Rodriguez-Mateos et al., 2009b) and induces the recruitment of ribosomal proteins Rpp1 and Rpp2, which built up the ribosomal stalk, required for interaction with translation factors (reviewed in Panse and Johnson, 2010). In parallel Arx1 is released from cytoplasmic pre-60S ribosomes in a Rei1 and Jjj1 dependent mechanism, which requires the prior action of Drg1 (Demoinet et al., 2007; Hung and Johnson, 2006; Lebreton et al., 2006; Lo et al., 2010; Meyer et al., 2007; Pertschy et al., 2007). Subsequent release of Tif6 by the GTPase Efl1 and Sdo1 from 60S subunits is a prerequisite for the association of 60S particles with mature 40S ribosomal subunits (Menne et al., 2007; Senger et al., 2001). Finally, the Lsg1 GTPase triggers the recycling of the export adaptor Nmd3 (see section 1.2, Lo et al., 2010), creating a translational active 60S subunit.

1.2 Nuclear Export of Ribosomal Subunits

The ribosomal subunits belong to the largest transport substrates that have to pass the nuclear pore complex (NPC). Pioneer studies showed that the export process of both subunits depends on the karyopherin export receptor Xpo1/Crm1 and is regulated by the small GTPase Ran (Hurt et al., 1999; Moy and Silver, 1999; Moy and Silver, 2002; Thomas and Kutay, 2003; Trotta et al., 2003; Zemp et al., 2009). Xpo1 is responsible for the export of multiple cargoes, each of them is recognized by the presence of a short nuclear export sequence (NES). Through the transient interaction with the FG-meshwork inside the NPC, Xpo1 facilitates the translocation process of the receptor-cargo complex towards the cytoplasm (reviewed in Chook and Blobel, 2001; Fried and Kutay, 2003).

In the case of 60S subunits, the essential NES is provided by the conserved and essential export adaptor Nmd3. Nmd3 binds via its N-terminal domain to the 60S particle (e.g. Arx1-TAP particle), whereas its C-terminus carries two NES sequences that are recognized by Xpo1 (Gadal et al., 2001; Hedges et al., 2006; Ho et al., 2000; Sengupta et al., 2010; Thomas and Kutay, 2003; Trotta et al., 2003). The binding site of Nmd3 on the pre-60S particle is in close proximity to the position of Rpl10 on mature 60S subunits (Hedges et al., 2006; SenGupta et al., 1996), but its direct binding partner (rRNA or protein) remains to be identified. Upon arrival in the cytoplasm the Xpo1-RanGTP-Nmd3-pre-60S complex is dissociated by RanGAP stimulated GTP hydrolysis. Subsequent release of Nmd3 is coupled to the incorporation of Rpl10 into pre-60S ribosomes (Hedges et al., 2005; West et al., 2005). Rpl10 in complex with its specific chaperon Sqt1 is recruited to the pre-60S particle, where the GTPase Lsg1 stimulates the exchange of Nmd3 for Rpl10 resulting in the release of Nmd3 and Sqt1 (Hedges et al., 2005; West et al., 2005).

It has been observed that the kinetics of the transport process is slowed down with increasing cargo size (Ribbeck and Gorlich, 2001). Therefore it appears feasible that the export of the large ribosomal subunit depends on additional nuclear export factors (Figure 4). Besides Xpo1, the heterodimeric export receptor Mex67-Mtr2 facilitates the export of the large, but not of the small subunit (Bassler et al., 2001; Strässer et al., 2000; Yao et al., 2007). *In vitro* binding assays

revealed that the Mex67-Mtr2 heterodimer can bind directly to nucleoporins and to 5S rRNA (Strässer et al., 2000; Yao et al., 2007). In addition, specific Mtr2 and Mex67 mutants showed defects in 60S export and are genetically linked to *nmd3* and *arx1* alleles (Bradatsch et al., 2007; Yao et al., 2007). Thus Mex67-Mtr2 fullfils all requirements of a bona fide export receptor for the 60S subunits.

Arx1 functions as a further export receptor of pre-60S particles. This unorthodox export factor binds to 60S subunits in the proximity of Rpl25 and interacts with the FG-repeats of nucleoporins via a specific binding pocket (Bradatsch et al., 2007; Hung and Johnson, 2006). Hereby, Arx1 might shield the surface of the pre-60S particle against the non-polar FG-meshwork inside the nuclear pore complexes, thereby facilitating translocation of pre-60S particles (Bradatsch et al., 2007). Moreover, the *arx1*Δ null mutation confers synthetic lethality with the other transport receptors/adaptors *nmd3, mex67 and mtr2* alleles (Bradatsch et al., 2007; Hung et al., 2008).

Another factor, which is functionally linked to the 60S export process, is Ecm1. Initially, Ecm1 was identified in a synthetic lethal screen with a *mtr2* mutant allele (Bassler et al., 2001) and was further shown to be genetically linked to Mex67, Arx1, Nmd3 and a number of nucleoporins (Bradatsch et al., 2007; Yao et al., 2010), B. Bradatsch and E.H. unpublished data). Ecm1 associates weakly with late pre-60S particles that also carry Nmd3, Mex67, and Arx1 (Yao et al., 2010). However, its precise role during 60S export still needs to be elucidated.

In contrast to the large subunit, the export mechanism for the small subunit remains unclear. It has been shown that Xpo1 and Ran are required for pre-40S translocation, but no NES-adaptor has been identified to date. Moreover, it has been discovered that depletion of few ribosomal proteins, namely Rps15, Rps10, Rps26, Rps2, Rps0 and Rps3 cause strong export defects (Ferreira-Cerca et al., 2005; Leger-Silvestre et al., 2004), suggesting a direct or an indirect involvement in pre-40S export. Bioinformatic analysis indicated that the pre-40S associated Dim2 (Schäfer et al., 2006; Schäfer et al., 2003) harbours a potential NES sequence (Vanrobays et al., 2008). In addition, the Rio2 kinase and the non-essential Ltv1, which are components of late 40S intermediates, carry a functional NES (Schäfer et al., 2006; Schäfer et al., 2003; Seiser et al., 2006; Zemp et al., 2009). Whilst these proteins may contribute to an efficient export, their NES

sequences are not essential for 40S export. Therefore, it seems likely that further, potentially essential, 40S export factors exists.

1.3 ATPases in Ribosome Biogenesis

The assembly of ribosomal subunits is one of the most energy consuming processes in dividing cells (Warner, 1999). Accordingly, there are several essential ATP and GTP consuming enzymes amongst the non-ribosomal factors involved in ribosome biogenesis (reviewed in Kressler et al., 2010; Strunk and Karbstein, 2009). These include 19 DExD/H-box ATPases, three kinases, three AAA-ATPases, two ABC proteins and six GTPases. It is believed that these enzymes provide the energy that is required to confer directionality to the assembly and maturation process. Here, it appears that the DExD/H-box ATPases are almost exclusively engaged in early, nucleolar assembly steps; whereas, the AAA-ATPases (e.g. Rea1) or GTPases (e.g. Nug1) are predominantly required for later steps in 60S assembly. This observation highlights the requirement for the action of different kinds of NTPases at distinct steps during the assembly of pre-ribosomal particles.

The largest class of NTPases involved in ribosome biogenesis are ATPases (also termed RNA helicases) of the DExD/H-box family, consisting of DEAD-, DEAH- and DExH-box proteins (de la Cruz et al., 2004). Genes encoding for DExD/H-box proteins are found in viral, prokaryotic and eukaryotic genomes and are involved in virtually all aspects of cellular RNA metabolism, including ribosome biogenesis, pre-mRNA splicing, mRNA export, translation initiation, and RNA turnover (reviewed in Bleichert and Baserga, 2007; Cordin et al., 2006). These ATPases display *in vitro* activities comprising RNA-dependent ATP hydrolysis, ATP-dependent RNA binding, ATP-dependent unwinding or strand separation of short double-stranded RNA or RNA/DNA duplexes, ATP-dependent dissociation of RNA-bound proteins, and ATP-independent annealing of complementary single-stranded RNA (Cordin et al., 2006; Jankowsky and Bowers, 2006; Jankowsky and Fairman, 2007; Linder and Lasko, 2006). However, DExD/H-box helicases generally have poor unwinding efficiency of long duplex substrates and their

anticipated *in vivo* substrates suggest that DExD/H-box proteins generally do not act as processive enzymes (Cordin et al., 2006; Jankowsky and Fairman, 2007). Due to their asscociation with early snoRNA decorated pre-ribosomal particles, the following functions had been proposed for DExD/H-box proteins: (i) remodelling and dissociation of RNA:RNA, RNA:protein or protein:protein interactions; (ii) rendering the pre-rRNA accessible for endo- or exonucleases and (iii) releasing snoRNP by unwinding of pre-rRNA:snoRNA duplexes. It is unlikely, that DExD/H-box ATPases in general trigger the release of snoRNAs (Bohnsack et al., 2008), however, a few DEAD-box ATPases may contribute to these processes (Bleichert and Baserga, 2007; Bohnsack et al., 2008; Kos and Tollervey, 2005; Liang and Fournier, 2006; Srivastava et al., 2010). Nevertheless, the specific substrates and the enzymatic function of most DExD/H-box ATPases are unknown.

All kinases shown to be involved in ribosome biogenesis, including Hrr25, Rio1, Rio2, have a predominant role in 40S formation. Hrr25, an isoform of casein kinase I, is a component of late pre-40S particles and has been shown to phosphorylate members of the Ltv1-Enp1-Rps3 subcomplex (Schäfer et al., 2006; Schäfer et al., 2003). A combination of *in vitro* maturation assays and EM studies has demonstrated that an Hrr25 mediated phosphorylation and subsequent dephosphorylation event of the Ltv1-Enp1-Rps3 complex is required for formation of the 40S ‘beak’ structure and for stable incorporation of Rps3 into 40S subunits. In contrast, the substrates of Rio1 and Rio2 within the ribosome assembly process are still elusive.

The ATPases Rix7, Rea1 and Drg1 belong to the superfamily of AAA-type ATPases (**A**TPases **a**ssociated with various cellular **a**ctivities). These proteins are characterised by a structurally conserved ATPase domain and are found in all organisms (reviewed in Erzberger and Berger, 2006; Ogura and Wilkinson, 2001; Vale, 2000). Independent of whether these ATPases harbour one (type I), two (type II), or six AAA-domains, they assemble into hexameric rings, which undergo structural changes during the ATPase cycle (Hanson and Whiteheart, 2005; Vale, 2000). It has been suggested that AAA-type ATPases utilize the energy from ATP hydrolysis to apply force onto their substrates, in order to induce structural rearrangements or substrate release (reviewed in Erzberger and Berger, 2006; Vale, 2000). Consistently, the cytoplasmic type II ATPase Drg1, has been

implicated in the release of Nog1, Rlp24 and Arx1 directly after the export of the pre-60S ribosome (Figure 4). Similarly, Rix7, a nuclear type II AAA-ATPase, has been proposed to stimulate the release of Nsa1 from nucleolar 60S particles (Kressler et al., 2008). However, no assay has been established to date, that demonstrates a direct role of these AAA-ATPases in the release of pre-ribosomal factors. The third AAA-ATPase involved in ribosome formation, Rea1, was identified as a component of the Nug1 and the Rix1 particle (Bassler et al., 2001; Nissan et al., 2002). This huge ATPase (~ 560 kDa) contains six AAA-protomers and is essential for 60S subunit formation and ITS2 processing (Galani et al., 2004). Subsequent work revealed that Rea1 catalyze the release of Rsa4 from nuclear pre-ribosomes and the release of the Ytm1-Erb1-Nop7 subcomplex from nucleolar pre-60S particles (see 3.2 Summary of Results).

The final class of ATP utilizing proteins in ribosome biogenesis are the ABC proteins. These ATPases are usually membrane transporters that utilize the energy from ATP hydrolysis to transport their cargoes against a concentration gradient. In has been discovered that two soluble members of the ABC proteins, namely Rli1 and Arb1, are involved in ribosome biogenesis (Dong et al., 2005; Yarunin et al., 2005). However, their function in ribosome biogenesis remains unclear till present.

1.4 GTPases in Ribosome Biogenesis

Many cellular processes are regulated by GTPases, which in general act as molecular switches. These enzymes have a G-domain, consisting of five conserved sequence motifs (G1-G5), including the characteristic Walker A motif (P-loop / G1) (Leipe et al., 2002) that can bind GTP. The GTP hydrolysis usually induces a conformational change within GTPases, that induces the molecular switch. To date, six GTPases (Bms1, Efl1/Ria1, Lsg1/Kre35, Nog1, Nug1, and Nug2/Nog2) have been demonstrated to be essential for ribosome biogenesis.

The GTPase Bms1 mediates the recruitment of Rcl1 to early pre-40S particles (Gelperin et al., 2001; Karbstein et al., 2005; Wegierski et al., 2001). The GTP bound form of Bms1 builds a complex with Rcl1, which is then recruited to

the U3 snoRNA within 90S particles (Karbstein and Doudna, 2006; Karbstein et al., 2005). In this context, the C-terminal domain of Bms1 may act as an intramolecular GTPase activator (GAP) that regulates the release of Bms1 from pre-ribosomal particles (Karbstein and Doudna, 2006; Karbstein et al., 2005).

The remaining GTPases are essential for 60S biogenesis. The conserved Nog1 is recruited to nucleolar pre-60S particles. Here Nog1 interacts genetically and physically with the ribosomal-like protein Rlp24 (Saveanu et al., 2003). After nuclear export, the ATPase Drg1 dissociates Nog1 and Rlp24 from the pre-ribosome (Pertschy et al., 2007). It has been speculated that Rlp24 is a placeholder for Rpl24 and Nog1 might regulate the corresponding exchange reaction (Saveanu et al., 2003).

The cytoplasmic GTPase Efl1/Ria1 is involved in the release of Tif6 from 60S pre-ribosomes. Upon binding of Elf1 to the cytoplasmic 60S pre-ribosomes, its GTPase activity is stimulated. Then, the subsequent conformational change induces the dissociation of Tif6 (Figure 3, 4) (Senger et al., 2001; Ulbrich et al., 2009). This release reaction is assisted by Sdo1, which is mutated in patients with the Shwachman-Diamond-Syndrome (Luz et al., 2009; Menne et al., 2007). Consistent with the finding that Tif6 prevents joining of the 60S pre-ribosome with the 40S subunit (Raychaudhuri et al., 1984), its removal is one of the latest maturation steps (Figure 4).

Nug1, Nug2/Nog2 and Lsg1/Kre35 belong to the unusual group of circularly permutated GTPases (cpGTPases), in which the characteristic GTPase motifs (G1-G2-G3-G4-G5) are switched in their order to G4-G1-G2-G3. Moreover they are lacking a distinct G5 motif, but instead they posses an unique G5* motif (DAR) ahead the G4 consensus sequence (Karbstein, 2007; Leipe et al., 2002). Moreover, the switch II region of the cpGTPases is missing key residues that stimulate GTP hydrolysis in small GTPases (Kim do et al., 2008). Therefore it's likely that these cpGTPases have a different mechanism of activation. Interestingly, cpGTPases appear to exclusively act in ribosome assembly, indicative of a specialised molecular role in rRNA metabolism. The cpGTPase Nug1 associates with nucleolar and nucleoplasmic 60S pre-ribosomes, which is mediated by its N-terminal RNA binding domain. Nug1 is functionally linked to export factors Mtr2, and Ecm1, but also to early factors like the Dbp10, Noc2, and

Noc3 (Bassler et al., 2001; Bassler et al., 2006; Yao et al., 2007). The properties of Nug1 are described and discussed in more detail in section 3.1 and 4.2. The essential Nug2 GTPase associates with nucleolar and nuclear pre-60S particles (Saveanu et al., 2001). However, to date no direct binding partner has been identified. In contrast, Lsg1 is only associated with cytoplasmic pre-60S particles. Here, Lsg1 is involved in the cytoplasmic release of Nmd3 and the incorporation of Rpl10 into the pre-60S ribosome (see section 1.2, Hedges et al., 2005; West et al., 2005). Yet, the mechanistic details of this process remained largely unknown.

1.5 Diseases Linked to Ribosome Biogenesis

Ribosomes are the machines, which translate the cellular proteins, a process which is essential for every dividing cell. Recent progress in genome sequencing has revealed that mild mutations in ribosomal proteins or assembly factors, are linked to various human diseases like Diamond-Blackfan anemia (DBA), dyskeratosis congenital (DC), Shwachman-Diamond Syndrome (SDS) or cartilage-hair hypoplasia (CHH) (reviewed in Freed et al., 2010; Ganapathi and Shimamura, 2008). Many of these diseases are associated with inherited bone marrow failure syndromes, which are characterised by a reduced number of blood cells. This might be due to the need for a high ribosome synthesis rate prior to the loss of the nucleus during erythropoiesis. Thus a reduced number of ribosomes might not allow for a sufficient production of α– and β-globin molecules.

Most of the diseases linked to ribosome biogenesis defects have a pre-disposition for cancer. Actively dividing cancer cells have a high demand for ribosomes, thus several cancer cell lines display increased expression of ribosomal and non-ribosomal factors involved in ribosome biogenesis (Dai and Lu, 2008). Moreover, it has been observed that the proto-oncogenic transcription factor myc stimulates ribosome assembly (Arabi et al., 2005; Gomez-Roman et al., 2006; Gomez-Roman et al., 2003; Grandori et al., 2005; Grewal et al., 2005). Thus, ribosome biogenesis appears to be also regulated by the cell cycle involving myc. On the opposite, an impaired ribosome assembly pathway may give a negative feedback signal to the cell cycle regulators and hence leads to a cell

cycle arrest or apoptosis: Accordingly, it was found that ribosomal protein Rpl11 could inhibit myc function. Moreover, ribosomal proteins like Rpl23, Rpl11, Rpl5 and Rps7, that are not associated with ribosomal subunits, were found to affect Mdm2 activity (Fumagalli et al., 2009; Lo and Lu, 2010; Sun et al., 2010) and references therein), a ubiquitin ligase that degrades the cell cycle regulator p53. Subsequently, increasing levels of p53 cause the synthesis of cell cycle inhibitors that inhibit cyclin-CDK complexes and thus stop cell cycle progression (Dai and Lu, 2008).

In summary, it seems contradictory that a defective ribosome biogenesis inhibits cell cycle progression and stimulates cancer development. However, a delayed progression in cell cycle could increase the selective pressure for mutations to suppress a reduced ribosome biogenesis and the negative feedback on the cell cycle. Finally, bypassing of the regulation may finally contribute to cancer development. These observations indicate that a detailed mechanistic understanding of the conserved pathways of ribosome biogenesis could aid in designing new strategies for cancer therapy or curing ribosomopathies.

2. Aim of the Work

The biogenesis of ribosomes in eukaryotic cells is a highly complex and dynamic process. Along that pathway the rRNA is transcribed, modified, folded, processed and assembled with ribosomal proteins. Many energy-consuming enzymes participate in ribosome biogenesis; however, their roles are not clear. To elucidate the mechanism of ribosome formation in eukaryotic cells, we sought to elucidate the role of the GTPase Nug1 and ATPase Rea1, which transiently associate with pre-60S particles.

Using mutational approaches we wanted to generate mutants of Nug1 and Rea1, characterize their cell biological phenotype and utilize them in genetic screens to identify their interaction partners and the functional network, in which they are embedded. Furthermore, we aimed to establish biochemical methods to allow the isolation and characterization of pre-ribosomal particles that are associated with Nug1 and Rea1, respectively. Last but not least, we aimed to purify these pre-ribosomal factors to study their enzymatic properties and obtain structural information. The combination of these different approaches may help us to elucidate the molecular roles of Nug1 and Rea1 in ribosome assembly.

3. Summary of Results

3.1 The GTPase Nug1 Binds to Pre-60S Particles via its N-terminal RNA-binding Domain

Baßler, Grandi, Gadal, Leßmann, Tollervey, Lechner and Hurt. (2001) Identification of a 60S pre-ribosomal particle that is closely linked to nuclear export. **Mol Cell** *8*, 645-656.

Baßler, Kallas and Hurt. (2006) The pre-ribosomal Nug1 factor reveals a central GTPase domain and an N-terminal RNA binding domain that mediates association with pre-60S subunits. **J Biol Chem** *281*, 24737-24744.

I have initially identified the GTPase Nug1 in genetic screens for factors that functionally interact with a mutant allele of the export receptor Mtr2. Bioinformatic analysis indicated that Nug1 comprises a highly conserved P-loop motif that is characteristic for GTPases. We demonstrated that Nug1 is an essential protein, that localises in the nucleolus and nucleoplasm and therefore termed it Nug1 (nucle(ol)lar GTPase). Since the nucleolar localisation indicated an involvement in ribosome biogenesis, temperature sensitive mutant alleles were generated and tested for defects in ribosome biogenesis. These *nug1* mutant alleles, when shifted to restrictive conditions, displayed an accumulation of pre-ribosomal particles inside the nucleus, rRNA processing defects, and a decrease of mature 60S subunits. Using a sucrose sedimentation assay, we showed that Nug1 associates with pre-60S particles. Subsequently, tandem affinity purifications (TAP, Puig et al., 2001) of Nug1-TAP as bait protein enabled us to isolate a highly specific and pure pre-ribosomal 60S particle (Figure 5). Mass spectrometry and Northern blot analysis revealed that this particle contained more than 20 non-ribosomal biogenesis factors, ribosomal proteins and pre-rRNA of the large subunit. Some of these non-ribosomal factors were already characterised as 60S biogenesis factors, whereas the remaining factors had an unknown function at this time. Among these non-ribosomal factors was also the AAA-ATPase Rea1 (see below; section 3.2). Concomitant to our isolation of the Nug1 particle, also other labs succeeded in the purification of pre-ribosomal particles using Nug2/Nog2, Nop7 and Ssf1 as bait proteins (Fatica et al., 2002; Harnpicharnchai et al., 2001; Saveanu et al., 2001). Subsequently, characteristic ribosome biogenesis factors of

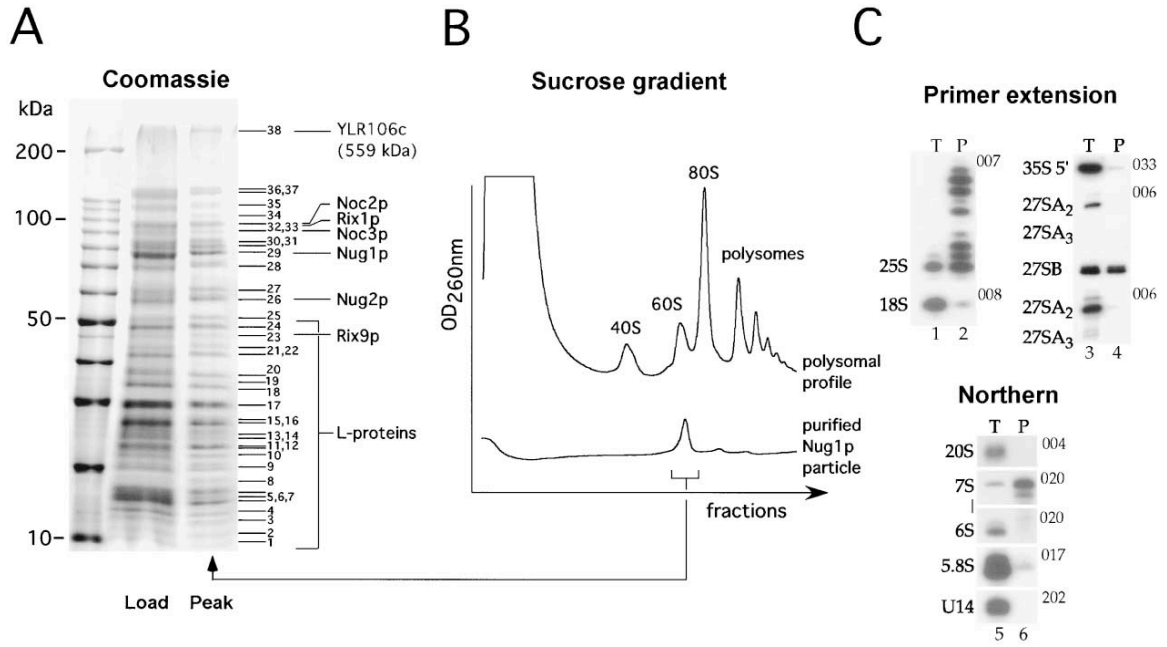

Figure 5. Nug1 is associated with pre-60S particles (Baßler et al., 2001)
(A) Nug1-TAP was affinity-purified, separated by SDS-PAGE, and analyzed by mass spectrometry. Load: Nug1 eluate from the Calmodulin-Sepharose column; Peak: 60S fraction isolated from the sucrose gradient after centrifugation of the Nug1 particle (see B). (B) Sedimentation behaviour of the Nug1 particle. (C) Analysis of rRNA in the purified Nug1 particle by primer extension and Northern hybridization. T, total RNA; P, Nug1 particle.

the Nug1 pre-ribosome were TAP-tagged and used to isolate pre-ribosomal particles of the large and small subunit (Grandi et al., 2002; Nissan et al., 2002; Schäfer et al., 2003). Thus, the identification of numerous novel biogenesis factors and finally the setup of a spatio-temporal map of pre-ribosomal particles along the ribosome biogenesis pathway (reviewed in Fatica and Tollervey, 2002; Fromont-Racine et al., 2003; Henras et al., 2008; Kressler et al., 2009; Tschochner and Hurt, 2003).

Analysis of the Nug1 primary sequence indicated that the Nug1 protein consists of three domains: an N-terminal domain, a middle domain, and a C-terminal domain. Genetic, cell biological and biochemical studies of Nug1 deletion constructs demonstrated that the N-terminal domain is required for the nucleolar/nuclear targeting of Nug1. Moreover, this N-domain showed RNA-binding activity and was essential for the binding of Nug1 to pre-60S particles. Interestingly, an N-terminal mutant of Nug1 was genetically linked to the nucleolar Noc2-Noc3 complex and the nucleolar helicase Dbp10. Therefore, these factors may either interact directly with the N-terminal domain or may be required to

generate the binding site for Nug1. The middle domain of Nug1 consists of a permutated GTPase motif (cpGTPase). At this time, it was unclear whether permutated GTPases could hydrolyze GTP. Purification of recombinant Nug1 and subsequent enzymatic analysis revealed that Nug1 has a low GTPase activity, which suggested that Nug1 require a GTPase activating protein (GAP) *in vivo* (see Discussion). The function of the essential C-domain remained unclear, however a mutation within this domain is linked to late biogenesis factors like *ecm1, bud20,* and *mtr2* mutants. To date, it has neither been possible to identify a direct binding partner of Nug1, nor to establish *in vitro* assays to test for the molecular function of Nug1, which is now the current research goal in our laboratory (see Discussion).

3.2 The AAA-ATPase Rea1 Acts at Multiple Stages during 60S Biogenesis

Ulbrich*, Diepholz*, Baßler*, Kressler, Pertschy, Galani, Böttcher, and Hurt. (2009) A Mechanochemical Removal of Biogenesis Factors from Nascent 60S Ribosomal Subunits. **Cell** *138*, 911-922.
* these three authors are contributed equally

Baßler, Kallas, Pertschy, Ulbrich, Thoms and Hurt. (2010) The AAA-ATPase Rea1 drives removal of biogenesis factors during multiple stages of 60S ribosome assembly. **Mol Cell** 38, 712-721

Initially, we identified the Rea1 ATPase as a co-purifying protein in the Nug1-TAP particle. Subsequently, Rea1 was found as a prominent component of the Rix1-TAP particle and was demonstrated to be essential for 60S biogenesis (Nissan et al., 2002; Galani et al., 2004). Bioinformatic analysis suggested that Rea1 (560 kDa) is a multi-domain protein with an N-terminal extension, six AAA+ type ATPase domains, a long α–helical linker region, a D/E rich domain and a C-terminal MIDAS domain (see Figure 6, Garbarino and Gibbons, 2002). Typically,

Figure 6: Domain organisation of Rea1 (see text for details)

MIDAS domains (**m**etal **i**on **d**ependent **a**dhesion **s**ite) are present in integrins, where they mediate protein-protein interactions (Astrof et al., 2006; Luo et al., 2007; Takagi, 2007). Using a yeast two hybrid assay we found that the Rea1 MIDAS domain interacts with the N-domain of Rsa4, an essential 60S biogenesis factor (De la Cruz et al., 2005). Bioinformatic analysis revealed that this N-terminal domain of Rsa4 is highly conserved within different eukaryotes. In addition it is also homologues to the N-terminal domain of Ytm1, a nucleolar 60S biogenesis factor that forms a tight complex with Erb1 and Nop7 (Miles et al., 2005; Tang et al., 2008). MIDAS domains usually coordinate a metal ion via a conserved motif. That metal ion is important for binding to a conserved E/D residue of the MIDAS binding partner (Craig et al., 2004). An *in vitro* binding assay demonstrated that Rea1 MIDAS binds directly to the N-domain of Rsa4 and Ytm1, respectively. Therefore we termed these domains MIDO (**M**IDAS **i**nteracting **do**main). Mutation of the metal ion coordinating residues (Rea1 DAA, Ytm1 E80A, Rsa4 E114D) abrogated the interaction and caused lethality. Further genetic analysis revealed a functional link between Rea1 and Ytm1 as well as between Rea1 and Rsa4. Significantly, overexpression of the Ytm1 E80A and the Rsa4 E114D mutants caused a dominant negative phenotype by blocking 60S biogenesis at a nucleolar stage (Ytm1 E80A) or nuclear stage (Rsa4 E114D). Consistent with the idea, that Rea1 interacts first with Ytm1, depletion of Rea1 resulted in a nucleolar arrest in 60S biogenesis, similar to the Ytm1 mutant. These findings revealed that Rea1 acts at multiple steps during 60S biogenesis.

Structural analysis of Rea1 by electron microscopy (EM) indicated that, similar to other AAA-type ATPases, the six ATPase domains of Rea1 formed a ring-like structure, whereas, the linker, the D/E rich and the MIDAS domain constitute a long tail that extended from the ring. EM analysis of the Rix1 pre-ribosome revealed that Rea1 was bound via the ring domain to the pre-ribosomal particle, close to the position of the Rix1-Ipi3-Ipi1 subcomplex (Figure 7), whereas the tail with the MIDAS at its tip protruded from the particle. The tail of Rea1 displayed an intrinsic flexibility with respect to the pre-ribosomal head, suggesting that the Rea1 tail could move towards the head and contact a MIDAS binding partner (Figure 7). However, antibody-labelling experiments showed that Rsa4 was not located at the tail of Rea1, but at the position, where the Rea1 MIDAS

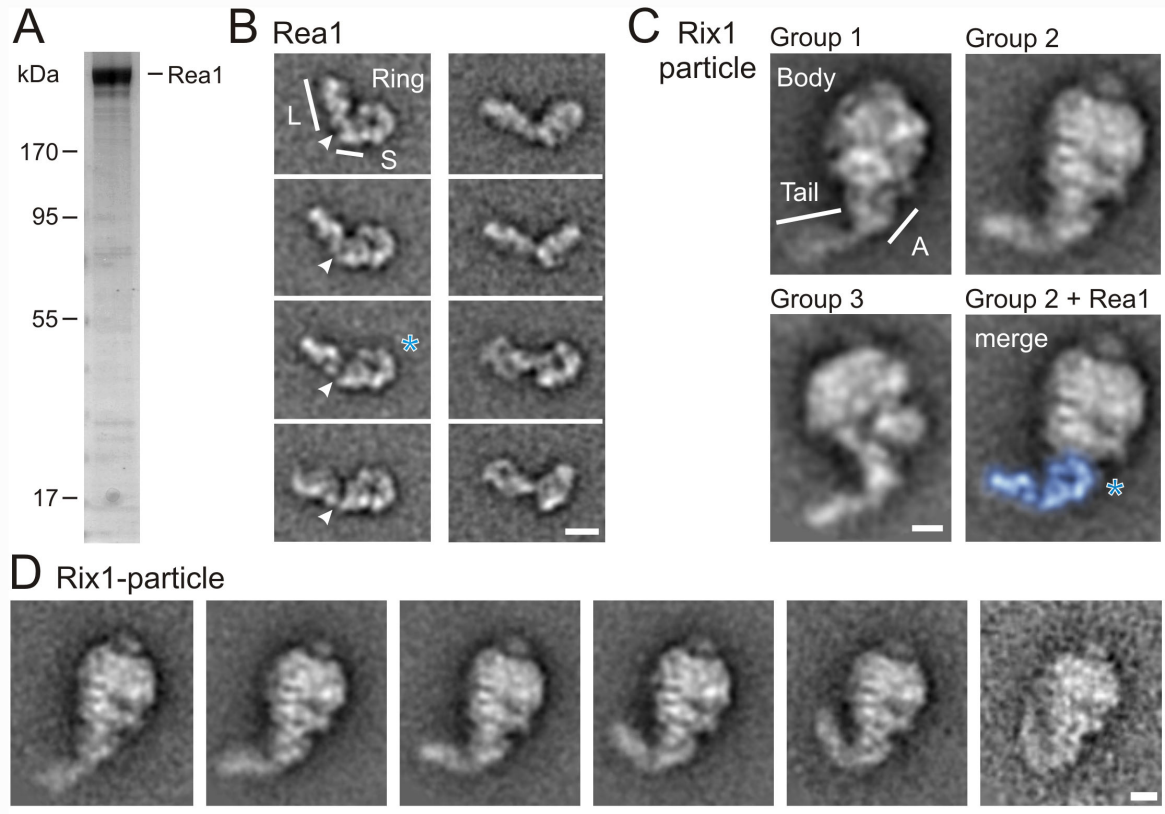

Figure 7. EM structure of Rea1 (A,B) and the Rix1 pre-60S particle (C,D) (Ulbrich et al., 2009) (B) The AAA-ATPase domain of Rea1 adopts a ring-like shape whereas the MIDAS locates to the tip of a tail structure. (C) A merge of Rea1 with the Rix1-particle reveals similar size and shape between Rea1 (blue) and the tail and attachment site within the Rix1-particle. (D) Rea1 can adopt different conformation within the Rix1 particle, suggesting a movement of the Rea1 tail during ribosome biogenesis.

domain was predicted to contact the body of the Rix1 pre-ribosome (see Figure 7).

Moreover, we observed that incubation of the Rix1 pre-ribosome with ATP causes dissociation of Rsa4, Rix1-Ipi3-Ipi1 complex and Rea1 from the pre-ribosome. This release reaction was depending on the hydrolysis of ATP, since ADP nor AMP-PNP treatment did not dissociate Rsa4 from the Rix1-particle. Moreover, the ATP-mediated release of biogenesis factors was depend on a functional Rea1-Rsa4 interaction, since a Rix1-particle, that carried the Rsa4 E114D mutant, was inert to ATP treatment. In order to test, whether Rea1 can also release Ytm1, we used a Rix1 pre-ribosome that was isolated from a Rea1 depleted background. This particle consisted of characteristic nucleolar biogenesis factors, including the Ytm1-Erb1- Nop7 subcomplex, but lacked nuclear factors like Rsa4. Upon incubation of this pre-ribosome with Rea1 and ATP, Ytm1 together with its binding partners Erb1 and Nop7 was released from the pre-ribosome.

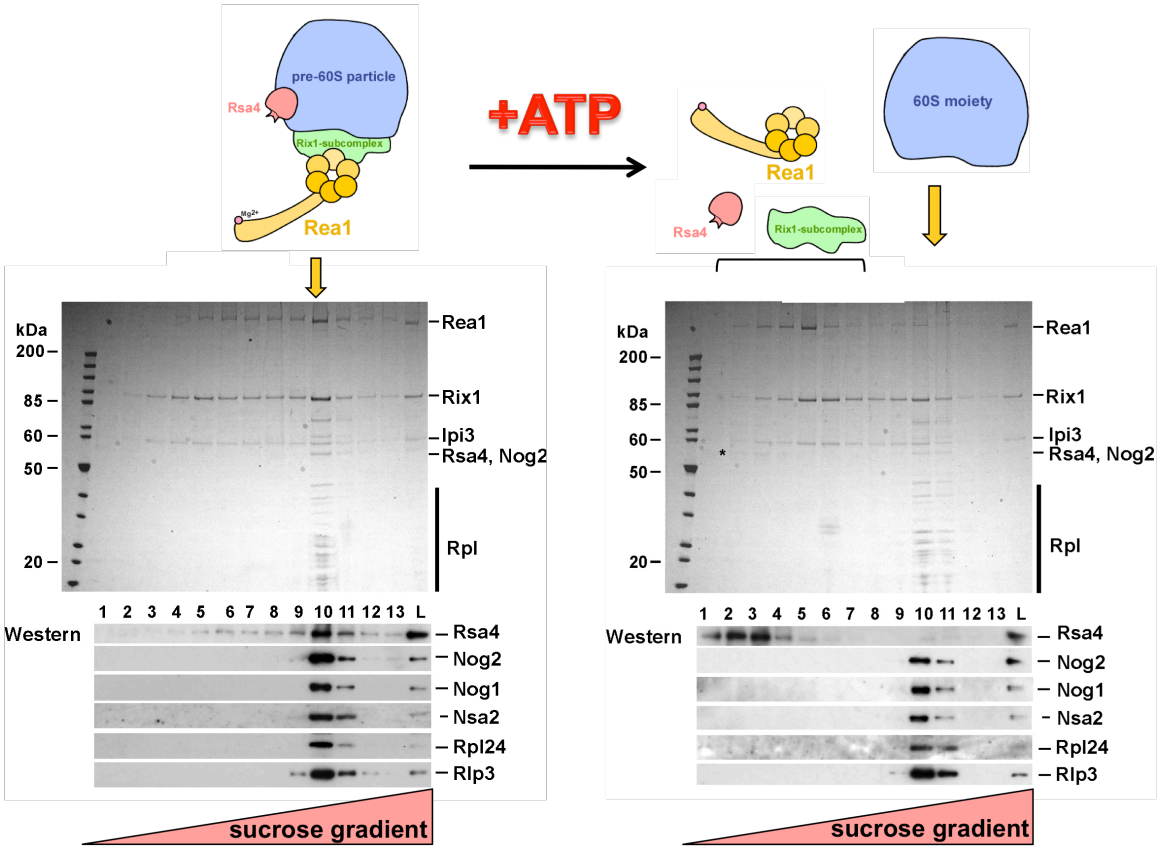

Figure 8. ATP-Dependent Release of Rsa4, Rea1 and the Rix1-Subcomplex from the Pre-60S Particle. Release of non-ribosomal factors from the pre-60S particle by ATP-treatment was monitored by sucrose gradient centrifugation. A purified Rix1-particle was incubated with ATP before loading on a sucrose gradient. After centrifugation the gradient was fractionated, and analysed by SDS-PAGE and Coomassie staining (upper part) or Western blotting.

Thus, a similar ATP and Rea1 dependent mechanism releases Rsa4 and Ytm1 from pre-ribosomal particles.

Taken together, we suggested a model in which Rea1 binds via the ATPase ring to the pre-ribosome. In a subsequent step the flexible tail, with the MIDAS at its tip, moves towards Rsa4, bound at the head of the pre-ribosome. Thus, Rea1 could be fixed at two different sites on the pre-ribosome, to generate a force by ATP hydrolysis that releases non-ribosomal factors.

This work shed light on the enzymatic function of Rea1 and identified important direct binding partners. However, several mechanistic questions remain open, which will be addressed in future studies (see Discussion).

4. Discussion and Conclusions

4.1 Biochemical Dissection of the Ribosome Assembly Pathway

Originally, I was interested in investigating the role of Mtr2 in nuclear export of mRNA. Together with Katja Sträßer, a former PhD student in the lab, I was able to show that the Mex67-Mtr2 complex binds directly to FG repeats of nuclear pore complexes and thus is the major export receptor for mRNA (Strässer et al., 2000). However, I discovered an unusual temperature sensitive *mtr2* mutant allele that unexpectedly, did not display an mRNA export defect, but was impaired in 60S ribosome biogenesis (Bassler et al., 2001). This finding then paved the way for characterizing the function of Mex67 in ribosome export (Yao et al., 2007).

Using a synthetic lethal (SL) screen, I identified *ecm1* and *nug1* mutants as genetic interaction partners of the *mtr2-33 mutant* allele. While characterising the molecular properties of Nug1, I found that the *in vivo* purification of Nug1 co-isolated a pre-60S particle. At this time the nature of pre-ribosomal particles was elusive. Pioneering work in the 1970s from Planta and Warner had shown that pre-rRNA associates with 90S, 66S and 43S precursor particles, but the composition of these particles remained unknown. 30 years later, the purification of a 60S pre-ribosome using Nug1 as bait protein, marked a breakthrough in studying ribosome biogenesis. Northern blot analysis and mass spectrometry revealed that the Nug1 pre-ribosome contained rRNA precursors, ribosomal proteins of the large subunit and more than 20 non-ribosomal factors. Here, several novel biogenesis factors could be identified. Subsequently, Tracy Nissan, a former Post-Doc in the Hurt lab, and I GFP- and TAP-tagged a number of these newly discovered 60S biogenesis factors, determined their cellular localization, and purified the associated pre-ribosomal particles and analyzed their protein and rRNA content (Nissan et al., 2002). These data enabled us to arrange the isolated pre-60S particles in a temporal order along the 60S biogenesis pathway. Thus, we could establish a chronological “map” of the maturation of pre-60S particles, which shows the temporal dynamics in binding and dissociation of biogenesis factors and allows the correlation of these factors with the associated rRNA intermediates.

4.2 Nug1, a Molecular Switch in 60S Biogenesis

The family of cpGTPases are characterized by a special arrangement of the GTPase motifs. Therefore, it was initially unclear, whether they could hydrolyze GTP and act as molecular switches like other types of GTPases. I could demonstrate that Nug1 has GTPase activity *in vitro*, but how the Nug1 mediated GTP hydrolysis cycle operates *in vivo* remained unclear. Moreover, Nug1 is capable of interacting directly with rRNA. Interestingly, all previously characterized cpGTPases are involved in the biogenesis of prokaryotic, eukaryotic or mitochondrial ribosomes. Several of these proteins display RNA binding activity (Anand et al., 2006) and the GTPase activity of some of them (e.g. prokaryotic Ylqf GTPase) could be stimulated upon binding to ribosomal particles (Matsuo et al., 2006; Matsuo et al., 2007; Uicker et al., 2006). Thus, it is possible that binding of rRNA is directly involved in the activation of the GTPase activity (Anand et al., 2006).

The eukaryotic cpGTPase Lsg1/Kre35 is involved in the recruitment and incorporation of the Rpl10 protein (Hedges et al., 2005; West et al., 2005). Nug1 displays a significant homology to Lsg1. Thus, Nug1 may also be involved in the incorporation of a ribosomal protein. Another possibility is that Nug1 functions as a placeholder: a critical position on the pre-ribosome that might be shielded by Nug1 until a (ribosomal) protein is recruited. To unravel this function it would be important to determine the binding position of Nug1 on the pre-ribosome and analyse the incorporation of adjacent ribosomal proteins. We know that the essential N-terminal domain of Nug1 binds to pre-ribosomes via an rRNA element, but the exact binding site of Nug1 remained unclear. To this end the newly established CRAC method (Granneman et al., 2009; Granneman et al., 2010) might help to identify rRNA-Nug1 contacts and thus could allow the identification of the ribosomal protein that interacts with Nug1.

The human homologue of Nug1 is called nucleostemin (NS) and was originally identified as a nucleolar factor enriched in stem cells and cancer cells (Cada et al., 2007; Tsai and McKay, 2002; Ye et al., 2008). NS is essential for cell proliferation and embryogenesis (Beekman et al., 2006; Zhu et al., 2006) and was shown to be involved in 60S biogenesis (Du et al., 2006; Romanova et al., 2009;

Rosby et al., 2009). Interestingly, it was observed that both overexpression and depletion of NS caused an increase in p53 protein levels (reviewed in Lo and Lu, 2010; Ma and Pederson, 2008). Elevated NS levels and subsequent relocation from the nucleolus to the nucleoplasm, leads to binding of NS to Mdm2 and thus to stabilization of p53. Conversely, depletion of NS, increased the free pool of ribosomal proteins and some of them like Rpl11 or Rpl5 in turn bind Mdm2. Because of these findings it has been proposed that NS might act as sensor for nucleolar stress (Lo and Lu, 2010), and thus is a potential molecular target for anti-cancer drug development (Lo and Lu, 2010). Therefore, a detailed understanding of Nucleostemin and Nug1 could stimulate the development of novel therapies for ribosomopathies and cancer.

4.3 Rea1, a Mechanoenzyme that Detaches Biogenesis Factors from Pre-60S Particles

By developing *in vitro* maturation assays, we demonstrated that the Rea1 ATPase acts at two subsequent steps in 60S ribosome biogenesis. First, Rea1 releases the Ytm1-Erb1-Nop7 subcomplex from nucleolar particles and subsequently, it detaches Rsa4 and the Rix1-Ipi3-Ipi1 subcomplex from nucleoplasmic particles. Thereby, the nucleolar step could be a prerequisite for progression of the pre-60S particle towards the nucleoplasm, whereas the subsequent nucleoplasmic step may pave the way for the recruitment of export factors to guide the particle to the cytoplasm.

In order to release Rsa4, Rea1 appears to bind simultaneously at two different sites on the pre-ribosome: the N-terminal ATPase ring binds in close proximity to the Rix1-Ipi3-Ipi1 subcomplex, and the C-terminal MIDAS domain contacts Rsa4. Thus, Rea1 could form a mechanochemical constellation where a conformational change within the ATPase domain creates a force to pull of Rsa4 (see Figures 8, and 9). Since the Rsa4 MIDO and the Ytm1 MIDO are homologous to each other and both interact with Rea1 via a conserved glutamate residue, it is feasible that Rea1 forms a similar mechanochemical constellation on nucleolar pre-ribosomes using Ytm1 as a docking site.

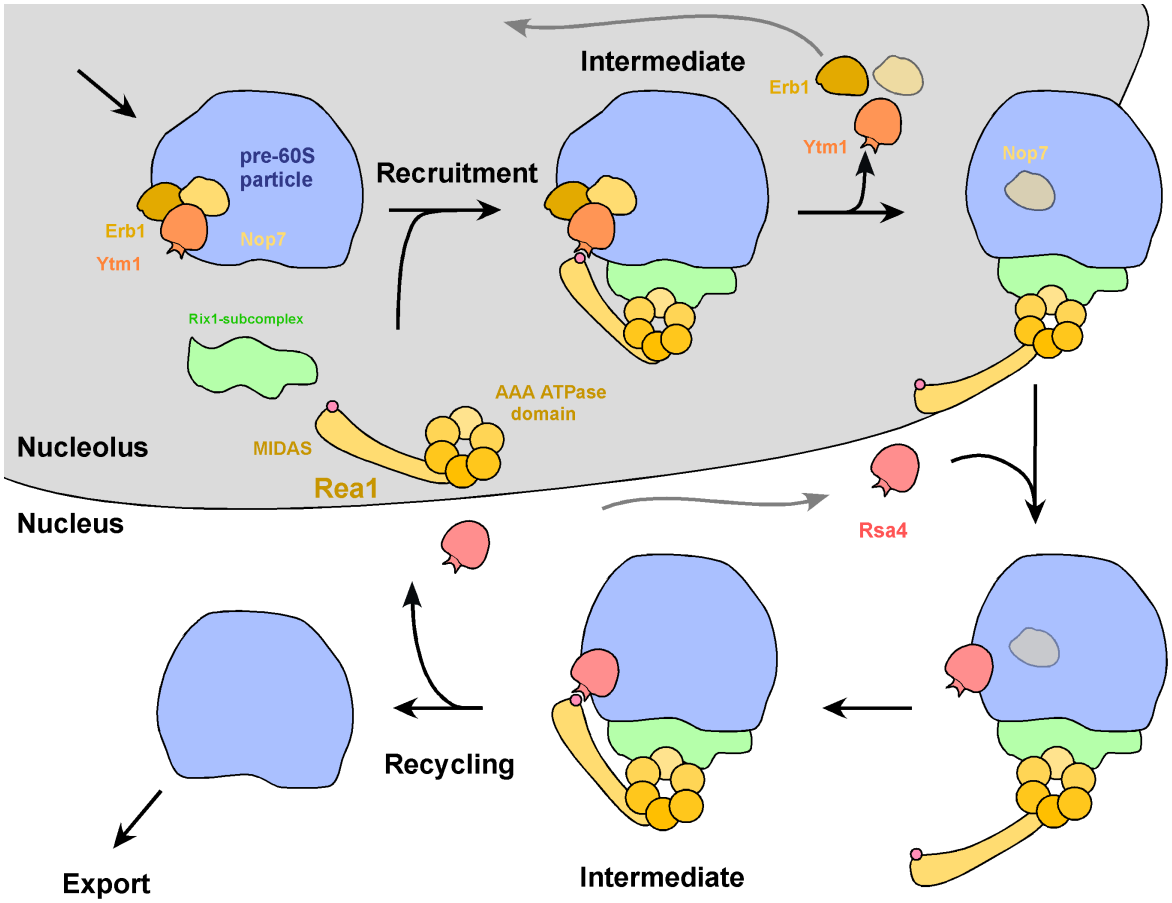

Figure 9. Working model of how Rea1 functions repeatedly as a mechanoenzyme to remove non-ribosomal factors from pre-60S particles (see text).

The direct binding partner(s) of the Rea1 ATPase ring domain remain elusive. The elevated levels of Rea1 in TAP purifications of either Rix1, Ipi3 or Ipi1 and the close neighbourhood on the pre-ribosomal particle, suggests that the Rix1-Ipi3-Ipi1 subcomplex acts as an adaptor complex for the ATPase ring domain. In line with that assumption, I uncovered that the release reaction of Ytm1 was only possible by using a substrate particle that contained the Rix1-Ipi3-Ipi1 subcomplex. Thus, the Rix1-Ipi3-Ipi1 subcomplex is a good candidate to serve as an adaptor for Rea1. This adaptor complex might also be responsible for the recruitment of the Rea1 ATPase. Alternatively, Rea1 could first be recruited via the MIDAS domain to Ytm1. To date, it remains unclear, whether Rea1 is repeatedly recruited and dissociated during the release reactions or whether it stays associated after the release of Ytm1 to be released later together with Rsa4.

It is likely that the force that drives the release reaction is created by conformational changes within the ATPase ring domain of Rea1. However, the

molecular basis of this force generation remains unclear. Bioinformatic analysis suggested that only the AAA ATPase domains 2, 3, 4 and 5 are active (Garbarino and Gibbons, 2002). Thereby, ATP loading, ATP hydrolysis and/or ADP release could induce the conformational change. Moreover, these reactions may occur in parallel or in a stepwise manner. In order to clarify these questions, we will perform a systematic site-specific mutagenesis analysis of the AAA domains. The analysis of these mutations should enable us to answer some of the open questions and reveal additional details of the Rea1-mediated release of biogenesis factors.

In order to achieve an effective release reaction, Rea1 needs to be concomitantly attached at both sites of the pre-ribosome. Thus, the Rea1-mediated power stroke should not be initiated prior to the correct attachment on both sites. In this scenario, binding of the N-terminal ATPase domains to the pre-ribosome might be a prerequisite for ATP-hydrolysis. Subsequent complex formation between MIDAS and MIDO may create a conformational change, which is then transmitted via the linker domain to the ATPase domains to initiate the release reaction. A comparable mechanism has been observed within the integrin receptor: the MIDAS domain changes from a closed conformation to an open state upon ligand binding and the according conformational change is then relayed to the opposite site of the receptor. Such a mechanism allows the communication between cytoplasm and the extracellular space via the integrin receptor (reviewed in Arnaout et al., 2005; Luo et al., 2007; Zhu et al., 2008). Analogously, also the Rea1 MIDAS might also adopt two different conformations, which allow Rea1 to sense for ligand binding.

In order to detach Rsa4 and Ytm1 from pre-ribosomal particles, the Rea1 MIDAS domains has to bind the MIDO domain with a high affinity. However, a tight interaction between MIDAS and MIDO needs to be disrupted, after the release reaction has occurred. Remarkably, it has been reported that the interaction between the MIDAS domain of integrin with its ligand is stabilized upon mechanical force (Astrof et al., 2006; Craig et al., 2004). Thus, the affinity of the Rea1 MIDAS to the MIDO of Rsa4 and Ytm1, respectively, could increase during the Rea1 power stroke to enable the release reaction. After detachment of Rsa4 or

Ytm1 the mechanical force decreases, which could cause a decline in affinity that would finally allow the disruption of the MIDAS-MIDO interaction.

Our studies demonstrated that the ATPase Rea1 and its interacting partners form a specific mechanochemical constellation that is used to remove biogenesis factors from nascent pre-ribosomal particles. To understand the mechanism of the Rea1 power stroke and its regulation, future studies are required to identify the direct binding partners of the ATPase domain, and to determine the structural properties of the ATPase-ring and the MIDAS domain in their different conformations. Rea1, Rsa4 and Ytm1 are evolutionary conserved from yeast to human, suggesting that the Rea1 mediated biogenesis step occurs in all eukaryotes. Thus, unravelling the function of Rea1 will encourage the general understanding of ribosome biogenesis in eukaryotes and its linkage to other cellular processes and diseases.

5. Acknowledgements

This work is dedicated to my family – Christine, Jonas, Benedikt & Maya.

At first place I would like to thank my mentor Prof. Dr. E. Hurt for continuous help and support during the course of this work. Further I like to acknowledge the people that contributed experiments, data and ideas to this project. Therefore special thanks to Martina Kallas, Cornelia Ulbrich, Meikel Diepholz, Bettina Böttcher, Brigitte Pertschy, Dieter Kressler, Paola Grandi, Tracy Nissan and many others.
Finally, I'm grateful for financial support by the Deutsche Forschungsgemeinschaft (DFG Sachbeihilfe HU363/10 01.04. 2003 – 31.03.2013)

6. List of Publication

6.1 Publications Related to the Topic of the Habilitation

6.1.1 Original Articles with First Authorship

- **Baßler**, Grandi, Gadal, Leßmann, Tollervey, Lechner and Hurt. (2001) Identification of a 60S pre-ribosomal particle that is closely linked to nuclear export. **Mol Cell** *8*, 645-656.
  (13,156)

- **Baßler**, Kallas and Hurt. (2006) The pre-ribosomal Nug1 factor reveals a central GTPase domain and an N-terminal RNA binding domain that mediates association with pre-60S subunits. **J Biol Chem** *281*, 24737-24744. (5,581)

- Ulbrich*, Diepholz*, **Baßler***, Kressler, Pertschy, Galani, Böttcher, and Hurt. (2009) A Mechanochemical Removal of Biogenesis Factors from Nascent 60S Ribosomal Subunits. **Cell** *138*, 911-922 . (29,887)
  * geteilte Coautorenschaft

- **Baßler**, Kallas, Pertschy, Ulbrich, Thoms and Hurt. (2010) The AAA-ATPase Rea1 drives removal of biogenesis factors during multiple stages of 60S ribosome assembly. **Mol Cell** *38*, 712-721 (13,156)

6.1.2 Original Articles with Coauthorship

- Sträßer, **Baßler** and Hurt. (2000) Binding of the Mex67p/Mtr2p heterodimer to FXFG, GLFG and FG repeat nucleoporins is essential for nuclear mRNA export. **J. Cell Biol** *150*, 695-706. (9,598)

- Grandi, Rybin, **Baßler**, Petfalski, Strauss, Marzioch, Schäfer, Kuster, Tschochner, Tollervey, Gavin and Hurt. (2002) 90S Pre-Ribosomes include the 35S Pre-rRNA, the U3 snoRNP, and 40S Subunit Processing Factors but predominately lack 60S Synthesis Factors. **Mol Cell** *10*, 1-20. (13,156)

- Nissan, **Baßler**, Petfalski, Tollervey and Hurt. (2002) The biochemistry of 60S pre-ribosome formation viewed from assembly in the nucleolus until export to the cytoplasm. **EMBO *21 (20)*** 5539-5547**.** (8,662)

- Milkereit, Strauß, **Baßler**, Gadal, Kühn, Schütz, Gas, Lechner, Hurt and Tschochner. (2003) A Noc-complex specifically involved in maturation and nuclear export of ribosomal 40S subunits. **J Biol Chem**. 278(6):4072-81. (5,581)

- Bradatsch, Katahira, Kowalinski, Bange, Yao, Sekimoto, Baumgartel, Boese, **Baßler**, Wild, Peters, Yoneda, Sinning and Hurt. (2007) Arx1 functions as an unorthodox nuclear export receptor for the 60S preribosomal subunit. **Mol Cell** *27*, 767-779. (13,156)

- Yao, Roser, Köhler, Bradatsch, **Baßler**, and Hurt. (2007) Nuclear export of ribosomal 60S subunits by the general mRNA export receptor Mex67-Mtr2. **Mol Cell** *26*, 51-62. (13,156)

6.1.3 Review Article

- Kressler, Hurt, **Baßler**. (2009) Driving ribosome assembly. **Biochim Biophys Acta**. Biochim Biophys Acta. Jun;1803(6):673-683. Epub 2009 Oct 30.

6.2 Publications not Related to the Topic of the Habilitation

- Saracino, **Baßler**, Muzzini, Hurt and Agostoni Carbone. (2004) The yeast kinase Swe1 is required for proper entry into cell cycle after arrest due to ribosome biogenesis and protein synthesis defects. **Cell Cycle**. (5):648-54 (3,314)

- Kispal, Sipos, Lange, Fekete, Bedekovics, Janaky, **Baßler**, Aguilar Netz, Balk, Rotte and Lill. (2005) Biogenesis of cytosolic ribosomes requires the essential iron-sulphur protein Rli1p and mitochondria. **EMBO J**.;24(3):589-98. (8,662)

- Beck, Sun, Adolf, Rutz, **Baßler**, Wild, Sinning, Hurt, Brügger, Bethune and Wieland. (2008). Membrane curvature induced by Arf1-GTP is essential for vesicle formation. **Proc Natl Acad Sci USA** *105*, 11731-11736. (9,598)

7. References

Anand, B., Verma, S.K., and Prakash, B. (2006). Structural stabilization of GTP-binding domains in circularly permuted GTPases: implications for RNA binding. Nucleic Acids Res *34*, 2196-2205.

Ansel, K.M., Pastor, W.A., Rath, N., Lapan, A.D., Glasmacher, E., Wolf, C., Smith, L.C., Papadopoulou, N., Lamperti, E.D., Tahiliani, M.*, et al.* (2008). Mouse Eri1 interacts with the ribosome and catalyzes 5.8S rRNA processing. Nat Struct Mol Biol *15*, 523-530.

Arabi, A., Wu, S., Ridderstrale, K., Bierhoff, H., Shiue, C., Fatyol, K., Fahlen, S., Hydbring, P., Soderberg, O., Grummt, I.*, et al.* (2005). c-Myc associates with ribosomal DNA and activates RNA polymerase I transcription. Nat Cell Biol *7*, 303-310.

Arnaout, M.A., Mahalingam, B., and Xiong, J.P. (2005). Integrin structure, allostery, and bidirectional signaling. Annu Rev Cell Dev Biol *21*, 381-410.

Astrof, N.S., Salas, A., Shimaoka, M., Chen, J., and Springer, T.A. (2006). Importance of force linkage in mechanochemistry of adhesion receptors. Biochemistry *45*, 15020-15028.

Bassler, J., Grandi, P., Gadal, O., Leßmann, T., Tollervey, D., Lechner, J., and Hurt, E.C. (2001). Identification of a 60S pre-ribosomal particle that is closely linked to nuclear export. Mol. Cell *8*, 517-529.

Bassler, J., Kallas, M., and Hurt, E. (2006). The Nug1 GTPase reveals and N-terminal RNA-binding domain that is essential for association with 60 S pre-ribosomal particles. J Biol Chem *281*, 24737-24744.

Bassler, J., Kallas, M., Ulbrich, C., Thoms, M., Pertschy.B., and Hurt, E. (2010). The AAA-ATPase Rea1 drives removal of biogenesis factors during multiple stages of 60S ribosome assembly. Mol. Cell *38*, 712-721.

Beekman, C., Nichane, M., De Clercq, S., Maetens, M., Floss, T., Wurst, W., Bellefroid, E., and Marine, J.C. (2006). Evolutionarily conserved role of nucleostemin: controlling proliferation of stem/progenitor cells during early vertebrate development. Mol Cell Biol *26*, 9291-9301.

Bleichert, F., and Baserga, S.J. (2007). The long unwinding road of RNA helicases. Mol Cell *27*, 339-352.

Bohnsack, M.T., Kos, M., and Tollervey, D. (2008). Quantitative analysis of snoRNA association with pre-ribosomes and release of snR30 by Rok1 helicase. EMBO Rep *9*, 1230-1236.

Bohnsack, M.T., Martin, R., Granneman, S., Ruprecht, M., Schleiff, E., and Tollervey, D. (2009). Prp43 bound at different sites on the Pre-rRNA performs distinct functions in ribosome synthesis. Mol Cell *36*, 583-592.

Bradatsch, B., Katahira, J., Kowalinski, E., Bange, G., Yao, W., Sekimoto, T., Baumgartel, V., Boese, G., Bassler, J., Wild, K.*, et al.* (2007). Arx1 functions as an unorthodox nuclear export receptor for the 60S preribosomal subunit. Mol Cell *27*, 767-779.

Cada, Z., Boucek, J., Dvorankova, B., Chovanec, M., Plzak, J., Kodets, R., Betka, J., Pinot, G.L., Gabius, H.J., and Smetana, K., Jr. (2007). Nucleostemin expression in squamous cell carcinoma of the head and neck. Anticancer Res *27*, 3279-3284.

Chook, Y.M., and Blobel, G. (2001). Karyopherins and nuclear import. Curr Opin Struct Biol *11*, 703-715.

Cordin, O., Banroques, J., Tanner, N.K., and Linder, P. (2006). The DEAD-box protein family of RNA helicases. Gene *367*, 17-37.

Craig, D., Gao, M., Schulten, K., and Vogel, V. (2004). Structural insights into how the MIDAS ion stabilizes integrin binding to an RGD peptide under force. Structure *12*, 2049-2058.

Dai, M.S., and Lu, H. (2008). Crosstalk between c-Myc and ribosome in ribosomal biogenesis and cancer. J Cell Biochem *105*, 670-677.

de la Cruz, J., Kressler, D., and Linder, P. (2004). Ribosomal subunit assembly. In The Nucleolus, M.O.J. Olson, ed. (Georgetown, Texas: Landes Bioscience/Eurekah.com), pp. 258-285.

De la Cruz, J., Sanz-Martinez, E., and Remacha, M. (2005). The essential WD-repeat protein Rsa4p is required for rRNA processing and intra-nuclear transport of 60S ribosomal subunits. Nucleic Acids Res *33*, 5728-5739.

Demoinet, E., Jacquier, A., Lutfalla, G., and Fromont-Racine, M. (2007). The Hsp40 chaperone Jjj1 is required for the nucleo-cytoplasmic recycling of preribosomal factors in Saccharomyces cerevisiae. RNA *13*, 1570-1581.

Dez, C., Froment, C., Noaillac-Depeyre, J., Monsarrat, B., Caizergues-Ferrer, M., and Henry, Y. (2004). Npa1p, a component of very early pre-60S ribosomal particles, associates with a subset of small nucleolar RNPs required for peptidyl transferase center modification. Mol Cell Biol *24*, 6324-6337.

Dong, J., Lai, R., Jennings, J.L., Link, A.J., and Hinnebusch, A.G. (2005). The novel ATP-binding cassette protein ARB1 is a shuttling factor that stimulates 40S and 60S ribosome biogenesis. Mol Cell Biol *25*, 9859-9873.

Dragon, F., Gallagher, J.E., Compagnone-Post, P.A., Mitchell, B.M., Porwancher, K.A., Wehner, K.A., Wormsley, S., Settlage, R.E., Shabanowitz, J., Osheim, Y.*, et*

al. (2002). A large nucleolar U3 ribonucleoprotein required for 18S ribosomal RNA biogenesis. Nature *417*, 967-970.

Du, X., Rao, M.R., Chen, X.Q., Wu, W., Mahalingam, S., and Balasundaram, D. (2006). The homologous putative GTPases Grn1p from fission yeast and the human GNL3L are required for growth and play a role in processing of nucleolar pre-rRNA. Mol Biol Cell *17*, 460-474.

Erzberger, J.P., and Berger, J.M. (2006). Evolutionary relationships and structural mechanisms of AAA+ proteins. Annu Rev Biophys Biomol Struct *35*, 93-114.

Fatica, A., Cronshaw, A.D., M., D., and Tollervey, D. (2002). Ssf1p prevents premature processing of an early pre-60S ribosomal particle. Mol. Cell *9*, 341-351.

Fatica, A., Oeffinger, M., Dlakic, M., and Tollervey, D. (2003). Nob1p is required for cleavage of the 3' end of 18S rRNA. Mol Cell Biol *23*, 1798-1807.

Fatica, A., Tollervey, D., and Dlakic, M. (2004). PIN domain of Nob1p is required for D-site cleavage in 20S pre-rRNA. Rna *10*, 1698-1701.

Ferreira-Cerca, S., Poll, G., Gleizes, P.E., Tschochner, H., and Milkereit, P. (2005). Roles of Eukaryotic Ribosomal Proteins in Maturation and Transport of Pre-18S rRNA and Ribosome Function. Mol Cell *20*, 263-275.

Freed, E.F., Bleichert, F., Dutca, L.M., and Baserga, S.J. (2010). When ribosomes go bad: diseases of ribosome biogenesis. Mol Biosyst *6*, 481-493.

Fried, H., and Kutay, U. (2003). Nucleocytoplasmic transport: taking an inventory. Cell Mol Life Sci *60*, 1659-1688.

Fromont-Racine, M., Senger, B., Saveanu, C., and Fasiolo, F. (2003). Ribosome assembly in eukaryotes. Gene *313*, 17-42.

Fumagalli, S., Di Cara, A., Neb-Gulati, A., Natt, F., Schwemberger, S., Hall, J., Babcock, G.F., Bernardi, R., Pandolfi, P.P., and Thomas, G. (2009). Absence of nucleolar disruption after impairment of 40S ribosome biogenesis reveals an rpL11-translation-dependent mechanism of p53 induction. Nat Cell Biol *11*, 501-508.

Gabel, H.W., and Ruvkun, G. (2008). The exonuclease ERI-1 has a conserved dual role in 5.8S rRNA processing and RNAi. Nat Struct Mol Biol *15*, 531-533.

Gadal, O., Strauss, D., Kessl, J., Trumpower, B., Tollervey, D., and Hurt, E. (2001). Nuclear export of 60S ribosomal subunits depends on Xpo1p and requires a NES-containing factor Nmd3p that associates with the large subunit protein Rpl10p. Mol. Cell. Biol. *21*, 3405-3415.

Galani, K., Nissan, T.A., Petfalski, E., Tollervey, D., and Hurt, E. (2004). Rea1, a Dynein-related Nuclear AAA-ATPase, Is Involved in Late rRNA Processing and Nuclear Export of 60 S Subunits. J Biol Chem *279*, 55411-55418.

Ganapathi, K.A., and Shimamura, A. (2008). Ribosomal dysfunction and inherited marrow failure. Br J Haematol *141*, 376-387.

Garbarino, J.E., and Gibbons, I.R. (2002). Expression and genomic analysis of midasin, a novel and highly conserved AAA protein distantly related to dynein. BMC Genomics *3*, 18-28.

Gelperin, D., Horton, L., Beckman, J., Hensold, J., and Lemmon, S.K. (2001). Bms1p, a novel GTP-binding protein, and the related Tsr1p are required for distinct steps of 40S ribosome biogenesis in yeast. RNA *7*, 1268-1283.

Gomez-Roman, N., Felton-Edkins, Z.A., Kenneth, N.S., Goodfellow, S.J., Athineos, D., Zhang, J., Ramsbottom, B.A., Innes, F., Kantidakis, T., Kerr, E.R.*, et al.* (2006). Activation by c-Myc of transcription by RNA polymerases I, II and III. Biochem Soc Symp, 141-154.

Gomez-Roman, N., Grandori, C., Eisenman, R.N., and White, R.J. (2003). Direct activation of RNA polymerase III transcription by c-Myc. Nature *421*, 290-294.

Grandi, P., Rybin, V., Bassler, J., Petfalski, E., Strauss, D., Marzioch, M., Schäfer, T., Kuster, B., Tschochner, H., Tollervey, D.*, et al.* (2002). 90S pre-ribosomes include the 35S pre-rRNA, the U3 snoRNP, and 40S subunit processing factors but predominantly lack 60S synthesis factors. Mol. Cell *10*, 105-115.

Grandori, C., Gomez-Roman, N., Felton-Edkins, Z.A., Ngouenet, C., Galloway, D.A., Eisenman, R.N., and White, R.J. (2005). c-Myc binds to human ribosomal DNA and stimulates transcription of rRNA genes by RNA polymerase I. Nat Cell Biol *7*, 311-318.

Granneman, S., and Baserga, S.J. (2004). Ribosome biogenesis: of knobs and RNA processing. Exp Cell Res *296*, 43-50.

Granneman, S., Kudla, G., Petfalski, E., and Tollervey, D. (2009). Identification of protein binding sites on U3 snoRNA and pre-rRNA by UV cross-linking and high-throughput analysis of cDNAs. Proc Natl Acad Sci U S A *106*, 9613-9618.

Granneman, S., Nandineni, M.R., and Baserga, S.J. (2005). The putative NTPase Fap7 mediates cytoplasmic 20S pre-rRNA processing through a direct interaction with Rps14. Mol Cell Biol *25*, 10352-10364.

Granneman, S., Petfalski, E., Swiatkowska, A., and Tollervey, D. (2010). Cracking pre-40S ribosomal subunit structure by systematic analyses of RNA-protein cross-linking. EMBO J.

Grewal, S.S., Li, L., Orian, A., Eisenman, R.N., and Edgar, B.A. (2005). Myc-dependent regulation of ribosomal RNA synthesis during Drosophila development. Nat Cell Biol *7*, 295-302.

Hanson, P.I., and Whiteheart, S.W. (2005). AAA+ proteins: have engine, will work. Nat Rev Mol Cell Biol *6*, 519-529.

Hedges, J., Chen, Y.I., West, M., Bussiere, C., and Johnson, A.W. (2006). Mapping the functional domains of yeast NMD3, the nuclear export adapter for the 60 S ribosomal subunit. J Biol Chem *281*, 36579-36587.

Hedges, J., West, M., and Johnson, A.W. (2005). Release of the export adapter, Nmd3p, from the 60S ribosomal subunit requires Rpl10p and the cytoplasmic GTPase Lsg1p. Embo J *24*, 567-579.

Henras, A.K., Dez, C., and Henry, Y. (2004). RNA structure and function in C/D and H/ACA s(no)RNPs. Curr Opin Struct Biol *14*, 335-343.

Henras, A.K., Soudet, J., Gerus, M., Lebaron, S., Caizergues-Ferrer, M., Mougin, A., and Henry, Y. (2008). The post-transcriptional steps of eukaryotic ribosome biogenesis. Cell Mol Life Sci *65*, 2334-2359.

Ho, J.H.N., Kallstrom, G., and Johnson, A.W. (2000). Nmd3p is a Crm1p-dependent adapter protein for nuclear export of the large ribosomal subunit. J.Cell Biol. *151*, 1057-1066.

Hung, N.J., and Johnson, A.W. (2006). Nuclear recycling of the pre-60S ribosomal subunit-associated factor Arx1 depends on Rei1 in Saccharomyces cerevisiae. Mol Cell Biol *26*, 3718-3727.

Hung, N.J., Lo, K.Y., Patel, S.S., Helmke, K., and Johnson, A.W. (2008). Arx1 is a nuclear export receptor for the 60S ribosomal subunit in yeast. Mol Biol Cell *19*, 735-744.

Hurt, E., Hannus, S., Schmelzl, B., Lau, D., Tollervey, D., and Simos, G. (1999). A Novel In Vivo Assay Reveals Inhibition of Ribosomal Nuclear Export in Ran-Cycle and Nucleoporin Mutants. J. Cell Biol. *144*, 389-401.

Jankowsky, E., and Bowers, H. (2006). Remodeling of ribonucleoprotein complexes with DExH/D RNA helicases. Nucleic Acids Res *34*, 4181-4188.

Jankowsky, E., and Fairman, M.E. (2007). RNA helicases--one fold for many functions. Curr Opin Struct Biol *17*, 316-324.

Karbstein, K. (2007). Role of GTPases in ribosome assembly. Biopolymers *87*, 1-11.

Karbstein, K., and Doudna, J.A. (2006). GTP-dependent formation of a ribonucleoprotein subcomplex required for ribosome biogenesis. J Mol Biol *356*, 432-443.

Karbstein, K., Jonas, S., and Doudna, J.A. (2005). An essential GTPase promotes assembly of preribosomal RNA processing complexes. Mol Cell *20*, 633-643.

Kemmler, S., Occhipinti, L., Veisu, M., and Panse, G.V. (2009). Yvh1 is required for a late maturation step in the 60S biogenesis pathway. . J. Cell Biol. *186*.

Kim do, J., Jang, J.Y., Yoon, H.J., and Suh, S.W. (2008). Crystal structure of YlqF, a circularly permuted GTPase: implications for its GTPase activation in 50 S ribosomal subunit assembly. Proteins *72*, 1363-1370.

Kos, M., and Tollervey, D. (2005). The Putative RNA Helicase Dbp4p Is Required for Release of the U14 snoRNA from Preribosomes in Saccharomyces cerevisiae. Mol Cell *20*, 53-64.

Kos, M., and Tollervey, D. (2010). Yeast pre-rRNA processing and modification occur cotranscriptionally. Mol Cell *37*, 809-820.

Kressler, D., Hurt, E., and Bassler, J. (2010). Driving ribosome assembly. Biochim Biophys Acta *1803*, 673-683.

Kressler, D., Roser, D., Pertschy, B., and Hurt, E. (2008). The AAA ATPase Rix7 powers progression of ribosome biogenesis by stripping Nsa1 from pre-60S particles. J Cell Biol *181*, 935-944.

Krogan, N.J., Peng, W.T., Cagney, G., Robinson, M.D., Haw, R., Zhong, G., Guo, X., Zhang, X., Canadien, V., Richards, D.P.*, et al.* (2004). High-definition macromolecular composition of yeast RNA-processing complexes. Mol Cell *13*, 225-239.

Lafontaine, D.L., and Tollervey, D. (2001). The function and synthesis of ribosomes. Nat Rev Mol Cell Biol *2*, 514-520.

Lamanna, A.C., and Karbstein, K. (2009). Nob1 binds the single-stranded cleavage site D at the 3'-end of 18S rRNA with its PIN domain. Proc Natl Acad Sci U S A *106*, 14259-14264.

Lebreton, A., Saveanu, C., Decourty, L., Rain, J.C., Jacquier, A., and Fromont-Racine, M. (2006). A functional network involved in the recycling of nucleocytoplasmic pre-60S factors. J Cell Biol *173*, 349-360.

Leger-Silvestre, I., Milkereit, P., Ferreira-Cerca, S., Saveanu, C., Rousselle, J.C., Choesmel, V., Guinefoleau, C., Gas, N., and Gleizes, P.E. (2004). The ribosomal protein Rps15p is required for nuclear exit of the 40S subunit precursors in yeast. Embo J *23*, 2336-2347.

Leipe, D.D., Wolf, Y.I., Koonin, E.V., and Aravind, L. (2002). Classification and evolution of P-loop GTPases and related ATPases. J Mol Biol *317*, 41-72.

Liang, X.H., and Fournier, M.J. (2006). The helicase Has1p is required for snoRNA release from pre-rRNA. Mol Cell Biol *26*, 7437-7450.

Linder, P., and Lasko, P. (2006). Bent out of shape: RNA unwinding by the DEAD-box helicase Vasa. Cell *125*, 219-221.

Lo, D., and Lu, H. (2010). Nucleostemin: Another nucleolar "Twister" of the p53-MDM2 loop. Cell Cycle *9*.

Lo, K.-Y., Li, Z., Wang, F., Marcotte, E., and Johnson, A.W. (2009). Ribosome stalk assembly requires the dual specificity phosphatase Yvh1 for the exchange of Mrt4 with P0. J. Cell Biol. *186*.

Lo, K.Y., Li, Z., Bussiere, C., Bresson, S., Marcotte, E.M., and Johnson, A.W. (2010). Defining the pathway of cytoplasmic maturation of the 60S ribosomal subunit. Mol Cell *39*, 196-208.

Luo, B.H., Carman, C.V., and Springer, T.A. (2007). Structural basis of integrin regulation and signaling. Annu Rev Immunol *25*, 619-647.

Luz, J.S., Georg, R.C., Gomes, C.H., Machado-Santelli, G.M., and Oliveira, C.C. (2009). Sdo1p, the yeast orthologue of Shwachman-Bodian-Diamond syndrome protein, binds RNA and interacts with nuclear rRNA-processing factors. Yeast *26*, 287-298.

Ma, H., and Pederson, T. (2008). Nucleostemin: a multiplex regulator of cell-cycle progression. Trends Cell Biol *18*, 575-579.

Martin, D.E., Powers, T., and Hall, M.N. (2006). Regulation of ribosome biogenesis: where is TOR? Cell Metab *4*, 259-260.

Matsuo, Y., Morimoto, T., Kuwano, M., Loh, P.C., Oshima, T., and Ogasawara, N. (2006). The GTP-binding protein YlqF participates in the late step of 50 S ribosomal subunit assembly in Bacillus subtilis. J Biol Chem *281*, 8110-8117.

Matsuo, Y., Oshima, T., Loh, P.C., Morimoto, T., and Ogasawara, N. (2007). Isolation and characterization of a dominant negative mutant of Bacillus subtilis GTP-binding protein, YlqF, essential for biogenesis and maintenance of the 50 S ribosomal subunit. J Biol Chem *282*, 25270-25277.

Mayer, C., and Grummt, I. (2006). Ribosome biogenesis and cell growth: mTOR coordinates transcription by all three classes of nuclear RNA polymerases. Oncogene *25*, 6384-6391.

Menne, T.F., Goyenechea, B., Sanchez-Puig, N., Wong, C.C., Tonkin, L.M., Ancliff, P.J., Brost, R.L., Costanzo, M., Boone, C., and Warren, A.J. (2007). The Shwachman-Bodian-Diamond syndrome protein mediates translational activation of ribosomes in yeast. Nat Genet *39*, 486-495.

Meyer, A.E., Hung, N.J., Yang, P., Johnson, A.W., and Craig, E.A. (2007). The specialized cytosolic J-protein, Jjj1, functions in 60S ribosomal subunit biogenesis. Proc Natl Acad Sci U S A *104*, 1558-1563.

Miles, T.D., Jakovljevic, J., Horsey, E.W., Harnpicharnchai, P., Tang, L., and Woolford, J.L., Jr. (2005). Ytm1, Nop7, and Erb1 form a complex necessary for maturation of yeast 66S preribosomes. Mol Cell Biol *25*, 10419-10432.

Milkereit, P., Gadal, O., Podtelejnikov, A., Trumtel, S., Gas, N., Petfalski, E., Tollervey, D., Mann, M., Hurt, E., and Tschochner, H. (2001). Maturation of Pre-Ribosomes Requires Noc-Proteins and is Coupled to Transport from the Nucleolus to the Nucleoplasm. Cell *105*, 499-509.

Moss, T., Langlois, F., Gagnon-Kugler, T., and Stefanovsky, V. (2007). A housekeeper with power of attorney: the rRNA genes in ribosome biogenesis. Cell Mol Life Sci *64*, 29-49.

Moy, T.I., and Silver, P.A. (1999). Nuclear export of the small ribosomal subunit requires the Ran-GTPase cycle and certain nucleoporins. Genes Dev. *13*, 2118-2133.

Moy, T.I., and Silver, P.A. (2002). Requirements for the nuclear export of the small ribosomal subunit. J. Cell Sci. *115*, 2985-2995.

Nissan, T.A., Bassler, J., Petfalski, E., Tollervey, D., and Hurt, E.C. (2002). 60S pre-ribosome formation viewed from assembly in the nucleolus until export to the cytoplasm. EMBO. J. *21*, 5539-5547.

Nissan, T.A., Galani, K., Maco, B., Tollervey, D., Aebi, U., and Hurt, E. (2004). A pre-ribosome with a tadpole-like structure functions in ATP-dependent maturation of 60S subunits. Mol Cell *15*, 295-301.

Ogura, T., and Wilkinson, A.J. (2001). AAA+ superfamily ATPases: common structure--diverse function. Genes Cells *6*, 575-597.

Osheim, Y.N., French, S.L., Keck, K.M., Champion, E.A., Spasov, K., Dragon, F., Baserga, S.J., and Beyer, A.L. (2004). Pre-18S ribosomal RNA is structurally compacted into the SSU processome prior to being cleaved from nascent transcripts in Saccharomyces cerevisiae. Mol Cell *16*, 943-954.

Panse, V.G., and Johnson, A.W. (2010). Maturation of eukaryotic ribosomes: acquisition of functionality. Trends Biochem Sci *35*, 260-266.

Perez-Fernandez, J., Roman, A., De Las Rivas, J., Bustelo, X.R., and Dosil, M. (2007). The 90S preribosome is a multimodular structure that is assembled through a hierarchical mechanism. Mol Cell Biol *27*, 5414-5429.

Pertschy, B., Saveanu, C., Zisser, G., Lebreton, A., Tengg, M., Jacquier, A., Liebminger, E., Nobis, B., Kappel, L., van der Klei, I.*, et al.* (2007). Cytoplasmic recycling of 60S preribosomal factors depends on the AAA protein Drg1. Mol Cell Biol *27*, 6581-6592.

Pertschy, B., Schneider, C., Gnädig, M., Schäfer, T., Tollervey, D., and Hurt, E. (2009). RNA helicase Prp43 and its co-factor Pfa1 promote 20S to 18S rRNA processing catalyzed by the endonuclease Nob1. J Biol Chem *284*, 35079-35091.

Puig, O., Caspary, F., Rigaut, G., Rutz, B., Bouveret, E., Bragado-Nilsson, E., Wilm, M., and Seraphin, B. (2001). The tandem affinity purification (TAP) method: a general procedure of protein complex purification. Methods *24*, 218-229.

Raychaudhuri, P., Stringer, E.A., Valenzuela, D.M., and Maitra, U. (1984). Ribosomal subunit antiassociation activity in rabbit reticulocyte lysates. Evidence for a low molecular weight ribosomal subunit antiassociation protein factor (Mr = 25,000). J Biol Chem *259*, 11930-11935.

Ribbeck, K., and Gorlich, D. (2001). Kinetic analysis of translocation through nuclear pore complexes. Embo J *20*, 1320-1330.

Rodriguez-Mateos, M., Abia, D., Garcia-Gomez, J.J., Morreale, A., de la Cruz, J., Santos, C., Remacha, M., and Ballesta, J.P. (2009a). The amino terminal domain from Mrt4 protein can functionally replace the RNA binding domain of the ribosomal P0 protein. Nucleic Acids Res *37*, 3514-3521.

Rodriguez-Mateos, M., Garcia-Gomez, J.J., Francisco-Velilla, R., Remacha, M., de la Cruz, J., and Ballesta, J.P. (2009b). Role and dynamics of the ribosomal protein P0 and its related trans-acting factor Mrt4 during ribosome assembly in Saccharomyces cerevisiae. Nucleic Acids Res *37*, 7519-7532.

Romanova, L., Grand, A., Zhang, L., Rayner, S., Katoku-Kikyo, N., Kellner, S., and Kikyo, N. (2009). Critical role of nucleostemin in pre-rRNA processing. J Biol Chem *284*, 4968-4977.

Rosby, R., Cui, Z., Rogers, E., deLivron, M.A., Robinson, V.L., and DiMario, P.J. (2009). Knockdown of the Drosophila GTPase nucleostemin 1 impairs large ribosomal subunit biogenesis, cell growth, and midgut precursor cell maintenance. Mol Biol Cell *20*, 4424-4434.

Rudra, D., and Warner, J.R. (2004). What better measure than ribosome synthesis? Genes Dev *18*, 2431-2436.

Sahasranaman, A., Jakovljevic, J., Strahler, J., Andrews, P., Maddock, J.R., and Woolford, J.L. (2009). A functional cluster of assembly factors regulate the exonuclease Rat1 to create precise 5´ends of 5.8S rRNA and is necessary for construction of the polypeptide tunnel. Oral presentation at the 8th Conference on Ribosome Synthesis, Regensburg, Germany.

Saveanu, C., Bienvenu, D., Namane, A., Gleizes, P.E., Gas, N., Jacquier, A., and Fromont-Racine, M. (2001). Nog2p, a putative GTPase associated with pre-60S subunits and required for late 60S maturation steps. EMBO J. *20*, 6475-6484.

Saveanu, C., Namane, A., Gleizes, P.E., Lebreton, A., Rousselle, J.C., Noaillac-Depeyre, J., Gas, N., Jacquier, A., and Fromont-Racine, M. (2003). Sequential

protein association with nascent 60S ribosomal particles. Mol Cell Biol *23*, 4449-4460.

Schäfer, T., Maco, B., Petfalski, E., Tollervey, D., Bottcher, B., Aebi, U., and Hurt, E. (2006). Hrr25-dependent phosphorylation state regulates organization of the pre-40S subunit. Nature *441*, 651-655.

Schäfer, T., Strauss, D., Petfalski, E., Tollervey, D., and Hurt, E.C. (2003). The path from nucleolar 90S to cytoplasmic 40S pre-ribosomes. EMBO J. *22*, 1370-1380.

Seiser, R.M., Sundberg, A.E., Wollam, B.J., Zobel-Thropp, P., Baldwin, K., Spector, M.D., and Lycan, D.E. (2006). Ltv1 is required for efficient nuclear export of the ribosomal small subunit in Saccharomyces cerevisiae. Genetics *174*, 679-691.

Senger, B., Lafontaine, D.L.J., Graindorge, J.-S., Gadal, O., Camasses, A., Sanni, A., GarnierJ.-M., Breitenbach, M., Hurt, E.C., and Fasiolo, F. (2001). The nucle(ol)ar Tif6p and Efl1p, a novel EF-2 like GTPase, are required for a late cytoplasmic step of ribosome synthesis. Mol. Cell *8*, 1363-1373.

SenGupta, D.J., Zhang, B., Kraemer, B., Pochart, P., Fields, S., and Wickens, M. (1996). A three-hybrid system to detect RNA-protein interactions in vivo. Proc Natl Acad Sci U S A *93*, 8496-8501.

Sengupta, J., Bussiere, C., Pallesen, J., West, M., Johnson, A.W., and Frank, J. (2010). Characterization of the nuclear export adaptor protein Nmd3 in association with the 60S ribosomal subunit. J Cell Biol *189*, 1079-1086.

Srivastava, L., Lapik, Y.R., Wang, M., and Pestov, D.G. (2010). Mammalian DEAD box protein Ddx51 acts in 3' end maturation of 28S rRNA by promoting the release of U8 snoRNA. Mol Cell Biol *30*, 2947-2956.

Steitz, T.A. (2008). A structural understanding of the dynamic ribosome machine. Nat Rev Mol Cell Biol *9*, 242-253.

Strässer, K., Bassler, J., and Hurt, E.C. (2000). Binding of the Mex67p/Mtr2p heterodimer to FXFG, GLFG, and FG repeat nucleoporins is essential for nuclear mRNA export. J. Cell Biol. *150*, 695-706.

Strunk, B.S., and Karbstein, K. (2009). Powering through ribosome assembly. RNA *15*, 2083-2104.

Sun, X.X., Wang, Y.G., Xirodimas, D.P., and Dai, M.S. (2010). Perturbation of 60 S ribosomal biogenesis results in ribosomal protein L5- and L11-dependent p53 activation. J Biol Chem *285*, 25812-25821.

Tang, L., Sahasranaman, A., Jakovljevic, J., Schleifman, E., and Woolford, J.L., Jr. (2008). Interactions among Ytm1, Erb1, and Nop7 required for assembly of the Nop7-subcomplex in yeast preribosomes. Mol Biol Cell *19*, 2844-2856.

Thomas, F., and Kutay, U. (2003). Biogenesis and nuclear export of ribosomal subunits in higher eukaryotes depend on the CRM1 export pathway. J. Cell Sci. *116*, 2409-2419.

Thomson, E., and Tollervey, D. (2010). The final step in 5.8S rRNA processing is cytoplasmic in Saccharomyces cerevisiae. Mol Cell Biol *30*, 976-984.

Trotta, C.R., Lund, E., Kahan, L., Johnson, A.W., and Dahlberg, J.E. (2003). Coordinated nuclear export of 60S ribosomal subunits and NMD3 in vertebrates. EMBO J. *22*, 2841-2851.

Tsai, R.Y., and McKay, R.D. (2002). A nucleolar mechanism controlling cell proliferation in stem cells and cancer cells. Genes Dev *16*, 2991-3003.

Tschochner, H., and Hurt, E. (2003). Pre-ribosomes on the road from the nucleolus to the cytoplasm. Trends Cell Biol. *13*, 255-263.

Uicker, W.C., Schaefer, L., and Britton, R.A. (2006). The essential GTPase RbgA (YlqF) is required for 50S ribosome assembly in Bacillus subtilis. Mol Microbiol *59*, 528-540.

Ulbrich, C., Diepholz, M., Bassler, J., Kressler, D., Pertschy.B., K., G., Böttcher, B., and Hurt, E. (2009). Mechanochemical Removal of Ribosome Biogenesis Factors from Nascent 60S Ribosomal Subunit. Cell *138*, 911-922.

Vale, R.D. (2000). AAA proteins: lords of the ring. J. Cell. Biol. *150*, 13-19.

Vanrobays, E., Gelugne, J.P., Gleizes, P.E., and Caizergues-Ferrer, M. (2003). Late cytoplasmic maturation of the small ribosomal subunit requires RIO proteins in Saccharomyces cerevisiae. Mol Cell Biol *23*, 2083-2095.

Vanrobays, E., Leplus, A., Osheim, Y.N., Beyer, A.L., Wacheul, L., and Lafontaine, D.L. (2008). TOR regulates the subcellular distribution of DIM2, a KH domain protein required for cotranscriptional ribosome assembly and pre-40S ribosome export. RNA *14*, 2061-2073.

Venema, J., and Tollervey, D. (1999). Ribosome synthesis in Saccharomyces cerevisiae. Annu.Rev.Genet. *33*, 261-311.

Warner, J.R. (1999). The economics of ribosome biosynthesis in yeast. Trends Biochem.Sci. *24*, 437-440.

Wegierski, T., Billy, E., Nasr, F., and Filipowicz, W. (2001). Bms1p, a G-domain-containing protein, associates with Rcl1p and is required for 18S rRNA biogenesis in yeast. RNA *7*, 1254-1267.

West, M., Hedges, J.B., Chen, A., and Johnson, A.W. (2005). Defining the order in which Nmd3p and Rpl10p load onto nascent 60S ribosomal subunits. Mol Cell Biol *25*, 3802-3813.

Yao, W., Roser, D., Kohler, A., Bradatsch, B., Bassler, J., and Hurt, E. (2007). Nuclear export of ribosomal 60S subunits by the general mRNA export receptor Mex67-Mtr2. Mol Cell *26*, 51-62.

Yao, Y., Demoinet, E., Saveanu, C., Lenormand, P., Jacquier, A., and Fromont-Racine, M. (2010). Ecm1 is a new pre-ribosomal factor involved in pre-60S particle export. RNA *16*, 1007-1017.

Yarunin, A., Panse, V.G., Petfalski, E., Dez, C., Tollervey, D., and Hurt, E.C. (2005). Functional link between ribosome formation and biogenesis of iron-sulfur proteins. Embo J *24*, 580-588.

Ye, F., Zhou, C., Cheng, Q., Shen, J., and Chen, H. (2008). Stem-cell-abundant proteins Nanog, Nucleostemin and Musashi1 are highly expressed in malignant cervical epithelial cells. BMC Cancer *8*, 108.

Zaher, H.S., and Green, R. (2009). Fidelity at the molecular level: lessons from protein synthesis. Cell *136*, 746-762.

Zemp, I., Wild, T., O'Donohue, M.F., Wandrey, F., Widmann, B., Gleizes, P.E., and Kutay, U. (2009). Distinct cytoplasmic maturation steps of 40S ribosomal subunit precursors require hRio2. J Cell Biol *185*, 1167-1180.

Zhang, J., Harnpicharnchai, P., Jakovljevic, J., Tang, L., Guo, Y., Oeffinger, M., Rout, M.P., Hiley, S.L., Hughes, T., and Woolford, J.L., Jr. (2007). Assembly factors Rpf2 and Rrs1 recruit 5S rRNA and ribosomal proteins rpL5 and rpL11 into nascent ribosomes. Genes Dev *21*, 2580-2592.

Zhu, J., Luo, B.H., Xiao, T., Zhang, C., Nishida, N., and Springer, T.A. (2008). Structure of a complete integrin ectodomain in a physiologic resting state and activation and deactivation by applied forces. Mol Cell *32*, 849-861.

Zhu, Q., Yasumoto, H., and Tsai, R.Y. (2006). Nucleostemin delays cellular senescence and negatively regulates TRF1 protein stability. Mol Cell Biol *26*, 9279-9290.

8. Copies of the Summarized Publications

(Including supplemental material and associated comments)

- **Baßler**, Grandi, Gadal, Leßmann, Tollervey, Lechner and Hurt. (2001) Identification of a 60S pre-ribosomal particle that is closely linked to nuclear export. **Mol Cell** *8*, 645-656.
  (13,156)

  Minireview: Warner JR. (2001) Nascent ribosomes. **Cell**. 107(2):133-6.

- **Baßler**, Kallas and Hurt. (2006) The pre-ribosomal Nug1 factor reveals a central GTPase domain and an N-terminal RNA binding domain that mediates association with pre-60S subunits. **J Biol Chem** *281*, 24737-24744. (5,581)

- Ulbrich*, Diepholz*, **Baßler***, Kressler, Pertschy, Galani, Böttcher, and Hurt. (2009) A Mechanochemical Removal of Biogenesis Factors from Nascent 60S Ribosomal Subunits. **Cell** *138*, 911-922
  (29,887)
  * geteilte Coautorenschaft

  Preview: Talkish J, Woolford JL Jr. (2009) The Rea1 tadpole loses its tail. Cell. 2009; 138(5):832-4.

- **Baßler**, Kallas, Pertschy, Ulbrich, Thoms and Hurt. (2010) The AAA-ATPase Rea1 drives removal of biogenesis factors during multiple stages of 60S ribosome assembly. **Mol Cell** *38*, 712-721 (13,156)

Molecular Cell, Vol. 8, 517–529, September, 2001, Copyright ©2001 by Cell Press

Identification of a 60S Preribosomal Particle that Is Closely Linked to Nuclear Export

Jochen Baßler,[1] Paola Grandi,[2] Olivier Gadal,[3] Torben Leßmann,[1] Elisabeth Petfalski,[1] David Tollervey,[4] Johannes Lechner,[5] and Ed Hurt[1,6]

[1] Biochemie-Zentrum Heidelberg
Im Neuenheimer Feld 328
69120 Heidelberg
[2] Cellzome GmbH
Meyerhofstrasse 1
69117 Heidelberg
Germany
[3] Institut Pasteur
25-28, Rue du Docteur Roux
75724 Paris Cedex 15
France
[4] Institute of Cell and Molecular Biology
University of Edinburgh
EH9 3JR Edinburgh
United Kingdom
[5] Mass Spectrometry Unit
Biochemie-Zentrum Heidelberg
69120 Heidelberg
Germany

Summary

A nuclear GTPase, Nug1p, was identified in a genetic screen for components linked to 60S ribosomal subunit export. Nug1p cosedimented with nuclear 60S preribosomes and was required for subunit export to the cytoplasm. Tagged Nug1p coprecipitated with proteins of the 60S subunit, late precursors to the 25S and 5.8S rRNAs, and at least 21 nonribosomal proteins. These included a homologous nuclear GTPase, Nug2p, the Noc2p/Noc3p heterodimer, Rix1p, and Rlp7p, each of which was implicated in 60S subunit export. Other known ribosome synthesis factors and proteins of previously unknown function, including the 559 kDa protein Ylr106p, also copurified. Eight of these proteins were copurified with nuclear pore complexes, suggesting that this complex represents the transport intermediate for 60S subunit export.

Introduction

The synthesis of the eukaryotic ribosome is a complex process which occurs mainly in the nucleolus; however, late maturation steps are thought to take place in the nucleoplasm and in the cytoplasm following nuclear export. Ribosome biogenesis begins with the transcription of the 35S and 5S pre-rRNAs, followed by rRNA processing and base modification to yield the mature 25S/28S, 18S, 5.8S, and 5S rRNA. Analyses in the yeast *Saccharomyces cerevisiae* have identified over 60 *trans*-acting factors, including rRNA modifying enzymes, endonucleases, exonucleases, RNA helicases, and proteins associated with the small nucleolar RNAs (snoRNAs) required for production of the mature 60S and 40S ribosomal subunits (for review see Kressler et al., 1999; Venema and Tollervey, 1999).

During transcription and processing, about 80 ribosomal proteins and many nonribosomal proteins assemble onto the pre-rRNAs, forming the preribosomal particles. These are not distinct species but dynamic structures, changing location and composition during ribosome biogenesis. However, little is known about the factors involved in maturation and transport of preribosomes within the nucleus and their subsequent export through the nuclear pores into the cytoplasm. To address this, in vivo assays have been developed in *S. cerevisiae* to study ribosomal export (Hurt et al., 1999; Moy and Silver, 1999). These analyses demonstrated that a subset of the nucleoporins and the Ran system are required for both large and small subunit export.

To identify factors involved in the export of the large ribosomal subunit, a bank of randomly generated ts mutants was screened for a ribosomal export defect. In the screen based on nuclear accumulation of Rpl25p-eGFP, several *RIX* (ribosomal export) components were identified (Gadal et al., 2001a, 2001b; Milkereit et al., 2001). One of these factors, *RIX5*, is allelic to the *RPL10* gene, which encodes the large subunit protein Rpl10p. Subsequent data showed that Nmd3p, which interacts with Rpl10p, acts as a NES-containing adaptor protein for Xpo1p-mediated nuclear export of 60S subunits (Ho et al., 2000; Gadal et al., 2001b). However, with the identification of Rpl10p, Nmd3p, and Xpo1p, the inventory of potential *cis*- and *trans*-acting factors during 60S ribosomal export is only at its beginning. Indeed, the genetic screen for *rix* mutants already yielded several further components required for intranuclear transport and export of 60S ribosomal subunits (e.g., Rix3p/Noc2p, Noc3p, and Noc1p; Milkereit et al., 2001) or late maturation of 60S subunits (e.g., Rix7p, an intranuclear AAA-type ATPase; Gadal et al., 2001a).

Here, we report a different approach to isolate factors involved in 60S subunit export. We identified a mutation in Mtr2p (*mtr2-33*), which impaired 60S subunit export in contrast to previously reported *mtr2* mutations that inhibited mRNA export (Kadowaki et al., 1994; Santos-Rosa et al., 1998). Genetic analysis of the *mtr2-33* allele led to the identification of two components, Ecm1p and Nug1p, that also function in 60S subunit export. Nug1p and its closely related homolog Nug2p belong to a previously uncharacterized family of conserved nuclear/nucleolar GTPases. Nug1p and Nug2p are associated with 60S preribosomes, and use of TAP-tagged Nug1p allowed the purification of a preribosomal particle. This contained large subunit proteins (L proteins) and at least 21 nonribosomal proteins including several Rix proteins, suggesting that it represents a late intermediate in 60S subunit assembly and export.

Results

An *mtr2* Allele with a Defect in Ribosomal Export Leads to the Identification of *ECM1*

Mtr2p is an essential mRNA export factor, which performs its function as part of a heterodimeric complex

[6] Correspondence: cg5@ix.urz.uni-heidelberg.de

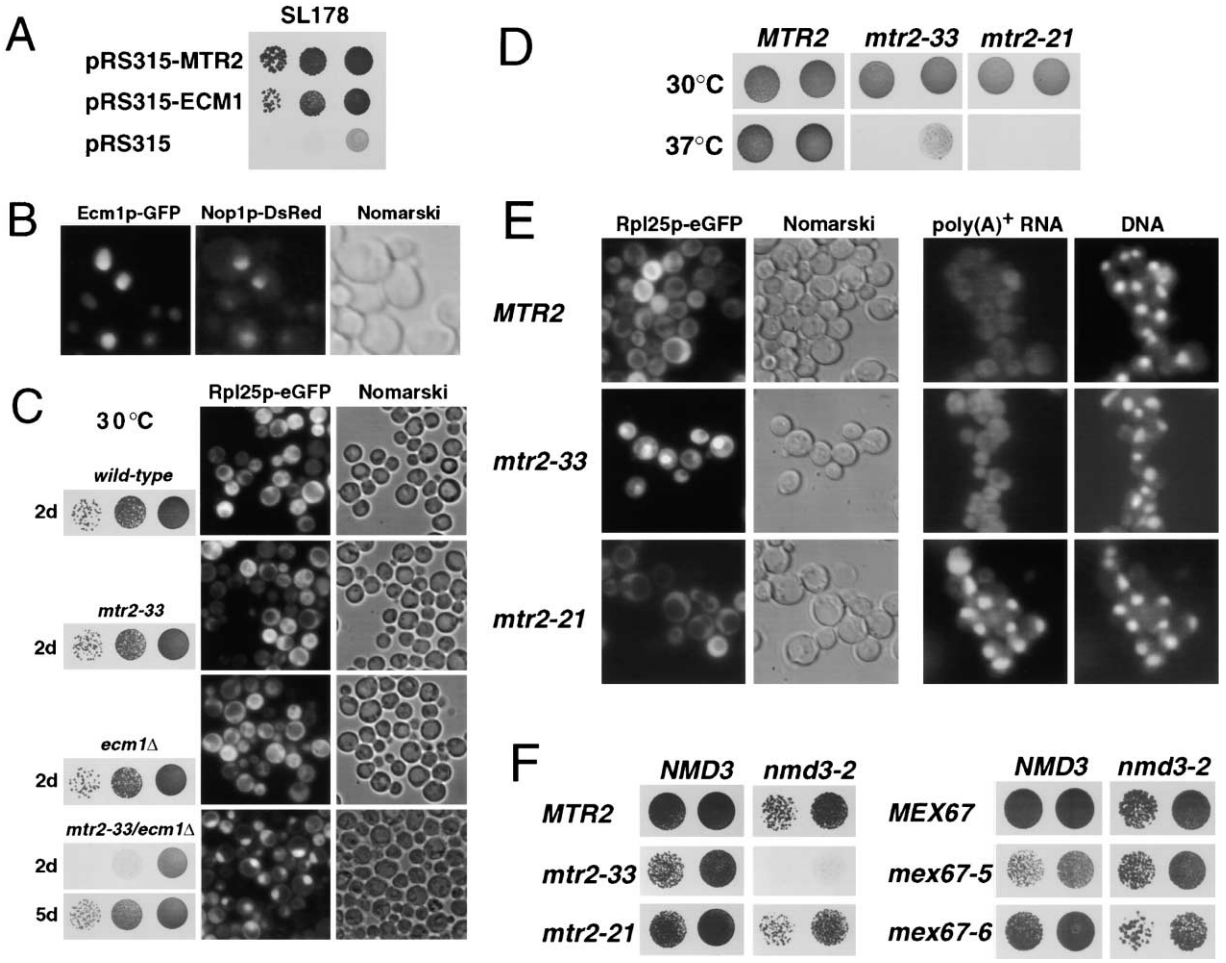

Figure 1. The *mtr2-33* Allele Exhibits a Functional Link to *ECM1*

(A) SL178 was transformed with plasmid pRS315-LEU2-MTR2, pRS315-LEU2-ECM1, or pRS315-LEU2. The synthetic lethal relationship was tested by spotting transformants on 5-FOA containing plates in 10^{-1} dilution steps. It was incubated for 6 days at 23°C. The screening strain and the sl mutant contained plasmids pHT4467-URA3-ADE3-MTR2 and pRS314-TRP1-mtr2-33.

(B) Ecm1p tagged with GFP localizes to the nucleus and nucleolus. The *ecm1*Δ strain was cotransformed with pRS315-ECM1-GFP and pRS314-NOP1-DsRed, and transformants were analyzed by fluorescence microscopy.

(C) A viable *mtr2-33*/*ecm1*Δ progeny is impaired in 60S subunit export. Left panel: the *MTR2* shuffle/*ecm1*Δ strain was transformed with the indicated *MTR2* and *ECM1* alleles, before transformants were spotted on 5-FOA containing plates. It was incubated at 30°C for 2 or 5 days. Right panel: the indicated strains were transformed with pRS316-RPL25eGFP, and 60S subunit export was analyzed at 30°C.

(D) Growth properties of *MTR2*, *mtr2-33*, and *mtr2-21* strains, incubated for 2 days at indicated temperature.

(E) 60S subunit export but not poly(A)$^+$ RNA export is impaired in *mtr2-33* cells at the restrictive temperature. The indicated strains were shifted for 1 hr to 37°C to analyze 60S subunit export (Rpl25p-eGFP) and 3 hr to 37°C to analyze poly(A)$^+$ RNA export. DNA was stained with DAPI.

(F) *mtr2-33* is functionally linked to *NMD3*. *NMD3*/*MTR2* or *NMD3*/*MEX67* double shuffle strains were transformed with the indicated plasmid-linked wild-type and mutant alleles. The synthetic lethal relationship was tested by spotting transformants on 5-FOA containing plates. It was incubated for 3 days at 30°C.

with Mex67p (Santos-Rosa et al., 1998). Most mutant alleles of *MTR2* are impaired in nuclear mRNA export (Santos-Rosa et al., 1998). However, *mtr2-33* (E106G, R109G) does not exhibit nuclear accumulation of poly(A)$^+$ RNA at the restrictive temperature (see below). To determine whether *mtr2-33* is impaired in another cellular pathway, we performed a synthetic lethal (sl) screen with this allele based on a red/white colony sectoring assay (see Experimental Procedures). Mutant SL178 was obtained from this screen, which forms red colonies on YPD (data not shown) and cannot grow on 5-FOA plates (Figure 1A). The wild-type allele of the gene causing synthetic lethality with *mtr2-33* in SL178 was cloned by complementation and shown to be *ECM1* (Figure 1A).

The genetic relation was also confirmed by generation of a haploid *ecm1*Δ/*mtr2* shuffle strain (Figure 1C). Combination of *mtr2-33* with the *ecm1* deletion resulted in a extremely slow-growing phenotype. These data show that the functions of Mtr2p and Ecm1p are genetically closely related. *ECM1*, which is not essential for cell growth (see below), was previously identified in a screen for mutants defective in cell wall biogenesis (Lussier et al., 1997); however, we were not able to reproduce this finding.

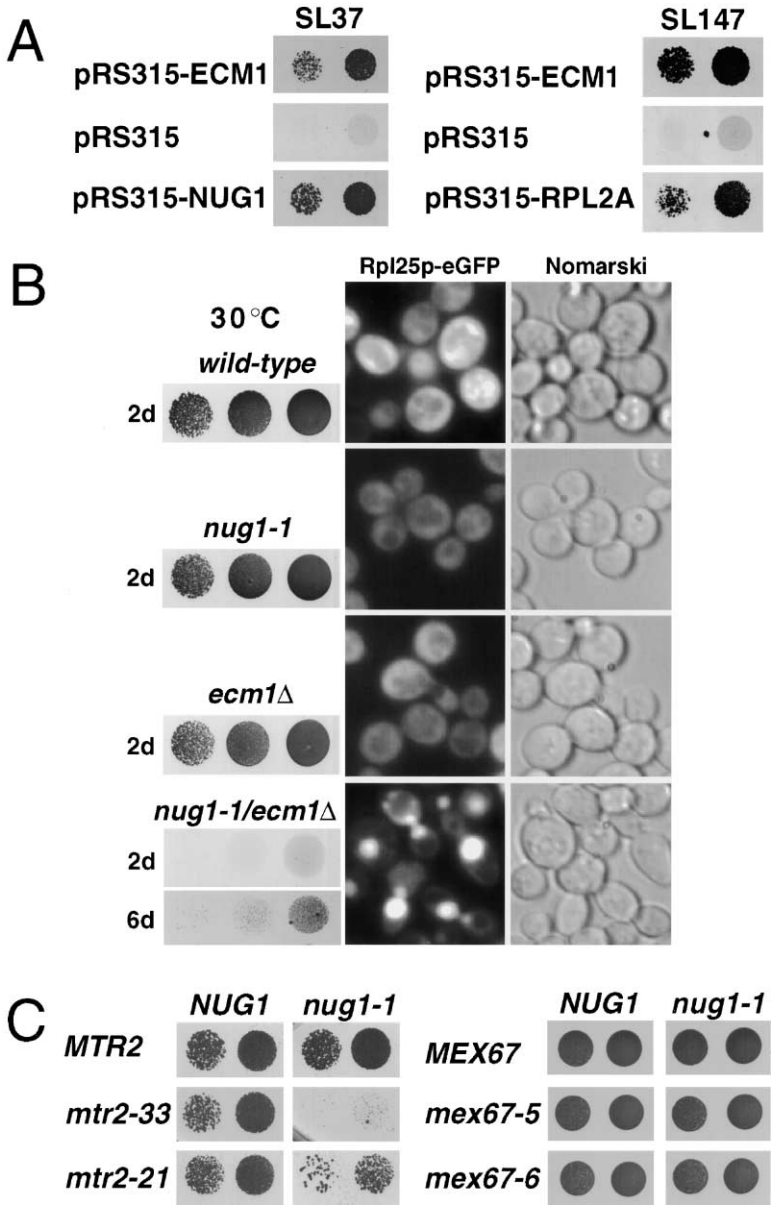

Figure 2. Identification of *NUG1*

(A) Isolation of *NUG1* and *RPL2A* in a synthetic lethal screen with the *ecm1*Δ allele. SL37 was transformed with pRS315-ECM1, empty pRS315, or pRS315-NUG1 (*YER006w*). SL147 was transformed with pRS315-ECM1, empty pRS315, or pRS315-RPL2A. Transformants were spotted in steps of 10^{-1} dilution on 5-FOA containing plates and incubated for 5 days at 30°C. Both sl mutants contained plasmid pHT4467Δ-URA3-ADE3-ECM1.

(B) Inhibition of 60S subunit export in the *nug1-1/ecm1*Δ double mutant. Left panel: a *NUG1*shuffle/*ecm1*Δ strain was transformed with the indicated plasmids. A synthetic lethal relationship was tested by spotting transformants on 5-FOA containing plates. It was incubated at 30°C for 2 or 6 days. Right panel: the indicated strains were transformed with pRS316-RPL25-eGFP, and analysis of 60S subunit export was performed at 30°C.

(C) Genetic interaction between *nug1-1* and *mtr2-33*. *NUG1/MTR2* or *NUG1/MEX67* double shuffle strains were transformed with the indicated plasmid-linked wild-type and mutant alleles, before transformants were spotted onto 5-FOA containing SDC-plates. It was incubated for 3 days at 30°C.

Ecm1p tagged with GFP is located in the nucleus, with a mild enrichment in the nucleolus (Figure 1B). This nucleolar localization prompted us to test if Ecm1p, together with Mtr2p, plays a role in nuclear export of ribosomes. Indeed, 60S subunit export is strongly impaired in the slow-growing *mtr2-33/ecm1*Δ double mutant but not in the single *ecm1*Δ or *mtr2-33* mutants when grown at 30°C (Figure 1C).

Moreover, the *mtr2-33* mutation causes accumulation of the large subunit reporter Rlp25p-eGFP inside the nucleus, when shifted to the restrictive temperature (Figure 1E; 37°C). In contrast, the *mtr2-21* mutant is defective in mRNA export but not in 60S subunit export (Figure 1E). Further evidence for a specific linkage of *MTR2* to the ribosome export machinery is the observation that *mtr2-33* but not *mtr2-21* is synthetically lethal with a *nmd3* mutant allele (Figure 1F). Nmd3p is a NES-containing adaptor protein for Xpo1p-mediated 60S subunit export (see Introduction). In contrast, *mex67* mutant alleles are not synergistically impaired when combined with the *nmd3-2* allele (Figure 1F). Taken all together, these data demonstrate that *MTR2* is linked in an allele-specific manner to ribosomal 60S subunit export and that this function of Mtr2p depends on Ecm1p.

Identification of Nug1p, a Nuclear Putative GTPase

As described above, Ecm1p plays a role in ribosomal export, but is not essential for this pathway. To identify the network of essential interaction partners of Ecm1p, we performed another synthetic lethal screen with the *ecm1*Δ allele and found two sl mutants (SL37 and SL147). SL147 is complemented by the gene encoding the ribosomal protein Rpl2Ap (Figure 2A). SL37 is complemented by *YER006w*, which encodes an essential protein that we termed Nug1p (for Nucle(ol)ar GTPase). Nug1p belongs to a large but previously uncharacterized

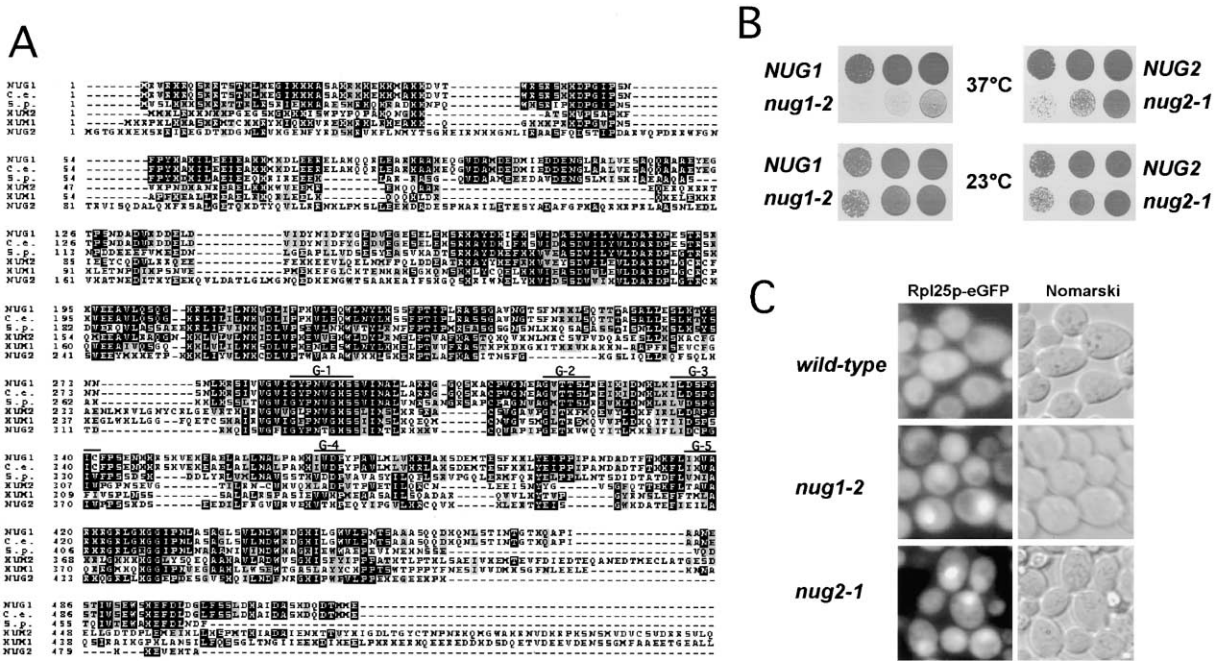

Figure 3. Temperature-Sensitive *nug1* and *nug2* Mutants Are Impaired in 60S Subunit Export

(A) Nug1p and Nug2p belong to a novel family of conserved GTPases. Multiple sequence alignment of Nug1p, Nug2p, and other homologs from human (HUM1, HUM2), *C. elegans* (C.e.), and *S. pombe* (S.p.) was done by ClustalW1.8. Conserved motifs G-1 > G-5, typically found in other GTPases (see Sprang, 1997), are indicated.

(B) Temperature-sensitive growth of *nug1-2* and *nug2-1* strains. Cells were spotted in 10^{-1} dilution steps on YPD plates and grown at the indicated temperatures.

(C) Inhibition of 60S subunit export in *nug1* and *nug2* ts mutants. Cells were shifted for 90 min (*nug1-2*) or 180 min (*nug2-1*) to 37°C, before nuclear accumulation of Rpl25p-eGFP was determined by fluorescence microscopy.

family of conserved putative GTPases and contains conserved nucleotide binding motifs G-1 to G-5, typically found in GTPases (see Figure 3A and Sprang, 1997).

In order to confirm the genetic interaction of *NUG1* with *ECM1* and possibly extend it to *MTR2*, the *nug1-1* allele was recovered from SL37. The *nug1-1* allele carries a single point mutation (R420P) that does not impair cell growth on its own in the tested temperature range from 23°C to 37°C. However, when *nug1-1* is combined with the *ecm1*Δ allele, a strong synergistic growth defect and a concomitant nuclear accumulation of the large subunit reporter Rpl25p-eGFP is observed (Figure 2B). Furthermore, *nug1-1* interacts genetically with *mtr2-33* but not with other *mtr2* or *mex67* ts alleles (Figure 2C). We conclude that Nug1p is involved in the nuclear export of 60S ribosomal subunits.

nug1 and *nug2* ts Mutants Are Impaired in 60S Subunit Export

A second ORF (*YNR053c*) in the yeast genome encodes another putative GTPase significantly homologous to Nug1p, which was designated Nug2p (Figure 3A). Since both *NUG1* and *NUG2* are essential (data not shown; see Table 1), they do not perform an identical function. To show a direct involvement of *NUG1* and *NUG2* in ribosomal export, ts mutants were generated (Figure 3B). Rpl25p-eGFP was efficiently exported in the *nug1-2* or *nug2-1* ts mutant strains grown at the permissive temperature. However, when *nug1-2* or *nug2-1* cells were shifted to the restrictive temperature, inhibition of 60S subunit export was observed (Figure 3C). Consistent with a large subunit export defect, *nug1* and *nug2* ts mutants exhibit a "half-mer" polysome phenotype and a decreased 60S to 40S subunit ratio on sucrose gradients when shifted to the restrictive temperature (Figure 4A). This shows that Nug1p and Nug2p are involved in the biogenesis of 60S but not in the production of 40S subunits.

Northern analysis of high molecular weight pre-rRNAs showed that the *nug1-2* and *nug2-1* alleles had little effect on processing (Figure 4B, left panel). Some accumulation of the 35S pre-rRNA and 23S RNA was seen, consistent with a mild inhibition of the early pre-rRNA cleavages at sites A_0, A_1, and A_2 on the 18S rRNA synthesis pathway. This was not, however, accompanied by any clear reduction in the mature 18S rRNA levels. Similar changes have been reported for almost all mutants with defects in the 60S subunit synthesis pathway, and these are very likely to be indirect effects (see Venema and Tollervey, 1999, for further discussion). In the *nug2-1* strain, some reduction in the 27SA and 27SB pre-rRNAs and the mature 25S rRNA was visible after transfer to 37°C, consistent with the polysome analysis. Little alteration in 25S synthesis was seen for the *nug1-2* strain.

Analysis of low molecular weight RNA (Figure 4B, right panel) showed some accumulation of intermediates between 7S and 6S in the *nug2-1* strain, suggesting that the normally high processivity of the exosome complex is mildly reduced. Moreover, the RNA species extending from site A_2 to site E (the 3′ end of the 5.8S rRNA), which

Table 1.

Protein	Band Number	RIX	Purification with NPCs	
Ribosomal L Proteins	1–24		Yes	Rpl1p (#14), Rpl2p (#17), Rpl3p (#24), Rpl4p (#21,22), Rpl5p (#18,19), Rpl6p (#10), Rpl7p (#14,15), Rpl8p (#17), Rpl9p (#11,13) Rpl11p (#9), Rpl12p (#8), Rpl13p (#14,15), Rpl14p (#5), Rpl15p (#11,12,15,16), Rpl16p (#11,12,13), Rpl18p (#11,12), Rpl19p (#13,14), Rpl20p (#9,10), Rpl21p (#9), Rpl25p (#6), Rpl26p (#5), Rpl27p (#6,7), Rpl28p (#7), Rpl31p (#4), Rpl32p (#5), Rpl33p (#3), Rpl35p (#5), Rpl36p (#2,3), Rpl38p (#1), Rpl39p (#1)
Nip7p	9			Null lethal, colocalized to both the cytoplasm and the nucleus, cosediments with free 60S ribosomal subunits, depletion causes accumulation of a 27S rRNA precursor, ts mutant accumulates halfmer-containing polysomes
Mrt4p	17			Null viable, mRNA turnover, required for an early step in mRNA decay
Kre32p	20		Yes	Null viable, localizes to the nucleus
Rlp7p	23	Rix9p		Null lethal, Ribosomal Like Protein required for the production of the large ribosomal subunit rRNAs. Cannot functionally substitue for ribosomal protein L7 (Rpl7Ap or Rpl7Bp)
YHR052w	25			Null lethal, unknown function
YNR053c	26	Nug2p	Yes	Null lethal, localizes to the nucleus
YCR072c	26			Null lethal, contains eight WD40 repeats
Has1p	27		Yes	Null lethal, localizes to the nuclear periphery and the nucleolus, has ATP/GTP-binding site motif A (P-loop), belongs to the DEAD box protein family of RNA helicases
YPL146c	28	Yes		Null lethal, localizes to the nucleolus and a portion of the nucleus
YDR101c	28			Null viable, unknown function
YER006w	29	Nug1p	Yes	Null lethal, localizes to the nucleus and the nucleolus, contains motifs typical of ATP/GTP-binding sites
Nog1p	30		Yes	Null lethal, localizes to the nucleus and the nucleolus, contains a GTP-binding domain
YGR103w	31		Yes	Null lethal, localizes to the nuclear rim, the nucleus and the nucleolus
Noc3p (YLR002c)	32	Noc3p		Null lethal, involved in nucleolar/nuclear transport of 60S preribosomal particle
Nop2	33			Null lethal, localizes to the nucleus and the nucleolus, required for pre-rRNA processing and 60S ribosome synthesis, has an ATP/GTP-binding site, some protein detected in cytoplasm, consistent with nuclear/cytosolic shuttling
YHR197w	33	Rix1p		Null lethal, localizes to the nucleoplasm
Noc2p (YOR206w)	33	Rix3p	Yes	Null lethal, localizes as crescent nucleolar and peripheral nuclear signals. Involved in nucleolar/nuclear transport of 60S preribosomal particle
Sda1p	34			Null lethal, localizes to the nucleus
Erb1p (YMR049c)	35,36			Null lethal, unknown function, may play a role in ribosome biogenesis
Spb1p	36			Null lethal, localizes to the nucleus and the nucleolus, involved in assembly of preribosomal particles in the biogenesis of the 60S ribosomal subunit
Dpb10p	37			Null lethal, DBP10 ''DEAD box protein,'' required for ribosome biogenesis, has ATP/GTP-binding site motif A (P loop), has N-terminal bipartite nuclear localization signal, localizes to the nucleus and enriched in the nucleolus
YLR106c	38			Null lethal, has multiple copies of ATP/GTP-binding site motif A (P loop)

Information in Table 1 was taken from YPD database (http://www.proteome.com/databases/index.html)

is a normal, minor species in the processing pathway, is lost, while the species from A_2 to C_2 (the 3′ end of the 7S pre-rRNA) was detected. Together, these data show that cleavage at site C_2 continues in the *nug2-1* strain, but digestion of the 7S pre-rRNA to the 6S pre-RNA by the exosome complex is partially inhibited.

Pulse-chase labeling of the *nug1-2* strain (Figure 4C) showed a delay in processing of the 35S pre-rRNA and delayed appearance of the 25S, 5.8S, and 18S rRNAs, consistent with results of Northern hybridization. However, rRNA synthesis remains robust, and the reduced incorporation is probably a consequence of the reduced growth rate of the mutant strain rather than a direct effect of processing inhibition.

The processing defects in the *nug1* and *nug2* mutant strains strongly support their direct involvement in ribosome synthesis. However, the mild phenotypes in the *nug1-2* and *nug2-1* mutant strains indicate that these alleles are not primarily defective in pre-rRNA cleavage. Nug1p and Nug2p are therefore likely to be directly involved in the correct assembly and/or transport of 60S ribosomal subunits.

Intranuclear Nug1p and Nug2p Associate with Preribosomal Particles

To test this model, we sought to determine the intracellular location of Nug1p and Nug2p and their association with preribosomal particles. GFP-tagged Nug1p or Nug2p

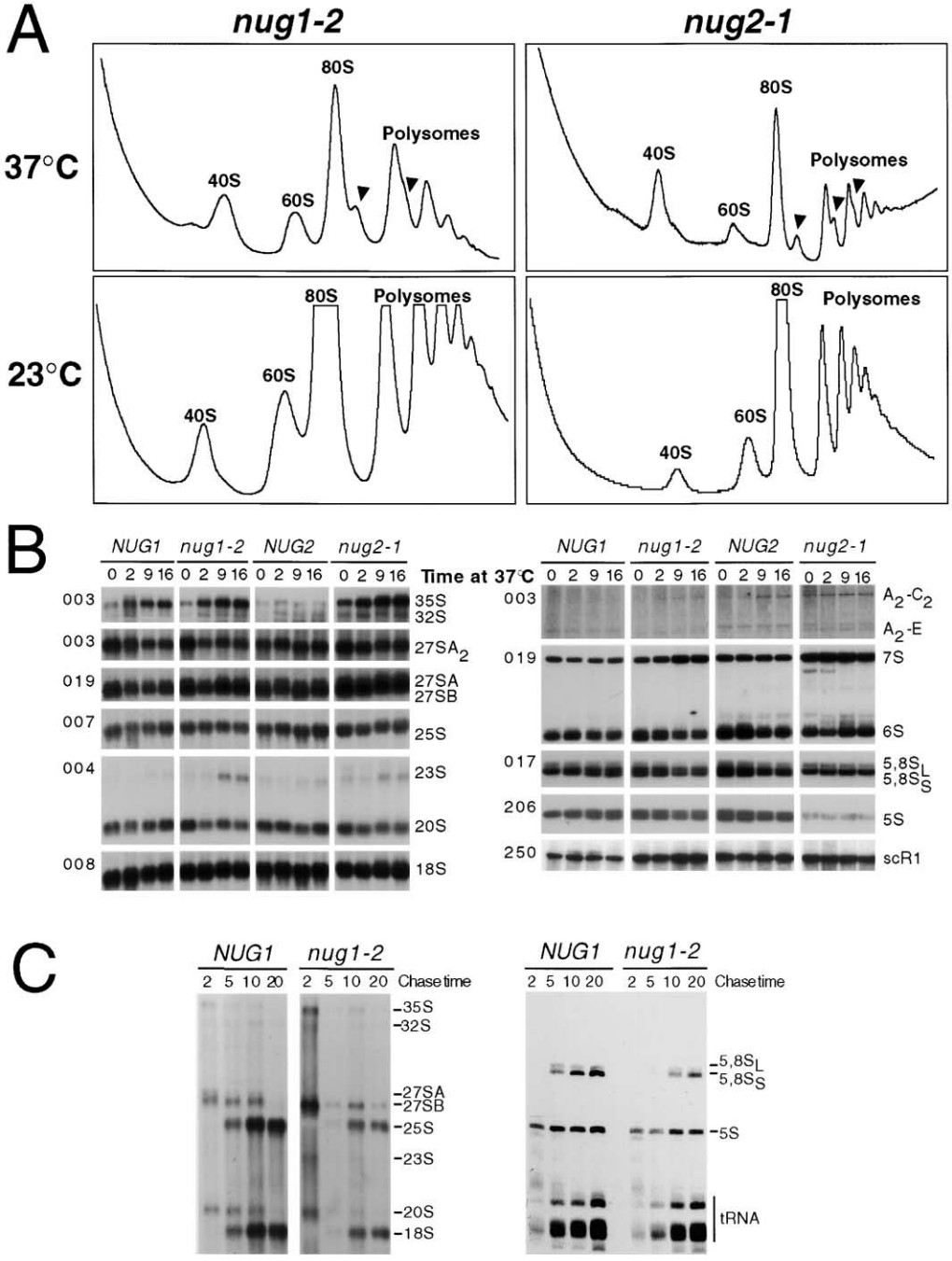

Figure 4. *nug1* and *nug2* ts Mutants Have Reduced Amounts of 60S Subunits but Are Only Slightly Impaired in rRNA Processing

(A) Analysis of polysomal ribosome fractions derived from *nug1-2* and *nug2-1* ts strains, grown at 23°C or shifted for 3 hr to 37°C. The UV profiles (OD_{260nm}) of the sucrose gradient are depicted, and "half-mer" polysomes (polysomes containing an unjoined 40S subunit at the initiation site) are indicated by arrow heads.

(B) Northern analysis of pre-rRNA and rRNA levels in the *nug1* and *nug2* mutant strains. RNA was extracted from strains grown at 23°C (0 time points) or after transfer to 37°C, separated on an agarose/formaldehyde gel (left panel) or a 6% polyacrylamide gel (right panel), and transferred for Northern hybridization. Oligos used are indicated on the left; RNA species detected are labeled on the right. The cytoplasmic scR1 (SRP) RNA was used as a loading control.

(C) Pulse-chase analysis. *NUG1* and *nug1-2* strains were shifted to 37°C for 2 hr, pulse-labeled with [^{3}H]uracil for 1 min, followed by the addition of excess cold uracil for 2, 5, 10, and 20 min. Total RNA was extracted, separated on 1.2% agarose-formaldehyde (upper panel) or 7% polyacrylamide-8 M urea gels (lower panel), transferred to a Nylon membrane, and visualized by fluorography. The 2 min time point for the *nug1-2* strain on the upper panel was probably mildly overloaded.

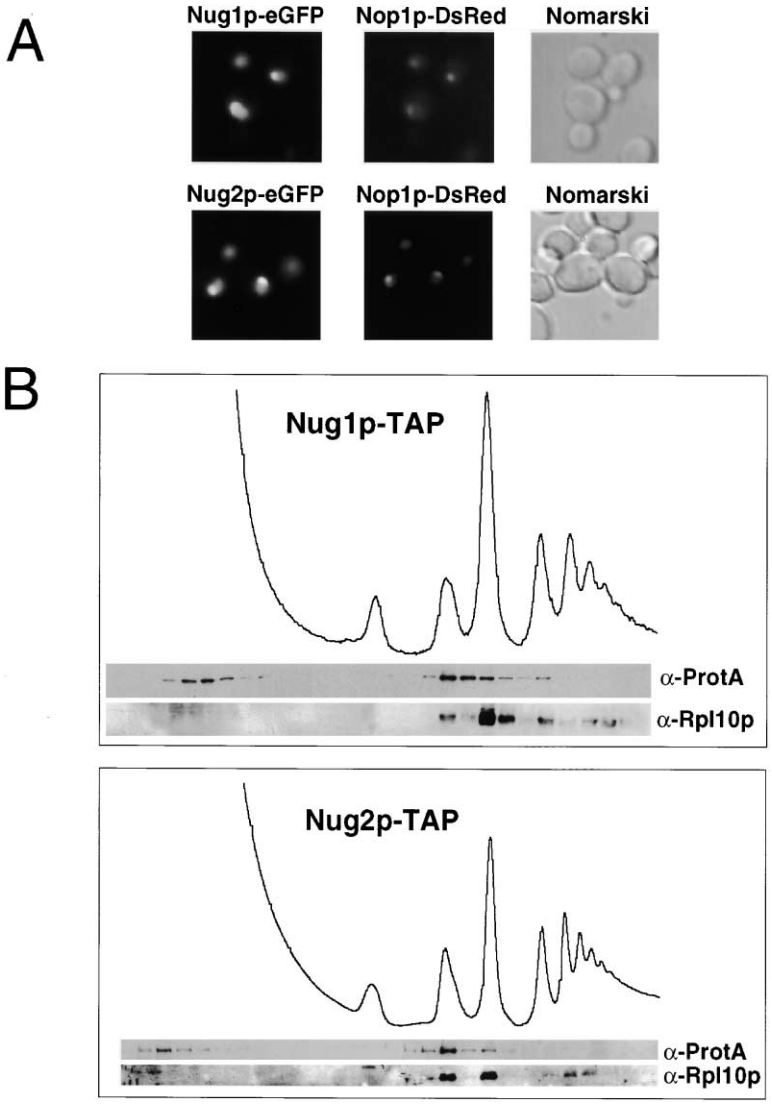

Figure 5. Nug1p and Nug2p Are Located in the Nucleus/Nucleolus and Associated with 60S Preribosomal Particles

(A) In vivo localization of Nug1p-GFP in the *nug1*Δ and Nug2p-GFP in the *nug2*Δ strain, in comparison to Nop1p-DsRed.

(B) Sedimentation behavior of Nug1p and Nug2p on sucrose gradients. Ribosomal and preribosomal particles derived from *nug1*Δ and *nug2*Δ strains, which express Nug1p-TAP and Nug2p-TAP, respectively, were analyzed by sucrose gradient centrifugation. Ribosomal profiles were determined by OD_{260nm} measurement of the gradient fractions. Western blot analysis of these gradient fractions reveals the position of Nug1p-TAP, Nug2p-TAP, and the 60S subunit marker Rpl10p.

are located exclusively in the nucleus, with a distribution throughout the entire nucleoplasm and enrichment in the nucleolus (Figure 5A). We conclude that Nug1p and Nug2p, similar to Ecm1p, have a location both in the nucleoplasm and in the nucleolus.

To find out whether Nug1p and Nug2p are associated with intranuclear preribosomal particles, whole-cell lysates derived from strains expressing TAP-tagged Nug1p or Nug2p (see below) were analyzed by sucrose gradient centrifugation. The OD_{260nm} profile of these sucrose gradients depicts the distribution of 40S and 60S subunits, 80S ribosomes, and polysomes. In addition, the sedimentation of the large subunit protein Rpl10p was determined by Western blot analysis. Apparently, Nug1p and Nug2p peak in a fraction of the sucrose gradient in which 60S ribosomal subunits sediment (Figure 5B). Moreover, Nug1p and, to a lesser extent, Nug2p, partition into lower fractions of the sucrose gradient, where larger preribosomal particles band. Finally, a pool of Nug1p and Nug2p is also found in the upper part of the sucrose gradient, where soluble proteins sediment (Figure 5B). This all suggests that Nug1p and Nug2p are bound to intranuclear 60S precursor particles.

Tandem Affinity Purification of Nug1p Reveals Association of this Protein with Ribosomal L Proteins and Many Nonribosomal Proteins

To identify the proteins, which directly interact with Nug1p and are part of these intranuclear 60S particles, Nug1p was tagged with the TAP cassette to allow tandem affinity purification (Rigaut et al., 1999). Nug1p-TAP is functional, since it fully complements the nonviable *nug1*Δ strain (data not shown). A two-step affinity purification was performed exploiting first the ProtA moiety (which binds to IgG-Sepharose), followed by TEV-proteolytic cleavage and a second affinity-purification step relying on the CBP (calmodulin binding peptide)-tag, which binds to Calmodulin-Sepharose. When purified Nug1p is analyzed by SDS-polyacrylamide gel electrophoresis and Coomassie staining, the Nug1p protein is the most prominent band (Figure 6A, band 29). Strikingly, a large number of other proteins copurify, and these

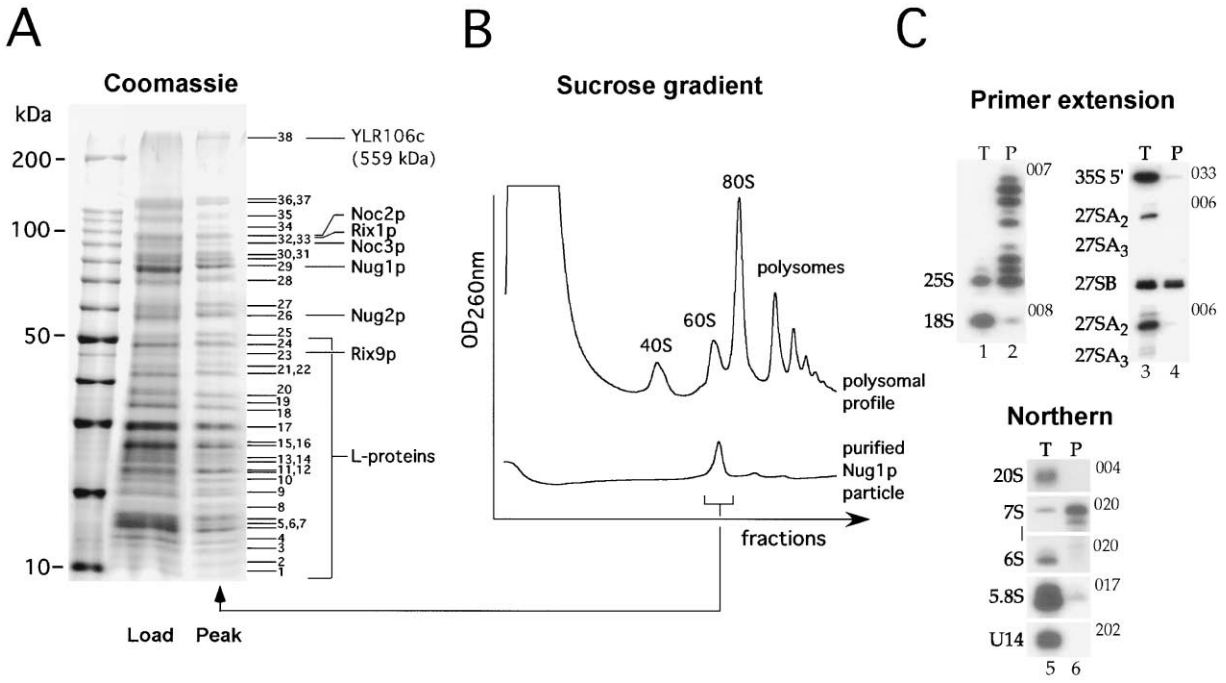

Figure 6. Nug1p Is Associated with Ribosomal L Proteins and Many Nonribosomal Proteins that Form a Stable 60S Particle

(A) Coomassie-stained gel. The Nug1p-TAP fusion protein, expressed in the *nug1*Δ null mutant, was purified by tandem affinity-purification as described under Experimental Procedures. Purified Nug1p was analyzed by SDS-10%–15% gradient polyacrylamide gel electrophoresis, and bands were visualized by Coomassie staining. The labeled bands were excised from the gel and identified by mass spectrometry. The position of Nug1p, Nug2p, Rix1p, Noc2p, Noc3p, Rix9p, YLR106c, and ribosomal L proteins are indicated. Load, final Nug1p eluate from the Calmodulin-Sepharose column; peak, 60S fraction isolated from the sucrose gradient after reisolation of the Nug1p particle by sucrose gradient centrifugation (see below). The left lane shows a 10 kDa protein ladder.

(B) Sedimentation behavior of the purified Nug1p particle on the sucrose gradient. The Nug1p eluate was applied onto a 10%–50% sucrose gradient, and the peak fraction sedimenting at 60S was analyzed by SDS-PAGE (depicted in [A]).

(C) Analysis of rRNA in the purified Nug1p particle by primer extension (lanes 1–4) and Northern hybridization (lanes 5 and 6). RNA was recovered from the double amount of precipitate as used in (A). 10% of this was used per lane and is compared to 0.5 μg of total RNA (lane 1) or 10 μg total RNA (lanes 3 and 5). Numbers indicate the oligos used. Oligo 006 hybridizes in ITS2, 3′ to site C_2, and the primer extension stops represent only the 27S pre-rRNA species. Two different exposures are shown to allow visualization of the stop corresponding to $27SA_3$ and the low level of precipitation of $27SA_2$. The bands joined by vertical lines show the same exposure from a single gel. T, total RNA or protein; P, RNA or protein present in the Nug1p particle.

were excised and identified by mass spectrometry (Table 1). In the low molecular weight range of the gel, many ribosomal L proteins (in total 30) but not S proteins were found (Table1). In contrast, the bands above 50 kDa correspond to nonribosomal proteins, most of which are essential, conserved, and possess orthologs in human, *Drosophila*, *C. elegans*, or *S. pombe* (Figure 6A and Table 1). Some of the Nug1p-associated, nonribosomal proteins were previously studied and implicated in ribosome biogenesis, including Rlp7p (Dunbar et al., 2000), the RNA helicases Has1p and Dbp10p, Nop2p (De Beus et al., 1994; Hong et al., 1997), and Nip7p (Zanchin et al., 1997). Interestingly, two of the Nug1p-copurifying bands exhibit homology to bona fide ribosomal L proteins but are not ribosomal proteins (e.g., Rlp7p, which is homologous to L7, and YHR052w, which is homologous to L1). Significantly, four of the Nug1p-associated proteins (Rix1p, Noc2p, Noc3p, and Rix9p) were previously identified in a genetic screen for ribosomal export (*rix*) mutants (Milkereit et al., 2001). Moreover, eight of the proteins (Nug1p, Nug2p, Noc2p, Kre32p, Has1p, YGR103w, YPL146c, and Nog1p) were previously reported to associate with purified nuclear pore complexes (NPC) and in vivo exhibit an intranuclear location with a concentration at the nuclear periphery (Rout et al., 2000). Finally, band 26 corresponds to Nug2p, the Nug1p homolog (Figure 6A and Table 1). These data suggest that Nug1p is associated with a 60S subunit precursor complex that associates with the NPC and includes several different proteins that are each required for export of the large subunit reporter Rpl25p-eGFP.

To find out whether tandem affinity purification of Nug1p yields a particle that has the L proteins and nonribosomal proteins stably associated, the final eluate from the Calmodulin-Sepharose column was applied on a sucrose gradient. This revealed that the purified Nug1p-containing particle sediments in the sucrose density gradient at a position close to the 60S subunits peak (Figure 6B). Importantly, all the ribosomal L proteins and associated nonribosomal proteins seen in the load fraction were still present in reisolated particle derived from the 60S peak fraction (Figure 6A, compare "Load" and "Peak"). This shows that the Nug1p containing particle is biochemically stable (see Discussion).

To determine which pre-rRNA species are present in the purified Nug1p particle (see Figure 6A), coprecipi-

tated RNA was analyzed by primer extension (Figure 6C, lanes 2 and 4) and Northern analysis (Figure 6C, lane 6). The large pre-rRNA species had undergone significant degradation during the extensive purification procedure and were therefore analyzed by primer extension. The Nug1p particle contained substantial amounts of the 25S rRNA compared to 18S rRNA (Figure 6C, lane 2). In addition to the mature 25S, substantial amounts of 5′ extended 25S were precipitated. The 5′ end of 25S is generated by exonucleases (Geerlings et al., 2001), and the extended species presumably represent late intermediates in 25S synthesis. The 27SB pre-RNA, the precursor to the 25S rRNA, was also coprecipitated (Figure 6C, lane 4). In contrast, little coprecipitation was observed for the 35S primary transcript or the $27SA_2$ and $27SA_2$ pre-rRNAs, which are earlier precursors in 60S subunit synthesis, confirming that Nug1p is specifically associated with late intermediates. Northern hybridization showed efficient recovery of the 7S pre-rRNA but lower recovery of the 6S pre-rRNA (Figure 6C, lane 6). The 5.8S rRNA was recovered, but apparently with lower efficiency than 25S. The 20S pre-rRNA, which is a component of the 40S preribosomes, and U14 snoRNA, were not detectably coprecipitated, confirming the specificity of precipitation. We conclude that Nug1p is stably associated with late rRNA precursors to 60S subunits.

The *rix1-1* Mutation Inhibits 60S Subunit Export but Has Little Effect on Pre-rRNA Processing

One of the Nug1p-associated proteins encoded by *YHR197w* was found in the screen for ribosomal export (*rix*) mutants (Figure 6A and Table 1, *RIX1*; see also Gadal et al., 2001b). The *rix1-1* mutant so isolated exhibits a strong accumulation of the Rpl25p-eGFP reporter throughout the entire nucleoplasm when shifted to the restrictive temperature (Figure 7A). Moreover, Rix1p tagged with GFP shows a nuclear location but, in contrast to Nug1p and Nug2p, no obvious nucleolar concentration (Figure 7B). Pre-rRNA processing was not clearly impaired in *rix1-1* cells for several hours after transfer to 37°C (Figure 7C). No defect in synthesis of the 7S pre-rRNA was seen, no intermediates in processing between 7S and 6S were detected, and the A_2-E intermediate was present at the same level as in the wild-type. At later time points (after 10 hr), a general reduction in pre-rRNA levels was seen (data not shown). This is likely due to a secondary consequence of the failure in subunit export and/or the inhibition of growth, since no specific processing defect could be observed. We conclude that, like *nug1-2* and *nug2-1*, the *rix1-1* strain is not primarily defective in pre-rRNA processing but is blocked in the export of 60S subunits from the nucleoplasm to the cytoplasm.

Discussion

The export of the major RNA species from the nucleus into the cytoplasm follows different routes. In the case of mRNA, RNA binding proteins assemble onto the mRNA to form export-competent mRNPs, which are then transported into the cytoplasm by a conserved export factor, the Mex67p/Mtr2p complex in yeast and the Tap/p15 complex in vertebrates (Katahira et al., 1999). Our knowledge of ribosomal export is more limited. Here, the chief difficulty has been untangling the nuclear export of the ribosomal subunits from the many other steps in their biogenesis. It is assumed that late preribosomes gain export competence either on reaching the nucleoplasm or immediately before entering the nuclear pores and that this is brought about by the binding or loss of nonribosomal protein components. While many nonribosomal proteins that are required for ribosome synthesis have been identified genetically, assigning specific functions to most of them has proved very difficult.

Here, we report the identification of a 60S subunit precursor particle, which contains a large number of associated nonribosomal proteins. Significantly, some of these components have been already demonstrated to play a role in the nuclear export of ribosomes. The biochemical purification of this 60S precursor was achieved by tandem affinity purification of an associated component Nug1p, which was found genetically via the mRNA export factor Mtr2p (see below). It is possible that the purified Nug1p particle is a mixture of discrete precursor species to 60S subunits, trapped in different stages of maturation. This could explain the sedimention behavior of Nug1p and Nug2p on the sucrose gradient and the association of Nug1p with 27SB and 7S pre-rRNAs, as well as the mature 25S and late intermediates in its 5′ processing. In contrast, the earlier processing intermediates 35S, $27SA_2$, or $27SA_3$ pre-rRNAs were coprecipitated with substantially lower efficiency. These results indicate that Nug1p associates with late pre-60S particles following processing at site B_1, which generates the 5′ end of the 27SB pre-rRNA, remains associated during cleavage of ITS2 at site C_2 that generates the 7S pre-rRNA, and dissociates shortly after 5′ maturation of the 25S rRNA.

Interestingly, among the Nug1p-associated proteinaceous components is the Noc2p/Noc3p complex that was previously shown to be required for a late step in 60S subunit export (Milkereit et al., 2001). It was suggested that during maturation of 90S to 66S preribosomes, Noc1p dissociates from Noc2p in the nucleolus and is replaced by Noc3p, which triggers movement of preribosomes from the nucleolus to the nucleoplasm. The Noc2p/Noc3p complex finally participates in export of 60S subunits into the cytoplasm. Consistent with a predominant nucleoplasmic localization of the purified preribosomal particle, it was associated with the Noc2p/Noc3p complex. In agreement with this model is also the finding that nucleolar Noc1p is absent from the Nug1p particle, as verified by Western blot analysis (data not shown).

Ribosomal proteins and eight of the 22 nonribosomal proteins identified in the pre-60S particle (see Table 1) were previously shown to purify with the NPC (Rout et al., 2000). While we cannot exclude the possibility that these are contaminants, we find this unlikely. Nug1p and Nug2p are not abundant yeast proteins. Moreover, the NPC purification, which involves several enrichment steps, contains other shuttling nucleocytoplasmic transport receptors and transport cargoes (Rout et al., 2000). We predict that the complex that we have characterized represents the nucleoplasmic transport substrate, whereas the (pre-

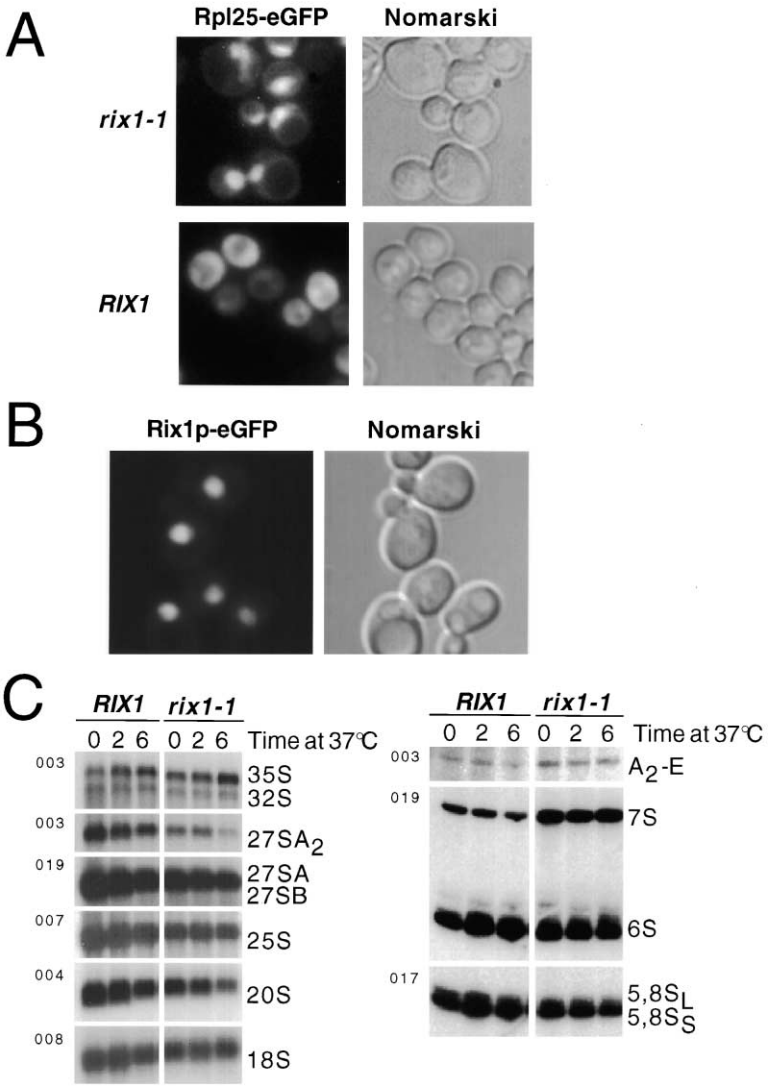

Figure 7. The *rix1-1* ts Mutant Is Not Impaired in rRNA Processing

(A) Nuclear accumulation of Rpl25p-eGFP in the *rix1-1* ts mutant shifted for 1 hr to 37°C. The *rix1-1* mutant complemented by a plasmid carrying the *RIX1* gene served as a control.

(B) In vivo localization of Rix1p-GFP in *rix1Δ* cells.

(C) Northern analysis of pre-rRNA processing in *rix1-1* and *RIX1* cells. Wild-type (*RIX1*) and *rix1-1* ts strains were analyzed following growth at 25°C (0 hr samples) and 2 and 6 hr after transfer to 37°C. Pre-rRNA species detected are indicated, as are the oligonucleotides used.

sumed) complexes that copurified with the NPC were preribosomes in transit through the pores. Indeed, we show that the particle containing Nug1p is very stable biochemically and resists extensive purification (see Figure 6). Whether the proteins present in the pre-60S complex but not found in the NPC preparation were dissociated at transport remains to be demonstrated. In the case of mRNA export, mRNA-associated proteins can be removed before or after export into the cytoplasm (Daneholt, 1999), and we predict that this will also be the case for ribosome export. Nmd3p was previously shown to act as an NES-containing shuttling adaptor protein for Xpo1p-mediated nuclear export of 60S subunits (Ho et al., 2000; Gadal et al., 2001b). However, Nmd3p was not identified in the purified Nug1p particle by mass spectrometry. This could mean that Nmd3p was present only in low amounts and thus escaped detection by mass spectrometry, or Nmd3p is not sufficiently stably associated with 60S precursor particles to resist tandem affinity purification of Nug1p.

Significantly, two predicted GTPases, Nug1p and Nug2p (see Figure 3A), which are located in the nucleoplasm and the nucleolus, are associated with the purified 60S precursor particles. Thus, Nug1p/Nug2p-mediated GTP-hydrolysis may be crucial for ribosomal export. So far, Ran is the only GTPase directly involved in nucleocytoplasmic transport. It is not known whether Nug1p and Nug2p have GTPase activity, which can be stimulated by a GAP. If this were the case, Nug1p and Nug2p (and possibly other factors) may dissociate from the 60S ribosomes upon GTP-hydrolysis, thereby triggering nuclear export or overcoming nuclear retention. Other possible functions of Nug1p/Nug2p-mediated GTP-hydrolysis might be to induce structural rearrangements of 60S precursor particles or to control rRNA maturation/modification, as a prerequisite for nuclear export. Since Nug1p and Nug2p are conserved during evolution, orthologs in higher eukaryotes are expected to perform a similar function. Two other conserved nucleolar GTPases, Nog1p and Bms1p, which are not otherwise related to Nug1p/Nug2p, were recently identified (Park et al., 2001; Wegierski et al., 2001). Bsm1p is required for processing on the pathway of 18S rRNA synthesis. Notably, Nog1p is also present in the Nug1p particle.

A remarkable protein associated with Nug1p is the essential and conserved ORF YLR106c (see Table 1). YLR106c is the largest known yeast protein (4910 amino acids, 559 kDa) and contains six tandemly arranged conserved AAA^+ cassettes, each about 250 amino acids in length, in its amino-terminal half. These domains are homologous to bacterial chaperone ATPases, which play a role in the assembly of oligomeric complexes (E.H., unpublished data). We suggest that YLR106c represents a chain of covalently linked chaperone ATPases that function in 60S subunit biogenesis. It is worth mentioning in this context that a nuclear AAA-type ATPase (Rix7p) was recently shown to be involved in ribosomal assembly and subsequent nuclear export (Gadal et al., 2001a).

Ribosomal export is closely dependent on correct rRNA processing, and instability of pre-rRNA processing intermediates is observed both in rRNA processing and export mutants (reviewed in Gadal et al., 2001a). However, earlier studies (Milkereit et al., 2001) and the work here suggest that both processes are not strictly coupled. This is exemplified by the *rix1-1*, *nug1-2*, and *nug2-1* strains, which are not clearly impaired in rRNA processing at the restrictive temperature but are strongly inhibited for 60S subunit export. This suggests that Rix1p, Nug1p, and Nug2p may be involved in late export (or assembly) steps at which feedback inhibition of pre-rRNA processing is less pronounced.

An unexpected finding of our study is that a particular *mtr2* mutant allele, *mtr2-33*, is specifically linked to ribosomal export but not to mRNA export. It was recently reported that the *mtr2-1* allele, which was isolated in a screen for mRNA export mutants (Kadowaki et al., 1994), is also impaired in 60S subunit export (Stage-Zimmermann et al., 2000). Since the genetic interaction of *mtr2-33* with *ECM1* and *NUG1* is highly specific, Mtr2p could have a role on its own in ribosomal export.

The role of Ecm1p in ribosomal export remains unclear. One possibility is that Ecm1p controls the availability of Mtr2p to act as a ribosome-specific export factor. On the other hand, we could not obtain any evidence that Mex67p is directly involved in ribosomal export. All *mex67* mutants tested so far show a normal nuclear export of 60S subunits (J.B., unpublished data).

In conclusion, we have reported the biochemical characterization of a preribosomal precursor to 60S subunits. This opens the way for a detailed analysis of the pathway of ribosome assembly and export, which have remained largely refractory to analysis by genetic approaches alone.

Experimental Procedures

Yeast Strains, DNA Recombinant Work, and Microbiological Techniques

Yeast strains used in this study are given as Supplemental Data (see Supplemental Table S1 online at http://www.molecule.org/cgi/content/full/8/3/517/DC1. Double disruption and double shuffle strains were constructed in an analogous way (Sträßer et al., 2000). Microbiological techniques and yeast work were done essentially as described (Santos-Rosa et al., 1998). DNA recombinant work was performed according to Maniatis et al. (1982).

Plasmids

The following plasmids used in this study were described previously: pUN100-DsRed-Nop1, pRS314-DsRed-Nop1, pRS316-Rpl25-eGFP, pRS315-Rpl25-eGFP, pRS314-NMD3, pRS314-nmd3-2, pRS315-RPS20-eGFP (Gadal et al., 2001b), pRS315-MTR2, pRS315-mtr2-21, YEp13-MTR2 (Santos-Rosa et al., 1998), pRS314-MEX67, pRS314-mex67-5, pHT4467 (Segref et al., 1997), pRS314-mex67-6 (Sträßer and Hurt, 2000), pRS314, pRS315 (Sikorski and Hieter, 1989), pRS416-NUG2 (Euroscarf), pBS1479 (Rigaut et al., 1999), and pft 27 (T.A. Fiedler et al., submitted). New plasmids used in this work are pRS314-MTR2, pRS314-mtr2-21, pHT4467-MTR2, pRS314-mtr2-33 (the *mtr2-33* ts allelel was constructed in the following way: an internal PstI fragment was excised from pRS315-mtr2-*22*, which is derived from a *mtr2* ts mutant collection, [Santos-Rosa et al., 1998] into pRS315-MTR2, replacing internal wild-type *Pst*I fragment, resulting in pRS314-mtr2-33 [E106G, R109G]), pRS315-mtr2-33, pRS314-ECM1, pRS315-ECM1, pRS315-ECM1-eGFP, pHT4467Δ-ECM1 (pHT4467Δ was obtained by replacing *Pvu*I fragment with *Pvu*I fragment from pft27, containing a 24 bp deletion in the *CEN6* region), pRS316-NUG1, pRS315-NUG1, pRS315-NUG2, pRS315-NUG1-eGFP, pRS315-NUG2-eGFP pRS315-RPL2A, pRS316-RIX1, pRS315-RIX1-eGFP, pRS315-NUG1-TAP, pRS315-NUG2-TAP, pRS315-nug1-1, pRS315-nug1-2, and pRS315-nug2-1.

Synthetic Lethal Screens and Cloning of ECM1, NUG1 RPL2A, and RIX1

Synthetic lethal (SL) screens with *mtr2-33* and *ecm1*Δ alleles, employing the screening strains MTR2sc and ECM1sc, respectively, and based on red/white colony sectoring, were performed according to Wimmer et al. (1992) and Segref et al. (1997). The wild-type genes, which complement SL178, SL37, and SL147, were cloned by transforming with a yeast genomic library in a *LEU2*-containing *ARS/CEN* plasmid, seletion for a red/white colony sectoring phenotype, and growth on 5-FOA-containing plates. From reisolated plasmids, the complementing ORFs were subcloned into pRS315 plasmids (SL178, pUN100-ECM1; SL37, pUN100-NUG1 [*YER006w*]; SL147, pUN100-RPL2A). *RIX1* was cloned as described previously (pUN100-RIX1) (Gadal et al., 2001b).

Generation of nug1 and nug2 ts Mutants by Mutagenic PCR

Generation of *nug1-2* ts mutants was performed by PCR-based mutagenesis as described before (Muhlrad et al., 1992; Santos-Rosa et al., 1998). About 5000 transformants were replica plated on 5-FOA containing plates. Ura^- colonies were tested for a ts phenotype at 37°C and growth at 23°C. Plasmids from identified ts mutants were isolated, and the plasmid-dependent ts phenotype was confirmed. The *nug2-1* ts mutant was generated in a similar way.

Sucrose Density Gradient Centrifugation

Isolation of ribosomes under low salt conditions by sucrose gradient centrifugation was performed as described (Tollervey et al., 1993), with the following modifications. 500 ml of a yeast culture was grown in YPD medium to an OD_{600nm} of 0.5–0.8 before cycloheximide was added to a final concentration of 100 μg/ml. Cells were harvested by centrifugation and washed in 10 ml ice-cold buffer A (20 mM HEPES [pH 7.5], 10 mM KCl, 2.5 mM $MgCl_2$, and 1 mM EGTA). 1.4 g glass beads (0.5 mm) was added to 0.5 ml of cell suspension. Cells were broken by 5 min shaking at 4°C on a shaking device (IKA Vibrax VXR). The suspension was centrifuged for 5 min at 14,000 rpm. The supernatant (300 μl) was loaded on a 10.5 ml 10%–50% sucrose gradient in buffer A without DTT and cycloheximide and centrifuged for 15 hr at 27,000 rpm in a SW40 rotor. A gradient collector (Foxy Jr from ISCO) was used to record the UV profile and collect 0.5 ml fractions, which were TCA-precipitated before SDS-PAGE and Western blot analysis.

Northern Blot Analysis

Northern hybridization in *nug1*, *nug2,* and *rix1-1* ts mutants was performed as described (Tollervey, 1987; Beltrame and Tollervey, 1992). Oligonucleotides used were: 003, TGTTACCTCTGGGCCC; 004, CGGTTTTAATTGTCCTA; 006, AGATTAGCCGCAGTTGG; 007, CTCCGCTTATTGATATGC; 008, CATGGCTTAATCTTTGAGAC; 013, GGCCAGCAATTTCAAGTTA; 017, GCGTTGTTCATCGATGC; 019, AACAGAATGTTTGAGAAGG; 020, TGAGAAGGAAATGACGCT; and 033, CGCTGCTCACCAATGG.

Mass Spectrometry

Tryptic peptides from Coomassie-stained proteins were prepared for mass spectrometry as described (Shevchenko et al., 1996), with the exception that C18 ZipTip pipette tips (Millipore) were used for the final purification according to the manufacturer's instructions. Analysis was performed on a Bruker Reflex III MALDI-TOF instrument, and proteins were identified using Mascot (Matrix Science) and the MSDB protein database. Ribosomal L5.e, L4-A/L4-B/L4.e.A/L4.e.B. and L3/L3.e. were identified by matching a peptide fingerprint of seven, eight, and six peptides, respectively, with an average mass accuracy of 13, 1.9, and 7.5 ppm, respectively. The remaining ribosomal proteins were identified by MS/MS data obtained from selected peptides after Post Source Decay. The MS/MS results were supported by peptide fingerprints (involving less than five peptides).

Miscellaneous

Poly(A)$^+$ RNA export was analyzed by in situ hybridization (Doye et al., 1994; Santos-Rosa et al., 1998). Affinity purification of TAP-tagged Nug1p protein was performed as described previously (Rigaut et al., 1999). SDS-PAGE and Western blot analysis were performed according to Siniossoglou et al. (1996). Fluorescence micrsocopy was done as described (Gadal et al., 2001a).

Acknowledgments

We would like to thank Dr. Trumpower for providing antibodies against Rpl10p, Dr. B. Seraphin (Gif-sur-Yvette, Orsay, France) for plasmid pBS1479, and Dr. J. Hegemann (Universität Düsseldorf, Germany) for plasmid ptf27. The excellent technical assistance of Daniela Strauß, Karina Deinert, Monika Lachner, and the help of Alex Löwer in cloning of *RIX1* is gratefully acknowledged. E.H. is recipient of grants from the Deutsche Forschungsgemeinschaft (SFB352 and Schwerpunktprogramm "Funktionelle Architektur des Zellkerns"), and O.G. is a holder of an HSFP fellowship. E.P. and D.T. were supported by the Wellcome Trust.

Received June 27, 2001; revised August 6, 2001.

References

Beltrame, M., and Tollervey, D. (1992). Identification and functional analysis of two U3 binding sites on yeast pre-ribosomal RNA. EMBO J. *11*, 1531–1542.

Daneholt, B. (1999). Pre-mRNP particles: from gene to nuclear pore. Curr. Biol. *9*, R412–R415.

De Beus, E., Brockenbrough, J.S., Hong, B., and Aris, J.P. (1994). Yeast *NOP2* encodes an essential nucleolar protein with homology to a human proliferation marker. J. Cell Biol. *127*, 1799–1813.

Doye, V., Wepf, R., and Hurt, E.C. (1994). A novel nuclear pore protein Nup133p with distinct roles in poly (A)$^+$ RNA transport and nuclear pore distribution. EMBO J. *13*, 6062–6075.

Dunbar, D.A., Dragon, F., Lee, S.J., and Baserga, S.J. (2000). A nucleolar protein related to ribosomal protein L7 is required for an early step in large ribosomal subunit biogenesis. Proc. Natl. Acad. Sci. USA *97*, 13027–13032.

Gadal, O., Strauß, D., Braspenning, J., Hoepfner, D., Petfalski, E., Philippsen, P., Tollervey, D., and Hurt, E.C. (2001a). A nuclear AAA-type ATPase (Rix7p) is required for biogenesis and nuclear export of 60S ribosomal subunits. EMBO J. *20*, 3695–3704.

Gadal, O., Strauß, D., Kessl, J., Trumpower, B., Tollervey, D., and Hurt, E. (2001b). Nuclear export of 60S ribosomal subunits depends on Xpo1p and requires a NES-containing factor Nmd3p that associates with the large subunit protein Rpl10p. Mol. Cell. Biol. *21*, 3405–3415.

Geerlings, T.H., Vos, J.C., and Raue, H.A. (2001). The final step in the formation of 25S rRNA in Saccharomyces cerevisiae is performed by 5′->3′ exonucleases. RNA *6*, 1698–1703.

Ho, J.H., Kallstrom, G., and Johnson, A.W. (2000). Nmd3p is a Crm1p-dependent adapter protein for nuclear export of the large ribosomal subunit. J. Cell. Biol. *151*, 1057–1066.

Hong, B., Brockenbrough, J.S., Wu, P., and Aris, J.P. (1997). Nop2p is required for pre-rRNA processing and 60S ribosome subunit synthesis in yeast. Mol. Cell. Biol. *17*, 378–388.

Hurt, E., Hannus, S., Schmelzl, B., Lau, D., Tollervey, D., and Simos, G. (1999). A novel *in vivo* assay reveals inhibition of ribosomal nuclear export in ran-cycle and nucleoporin mutants. J. Cell Biol. *144*, 389–401.

Kadowaki, T., Hitomi, M., Chen, S., and Tartakoff, A.M. (1994). Nuclear mRNA accumulation causes nucleolar fragmentation in yeast *mtr2* mutant. Mol. Biol. Cell *5*, 1253–1263.

Katahira, J., Sträßer, K., Podtelejnikov, A., Mann, M., Jung, J.J., and Hurt, E.C. (1999). The Mex67p-mediated nuclear mRNA export pathway is conserved from yeast to human. EMBO J. *18*, 2593–2609.

Kressler, D., Linder, P., and De La Cruz, J. (1999). Protein *trans*-acting factors involved in ribosome biogenesis in *Saccharomyces cerevisiae*. Mol. Cell. Biol. *19*, 7897–7912.

Lussier, M., White, A.M., Sheraton, J., Di Paolo, T., Treadwell, J., Southard, S.B., Horenstein, C.I., Chen-Weiner, J., Ram, A.F.J., Kapteyn, J.C., et al. (1997). Large scale identification of genes involved in cell surface biosynthesis and architecture in *Saccharomyces cerevisiae*. Genetics *147*, 435–450.

Maniatis, T., Fritsch, E.T., and Sambrook, J. (1982). Molecular Cloning: A Laboratory Manual (Cold Spring Harbor, New York: Cold Spring Harbor Laboratory Press).

Milkereit, P., Gadal, O., Podtelejnikov, A., Trumtel, S., Gas, N., Petfalski, E., Tollervey, D., Mann, M., Hurt, E., and Tschochner, H. (2001). Maturation of pre-ribosomes requires noc-proteins and is coupled to transport from the nucleolus to the nucleoplasm. Cell *105*, 499–509.

Moy, T.I., and Silver, P.A. (1999). Nuclear export of the small ribosomal subunit requires the Ran-GTPase cycle and certain nucleoporins. Genes Dev. *13*, 2118–2133.

Muhlrad, D., Hunter, R., and Parker, R. (1992). A rapid method for localized mutagenesis of yeast genes. Yeast *8*, 79–82.

Park, J.H., Jensen, B.C., Kifer, C.T., and Parsons, M. (2001). A novel nucleolar G-protein conserved in eukaryotes. J. Cell Sci. *114*, 173–185.

Rigaut, G., Shevchenko, A., Rutz, B., Wilm, M., Mann, M., and Séraphin, B. (1999). A generic protein purification method for protein complex characterization and proteome exploration. Nat. Biotech. *17*, 1030–1032.

Rout, M.P., Aitchison, J.D., Suprapto, A., Hjertaas, K., Zhao, Y., and Chait, B.T. (2000). The yeast nuclear pore complex: composition, architecture, and transport mechanism. J. Cell Biol. *148*, 635–651.

Santos-Rosa, H., Moreno, H., Simos, G., Segref, A., Fahrenkrog, B., Panté, N., and Hurt, E. (1998). Nuclear mRNA export requires complex formation between Mex67p and Mtr2p at the nuclear pores. Mol. Cell. Biol. *18*, 6826–6838.

Segref, A., Sharma, K., Doye, V., Hellwig, A., Huber, J., Lührmann, R., and Hurt, E.C. (1997). Mex67p which is an essential factor for nuclear mRNA export binds to both Poly(A)$^+$ RNA and nuclear pores. EMBO J. *16*, 3256–3271.

Shevchenko, A., Wilm, M., Vorm, O., and Mann, M. (1996). Mass spectrometric sequencing of proteins from silver stained gels. Anal. Chem. *68*, 850–858.

Sikorski, R.S., and Hieter, R. (1989). A system of shuttle vectors and yeast host strains designed for efficient manipulation of DNA in *Saccharomyces cerevisiae*. Genetics *122*, 19–27.

Siniossoglou, S., Wimmer, C., Rieger, M., Doye, V., Tekotte, H., Weise, C., Emig, S., Segref, A., and Hurt, E.C. (1996). A novel complex of nucleoporins, which includes Sec13p and a Sec13p homolog, is essential for normal nuclear pores. Cell *84*, 265–275.

Sprang, S.R. (1997). G protein mechanisms: insights from structural analysis. Annu. Rev. Biochem. *66*, 639–678.

Stage-Zimmermann, T., Schmidt, U., and Silver, P.A. (2000). Factors affecting nucler export of the 60S subunits in vivo. Mol. Biol. Cell. *11*, 3777–3789.

Sträßer, K., and Hurt, E.C. (2000). Yra1p, a conserved nuclear RNA binding protein, interacts directly with Mex67p and is required for mRNA export. EMBO J. *19*, 410–420.

Sträßer, K., Baßler, J., and Hurt, E.C. (2000). Binding of the Mex67p/Mtr2p heterodimer to FXFG, GLFG, and FG repeat nucleoporins is essential for nuclear mRNA export. J. Cell Biol. *150*, 695–706.

Tollervey, D. (1987). A yeast small nuclear RNA is required for normal processing of pre-ribosomal RNA. EMBO J. *6*, 4169–4175.

Tollervey, D., Lehtonen, H., Jansen, R.P., Kern, H., and Hurt, E.C. (1993). Temperature-sensitive mutations demonstrate roles for yeast fibrillarin in pre-rRNA processing, pre-rRNA methylation, and ribosome assembly. Cell *72*, 443–457.

Venema, J., and Tollervey, D. (1999). Ribosome synthesis in *Saccharomyces cerevisiae*. Annu. Rev. Genet. *33*, 261–311.

Wegierski, B., Billy, E., Nasr, F., and Filipowicz, W. (2001). Bms1p, a G-domain-containing protein, associates with Rcl1p and is required for 18S rRNA biogenesis in yeast. RNA, in press.

Wimmer, C., Doye, V., Grandi, P., Nehrbass, U., and Hurt, E. (1992). A new subclass of nucleoporins that functionally interacts with nuclear pore protein NSP1. EMBO J. *11*, 5051–5061.

Zanchin, N.I.T., Roberts, P., DeSilva, A., Sherman, F., and Goldfarb, D.S. (1997). *Saccharomyces cerevisiae* Nip7p is required for efficient 60S ribosome subunit biogenesis. Mol. Cell. Biol. *17*, 5001–5015.

Supplementary data - Baßler et al., 2001

Yeast strains

NAME	**Genotype**	**Origin**
RS453	MATa or MATα, *ura3, trp1, leu2, ade2, his3, mtr2Δ::HIS3*	(Hurt et al., 1999)
MTR2sc	*MATa, ura3, trp1, leu2, ade2, ade3, his3, mtr2Δ::HIS3* *+pHT4467-MTR2 (ARS/CEN ADE3 URA3 MTR2)* *+pRS314-mtr2-33 (ARS/CEN TRP1 mtr2-33)*	This study
SL178	*MATa, ura3, trp1, leu2, ade2, ade3, his3, mtr2Δ::HIS3, ecm1-1* *+pHT4467-MTR2 (ARS/CEN ADE3 URA3 MTR2)* *+pRS314-mtr2-33 (ARS/CEN TRP1 mtr2-33)*	This study; isolated in a SL screen with *mtr2-33*
MTR2 shuffle	*MATa or MATα, ura3, trp1, leu2, ade2, his3, mtr2Δ::HIS3* *+pRS316-MTR2 (ARS/CEN URA3 MTR2)*	(Santos-Rosa et al., 1998)
MEX67 shuffle	*MATa or MATα, ura3, trp1, leu2, ade2, his3, mex67Δ::HIS3* +pRS316-MEX67 (*ARS/CEN URA3* MEX67)	(Segref et al., 1997)
Y10348 (ecm1Δ)	*MATα, ura3, lys2, leu2, ecm1::kanMX4*	Euroscarf
*ecm1*Δ	*MATa, ura3, leu2, trp1, ade2, ecm1::kanMX4*	This study; isolated from cross of Y10348 with MTR2 shuffle
*MTR2 shuffle/ecm1*Δ	*MATa, ura3, leu2, trp1, ade2, mtr2Δ::HIS3, ecm1::kanMX4* *+pRS316-MTR2 (ARS/CEN URA3 MTR2)*	This study; isolated from cross of Y10348 with MTR2 shuffle
NMD3 shuffle	*MATa, his3, leu2, lys2, ura3, nmd3Δ::kanMX4* *+pRS316-NMD3 (ARS/CEN URA3 NMD3)*	(Gadal et al., 2001b)
MTR2/NMD3 double shuffle	*MATa, his3, ura3, leu2, trp1, ade2, mtr2Δ::HIS3, nmd3::kanMX4* *+pRS316-MTR2 (ARS/CEN URA3 MTR2)* *+pRS316-NMD3 (ARS/CEN URA3 NMD3)*	This study; isolated from cross of NMD3 shuffle with MTR2 shuffle
MEX67/NMD3 double shuffle	*MATa, his3, ura3, leu2, trp1, ade2, LYS2, mex67Δ::HIS3, nmd3::kanMX4* *+pRS316-MEX67 (ARS/CEN URA3 MEX67)* *+pRS316-NMD3 (ARS/CEN URA3 NMD3)*	This study; isolated from cross of NMD3 shuffle with MEX67 shuffle
ECM sc	*MATα, ura3, leu2, trp1, ade2, ade3, ecm1::kanMX4* *+pHT4467-ECM1 (ARS/CEN ADE3 URA3 ECM1)*	This study

SL37	*MATα, ura3, leu2, trp1, ade2, ade3, ecm1::kanMX4, nug1-1 +pHT4467-ECM1 (ARS/CEN ADE3 URA3 ECM1)*	This study; isolated in a SL screen with *ecm1Δ*
SL147	*MATα, ura3, leu2, trp1, ade2, ade3, ecm1::kanMX4 rpl2a-1 +pHT4467-ECM1 (ARS/CEN ADE3 URA3 ECM1)*	This study; isolated in a SL screen with *ecm1Δ*
NUG1 shuffle (TRP1)	*MATa or MATα, ura3, TRP1, leu2, his3, lys2 nug1::kanMX4 +pRS316-NUG1 (ARS/CEN URA3 NUG1)*	Derived by sporulation of Euroscarf strain Y20327
NUG1 shuffle	*MATa, his3, ura3, leu2, trp1, ADE2, LYS2, nug1::kanMX4 +pRS316-NUG1 (ARS/CEN URA3 NUG1)*	This study; isolated from cross of *NUG1 TRP1* shuffle with *MEX67* shuffle
MTR2/NUG1 double shuffle	*MATα, his3, ura3, leu2, trp1, ADE2, LYS2, mtr2Δ::HIS3, nmd3::kanMX4 +pRS316-MTR2 (ARS/CEN URA3 MTR2) +pRS316-NUG1 (ARS/CEN URA3 NUG1)*	This study isolated from cross of *NUG1* shuffle with *MTR2* shuffle
NUG1 shuffle/ecm1Δ	*his3, ura3, leu2, trp1, ADE2, lys2 ecm1Δ::kanMX4, nug1::kanMX4 +pRS316-NUG1 (ARS/CEN URA3 NUG1)*	This study isolated from cross of *NUG1* shuffle with *ecm1Δ*
NUG1/MEX67 double shuffle	*MATα, his3, ura3, leu2, trp1, ade2, lys2 mex67Δ::HIS3, nug1::kanMX4 +pRS316-MEX67 (ARS/CEN URA3 MEX67) +pRS316-NUG1 (ARS/CEN URA3 NUG1)*	This study isolated from cross of NUG1 shuffle with MEX67 shuffle
NUG2 shuffle (TRP1)	*MATa or MATα, ura3, TRP1, leu2, his3, lys2 nug2::kanMX4 +pRS416-NUG2 (ARS/CEN URA3 NUG2)*	Derived by sporulation of Euroscarf strain Y26080
NUG2 shuffle	*MATα, ura3, trp1, leu2, his3, lys2 nug2::kanMX4* +pRS416-NUG2 (ARS/CEN URA3 NUG2)	This study isolated from cross of NUG2 TRP1 shuffle with RS453
FY86	*MATα, ura3, leu2, his3 (RIX1)*	(Gadal et al., 2001b)
FY23	*MATa, ura3, leu2, trp1 (RIX1)*	(Gadal et al., 2001b)
rix1-1	*MATa, ura3, trp1, leu2, his3, rix1-1*	Cross of FY23 with mutagenized FY86 isolated from ts bank
RIX1 shuffle	*MATa, ura3 , leu2, his3, lys2 rix1::kanMX4 +pRS316-RIX1 (ARS/CEN URA3 RIX1)*	Derived by sporulation of Euroscarf strain Y22891

Cell, Vol. 107, 133–136, October 19, 2001, Copyright ©2001 by Cell Press

Nascent Ribosomes

Minireview

Jonathan R. Warner[1]
Department of Cell Biology
Albert Einstein College of Medicine
Bronx, New York 10461

The conversion of a ribosomal RNA transcript to a cytoplasmic ribosome requires hundreds of accessory RNA and protein factors. Two papers published recently in *Molecular Cell* provide first looks at the association of these processing factors with the intermediates in ribosome synthesis (Harnpicharnchai et al., 2001; Bassler et al., 2001).

Processing of the ribosomal RNA transcript and its assembly into ribosomal subunits has turned out to be far more intricate, and interesting, than originally imagined. The early success in reconstituting a functional bacterial small subunit from purified RNA and ribosomal proteins (Traub and Nomura, 1968) sent a misleading signal about how complex a process this is in vivo, at least in eukaryotic cells. This is evident from the identification within the past few years of more than 100 proteins and at least an equal number of small nucleolar RNAs (snoRNAs) involved in ribosome formation in the yeast *Saccharomyces cerevisiae* (reviewed in Kressler et al., 1999 and Venema and Tollervey, 1999; see also http://www.expasy.ch/linder/proteins.html). A hint of this complexity was suggested by early work showing that ribosomal precursor RNA from HeLa nucleoli could be isolated in the form of particles that contain not only newly formed ribosomal proteins destined for export with the completed ribosomal subunit but also an equally large number of proteins that recycle within the nucleolus (Warner and Soeiro, 1967; Kumar and Warner, 1972).

The RNAs of Ribosome Formation

In *S. cerevisiae*, there are two major elements to the processing of the ribosomal RNA itself. One is the conversion of a single 7 kb 35S transcript to three smaller molecules: 18S rRNA that is the core of the 40S ribosomal subunit, and the H-bonded complex 25S::5.8S rRNA that is the core of the 60S ribosomal subunit (Figure 1). At least four of the snoRNAs participate in the cleavage reactions shown in Figure 1. For only one, a relative of RNase P termed MRP, is there evidence that it acts as an endonuclease. The other major element of processing is the modification of nucleotides, the 2′-O-methylation of ribose residues, and the conversion of uridine residues to pseudouridine. A major step forward came from the recognition that most of the snoRNAs carry a region complementary to rRNA, and that one class, the "C+D box" RNAs, is responsible for directing the 2′-O methylation at 55 sites in the rRNA (Kiss-László et al., 1996) while the "H+ACA box" RNAs are responsible for directing the formation of pseudouridine at 45 sites in the rRNA (Ni et al., 1997). Each set of snoRNAs has its own set of proteins, including Nop1p, perhaps the methylase, and Cbf5p, thought to be the pseudouridylase.

The Proteins of Ribosome Formation

The identification of the many proteins that participate in the processing of ribosomal RNA, its assembly with ribosomal proteins, and its export to the cytoplasm, has been a tour de force of genetic bootstrapping in *S. cerevisiae*, starting with mutants in one component and using visual or synthetic lethal screens or high-copy suppression to identify new ones. Most of them represent essential genes. Mutation of the gene or depletion of the protein leads to inefficient or lack of formation of either the 40S subunit, the 60S subunit, or, rarely, both. In many cases, there is a slight accumulation of one or more of the intermediates shown in Figure 1 or of an aberrant intermediate. However, the accumulation represents only a minor part of the flux of RNA through the processing system. Improperly processed molecules are rapidly degraded.

What are the proteins that have been implicated in ribosome synthesis (see reviews cited above)? Not surprisingly, there are nucleases, including a truly remarkable collection of 11 exonucleases in a complex termed the "exosome." While the latter are employed in trimming the ends of the final products, only a single endonuclease has yet been identified, an RNase III type of double-stranded nuclease that generates the initial 3′ end of the 35S transcript. As yet, we know no endonuclease responsible for the major cleavage steps shown in Figure 1.

Another group are the putative helicases, of which at least 16 have been implicated in ribosome assembly (reviewed by Tanner and Linder, 2001). These have been classified only on the basis of sequence; no ATP-dependent helicase activity has yet been demonstrated. Presumably, they are involved in the association/dissociation of the pre-rRNA with the snoRNAs, in the enormously complex folding of the rRNAs themselves that is found in the mature ribosome, as well as in the rearrangement of protein-RNA interactions (Jankowsky et al., 2001). However, no helicase has yet been identified with a discrete step in the processing of the pre-rRNA.

Although crystal structures of ribosomal particles show the ribosomal proteins mostly on the exterior of the rRNA core, they also provide numerous examples in which a domain of a ribosomal protein is buried deep within the structure, in a configuration that could only occur during the folding of the rRNA (Ramakrishnan and Moore, 2001). Yet, in few cases has any accessory protein been implicated in assembly of the ribosomal proteins. One possible example stems from the observation that lethality of the deletion of *RRP7* is suppressed by the overexpression of ribosomal protein S27, suggesting that Rrp7p might assist in the assembly of this particular ribosomal protein (Baudin-Baillieu et al., 1997).

One problem for the cell is to maintain directional control over the assembly line, in particular to have mechanisms that determine when one step has been completed and the next can begin. The Noc1, 2, and 3

[1] Correspondence: warner@aecom.yu.edu

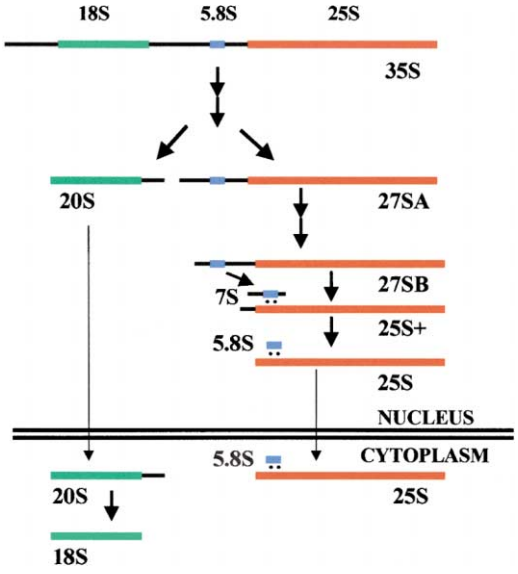

Figure 1. A Simplified Version of the Processing of the 35S Pre-rRNA Transcript of *S. cerevisiae* to the Mature 18S and 25:5.8S Species

20S RNA is transported to the cytoplasm where it is processed to 18S. 27S RNA is processed to mature 25:5.8S in the nucleus and then transported to the cytoplasm. Although only the RNAs are shown, each is accompanied by a great many proteins, the subject of two papers in a recent *Molecular Cell* (Harnpicharnchai et al., 2001; Bassler et al., 2001).

proteins appear to participate in this process. The data suggest that Noc1p and Noc2p associate with each other and with the assembling ribosomal subunit at an early stage; the conversion of a Noc1p-Noc2p to a Noc2p-Noc3p interaction may signal a nearly completely processed ribosomal subunit that is ready for export (Milkereit et al., 2001).

A recent search for mutants involved in the export process has turned up another 35 genes, that range from *RPL10*, encoding one of the ribosomal proteins, to an AAA-type ATPase that is postulated to be involved in rearranging the particle in preparation for export (Gadal et al., 2001). Although one can speculate endlessly about the role of individual proteins implicated in this complex pathway, it is rare that a verifiable function can be assigned to any one of them.

The Ribonucleoproteins of Ribosome Formation

We expect that each of these proteins will be associated with the developing ribosome only transiently, when it is carrying out its appointed task. Yet almost entirely missing from the experimental approaches thus far has been a determination of which proteins and which RNAs are associated at a particular stage of the formation of the ribosome. Two recent papers address this issue. Focusing on processing itself, Harnpicharnchai et al. (2001) have identified Nop7p as participating in the conversion of 27S to 25S rRNA. Focusing on factors involved in the transport of 60S subunits to the cytoplasm, Bassler et al. (2001) have identified a group of proteins that may represent an export complex, one of which is Nug1p, a putative GTPase. What marks these papers as a major advance over earlier work is that each group, using the tandem affinity purification (TAP) protocol (Rigaut et al., 1999) with wild-type Nop7p and Nug1p, respectively, has purified the ribonucleoprotein particles with which they are associated, particles that may represent a snapshot of nascent ribosomes at a particular stage of development (Figure 2).

Surprisingly, given that the phenotypes of *nop7* and *nug1* mutants suggest that the particles purified with the Nug1p-tag would be more mature, the complement of RNA in the two particles was largely the same, namely the 27SB, 25S+, and 7S precursors of the 25S and 5.8S mature species, representing the later steps of processing (see Figure 1). Relatively little mature 25S RNA was present, and no 20S or 18S species. The snoRNAs involved in early steps of rRNA processing were barely detectable. Thus, each particle represents a late stage in the maturation of the 60S ribosomal subunit.

Fractionation of the particles followed by mass spectrometry has led to the identification of a rich complement of proteins. In spite of their similar RNA content, the particles are substantially different. While each had about two thirds of the 45 proteins of the 60S subunit, and mostly the same ones, the Nop7p-tag particle also contained several proteins destined for the 40S subunit. Since the 35S pre-rRNA in this preparation, while detectable, seems insufficient to account for their presence, we are left to wonder whether the ribosomal proteins may be playing more than a structural role.

Most interesting, however, are the nonribosomal proteins identified within these particles, 23 with the Nop7-tag and 21 with the Nug1-tag. The intriguing, and promising, result is that these show only 25% overlap. While Nop7p was found on the Nug1p-tagged particles, the converse was not true, suggesting some experimental limitations. Nevertheless, these two particles clearly bear quite divergent sets of nucleolar proteins. Given the similarity of the RNA complement, this result suggests that a limiting step in rRNA processing is the remodeling of the protein complement of the intermediate particles. Surprisingly, Bassler et al. (2001), although purifying their particle based on a protein thought to be involved in the export process, found relatively little mature 25S and 5.8S rRNAs. Does this result imply that export is closely coupled to the final steps of rRNA processing?

Although many of the proteins found in the purified particles had previously been identified as participating in ribosome synthesis, each group found new ones. Harnpicharnchai et al. (2001) analyzed genes encoding seven novel proteins; in each case, loss or depletion of the protein leads to deficient 60S ribosome synthesis. Erb1p, only recently described as essential for maturation of 25S rRNA (Pestov et al., 2001), was found on both particles. Reassuringly, Bassler et al. (2001) found Noc2p and Noc3p, identified with late stages of maturation, but not Noc1p, representative of earlier stages (Milkereit et al., 2001). They found eight proteins that had previously copurified with nuclear pore complexes (Rout et al., 2000), only some of which had also been implicated in nuclear export of the ribosome (Gadal et al., 2001). They did not, however, find Nmd3p, the protein most convincingly identified as a chaperone for the nuclear to cytoplasmic transfer of 60S subunits (Ho et al., 2000). Intriguingly, one member of the particle purified

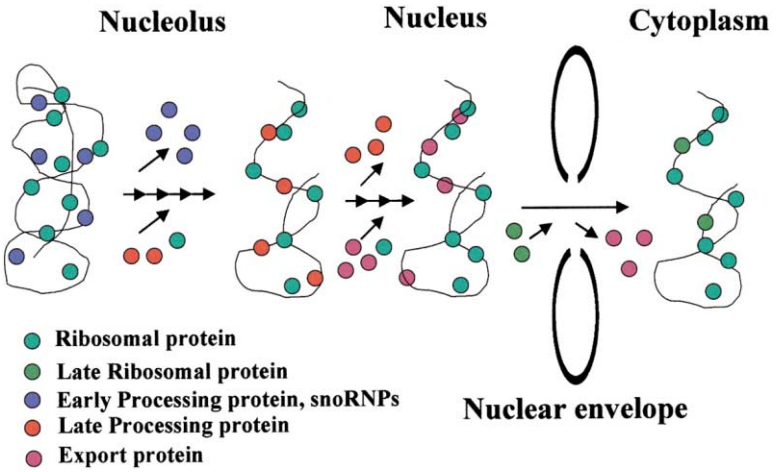

Figure 2. A Simplified View of Several Species of Nascent Ribosomes as They Develop and Are Exported to the Cytoplasm

Although drawn as if there is a complete exchange of nonribosomal proteins at each step, undoubtedly there are many that remain associated with the nascent ribosome through several processing steps. Note that a few of the ribosomal proteins associate late in the process, perhaps even in the cytoplasm.

with the Nug1-tag was derived from the largest ORF represented in the yeast genome, once again a protein without an evident function.

These are still early days for this technique. There is, as yet, no direct demonstration that there is a precursor-product relationship between the Nop7-tag and the Nug1-tag particles, nor between either particle and 60S cytoplasmic subunits. The similarity of the RNAs in particles with such different proteins complements raises some concerns.

Nevertheless, the results reported in these two papers are important on two fronts: (1) the identification of many new proteins, whose role in ribosome synthesis must now be determined, and (2) the demonstration that application of the TAP-tag to a complex, yet evanescent particle (lifetime probably $<$1 min.) yields the real McCoy, with few if any extraneous proteins. Judicious choice of the proteins to be tagged should, in the near future, supply a series of nascent ribosomes, representing the many stages in processing of the 35S rRNA transcript and its assembly with ribosomal proteins. Each such particle will provide an extra dimension for analysis of the course of this exceptionally complex process. In time, we may even learn what these proteins are doing and how they are arranged on the nascent ribosomes.

Furthermore, these papers demonstrate the exceptional suitability of *S. cerevisiae* for this kind of study. Its genetics enables identification of the proteins to be used as tags and then confirmation of the participation of novel proteins that are found in the particles. It has been most reassuring to learn that a large proportion of the factors described in *S. cerevisiae* have counterparts in mammalian organisms, suggesting that the fundamental organization of the formation of ribosomes has been conserved through evolution.

As satisfying as these two papers are, it is clear that a full understanding of rRNA processing will not yield to analysis only of steps from 35S pre-rRNA to mature rRNA. This is complete in a couple of minutes, while transcription of the 7 kb 35S pre-rRNA transcript probably consumes at least 5 min. Recent experience with Pol II demonstrates that many factors can associate with RNA during the transcription process. Do analogous events take place during Pol I transcription? One hint is the observation that in *S. cerevisiae* methylation of the rRNA occurs, apparently cooperatively, immediately after the completion of transcription (Udem and Warner, 1972). This implies that the snoRNAs associate with the growing chain as it is being transcribed, a reasonable way to prevent unwanted folding arrangements. Which of the proteins accompany them? What triggers the methylation (and the presumably concomitant pseudouridylation)? What is the form of the nascent ribosome at this first step of gestation?

Selected Reading

Bassler, J., Grandi, P., Gadal, O., Lessmann, T., Tollervey, D., Lechner, J., and Hurt, E. (2001). Mol. Cell *8*, 517–529.

Baudin-Baillieu, A., Tollervey, D., Cullin, C., and Lacroute, F. (1997). Mol. Cell. Biol. *17*, 5023–5032.

Gadal, O., Strauss, D., Kessl, J., Trumpower, B., Tollervey, D., and Hurt, E. (2001). Mol. Cell. Biol. *21*, 3405–3415.

Harnpicharnchai, P., Jakovljevic, J., Horsey, E., Miles, T., Roman, J., Rout, M., Meagher, D., Imai, B., Guo, Y., Brame, C.J., et al. (2001). Mol. Cell *8*, 505–515.

Ho, J.H., Kallstrom, G., and Johnson, A.W. (2000). J. Cell Biol. *151*, 1057–1066.

Jankowsky, E., Gross, C.H., Shuman, S., and Pyle, A.M. (2001). Science *291*, 121–125.

Kiss-László, Z., Henry, Y., Bachellerie, J.P., Caizergues-Ferrer, M., and Kiss, T. (1996). Cell *85*, 1077–1088.

Kressler, D., Linder, P., and de la Cruz, J. (1999). Mol. Cell. Biol. *19*, 7897–7912.

Kumar, A., and Warner, J.R. ((1972). J. Mol. Biol. *63*, 233–246.

Milkereit, P., Gadal, O., Podtelejnikov, A., Trumtel, S., Gas, N., Petfalski, E., Tollervey, D., Mann, M., Hurt, E., and Tschochner, H. (2001). Cell *105*, 499–509.

Ni, J., Tien, A.L., and Fournier, M.J. ((1997). Cell *89*, 565–573.

Pestov, D.G., Stockelman, M.G., Strezoska, Z., and Lau, L.F. (2001). Nucleic Acids Res. *29*, 3621–3630.

Ramakrishnan, V., and Moore, P.B. (2001). Curr. Opin. Struct. Biol. *11*, 144–154.

Rigaut, G., Shevchenko, A., Rutz, B., Wilm, M., Mann, M., and Seraphin, B. (1999). Nat. Biotechnol. *17*, 1030–1032.

Rout, M.P., Aitchison, J.D., Suprapto, A., Hjertaas, K., Zhao, Y., and Chait, B.T. (2000). J. Cell Biol. *148*, 635–651.

Tanner, N.K., and Linder, P. (2001). Mol. Cell *8*, 251–262.

Traub, P., and Nomura, M. (1968). Proc. Natl. Acad. Sci. U. S. A *59*, 777–784.

Udem, S.A., and Warner, J.R. (1972). J. Mol. Biol. *65*, 227–242.

Venema, J., and Tollervey, D. (1999). Annu. Rev. Genet. *33*, 261–311.

Warner, J.R., and Soeiro, R. (1967). Proc. Natl. Acad. Sci. USA *58*, 1984–1990.

THE JOURNAL OF BIOLOGICAL CHEMISTRY VOL. 281, NO. 34, pp. 24737–24744, August 25, 2006

The NUG1 GTPase Reveals an N-terminal RNA-binding Domain That Is Essential for Association with 60 S Pre-ribosomal Particles*[S]

Received for publication, May 4, 2006, and in revised form, June 23, 2006 Published, JBC Papers in Press, June 27, 2006, DOI 10.1074/jbc.M604261200

Jochen Bassler[1], **Martina Kallas, and Ed Hurt**[1,2]

From the Biochemie-Zentrum der Universität Heidelberg, 69120 Heidelberg, Germany

The putative yeast GTPase Nug1, which is associated with several pre-60 S particles in the nucleolus and nucleoplasm, consists of an N-terminal domain, which is found only in eukaryotic orthologues, and middle and C-terminal domains that are conserved throughout eukaryotes, bacteria, and archaea. Here, we analyzed the role of the eukaryote-specific Nug1 N-domain (Nug1-N). We show that the essential Nug1-N is sufficient and necessary for nucle(ol)ar targeting and association with pre-60 S particles. Nug1-N exhibits RNA binding activity and is genetically linked in an allele-specific way to the pre-60 S factors Noc2, Noc3, and Dbp10. In contrast, the middle domain, which exhibits a circularly permuted GTPase fold and an intrinsic GTP hydrolysis activity *in vitro*, is not essential for cell growth. The conserved Nug1 C-domain, which has a yet uncharacterized fold, is also essential for ribosome biogenesis. Our findings suggest that Nug1 associates with pre-60 S subunits via its essential N-terminal RNA-binding domain and exerts a non-essential regulative role in pre-60 S subunit biogenesis via its central GTPase domain.

Ribosome synthesis in eukaryotic cells is a strictly coordinated multistep process. It requires transcription by the three RNA polymerases to generate the pre-rRNAs (by polymerase I and polymerase III) and mRNAs (by polymerase II) that encode the ribosomal proteins and the non-ribosomal factors involved in ribosome biogenesis. Concomitant to transcription, early trans-acting factors together with small nucleolar ribonucleoparticles and ribosomal proteins are recruited to the 35 S pre-rRNA to form the 90 S pre-ribosome/small subunit processome (1, 2). Within this early 90 S pre-ribosome intermediate, various rRNA modification/processing events occur, including methylation, pseudouridylation, and cleavage of pre-rRNA at sites A_0 and A_1. Subsequently, cleavage at site A_2 leads to a splitting of the 90 S precursor particle yielding the earliest pre-40 S and pre-60 S subunits (reviewed in Refs. 3 and 4). Depending on the growth state, the latter cleavage can occur co-transcriptionally or post-trancriptionally in yeast (5). Upon further maturation, nearly all 90 S factors dissociate, and a small number of new factors are recruited (6). The derived nuclear pre-40 S particle contains Rps proteins, 20 S pre-rRNA, and a few non-ribosomal factors. Lastly, the pre-40 S particle is exported to cytoplasm, where final maturation of the 40 S subunit takes place.

In contrast, the early nucleolar pre-60 S particles contain a huge number of factors (~40–50), among which are methyltransferases, RNA helicases, ATPases, and GTPases (7). Subsequent maturation steps include processing of the 27 S rRNA into 25 S and 5.8 S rRNA, incorporation of 5 S rRNA and transport of the pre-60 S subunit to the nucleoplasm. During these processes, the composition of the particles is simplified until export competence is achieved by recruitment of export factors including Nmd3 and Mtr2 and possibly others (7). It is assumed that the heterotrimeric Nmd3-Xpo1-RanGTP complex, which assembles onto the transport-competent pre-60 S subunit, mediates export through the nuclear pore complex into the cytoplasm. Subsequently, the late non-ribosomal factors dissociate from the 60 S subunit by mechanisms, which also involve GTPases (8).

Significant insight into the formation and transport of pre-ribosomal particles has been achieved over the past several years (for review, see Refs. 9–11). Due to extensive proteomic analyses of pre-ribosomal particles, the vast majority of non-ribosomal factors involved in ribosome synthesis have been identified, and their approximate site of action is beginning to be understood. Moreover, the structural organization of a few pre-ribosomal particles has been determined by electron microscopy (12, 13). Notably, structural rearrangement of a late pre-40 S particle was followed during *in vitro* maturation and was found to be dependent upon phosphorylation and dephosphorylation events (13). Regulation of pre-60 S subunit biogenesis appears to be strongly dependent on the function of several putative GTPases in yeast, including Nug1,[3] Nug2/Nog2, and Lsg1/Kre35 (8, 14–18), all belonging to a novel G-family (called YawG) that are earmarked by a permutated order of GTP motifs within the GTP-binding domain (19). Here, we studied one member of these putative GTPases, Nug1. We found that

* The costs of publication of this article were defrayed in part by the payment of page charges. This article must therefore be hereby marked "*advertisement*" in accordance with 18 U.S.C. Section 1734 solely to indicate this fact.
[S] The on-line version of this article (available at http://www.jbc.org) contains a supplemental figure and two tables.
[1] Supported by the Deutsche Forschungsgemeinschaft (Grant Hu363/10-1).
[2] To whom correspondence should be addressed: Biochemie-Zentrum der Universität Heidelberg, Im Neuenheimer Feld 328, 69120 Heidelberg, Germany. Tel.: 49-6221-544173; Fax: 49-6221-54-4369; E-mail: cg5@ix.urz.uni-heidelberg.de.

[3] The abbreviations used are: Nug, nuclear/nucleolar GTPase; GST, glutathione *S*-transferase; RbgA, ribosome biogenesis GTPaseA; RsgA, ribosome small subunit-dependent GTPaseA; Rps, ribosomal protein small subunit; TAP, tandem affinity purification; EGFP, enhanced green fluorescent protein; mRFP, monomeric red fluorescent protein; TEV, tobacco etch virus; SL, synthetic lethal; 3-AT, 3-aminotriazole; SDC, synthetic dextrose complete-medium; FOA, 5-fluoroorotic acid; HE-EGFP, high efficiency EGFP filter.

Supplemental Material can be found at: http://www.jbc.org/cgi/content/full/M604261200/DC1

the essential N-terminal Nug1 domain targets Nug1 to the nucleolus/nucleus, mediates association with pre-60 S particles, and exhibits RNA binding activity. In contrast, the middle part of Nug1, which comprises the GTPase fold, is not essential for cell growth and thus may fulfill a redundant role with other GTPases involved in ribosome biogenesis.

EXPERIMENTAL PROCEDURES

Plasmids, Strains, DNA Recombinant Work, and Microbiological Techniques—Yeast strains and plasmids used in this study are listed in supplemental Tables 1 and 2. Double knockout strains were generated as described previously (20). DNA recombinant work was done according to (21) using *Escherichia coli* strain *DH5α*.

Live Cell Imaging—Prior to imaging, cells were grown in SDC-leu liquid medium (30 °C) until logarithmic phase. Fluorescence microscopy was performed using an Imager Z1 (Carl Zeiss) with a ×100 NA 1.4 Plan-Apo-Chromat Oil immersion lens (Carl Zeiss) and DICIII, HE-EGFP, or HE-Cy3 filter set, respectively. Pictures were acquired with an AxioCamMRm camera (Carl Zeiss) and software AxioVision 4.3 (Carl Zeiss) at resolution 1388 × 1040 (Binning 1 × 1, gain factor 1). Pictures were exported as jpg files and processed in PhotoShop 7.0 for gray levels.

GTP Hydrolysis Assays—Recombinant GST-TEV-Nug1 or GST-TEV-Nug1–4G mutant was expressed from *E. coli* Star^{+}, purified via GST affinity purification, and eluted by incubation with TEV protease. GST-Nug1–4G is a mutant of Nug1, in which the G1 consensus motif GKSS was mutated to 4 glycines (GGGG). Eluted proteins were further purified by ion exchange chromatography (MonoS/GE Healthcare) and gel filtration (Superdex^{TM} 200/GE Healthcare) and concentrated using ULTRAFREE 0.5 with Biomax-10K NMWL membrane (Millipore). Cell lysis buffer contained 100 mM KOAc, 400 mM NH_4Cl, 100 mM NaCl, 5 mM $MgCl_2$, 20 mM HEPES, pH 7.5. Subsequent purification steps were performed in the same buffer with 200 mM NH_4Cl. For the GTPase assay, the purified protein was incubated with [γ-^{32}P]GTP at 30 °C. To stop the reaction, SDS was added. The cleaved radioactive [γ-^{32}P]phosphate was separated by thin layer chromatography and visualized by autoradiography.

Kinetic analysis of Nug1-mediated GTP hydrolysis was performed using a colorimetric assay according to Ref. 22. Purified Nug1 (80 μl) was mixed with 20 μl of various concentrations GTP to obtain 16–30 μM Nug1 and 0.4, 1, 2, 4, or 10 mM GTP and incubated at 30 °C. Aliquots (15 μl) were taken in 45-min intervals, and the reaction was stopped by freezing in liquid N_2. The amount of hydrolyzed phosphate was determined by incubation with 885 μl of malachite green solution (0.3 g of malachite green, 2 g of ammonium molybdate, 0.5 g of Triton in 1 liter of 1 N HCl). The colorimetric reaction was terminated after 3 min by adding 100 μl of sodium citrate (34 g/100 ml). Finally, A_{600} was measured after a 30–90-min incubation. The catalytic constant was derived from $k_{cat} = \nu_{max}/c_{Nug1}$. ν_{max} was calculated using a Lineweaver-Burk plot, and c_{Nug1} was determined by A_{280} in a NanoDrop© 1000 spectrophotometer.

RNA-Electrophoresis Mobility Shift Assay—Nug1-N was incubated with RNase during incubation with nickel-nitrilotriacetic acid resin (Qiagen). Subsequently, Nug1-N was eluted by imidazole and applied to a gel filtration column containing Superdex^{TM}-200 (Amersham Biosciences). All purification steps were performed in buffer containing 50 mM KOAc, 100 mM NH_4Cl, 50 mM NaCl, 10 mM $MgOAc_2$, and 20 mM HEPES, pH 7.0. *In vitro* transcription of 5 S RNA was performed using linearized plasmid DNA carrying the 5 S rRNA gene under the control of T7 promoter (pET9D-5 S-RNA). Total yeast tRNA was purchased from Sigma. RNA binding assays were performed at room temperature (23 °C) in protein purification buffer. Samples were analyzed by loading on 8% polyacrylamide gels (0.5× Tris-borate-EDTA) containing ethidium bromide to visualize RNA under UV light.

Miscellaneous—The following published methods were applied: three-hybrid interactions on SDC-trp-leu-ura-his+5 mM 3-AT (23), sedimentation analysis (14), affinity purification of tandem affinity purification (TAP)-tagged Nug1 constructs (24), Western blot analysis using anti-protein-A (DAKO) (25), and NuPage 4–12% polyacrylamide gel (Invitrogen) followed by Coomassie Brilliant Blue G Colloidal (Sigma) staining according to the manufacturer's instructions and mass spectrometry (14).

RESULTS

Domain Analysis of the Nug1 Protein—Inspection of primary amino acid sequence suggests that Nug1 consists of three domains (Fig. 1 and supplemental figure Fig. S1). An N-terminal domain (residues 1–154), which is conserved within the Nug1 orthologues (nucleostemin family), a middle domain (residues 155–344), which has a highly conserved GTPase fold with permutated G1–5 motifs and a conserved C-terminal domain (residues 345–520) lacking known motifs. The protein fold of the latter two domains most likely resembles the prokaryotic RbgA fold, whose x-ray structure is known (see "Discussion"). To determine whether all three domains of Nug1 are essential for cell growth, a deletion analysis was performed (Fig. 1*A*). In the case of the N-domain, removal of the first 37 amino acids (*nug1-ΔN1*) exhibited a slightly reduced growth rate, whereas deletion of the first 100 amino acids or the entire N-domain caused a lethal phenotype (*nug1-ΔN;* Fig. 1*A*). In the case of the C-terminal domain, deletion of the last 52 non-conserved residues did not affect the growth rate, but further (last 116 amino acids) or complete deletion of the conserved C-domain (last 176 amino acids; *nug1-ΔC*) resulted in lethality (data not shown and Fig. 1*A*). Unexpectedly, deletion of the M-domain containing the GTPase fold resulted only in a slightly reduced growth rate (*nug1-ΔM;* Fig. 1*A*). In contrast, deletion of the M-domain in the homologous putative GTPase Nug2 (Fig. 1*B*) or point mutations in the GTPase motifs caused lethality (15). These results suggest that the putative Nug1 GTPase has essential N- and C-domains, which enclose the central but non-essential putative GTPase domain.

Purified Nug1 Exhibits GTPase Activity—The finding that the Nug1 middle domain with a predicted GTPase fold is not essential for growth prompted us to test for Nug1 GTPase activity. Thus, we expressed GST-tagged Nug1 in *E. coli* and purified it via GSH affinity, ionic exchange, and gel filtration chromatography (Fig. 2*A*). As a negative control, we purified in the

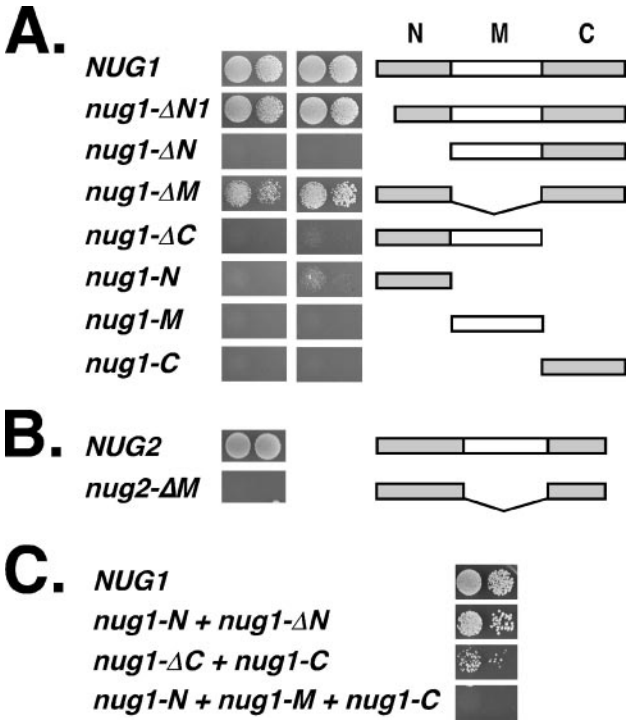

FIGURE 1. **Nug1 consists of functionally different N-, M-, and C-domains.** *A,* deletion analysis of the three Nug1 domains. Wild-type and deletion constructs, C-terminally fused to EGFP, were transformed into the Nug1 shuffle strain. *Left panel*, growth behavior after 3 and 6 days at 30 °C on SDC+FOA plates. Note that N-terminal or C-terminal tagging of Nug1 did not affect growth of the corresponding strains when tested at 23, 30, and 37 °C (data not shown). *Right panel*, schematic drawing of the Nug1 constructs; borders of the constructs are given in supplemental Table 2. *B,* deletion of Nug2-M domain is lethal. Nug2 shuffle strain was transformed with plasmids encoding Nug2-TAP or Nug2-ΔM-TAP. Growth behavior on SDC+FOA is shown after 6 days at 30 °C. *C,* Nug1 domain constructs show trans-complementation. Nug1 shuffle strain was transformed with plasmids pRS315-NUG1-TAP (*NUG1*), pRS314-nug1-ΔN and pRS313-nug1-N-EGFP (*nug1-N* + *nug1-ΔN*), pRS315-nug1-ΔC-TAP and pRS314-nug1-C (*nug1-ΔC* + *nug1-C*), and pRS313-nug1-N-EGFP, pRS315-nug1-M-TAP, and pRS314-nug1-C (*nug1-N* + *nug1-M* + *nug1-C*). Transformants were spotted on SDC+FOA plates, and growth is shown after 3 days at 30 °C.

same manner GST-Nug1–4G that is a mutant form of Nug1, containing an inactive Walker A motif (see "Experimental Procedures"). This Nug1–4G construct was expected to be inactive in GTP hydrolysis.

The purified GST-tagged Nug1 and Nug1–4G proteins were tested *in vitro* for GTP hydrolysis activity by incubation with γ-^{32}P-labeled GTP. The release of [γ-^{32}P]phosphate was followed by thin layer chromatography in combination with autoradiography (Fig. 2*B*). This analysis revealed that purified recombinant Nug1 exhibits a distinct GTPase activity (Fig. 2*B*), which is largely abolished in the Nug1–4G mutant. Thus, it is likely that Nug1 has GTP hydrolysis activity *in vivo*.

For further characterization of the Nug1 GTPase activity, we determined the enzymatic parameters using a colorimetric assay (22). Purified Nug1 was incubated with various concentrations (0.2–10 mM) of GTP, and the amount of generated PO_4^{3-} was determined (see "Experimental Procedures"). Lineweaver-Burk plot analysis revealed a K_m of 0.2 mM ± 0.1 mM and k_{cat} of 0.11 min^{-1} ± 0.01 min^{-1} for the GTP hydrolysis reaction ("Experimental Procedures"). Notably, for *E. coli* RsgA (a Nug1 homolog), similar kinetic parameters for the intrinsic GTPase activity were reported (26, 27). We conclude from our studies that purified Nug1 has an intrinsic GTP hydrolysis activity (see "Discussion").

Trans-complementation by the Various Nug1 Domains—In the course of our studies, we found that N-terminal truncations of Nug1 could be rescued by co-expression of an intact N-domain. Therefore, we tested whether the essential Nug1 domains, when separated from each other but co-expressed in the same cell, would allow for trans-complementation. Co-expression of the split N-domain together with the Nug1-ΔN construct revealed efficient complementation of the otherwise lethal *nug1* null mutant (Fig. 1*C*). Moreover, co-expression of the C-domain together with the Nug1-ΔC construct could complement the *nug1* null mutant (Fig. 1*C*). This suggests that the various Nug1 domains perform unique but overlapping functions.

The Nug1-N Domain Exhibits Nucle(ol)ar Targeting and Pre-ribosome Binding Properties—To determine how the three Nug1 domains contribute to nuclear and/or nucleolar targeting and association with pre-60 S particles, we tagged the individual domains or various combinations of them (ΔN, ΔM, ΔC) with either EGFP or TAP and analyzed their subcellular location and association with pre-60 S particles. The EGFP-tagged Nug1-N domain, as well as the Nug1-ΔC and Nug1-ΔM constructs, localized to the nucleolus/nucleoplasm with a distribution that is similar to that of the endogenous Nug1 (Fig. 3). The nucleolar localization of these constructs was confirmed by co-localization with the nucleolar marker Nop1 tagged with mRFP. Interestingly, expression of frag-

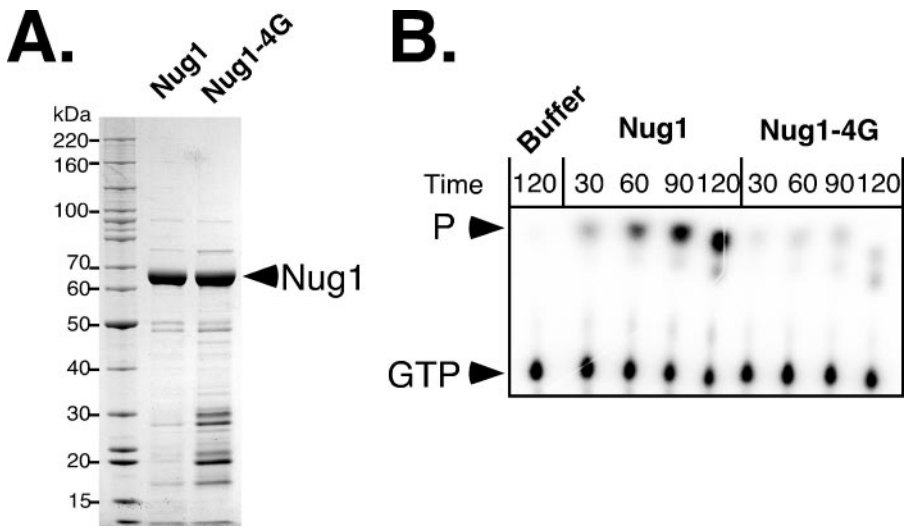

FIGURE 2. **Nug1 has intrinsic GTPase activity.** *A,* bacterially expressed and purified wild-type Nug1 and mutant Nug1–4G (see "Experimental Procedures") were analyzed on a SDS 4–12% polyacrylamide gel and visualized by Coomassie Blue staining. A protein standard is indicated at the *left*. *B,* 5 nM Nug1 or 8 nM Nug1–4G were mixed with γ-^{32}P-labeled 0.05 mM GTP in reaction buffer and incubated at 30 °C for 30, 60, 90, or 120 min before the reaction was stopped and the mixture analyzed with TLC. Migration behavior of [γ-^{32}P]GTP and [γ-^{32}P]phosphate is indicated at the *left* with GTP or *P*, respectively.

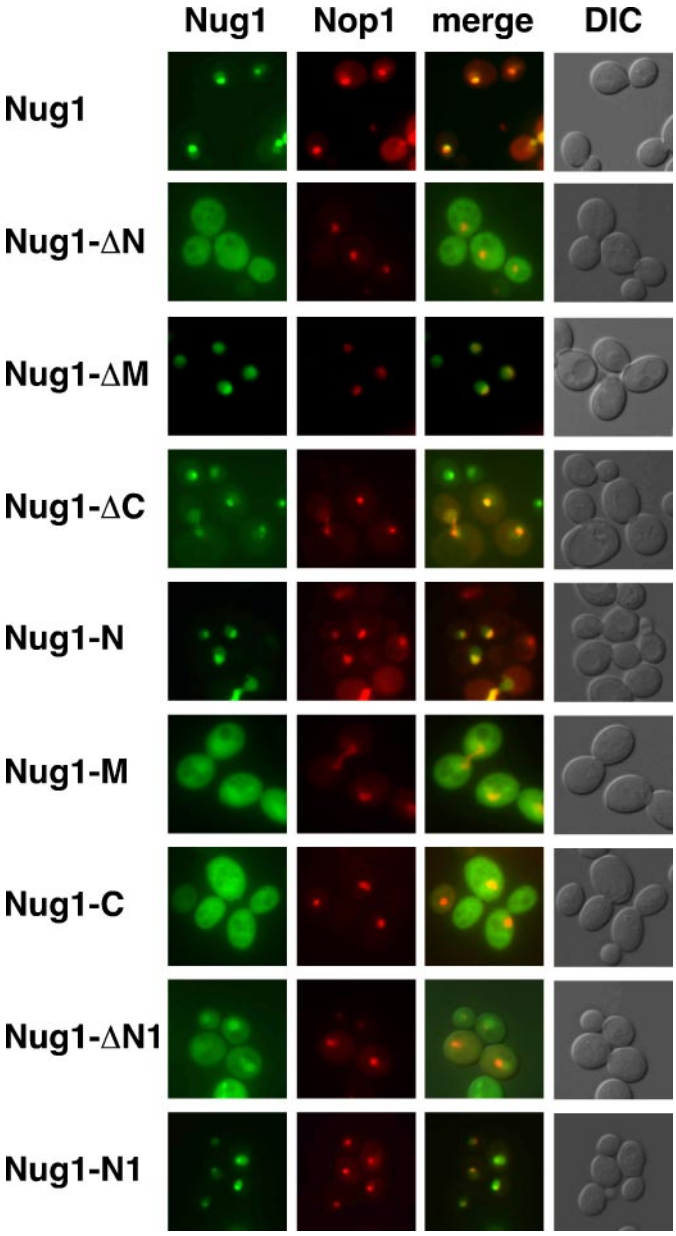

FIGURE 3. **Subcellular localization of Nug1 domain constructs.** The indicated Nug1 constructs were C-terminally fused to EGFP and analyzed for co-localization with mRFP-NOP1 in exponentially growing yeast cells (Nug1 shuffle strain) by fluorescence microscopy (see "Experimental Procedures"). Representative pictures of yeast cells show the signals for EGFP (Nug1), mRFP (Nop1), an overlay of EGFP with mRFP (*merge*), and differential interference contrast (*DIC*).

ments that lacked the N-domain (*e.g.* Nug1-ΔN) revealed a predominantly cytoplasmic location with a weak nuclear signal (Fig. 3). Altogether the data suggest that the N-domain of Nug1 when attached to a reporter protein can mediate nucle(ol)ar localization.

To further delimit the nucle(ol)ar targeting signal, the first 39 amino acids of the N-domain, which is rich in positively charged amino acids (M**R**V**RKR**QS**RR**TST**K**L**K**EGI**KKK**ASA-**HRKK**E**KK**MA**KK**DVT; pI = 11.76), were fused to EGFP. In contrast, the second half of the N-domain is acidic (pI = 4.37). As seem in Fig. 3, the N-terminal basic sequence of Nug1 (Nug1-N1) is sufficient to target the attached EGFP reporter to the nucleus/nucleolus. Conversely, a construct lacking the first 37 amino acids from Nug1 (Nug1-ΔN1-EGFP) no longer mediated nucleolar accumulation but was still able to target to the nucleus. Moreover, a fraction of Nug1-ΔN1-EGFP was also detected in the cytoplasm (Fig. 3). In conclusion, the N-terminal end of Nug1 exhibits a basic sequence that is sufficient and necessary for nucleolar accumulation of Nug1.

To correlate nucle(ol)ar location of Nug1-N with binding to 60 S pre-ribosomes, we performed sucrose gradient centrifugation to analyze the association of wild-type Nug1 and its various truncation constructs with pre-60 S subunits (Fig. 4). The $A_{260\ nm}$ profile of these gradients shows the sedimentation of 40 S and 60 S subunits, 80 S ribosomes, and polysomes (Fig. 4, *upper panels*). The sedimentation of the TAP-tagged wild-type and mutant Nug1 proteins was determined by Western analysis (Fig. 4, *lower panels*). Interestingly, wild-type Nug1 and the N-terminal constructs Nug1-N and Nug1-N1 are associated with high molecular weight complexes, presumably pre-60 S particles. In contrast, constructs lacking the N-terminal domain (Nug1-ΔN) or part of it (Nug1-ΔN1) did not associate with the high molecular particles and were mainly detected in the fractions of the gradient, containing the soluble proteins (Fig. 4). Notably, Nug1-N1 revealed a broad distribution with large complexes (in the range of pre-60 S particles). Notably, if endogenous Nug1 was absent, the viable Nug1-ΔN1-(38–520) was also weakly associated with large structures. These data indicate that the entire N-domain is necessary and sufficient for association with large assemblies, which likely correspond to pre-60 S subunits.

To show a direct association with pre-60 S particles, we performed tandem affinity purification of various Nug1 constructs. Significantly, when TAP-tagged Nug1-N was affinity-purified, it co-precipitated pre-60 S subunits that contained a set of non-ribosomal factors, the most prominent ones being Dbp10, Erb1, Nop2, Nop7, Noc3, Nog1, Has1, and Nug2 (Fig. 5). The same pre-60 S factors were also co-enriched when full-length Nug1-TAP was affinity-purified (Fig. 5). Purification of the Nug1-N1 construct, which has a shortened N-domain, caused substantial loss of these pre-60 S factors, but association with 60 S subunits was not abolished. Thus, Nug1-N1 may exhibit a relatively unspecific binding to 60 S subunits. Consistent with this interpretation, Nug1-N1 was also detected in fractions corresponding to polysomes (Fig. 4). In contrast, affinity purification of TAP-tagged Nug1-ΔN or Nug1-ΔN1 lacking the entire N-domain or part of it, respectively, revealed a complete loss of both pre-60 S factors and ribosomal Rpl proteins (Fig. 5). Taken together, the data showed that the N-domain of Nug1 confers nucle(ol)ar location and association with pre-60 S particles that exhibit a typical set of pre-60 S factors. However, the middle and C-domain of Nug1 (Nug1-ΔN) are not significantly associated with pre-60 S particles under the biochemical conditions tested.

The N-terminal Domain of Nug1 Interacts with RNA—The observation that the N-domain of Nug1 mediates recruitment to the pre-60 S subunit suggested that it binds to the particle through either a protein or an RNA interaction. Notably, we observed that recombinant Nug1 purified from *E. coli* co-enriched RNA.[4] Therefore, we sought to test whether Nug1 via its

[4] J. Bassler and E. Hurt, unpublished results.

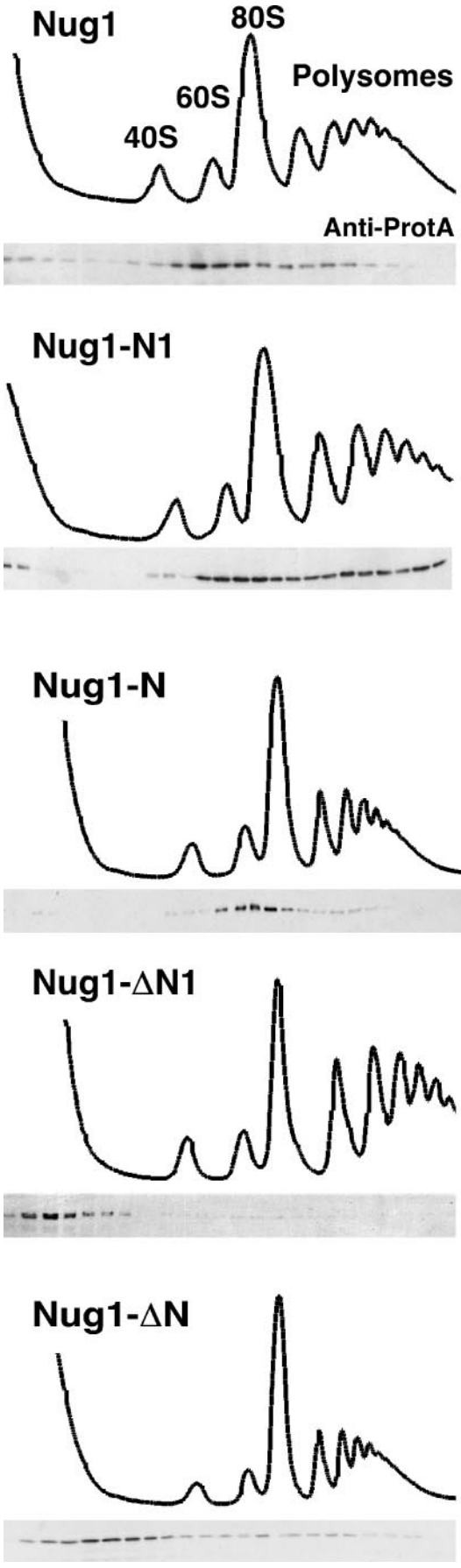

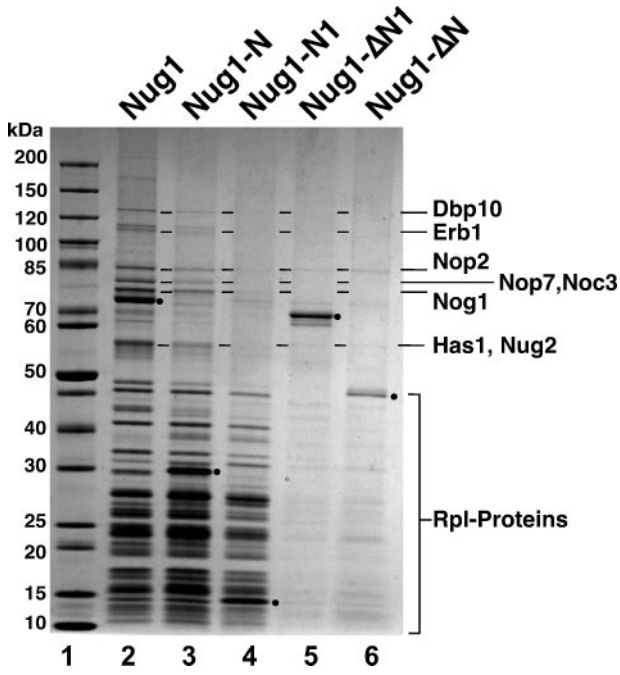

FIGURE 5. **Purification of Nug1 domain constructs.** The indicated Nug1 domain constructs, all tagged with the TAP epitope, were affinity-purified by the TAP-method (see "Experimental Procedures"). Purified Nug1 domain constructs were analyzed on an SDS 4–12% gradient polyacrylamide gel followed by Coomassie Blue staining. The Nug1 bait proteins are marked by *filled circles*. Prominent bands of the Nug1-N purification were identified by mass spectrometry and are indicated on the *right*.

N-domain can bind to RNA in general. As a first approach, we employed the yeast three-hybrid system to test for a possible interaction of Nug1 with RNA (23,28) (Fig. 6*A*). In the past, several specific RNA-protein interactions have been demonstrated in the three-hybrid system including interaction between ribosomal protein Rps14 and helix 23 of 18 S rRNA (29). We could validate interaction of Rps14 with helix 23 rRNA in our three-hybrid analysis, but Nug1 did not interact with helix 23 rRNA (Fig. 6*B*). Notably, Nug1 revealed a strong three-hybrid interaction with 5 S rRNA (Fig. 6*B*). However, no three-hybrid interaction was observed between Nug1 and 5.8 S rRNA or reverse 5 S rRNA. Additional controls revealed that Rps14 did not interact with 5 S, 5.8 S, and reverse 5 S rRNA (Fig. 6*B*). Since the N-domain of Nug1 mediates binding to pre-60 S subunits, we tested whether Nug1-N interacts with 5 S rRNA in the three-hybrid assay. As shown in Fig. 6*C*, the Nug1-N construct, but not Nug1-ΔN, exhibited a three-hybrid interaction with 5 S rRNA.

To confirm that Nug1 binds directly to RNA via its N-domain, we performed RNA electrophoresis mobility shift assays. First, the Nug1 N-terminal domain was expressed in *E. coli* as His_6-Nug1-N and purified to homogeneity by nickel-nitrilotri-

FIGURE 4. **Sedimentation of Nug1 domain constructs on sucrose gradients.** The indicated Nug1 domain constructs were fused C-terminally to the TAP tag and expressed in a *NUG1*$^+$ background. Cell lysates derived from these strains were centrifuged on 10–50% sucrose gradients, and the absorption profile of these gradients at A_{260} is shown (*upper panels*). Peaks representing 40 S, 60 S, 80 S, and polysomes are indicated. Fractions were collected from these sucrose gradients and analyzed by Western blotting (anti-protein A (*Anti-ProtA*)) to detect Nug1 and the various Nug1 domain constructs (*lower panels*).

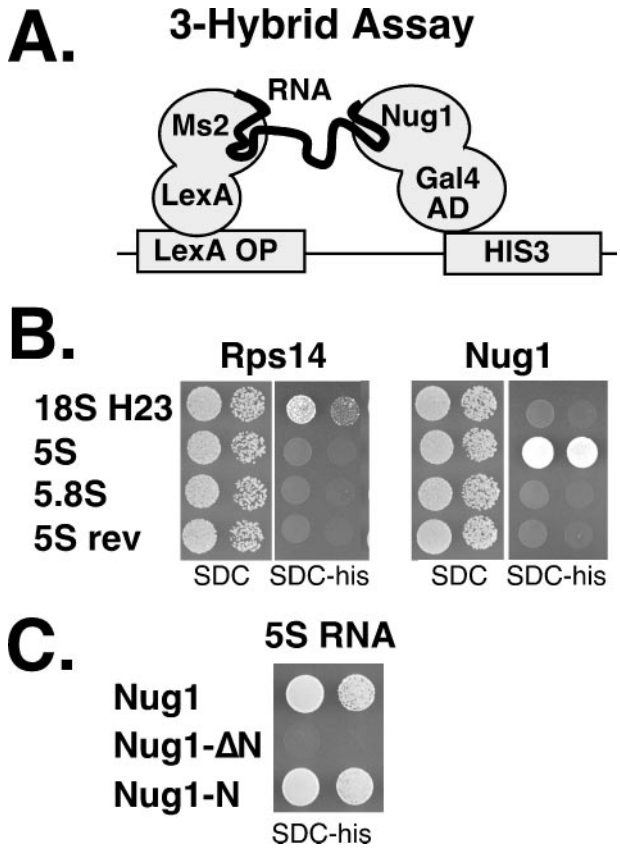

FIGURE 6. **The Nug1-N domain interacts with 5 S rRNA in the three-hybrid assay.** *A,* schematic drawing of the principle of the three-hybrid assay. LexA-MS2 fusion protein is targeted via LexA to LexA operator (*LexA OP*). MS2 binds to its cognate RNA, which is fused to the RNA of interest. Protein of interest to be tested for RNA interaction (*e.g. NUG1*) is fused to the *GAL4* activation domain (*GAL4 AD*). Interaction of Nug1 with RNA induces expression of the *HIS3* reporter gene. *B,* the L40-coat yeast strain was transformed with pACTII-NUG1 or pACTII-RPS14, respectively, and various p3A-MS2 vectors expressing indicated the RNAs fused to MS2 RNA. Transformants were spotted in 10^{-1} dilution steps on SDC-leu-trp-ura (*SDC*; *left panel*) and SDC-leu-trp-ura-his plates containing 5 mM 3-AT (*SDC-his*; *right panel*). Growth behavior is shown after 4 days of incubation at 30 °C. A similar doubling time could be observed on SDC-his plates up to 15 mM 3-AT (data not shown). *rev*, reverse. *C,* the L40-coat yeast strain was co-transformed with pACTII-NUG1 (1–520), pACTII-NUG1-ΔN (residues 146–520), or pACTII-NUG1-N (residues 1–145), respectively, and p3A MS2–5 S rRNA vector expressing 5 S rRNA. Transformants were spotted in 10^{-1}dilution steps on SDC-leu-trp-ura-his plates containing 5 mM 3-AT (SDC-his). Growth phenotype is shown after 3 days incubation at 30 °C.

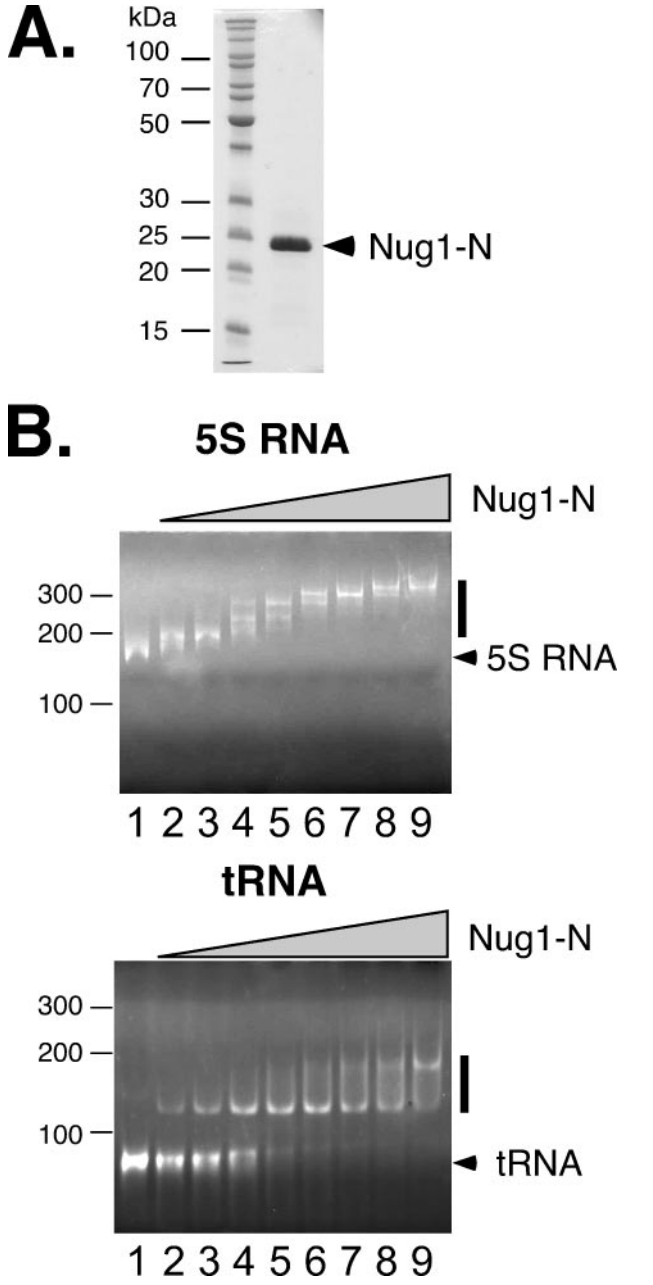

FIGURE 7. **Nug1-N binds directly to RNA.** *A,* recombinant His_6-Nug1-N (residues 1–145) was purified via affinity purification and gel filtration. Purified His_6-Nug1-N was analyzed on a SDS 4–12% polyacrylamide gel and visualized by Coomassie Blue staining. *B,* 5 S rRNA (*upper panel*) and tRNA (*lower panel*) were incubated with no protein (*lane 1*) and increasing amounts of His_6-Nug1-N (*lanes 2–9*). The size of the RNA ladder (in nucleotides) is indicated at the *left side* of the gel. Non-shifted RNA is marked by an *arrow*, and the formation of RNA-protein complexes is indicated by a *dark line* on the *right*.

acetic acid affinity purification and subsequent gel filtration on Superdex^{TM}200 (Fig. 7*A*). As an RNA substrate, we used *in vitro* synthesized 5 S rRNA and commercially available yeast tRNA. We observed that 5 S rRNA, but also tRNA, were efficiently retarded in their migration on the native polyacrylamide gel (band shift) when increasing amounts of the Nug1 N-domain were added (Fig. 7*B*). The formation of Nug1-N/5 S rRNA complexes was still observed in buffers that contained high salt (*e.g.* 500 mM NaCl). Since *nug1-ΔN1* or *nug1-1* mutants are not genetically linked to *rpl5* or 5 S rRNA mutants (data not shown), we assume that *in vitro* binding of Nug1 to 5 S rRNA and tRNA reflects a general RNA binding activity of the Nug1 N-domain. However, it remains to be shown whether *in vivo* Nug1 binds to 5 S rRNA or to another rRNA species within the pre-60 S subunit (see "Discussion").

NUG1 via Its N-terminal Domain Genetically Interacts with pre-60 S Factors NOC2, NOC3, DBP10, and BUD20—To characterize the functional interaction of the Nug1 N-domain with components of the pre-60 S subunit *in vivo*, we performed a synthetic lethal (SL) screen with the *nug1-ΔN1* allele using a red-white colony-sectoring assay (14). From this SL screen, we could isolate synthetic lethal mutants SL46, SL78, and SL105 that were complemented by *DBP10*, *NOC3*, and *BUD20*, respectively. Noc3 and Dbp10 are known pre-60 S factors that are essential for 60 S subunit biogenesis (30, 31) and co-purify

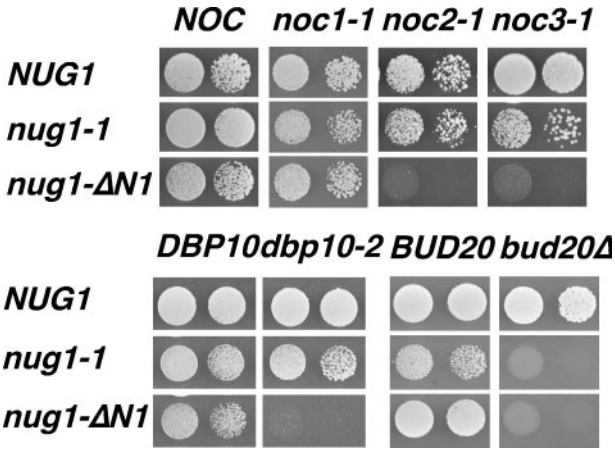

FIGURE 8. **Nug1-ΔN1 is synthetically lethal with *noc2-1*, *noc3-1*, and *dbp10-2* mutant alleles.** Double disruptions strains (see supplemental Table 1) were transformed with plasmids harboring the indicated wild-type and mutant alleles. Transformants were spotted in 10^{-1} dilution steps on SDC+FOA plates and grown at 30 °C for 5 days.

with the Nug1 pre-ribosomal particle (7, 14). Likewise, the non-essential Bud20 was found in several pre-60 S particles that also contained Nug1 (32, 33). Affinity purification of Bud20-TAP co-enriched a late pre-60 S particle that contained several pre-60 S factors including Nug1 (data not shown).

To confirm the genetic interactions between Nug1-N domain and the various pre-60 S factors, we directly combined mutant alleles of *nug1* with mutant alleles of *dbp10* and *noc3* (see "Experimental Procedures"). Noc3 is part of the nuclear Noc2-Noc3 complex that replaces the nucleolar Noc1 from the Noc1-Noc2 complex during pre-60 S biogenesis (30). Therefore, we tested for a genetic interaction between *noc1-1* and *noc2-1* alleles with *nug1-ΔN1*. This analysis revealed that the *nug1-ΔN1*, but not *nug1-1*, which carries a mutation in the C-domain (R420P), is synthetically lethal with *noc2-1* and *noc3-1*. Notably, *nug1-ΔN1* is not SL with *noc1-1* (Fig. 8). Moreover, *dbp10-2* is synthetically lethal with *nug1-ΔN1* but not with *nug1-1*. These results correlate with the findings that Noc2-Noc3 and Dbp10 are present in the Nug1 particle, whereas Noc1 is absent (7, 14). In contrast, *bud20Δ* is genetically linked to several *nug1* mutant alleles, which are not restricted to the Nug1 N-terminal domain (Fig. 8 and data not shown). Interestingly, the *mtr2-33 allele,* which was shown to be SL with the C-terminal mutant *nug1-1* (14), is not linked to the *nug1-ΔN1* mutation (data not shown). Moreover, other factors present in the Nug1 pre-60 S particle such as Rlp7, Rea1, Nop7, and Nsa3 did not show genetic interactions with the various *nug1* mutants (data not shown). Thus, the genetic analyses revealed that Noc2-Noc3 and Dbp10 are specifically linked to the N-domain of Nug1.

DISCUSSION

In this study, we showed that the N-terminal domain of Nug1 is essential for the correct nucle(ol)ar localization and association with pre-60 S particles. Moreover, we demonstrated that the Nug1-N domain binds directly to RNA. Due to this general binding activity, we suggest that Nug1 binds to the rRNA of the pre-60 S subunit. However, additional pre-60 S factors could play a role in targeting Nug1 to its specific site(s) at the pre-60 S particle.

Sequence analysis revealed that Nug1 belongs to the family of YawG GTPases characterized by permutated GTP motifs (19). Significantly, many of these GTPases have been described to function in ribosome biogenesis. It was demonstrated that yeast Nug1, Nug2/Nog2, and Lsg1/Kre35, which all are YawG family members, are essential for 60 S subunit maturation (8, 14–17). Furthermore, another YawG member, Mtg1, was suggested to play a role in assembly of the mitochondrial large ribosomal subunit (34). In *Saccharomyces pombe,* it was demonstrated that the Nug1 homologue Grn1 is involved in 60 S biogenesis (35).

Do these GTPases with permutated GTP motifs have related roles in large subunit biogenesis? Recently, the three-dimensional structures of two members of this family, RsgA (ribosome small subunit-dependent GTPaseA/YjeQ (36)) and RbgA (ribosome biogenesis GTPaseA/Ylqf (Protein Data Bank accession number 1PUJ)),[5] have been solved. Despite the permutated order, the GTP-binding pocket is highly homologous to those of classical GTPases. Significantly, the prokaryotic GTPases have different N- and C-terminal domains, indicative of different functions *in vivo*. RsgA binds to the small 30 S subunit, which is mediated by the N terminus (27, 38). This domain has an OB fold (26, 36) that is characteristic for a class of RNA-binding proteins. Moreover, RsgA has an intrinsic GTPase activity (k_{cat} = 0.13 min^{-1} at 23 °C; ref. 38) that is similar to the activity determined for Nug1 (k_{cat} of 0.11 min^{-1} ± 0.01 min^{-1}). Significantly, the intrinsic GTP hydrolysis activity of Nug1 is ~20–100 times higher than the GTP hydrolysis activity of Rab GTPases. However, Rab GTPases that are stimulated by GTPase-activating protein have a still ~5–20 times higher GTPase activity than the intrinsic Nug1 GTPase activity (39, 40). Therefore, it remains to be shown whether a GTPase-activating protein exists for Nug1. Interestingly, RsgA GTPase activity could be stimulated 80-fold by the small subunit (27). Thus, binding of Nug1 to pre-60 S subunits could regulate its GTPase activity.

Significantly, the C-domain of the essential RbgA, which is involved in 50 S biogenesis (41), shares homology to the Nug1-C domain (supplemental figure Fig. S1). Moreover, modeling of the Nug1 sequence, based on the structure of RbgA, revealed that the R420P mutation in *nug1-1* is in an exposed helix that is part of the C-domain. It is possible that the C-domain recruits pre-60 S factors, which is regulated by the middle GTPase domain.

The human homologue of Nug1 is nucleostemin (supplemental figure Fig. S1). Despite the high sequence homology, nucleostemin was not able to complement a *nug1* or *nug2* deletion strain.[6] Notably, nucleostemin is highly expressed in stem and cancer cells but is down-regulated in differentiated cells, suggesting that nucleostemin is involved in regulation of cell proliferation and cell cycle progression (42–44). These findings would be consistent with a role of nucleostemin in ribosome biogenesis since dividing cells are highly dependent on newly

[5] R. Kniewel, J. Buglino, and C. D. Lima, personal communication.
[6] J. Bassler, unpublished results.

synthesized ribosomal subunits. Similar to our findings with Nug1, it was reported that the nucleolar localization of nucleostemin depends on the first 46 amino acids (42). Moreover, the nucleolar location of nucleostemin was shifted toward the nucleoplasm upon mutation of the G1 motif (37).

Taken together, our studies suggest that Nug1 binds to pre-60 S particles in the nucleolus and accompanies them to the nucleoplasm. Binding of Nug1 to pre-60 S subunits is mediated by an N-terminal RNA-binding domain, which is functionally linked to the Noc2/Noc3 complex and to the RNA helicase Dbp10. Future analysis will reveal the role of the Nug1 GTPase domain and other trans-acting factors in regulating these various 60 S biogenesis steps.

Acknowledgments—We are grateful to Dr. John Woolford for sending plasmid pACTII-RPS14, Dr. Marvin Wickens for yeast strain L40 and plasmid pIIIA/MS2-1, Dr. Patrick Linder for the DBP10 strain and plasmids, Dr. Sylvie Camier-Thuillier for providing plasmids pRSC3, pOK3, and pOK8, and Dr. Olivier Gadal for sharing the unpublished plasmid pUN100-mRFP-NOP1.

REFERENCES

1. Dragon, F., Gallagher, J. E., Compagnone-Post, P. A., Mitchell, B. M., Porwancher, K. A., Wehner, K. A., Wormsley, S., Settlage, R. E., Shabanowitz, J., Osheim, Y., Beyer, A. L., Hunt, D. F., and Baserga, S. J. (2002) *Nature* **417,** 967–970
2. Grandi, P., Rybin, V., Bassler, J., Petfalski, E., Strauss, D., Marzioch, M., Schafer, T., Kuster, B., Tschochner, H., Tollervey, D., Gavin, A. C., and Hurt, E. (2002) *Mol. Cell* **10,** 105–115
3. Kressler, D., Linder, P., and de La Cruz, J. (1999) *Mol. Cell Biol.* **19,** 7897–7912
4. Venema, J., and Tollervey, D. (1999) *Annu. Rev. Genet.* **33,** 261–311
5. Osheim, Y. N., French, S. L., Keck, K. M., Champion, E. A., Spasov, K., Dragon, F., Baserga, S. J., and Beyer, A. L. (2004) *Mol. Cell* **16,** 943–954
6. Schäfer, T., Strauss, D., Petfalski, E., Tollervey, D., and Hurt, E. (2003) *EMBO J.* **22,** 1370–1380
7. Nissan, T. A., Bassler, J., Petfalski, E., Tollervey, D., and Hurt, E. (2002) *EMBO J.* **21,** 5539–5547
8. Hedges, J., West, M., and Johnson, A. W. (2005) *EMBO J.* **24,** 567–579
9. Tschochner, H., and Hurt, E. (2003) *Trends Cell Biol.* **13,** 255–263
10. Fromont-Racine, M., Senger, B., Saveanu, C., and Fasiolo, F. (2003) *Gene* (*Amst.*) **313,** 17–42
11. Granneman, S., and Baserga, S. J. (2004) *Exp. Cell Res.* **296,** 43–50
12. Nissan, T. A., Galani, K., Maco, B., Tollervey, D., Aebi, U., and Hurt, E. (2004) *Mol. Cell* **15,** 295–301
13. Schäfer, T., Maco, B., Petfalski, E., Tollervey, D., Böttcher, B., Aebi, U., and Hurt, E. (2006) *Nature* **441,** 651–655
14. Bassler, J., Grandi, P., Gadal, O., Lessmann, T., Petfalski, E., Tollervey, D., Lechner, J., and Hurt, E. (2001) *Mol. Cell* **8,** 517–529
15. Saveanu, C., Bienvenu, D., Namane, A., Gleizes, P. E., Gas, N., Jacquier, A., and Fromont-Racine, M. (2001) *EMBO J.* **20,** 6475–6484
16. Saveanu, C., Namane, A., Gleizes, P. E., Lebreton, A., Rousselle, J. C., Noaillac-Depeyre, J., Gas, N., Jacquier, A., and Fromont-Racine, M. (2003) *Mol. Cell Biol.* **23,** 4449–4460
17. Kallstrom, G., Hedges, J., and Johnson, A. (2003) *Mol. Cell Biol.* **23,** 4344–4355
18. West, M., Hedges, J. B., Chen, A., and Johnson, A. W. (2005) *Mol. Cell Biol.* **25,** 3802–3813
19. Leipe, D. D., Wolf, Y. I., Koonin, E. V., and Aravind, L. (2002) *J. Mol. Biol.* **317,** 41–72
20. Strässer, K., Bassler, J., and Hurt, E. (2000) *J. Cell Biol.* **150,** 695–706
21. Maniatis, T., Fritsch, E. T., and Sambrook, J. (1982) *Molecular Cloning: A Laboratory Manual*, Cold Spring Harbor Laboratory, Cold Spring Harbor, NY
22. Fiske, L. M., and Subbarow, Y. (1925) *J. Biol. Chem.* **66,** 375–389
23. Bernstein, D. S., Buter, N., Stumpf, C., and Wickens, M. (2002) *Methods* **26,** 123–141
24. Rigaut, G., Shevchenko, A., Rutz, B., Wilm, M., Mann, M., and Seraphin, B. (1999) *Nat. Biotechnol.* **17,** 1030–1032
25. Siniossoglou, S., Wimmer, C., Rieger, M., Doye, V., Tekotte, H., Weise, C., Emig, S., Segref, A., and Hurt, E. C. (1996) *Cell* **84,** 265–275
26. Daigle, D. M., Rossi, L., Berghuis, A. M., Aravind, L., Koonin, E. V., and Brown, E. D. (2002) *Biochemistry* **41,** 11109–11117
27. Himeno, H., Hanawa-Suetsugu, K., Kimura, T., Takagi, K., Sugiyama, W., Shirata, S., Mikami, T., Odagiri, F., Osanai, Y., Watanabe, D., Goto, S., Kalachnyuk, L., Ushida, C., and Muto, A. (2004) *Nucleic Acids Res.* **32,** 5303–5309
28. SenGupta, D. J., Zhang, B., Kraemer, B., Pochart, P., Fields, S., and Wickens, M. (1996) *Proc. Natl. Acad. Sci. U. S. A.* **93,** 8496–8501
29. Fewell, S. W., and Woolford, J. L., Jr. (1999) *Mol. Cell Biol.* **19,** 826–834
30. Milkereit, P., Gadal, O., Podtelejnikov, A., Trumtel, S., Gas, N., Petfalski, E., Tollervey, D., Mann, M., Hurt, E., and Tschochner, H. (2001) *Cell* **105,** 499–509
31. Burger, F., Daugeron, M. C., and Linder, P. (2000) *Nucleic Acids Res.* **28,** 2315–2323
32. Ho, Y., Gruhler, A., Heilbut, A., Bader, G. D., Moore, L., Adams, S. L., Millar, A., Taylor, P., Bennett, K., Boutilier, K., Yang, L., Wolting, C., Donaldson, I., Schandorff, S., Shewnarane, J., Vo, M., Taggart, J., Goudreault, M., Muskat, B., Alfarano, C., Dewar, D., Lin, Z., Michalickova, K., Willems, A. R., Sassi, H., Nielsen, P. A., Rasmussen, K. J., Andersen, J. R., Johansen, L. E., Hansen, L. H., Jespersen, H., Podtelejnikov, A., Nielsen, E., Crawford, J., Poulsen, V., Sorensen, B. D., Matthiesen, J., Hendrickson, R. C., Gleeson, F., Pawson, T., Moran, M. F., Durocher, D., Mann, M., Hogue, C. W., Figeys, D., and Tyers, M. (2002) *Nature* **415,** 180–183
33. Gavin, A. C., Bosche, M., Krause, R., Grandi, P., Marzioch, M., Bauer, A., Schultz, J., Rick, J. M., Michon, A. M., Cruciat, C. M., Remor, M., Hofert, C., Schelder, M., Brajenovic, M., Ruffner, H., Merino, A., Klein, K., Hudak, M., Dickson, D., Rudi, T., Gnau, V., Bauch, A., Bastuck, S., Huhse, B., Leutwein, C., Heurtier, M. A., Copley, R. R., Edelmann, A., Querfurth, E., Rybin, V., Drewes, G., Raida, M., Bouwmeester, T., Bork, P., Seraphin, B., Kuster, B., Neubauer, G., and Superti-Furga, G. (2002) *Nature* **415,** 141–147
34. Barrientos, A., Korr, D., Barwell, K. J., Sjulsen, C., Gajewski, C. D., Manfredi, G., Ackerman, S., and Tzagoloff, A. (2003) *Mol. Biol. Cell* **14,** 2292–2302
35. Du, X., Rao, M. R., Chen, X. Q., Wu, W., Mahalingam, S., and Balasundaram, D. (2006) *Mol. Biol. Cell* **17,** 460–474
36. Shin, D. H., Lou, Y., Jancarik, J., Yokota, H., Kim, R., and Kim, S. H. (2004) *Proc. Natl. Acad. Sci. U. S. A.* **101,** 13198–13203
37. Tsai, R. Y., and McKay, R. D. (2005) *J. Cell Biol.* **168,** 179–184
38. Daigle, D. M., and Brown, E. D. (2004) *J. Bacteriol.* **186,** 1381–1387
39. De Antoni, A., Schmitzova, J., Trepte, H. H., Gallwitz, D., and Albert, S. (2002) *J. Biol. Chem.* **277,** 41023–41031
40. Albert, S., and Gallwitz, D. (1999) *J. Biol. Chem.* **274,** 33186–33189
41. Uicker, W. C., Schaefer, L., and Britton, R. A. (2006) *Mol. Microbiol.* **59,** 528–540
42. Tsai, R. Y., and McKay, R. D. (2002) *Genes Dev.* **16,** 2991–3003
43. Sijin, L., Ziwei, C., Yajun, L., Meiyu, D., Hongwei, Z., Guofa, H., Siguo, L., Hong, G., Zhihong, Z., Xiaolei, L., Yingyun, W., Yan, X., and Weide, L. (2004) *J. Exp. Clin. Cancer Res.* **23,** 529–538
44. Liu, S. J., Cai, Z. W., Liu, Y. J., Dong, M. Y., Sun, L. Q., Hu, G. F., Wei, Y. Y., and Lao, W. D. (2004) *World J. Gastroenterol.* **10,** 1246–1249

ONLINE SUPPLEMENTARY DATA

Figure S1: Nug1 is homologous to nucleostemin (NS) and RbgA/Ylqf. Sequence alignment was done using CustalW and displayed with Boxshade (available at www.ch.embnet.org). N-terminal RNA binding domain is marked in green, NLS in black, GTP binding motifs in red and C-terminal domain in blue. Borders of constructs used in this study are indicated.

Table I: *S. cerevisiae* strains used in this study

Table II: Plasmids used in this study

supplementary Figure S1

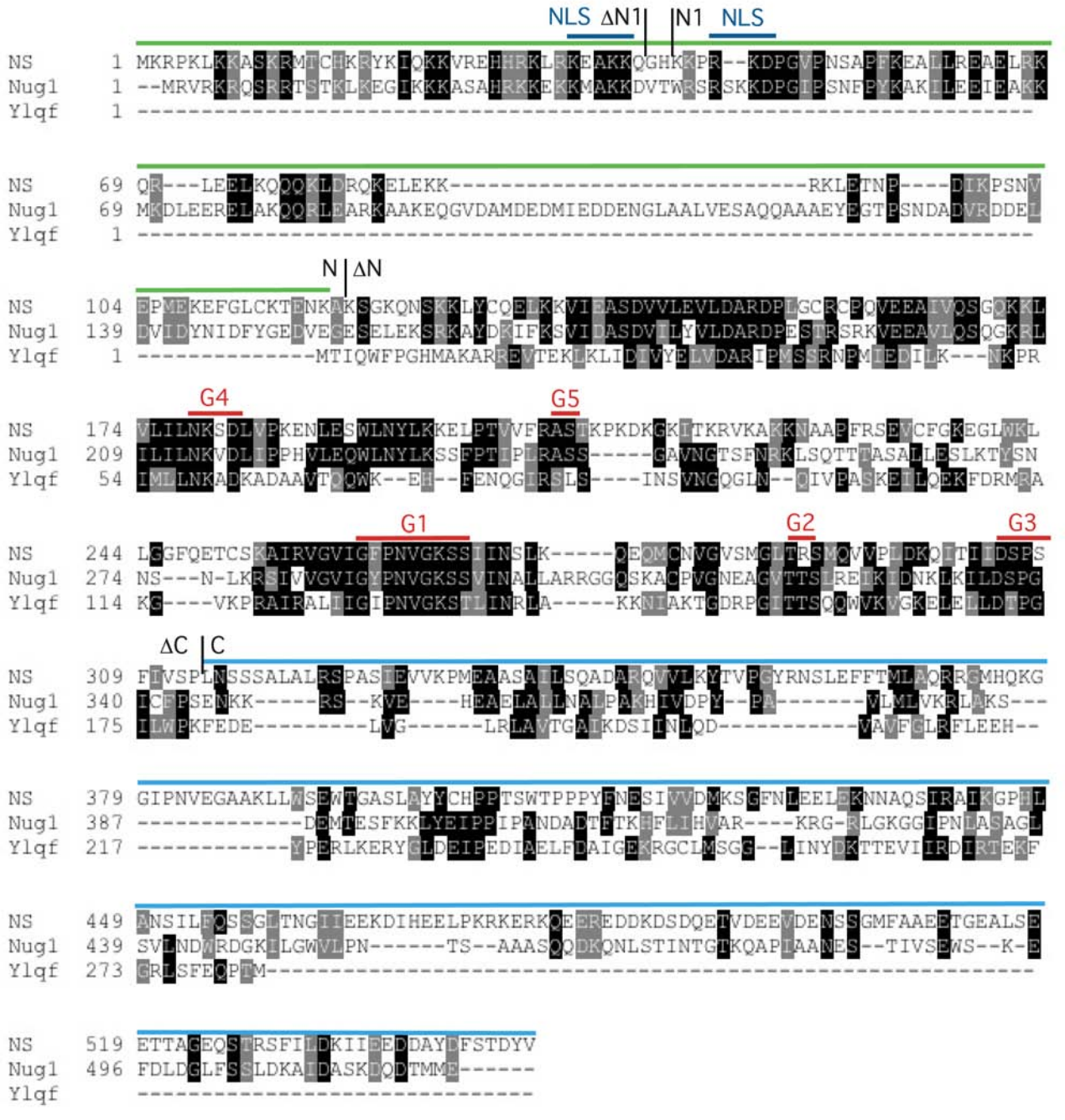

Table I: ***S. cerevisiae*** **strains used in this study**

Name	Genotype	Reference
NUG1 shuffle	*MATa*, *his3*, *ura3*, *leu2*, *trp1*, *nug1*::*kanMX4* + pRS316-NUG1	(14)
NUG2 shuffle	*MATa*, *his3*, *ura3*, *leu2*, *trp1*, lys2, *nug1*::*kanMX4* + pRS416-NUG2	(14)
L40-coat	*MATa*, *his3-200, ura3-52, leu2-3, 112, trp1-1, ade2, LYS2::(lexA op)-HIS3*, LexA-MS2 coat (*TRP1*)	(28)
nug1ΔN pzf1Δ	*his3*, *ura3*, *leu2*, *trp1*, *nug1*::*kanMX4*, *pzf1*::*kanMX4* + pRS315-nug1-ΔN1 + pJA230 (*ARS*/*CEN, URA3, PZF1*))	this study
NUG1 pzf1Δ	*his3*, *ura3*, *leu2*, *trp1*, *nug1*::*kanMX4*, *pzf1*::*kanMX4* + pRS315-NUG1 + pJA230 (*ARS*/*CEN, URA3, PZF1*))	this study
nug1Δ noc1Δ	*MATa*, *his3*, *ura3*, *leu2*, *trp1*, ade*2*, *nug1*::*kanMX4*, *noc1::HIS3*, + pRS316-NUG1 + YCplac33-NOC1)	this study
nug1Δ noc2Δ	*MATa*, *his3*, *ura3*, *leu2*, *trp1*, *ade2*, *nug1*::*kanMX4 noc2*::*HIS3* + pRS316-NUG1, pRS316 NOC2	this study
nug1Δ noc3Δ	*MATa*, *his3*, *ura3*, *leu2*, *trp1*, *nug1*::*kanMX4 noc3*::*HIS3* + pRS316-NUG1, pRS316-NOC3	this study
nug1Δ dbp10Δ	*MATa*, *his3*, *ura3*, *leu2*, *trp1*, *nug1*::*kanMX4, dbp10*::*KanMX* + pRS316-NUG1 + pRS314-DBP10	this study
nug1Δ bud20Δ	*MATa*, *his3*, *ura3*, *leu2*, *trp1*, *nug1*::*kanMX4, bud20*::*KanMX* + pRS316-NUG1	this study

Table II: **Plasmids used in this study**

Name	Genotype	Reference
pRS315-NUG1-eGFP	*ARS/CEN, LEU2,* P_{NUG1} *NUG1-eGFP*	(14)
pRS315-nug1-4G-eGFP	*ARS/CEN, LEU2,* P_{NUG1} *nug1-eGFP (G292G, K293G, S294G, S295G)*	this study
pRS315-nug1-N1-eGFP	*ARS/CEN, LEU2,* P_{NUG1} *nug1-eGFP (1-39 aa)*	this study
pRS315-nug1-N-eGFP	*ARS/CEN, LEU2,* P_{NUG1} *nug1-eGFP (1-154 aa)*	this study
pRS315-nug1-M-eGFP	*ARS/CEN, LEU2,* P_{NUG1} *nug1-eGFP (155-344 aa)*	this study
pRS315-nug1-C-eGFP	*ARS/CEN, LEU2,* P_{NUG1} *nug1-eGFP (345-520 aa)*	this study
pRS315-nug1-ΔN1-eGFP	*ARS/CEN, LEU2,* P_{NUG1} *nug1-eGFP (38-520 aa)*	this study
pRS315-nug1-ΔN-eGFP	*ARS/CEN, LEU2,* P_{NUG1} *nug1-eGFP (155-520 aa)*	this study
pRS315-nug1-ΔM-eGFP	*ARS/CEN, LEU2,* P_{NUG1} *nug1-eGFP (1-154 aa;345-520 aa)*	this study
pRS315-nug1-ΔC-eGFP	*ARS/CEN, LEU2,* P_{NUG1} *nug1-eGFP (1-344 aa)*	this study
pRS313-nug1-N-eGFP	*ARS/CEN, LEU2,* P_{NUG1} *nug1-eGFP (1-154 aa)*	this study
pRS314 mRFP NOP1	*ARS/CEN TRP1,* P_{NOP1} *mRFP-NOP1* derived from *pUN100-mRFP-NOP1* (O. Gadal, unpublished material).	this study
pRS315-NUG1-TAP	*ARS/CEN, LEU2,* P_{NUG1} *NUG1-TAP*	(14)
pRS315-nug1-4G-TAP	*ARS/CEN, LEU2,* P_{NUG1} *nug1-TAP (G292G, K293G, S294G, S295G)*	this study
pRS315-nug1-N1-TAP	*ARS/CEN, LEU2,* P_{NUG1} *nug1-TAP (1-39 aa)*	this study
pRS315-nug1-N-TAP	*ARS/CEN, LEU2,* P_{NUG1} *nug1-TAP (1-154 aa),*	this study
pRS315-nug1-ΔC-TAP	*ARS/CEN, LEU2,* P_{NUG1} *nug1-TAP (1-344 aa)*	this study
pRS315-nug1-ΔN1-TAP	*ARS/CEN, LEU2,* P_{NUG1} *nug1-TAP (38-520 aa)*	this study
pRS315-nug1-ΔN-TAP	*ARS/CEN, LEU2,* P_{NUG1} *nug1-TAP (155-520 aa)*	this study
pRS315-nug1-C-TAP	*ARS/CEN, LEU2,* P_{NUG1} *nug1-TAP (345-520 aa).*	this study

Table II: **Plasmids used in this study** (continued)

Name	Genotype	Reference
pRS314-nug1-C	*ARS/CEN, TRP1, P_{NUG1} nug1 (345-520 aa)*	this study
pRS314-nug1-ΔN	*ARS/CEN, TRP1, P_{NUG1} nug1 (155-520 aa)*	this study
pRS314-nug1-1	*ARS/CEN, TRP1, P_{NUG1} nug1 (R420P)*	(14)
pRS314-nug1-2	*ARS/CEN, TRP1, P_{NUG1} nug1 (K22R, L61S, Q81R, Q202R, T409A, L415S)*	(14)
pRS314-nug1-ΔN1	*ARS/CEN, TRP1, P_{NUG1} nug1 38-520 aa*	this study
pRS315-nug1-ΔN1	*ARS/CEN, LEU2, P_{NUG1} nug1 38-520 aa*	this study
pRS316-NUG1	*ARS/CEN, URA3, P_{NUG1} NUG1*	(14)
pRS416-NUG2	*ARS/CEN, URA3, P_{NUG2} NUG2*	
pRS315-NUG2-TAP	*ARS/CEN, LEU2, P_{NUG1} NUG2-TAP*	(14)
pRS315-NUG2-ΔM-TAP	*ARS/CEN, LEU2, P_{NUG1} NUG2-TAP (1-194 aa; G;378-486 aa)*	this study
pT7-NUG1-N	*ori, Kan^R $lacI^q$, P_{T7} NUG1 (1-145 aa)*	this study
pProHTb-HIS-TEV-GST-TEV-NUG1	*ori, AmpR, lacIq, P_{trc}, HIS-TEV-GST-TEV-NUG1*	this study
pProHTb-HIS-TEV-GST-TEV-nug1-4G	*ori, AmpR, lacIq, P_{trc}, HIS-TEV-GST-TEV-nug1 (G292G, K293G, S294G, S295G)*	this study
pET9D-5S-RNA	*ori, KanR, lacIq, P_{T7}, 5S RNA (RE site SpeI)*	this study
pACTII-NUG1	*2m, LEU2, P_{ADH1}, GAL4-HA-NUG1, T_{ADH}*	this study
pACTII-NUG1-ΔN	*2m, LEU2, P_{ADH1}, GAL4-HA-NUG1 (146-520 aa), T_{ADH}*	this study
pACTII-NUG1-N	*2m, LEU2, P_{ADH1}, GAL4-HA-NUG1 (1-145 aa), T_{ADH}*	this study
JBW4130	*pACTII RPS14;* *2m, LEU2, P_{ADH1}, GAL4-HA-RPS14, T_{ADH}*	(29)
pIIIA/MS2-1	*2m, URA3, ADE2, P_{PolIII}, MS2 sites, T_{PolIII}*	(28)
p3A-MS2-1	*2m, URA3, ADE2, P_{PolIII}, MS2 sites, T_{PolIII}* (Vector contains unique XmaI & SpeI sites for insertion of RNA Sequences)	this study
p3A-MS2-18S H23	*2m, URA3, ADE2, P_{PolIII}, MS2-18SH23, T_{PolIII}*	this study
p3A-MS2-5S	*2m, URA3, ADE2, P_{PolIII}, MS2-5S, T_{PolIII}*	this study
p3A-MS2-5Sreverse	*2m, URA3, ADE2, P_{PolIII}, MS2-5Srev, T_{PolIII}*	this study
p3A-MS2-5.8S	*2m, URA3, ADE2, P_{PolIII}, MS2-5.8S, T_{PolIII}*	this study
pRS315-BUD20	*ARS/CEN, LEU2, BUD20*	this study
pRS314-BUD20	*ARS/CEN, TRP1, BUD20*	this study
pRS315-DBP10	*ARS/CEN, LEU2, DBP10*	this study
pRS315-dbp10-2	*ARS/CEN, LEU2, dbp10-2* (Mutant was isolated from SL 46 by PCR)	this study
pNOPPA1L noc1-1	*ARS/CEN, LEU2, P_{NOP1}, ptA-TEV-noc1-1, T_{ADH1}*	(30)
pRS315 noc2-1	*ARS/CEN, LEU2, noc2-1* *noc2-1* was amplified from Rix3 (30)	this study
pNOPPA1L noc3-1	*ARS/CEN, LEU2, P_{NOP1}, ptA-TEV-noc3-1, T_{ADH1}*	(30)

Cell

Mechanochemical Removal of Ribosome Biogenesis Factors from Nascent 60S Ribosomal Subunits

Cornelia Ulbrich,[1,4] Meikel Diepholz,[2,4] Jochen Baßler,[1,4] Dieter Kressler,[1] Brigitte Pertschy,[1] Kyriaki Galani,[1,2] Bettina Böttcher,[2,3,*] and Ed Hurt[1,*]

[1]Biochemie-Zentrum der Universität Heidelberg, Im Neuenheimer Feld 328, 69120 Heidelberg, Germany
[2]EMBL, Meyerhofstrasse 1, 69117 Heidelberg, Germany
[3]University of Edinburgh, School of Biological Sciences, King's Buildings, Mayfield Road, Edinburgh EH9 3JR, UK
[4]These authors contributed equally to this work
*Correspondence: ed.hurt@bzh.uni-heidelberg.de (E.H.), bettina.boettcher@ed.ac.uk (B.B.)
DOI 10.1016/j.cell.2009.06.045

SUMMARY

The dynein-related AAA ATPase Rea1 is a preribosomal factor that triggers an unknown maturation step in 60S subunit biogenesis. Using electron microscopy, we show that Rea1's motor domain is docked to the pre-60S particle and its tail-like structure, harboring a metal ion-dependent adhesion site (MIDAS), protrudes from the preribosome. Typically, integrins utilize a MIDAS to bind extracellular ligands, an interaction that is strengthened under applied tensile force. Likewise, the Rea1 MIDAS binds the preribosomal factor Rsa4, which is located on the pre-60S subunit at a site that is contacted by the flexible Rea1 tail. The MIDAS-Rsa4 interaction is essential for ATP-dependent dissociation of a group of nonribosomal factors from the pre-60S particle. Thus, Rea1 aligns with its interacting partners on the preribosome to effect a necessary step on the path to the export-competent 60S subunit.

INTRODUCTION

The assembly of eukaryotic ribosomal subunits, which are composed of ribosomal RNA (25S/28S, 18S, 5.8S, and 5S rRNA) and about 80 ribosomal proteins, takes successively place in the nucleolus, nucleoplasm and cytoplasm. This complicated process is initiated by transcription of a large pre-rRNA precursor, which is subsequently modified, processed and assembled with the ribosomal proteins. At the beginning of ribosome synthesis, a huge (90S) precursor particle is formed that is then split to induce the formation of the pre-60S and pre-40S particles, which each follow separate biogenesis and export routes (Fromont-Racine et al., 2003; Granneman and Baserga, 2004; Henras et al., 2008; Tschochner and Hurt, 2003; Zemp and Kutay, 2007).

Proteomic approaches have revealed more than 150 non-ribosomal factors, which transiently associate with these nascent 60S and 40S subunits during ribosome biogenesis. It is assumed that these factors drive the multiple maturation steps in a temporally and spatially ordered fashion. Some of these preribosomal factors have domains homologous to ATPases or GTPases suggesting that they trigger energy-consuming steps. Among these types of factors are three AAA-type ATPases that are specifically involved in 60S subunit biogenesis. In general AAA-type ATPases apply force on their substrates upon ATP hydrolysis, which can trigger structural rearrangements or substrate release (Erzberger and Berger, 2006; Vale, 2000). The activity of the AAA ATPase Drg1 is required for the release of shuttling proteins from the pre-60S particles shortly after nuclear export (Pertschy et al., 2007). The other characterized AAA ATPase Rix7 mediates the release of a specific pre-60S factor, Nsa1, from the evolving nascent 60S subunit in the nucleus (Kressler et al., 2008). Finally, the large ~550 kDa AAA ATPase Rea1 (also called Midasin or Mdn1) is associated with pre-60S subunits and its ATPase domain is distantly related to the motor protein dynein heavy chain (Nissan et al., 2002). Rea1 has several distinct domains, an N-terminal extension (35 kDa), followed by an ATPase domain containing six tandem AAA protomers (between 28 and 40 kDa each), a linker domain (260 kDa), a D/E-rich domain (approximately 70 kDa) and a carboxy-terminal domain (30 kDa) that possesses a MIDAS (*m*etal *i*on-*d*ependent *a*dhesion *s*ite), which is homologous to the I-domain of integrins (Garbarino and Gibbons, 2002).

Rea1, which is the largest yeast protein and highly conserved in evolution, was identified as a specific component of an intermediate pre-60S particle that is located in the nucleoplasm and carries the salt-stable Rix1-Ipi3-Ipi1 subcomplex (Galani et al., 2004; Krogan et al., 2004; Nissan et al., 2004). Genetic analyses demonstrated that Rea1, like the members of the Rix1-subcomplex, is required for 60S subunit formation and ITS2 processing, a late pre-rRNA processing step generating the mature 5.8S rRNA from the 7S pre-rRNA (Galani et al., 2004).

Electron microscopic (EM) analysis revealed a tadpole-like shape of the pre-60S particle carrying Rea1 and the Rix1-subcomplex (Nissan et al., 2004). The head region of this particle was assigned to the 60S part and the tail extension was suggested to carry preribosomal factors including Rea1 (Nissan

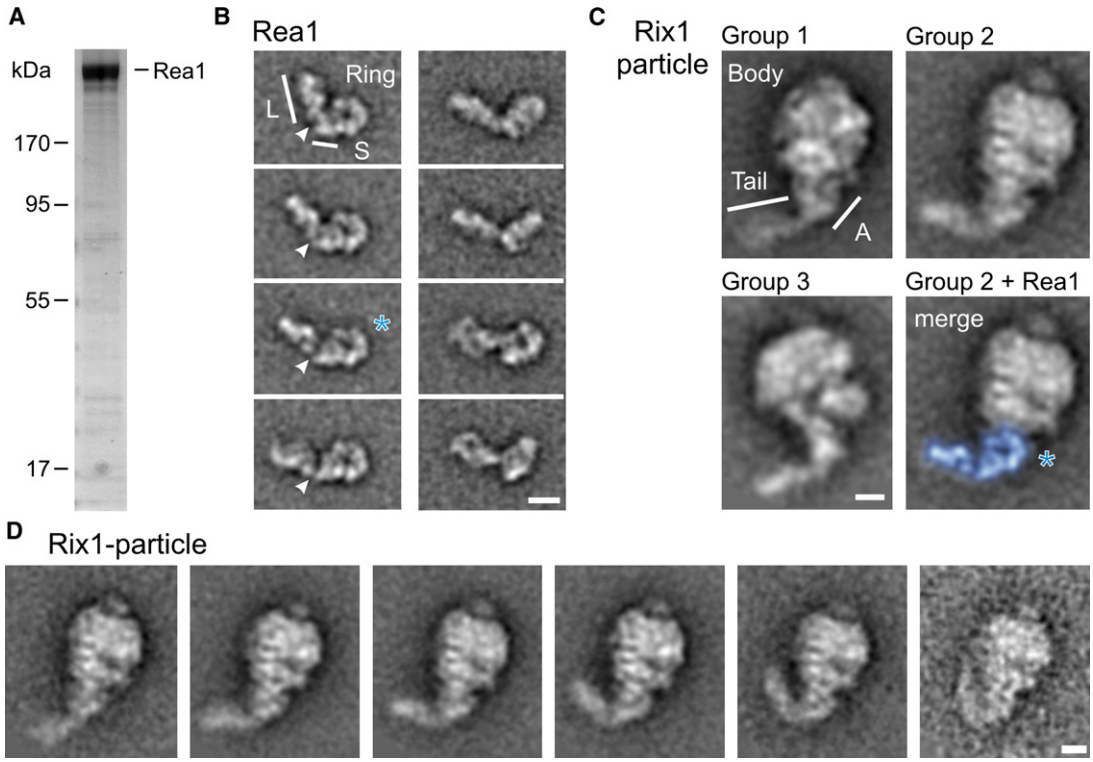

Figure 1. Identification of Position and Dynamics of Rea1 on the Rix1 Pre-60S Particle

(A) Affinity-purified TAP-Rea1 devoid of preribosomal and ribosomal proteins was analyzed by SDS-PAGE and Coomassie staining. Indicated at the left is the molecular weight protein standard in kDa.

(B) Eight representative class averages of the Rea1 molecule. Class averages in the left column show the ring-like shape of the compact domain that connects via a short segment (S) to a longer segment (L) in the elongated tail. The relative orientation of the ring and the short segment does not change significantly, whereas the long tail-segment adopts different positions. The virtual hinge between long segment and short segment is indicated by an arrow-head. The right column shows other orientations of the Rea1 molecule, in which the ring-shaped domain is rotated out of plane. The scale bar represents 10 nm.

(C) The three most representative groups of tail-containing Rix1-particle classes. Major structural landmarks in the Rix1-particle are indicated in group 1 (body, tail and attachment site abbreviated as "A"). Particles that classified into groups 1-3 represent 87% of all tail-containing particles (group 1: 52%, group 2: 24%, and group 3: 11%). For comparison, one Rea1 class average (marked by a blue star in [B]) was overlaid to the tail regions of a group 2 Rix1-particle class average ([C] merge with Rea1*). The overlay shows a good agreement in size and shape between the isolated Rea1 molecule (blue) and the tail and attachment site within the Rix1-particle. The scale bar represents 10 nm.

(D) Movement of the Rea1 tail in the Rix1-particle. Averages of Rix1-particles with the same projection of the body displayed different angular orientations of the tail. The averages are also shown as frames in Movie S2. The first five averages represent one of the five groups in the histogram shown in Figure S2B. The sixth average is a subpopulation of the fifth group in which the tip of the tail appears to make contact to the body of the Rix1-particle. The scale bar represents 10 nm.

et al., 2004). Thus, it was proposed that the AAA ATPase Rea1 could power an ATP-dependent maturation step during 60S subunit formation, but how Rea1 could fulfill this function remained elusive.

Here, we show by electron microscopy that Rea1 consists of two main structural parts, an AAA motor domain, which is stably bound to the pre-60S particle, and a long tail that points away from the preribosome. The Rea1 tail is hinged to the rest of the pre-60S particle enabling the MIDAS at the carboxy-terminal end of the tail to create contact with a distant site on the Rix1 pre-60S particle, where the preribosomal factor Rsa4 is located. Importantly, the Rea1 MIDAS can physically interact with Rsa4. In vivo, site-specific mutants mapping in either the MIDAS or Rsa4 abrogate this interaction and cause a robust 60S subunit export defect. Thus, Rea1 can make contact to the pre-60S subunit at two separate sites, to Rsa4 via the tip of the tail carrying the MIDAS and via the AAA ATPase domain close to the Rix1-complex. In this constellation, the Rea1 motor domain generates force upon ATP hydrolysis to irreversibly remove pre-60S factors, thereby conferring export competence to the pre-60S subunit.

RESULTS

EM Analysis of Isolated Rea1 and of Rea1 Attached to the Rix1-Purified Pre-60S Particle

The conserved AAA ATPase Rea1 is associated with an intermediate pre-60S particle (termed Rix1-particle) in the nucleoplasm that typically carries the salt-stable Rix1-Ipi1-Ipi3 complex (termed Rix1-subcomplex). To elucidate the role of Rea1 in 60S subunit biogenesis, we sought to assign its position within the Rix1-particle. Therefore, we purified Rea1 by tandem affinity-purification (Figure 1A). The negatively stained Rea1 molecules

were examined by EM and single particle analysis (Figure 1B and Table S1 available with this article online). The selected class averages of Rea1 showed an elongated molecule consisting of a ring-like structure with a diameter of 12 ± 1 nm and an elongated "tail" (Figure 1B). The tail consists of a longer (14 ± 1 nm) and a shorter segment (3 ± 1 nm). The latter connects the tail to one side of the ring. Both segments appear to be flexibly hinged as seen in different class averages that show a similar arrangement of the ring and short tail-segment, but different orientations of the long tail-segment (Figure 1B, left column, and Movie S1).

Next, we negatively stained the pre-60S particles purified via the Rix1-TAP bait and calculated class averages. Class averages of the majority of particles (~70%) showed a tadpole-like shape (Nissan et al., 2004) consisting of a tail which is connected via an attachment site to the main body (Figure 1C). More than 85% of the tail-containing particles clustered into only three groups with different views of the body and the tail mostly protruding to one side with a certain degree of flexibility (Figures 1C, 1D, and S1). Class averages of the remaining ~30% of particles did not show a tail and were generally less well defined suggesting greater variability (Figure S1).

Comparison of class averages of the tail-containing pre-60S particles and isolated Rea1 protein showed that the shape of the tail resembled the characteristic shape of purified Rea1 (compare Figures1B and 1C). This observation was further confirmed by overlays between class averages of Rea1 and the Rix1-particle. In these overlays the globular domain of the Rea1 molecule is seen at the attachment site between tail and the body of the pre-60S subunit (Figure 1C, merge with Rea1). This positioning of Rea1 within the Rix1-particle was consistent with earlier antibody labeling that localizes the N-terminus of Rea1, which directly precedes the AAA domain, close to the attachment site in the pre-60S particle (Nissan et al., 2004). Vice versa, the C-terminal MIDAS domain of Rea1 was assumed to be located most distant to the N-terminus at the tip of the Rea1 tail (see Introduction). To test this hypothesis, Rea1 was modified C-terminally with a triple HA-tag, and the affinity-purified Rix1-particle was analyzed by immuno-EM using antibodies against HA. Class averages of labeled Rix1-particles showed enlarged tips of the tails (Figure 2A), thus verifying the localization of the C-terminal MIDAS-domain close to the end of the tail. We conclude that Rea1's globular domain contains the N-terminal domain and the following six AAA-ATPase protomers, whereas the tail consists of the other described motifs (i.e., linker, D/E-rich and MIDAS domains; see Introduction) with MIDAS at or close to the tip of the tail.

It is still unknown where the 60S-moiety is positioned within the body of the Rix1-particle. Therefore, we determined where 60S marker proteins (Rpl) are located within the Rix1-particle. We performed immuno-EM to localize the ribosomal proteins Rpl5, which is part of the central protuberance in the mature 60S subunit, and Rpl3, which is positioned at the opposite side of the 60S moiety (Spahn et al., 2001). For antibody labeling, Rpl3 and Rpl5 were fused to a C-terminal triple HA-tag and functionally expressed in the Rix1-TAP strain. In the class averages of Rix1-particles carrying Rpl3-HA the HA-antibody bound close to the top of the body and pointed to the side of the tail, whereas in the Rpl5-HA carrying pre-60S subunits the extra density of the HA-antibody was detected at the opposite side above the attachment site (Figure 2A). Due to the flexibility of the bound antibody, these class averages showed less detail than class averages of Rix1-particles without bound antibody (Figure 2B). Therefore, we confirmed the significance of this antibody labeling by counting the occurrence of additional densities in a given segment at the periphery of the Rix1-particle in raw images. In all experiments, the segment, in which the extra density was seen in the class averages, contained significantly more peripheral densities than the other five segments (Figure S2A). Taken together this analysis located two spatially distant Rpl proteins of the 60S moiety and placed the central protuberance close to the AAA ATPase domain of Rea1.

Since it was hypothesized that Rea1 could bind via the Rix1-subcomplex to the 60S subunit (Nissan et al., 2004), we aimed to determine the position of Rix1, Ipi1 and Ipi3 by antibody labeling of HA-tagged proteins in negatively stained pre-60S particles. Whereas the antibody against Rix1-HA was found close to the globular domain of Rea1, the antibody against Ipi3-HA was located above Rix1 and close to Rpl5 (Figures 2A and 2C). Ipi1 could not be localized due to inefficient labeling (data not shown). These data suggest that the Rix1-subcomplex is sandwiched between the AAA-ATPase domain and the 60S subunit joining surface and thus could serve as possible adaptor between these two entities.

A Flexible Rea1 Tail Could Bring the MIDAS in Proximity to Rsa4 to Allow a MIDAS-Rsa4 Contact

Class averages with similar projections of the body of the Rix1-particle often displayed the tail in different angles with respect to the main axis of the body, suggesting flexibility of the tail. To quantify this flexibility further, we grouped particles with the same projection of the body by supervised classification and sub-classified these particles according to the features in the tail region by multivariate statistical analysis. The largest flexibility was observed for 'Group 2' Rix1-particles (see Figure 1C). Their class averages indicated that Rea1's tail is flexible around a virtual hinge close to the AAA ATPase domain (Figure 1D and Movie S2) and covers an angular range of ~120° (Figure S2B). The favored orientation of the tail is in the middle of this angular range. In a few particles the tip of the tail comes close to the pre-60S body and may even contact a discrete region on the pre-60S subunit, which is below the location of Rpl3, but distant to the binding site of the Rea1 AAA ATPase domain (Figure 1D). Since the tail region of Rea1 contains the MIDAS, a well-known motif mediating protein-protein interaction, it is possible that the tail movement brings the MIDAS close to another factor on the pre-60S particle to allow for a direct contact.

To find out if the Rea1 MIDAS indeed could develop a physical connection to a second site on the pre-60S subunit, we searched for factors that interact with the Rea1 MIDAS domain. Valid candidates are proteins, which co-purify with the Rix1-particle. In the past, several factors have been reported to be associated with the Rix1-particle. Re-investigation of these bands by SDS-PAGE of the purified Rix1-particle confirmed that the Rix1-Ipi1-Ipi3 subcomplex is highly enriched (Figure 3A). Additional prominent bands in the Rix1-particle were Rea1, Rsa4, Nsa2, Arx1 and the GTPases Nog1, Nog2 and Nug1 (Galani et al., 2004;

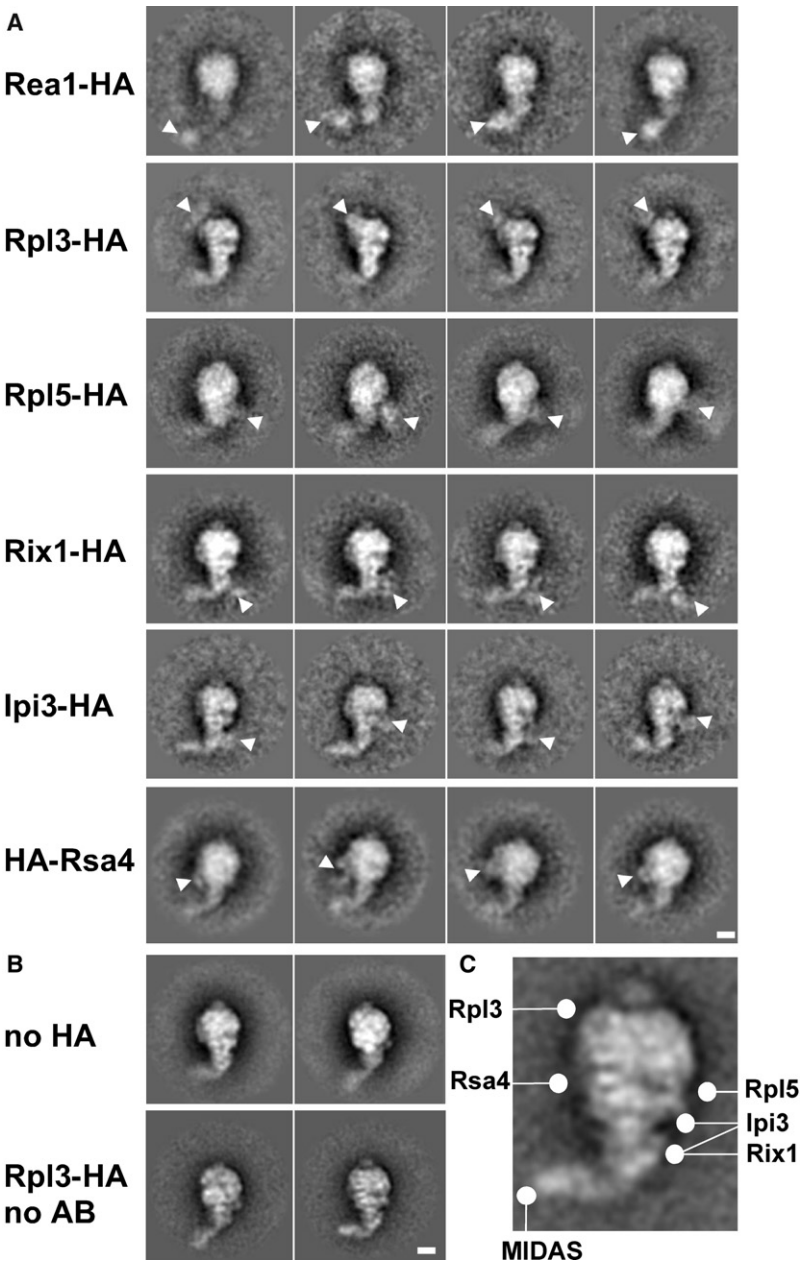

Figure 2. Positioning of Ribosomal Proteins and Preribosomal Factors on the Rix1-Particle

(A) Class averages of HA-antibody labeled negatively stained Rix1-particles purified via the Rix1-TAP bait. The HA-labeled protein is indicated on the left. Rea1, Rpl5 and Rpl3 carried a C-terminal HA-tag, Rsa4 had an N-terminal HA-tag. In the case of Rix1 and Ipi3, the HA-tag was inserted at the C terminus before the TAP-tag. Ipi3-TAP was shown to purify the same particles as Rix1-TAP (Nissan et al., 2004). White arrowheads indicate the position of the antibody-dependent extra density.

(B) Negative controls for antibody labeling. Class averages of Rix1-particles that did not carry the HA-tag but were incubated with HA-antibodies (upper row). No extra density of a contaminating antibody is visible. Rix1-particles containing the HA-tag on Rpl3 were affinity-purified without the HA-antibody (lower row). The scale bar represents 10 nm.

(C) Class average of the Rix1-particle with the approximate positions of all localized proteins.

Nissan et al., 2002; Nissan et al., 2004). Western blotting revealed that Rsa4 and Nog2 co-purified mainly with the Rix1-particle, whereas Nog1, Nsa2 and Tif6 were also found in earlier and later pre-60S particles (Figure 3B).

To identify the factor(s) present on the Rix1-particle that potentially could bind to the MIDAS in the Rea1 tail, we performed yeast 2-hybrid assays. Among the analyzed factors, only Rsa4 exhibited a robust 2-hybrid interaction with the Rea1 MIDAS bait, whereas Nog2, Nog1, Nsa2, Rix1, Ipi3, and Ipi1 did not interact (Figure 3C). Further investigations demonstrated that the domain with the predicted MIDAS fold (residues 4700-4910 in Rea1) plus an adjacent sequence (4620-4699) and the highly conserved N-domain of Rsa4 (residues 20-128) were necessary for the 2-hybrid interaction (Figure 4A, see also Figures S3A, S3B, S4A, and data not shown). Consistent with this finding, NOTCHLESS, the plant homolog of Rsa4, exhibits a 2-hybrid interaction with the Rea1 homolog Midasin (Chantha and Matton, 2006). To test whether Rsa4 and Rea1 can directly interact, we co-expressed His-Rsa4 and GST-MIDAS in *E. coli*. Affinity-purification of GST-MIDAS from a bacterial lysate revealed a strong co-enrichment of Rsa4 (Figure 4B) showing that the MIDAS of Rea1 binds directly to Rsa4.

To determine whether the position of Rsa4 within the Rix1-particle could be consistent with a physical interaction between Rsa4 and the Rea1 MIDAS, we performed immuno-EM as described above. This analysis showed that HA-Rsa4 is located in the center of the body pointing to the side of the tail (Figures 2 and S2A). The area defined by antibody labeling of Rsa4 overlaps with the site where the tail contacts the body of the Rix1-particle (Figure 1D). Altogether, these data indicate that a movement of the Rea1 tail brings the Rea1 MIDAS in proximity to Rsa4 and thus could allow in vivo a physical contact between these two proteins on the pre-60S subunit.

The Rea1 MIDAS-Rsa4 Interaction Resembles the Classical Integrin MIDAS-Ligand Interaction

To investigate the mechanism by which the Rea1 MIDAS binds to Rsa4, we took advantage of the structural knowledge of how an integrin MIDAS interacts with its ligand (i.e., extracellular matrix protein). Crystal structures of MIDAS-ligand complexes show that the MIDAS ion (mainly Mg^{2+}) at the integrin–ligand interface is coordinated by five conserved residues of the MIDAS fold (consensus DxSxS-x_{70}-T-x_{30}-(S/T)DG) and the sixth coordination residue (either E or D) is provided by the ligand (Arnaout

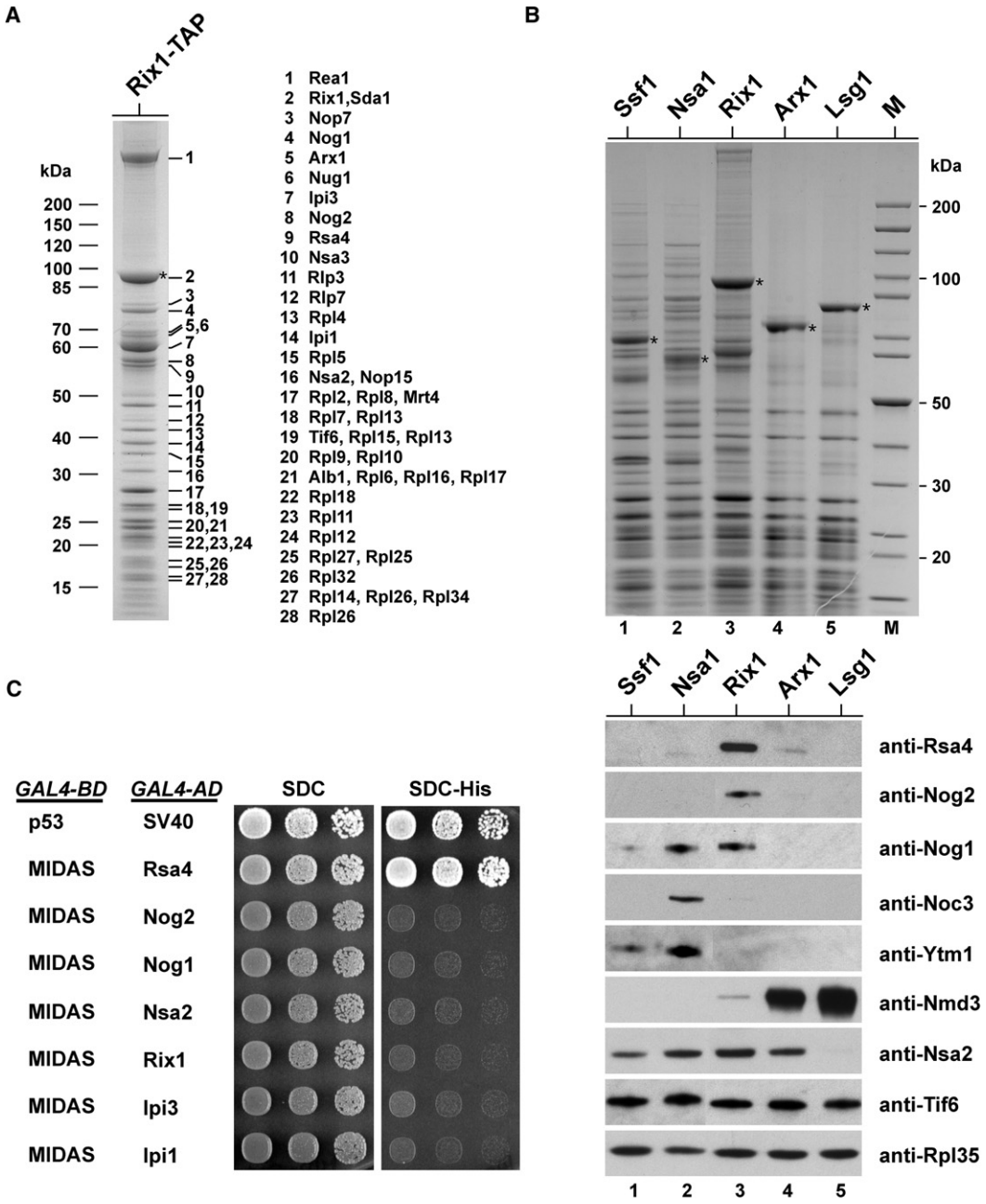

Figure 3. Rsa4 Associates with the Rix1 Pre-60S Particle and Interacts with the Rea1 MIDAS in the 2-Hybrid Assay

(A) Protein composition of the pre-60S particle used for electron microscopic analysis. The final EGTA eluate of Rix1-TAP was analyzed by 4%–12% gradient SDS-PAGE and Coomassie staining. The indicated protein bands (1 to 28) were identified by mass spectrometry.

(B) Rsa4 and Nog2 are co-enriched within the Rix1 pre-60S particle. The final eluates of tandem affinity purifications (TAP) using the bait proteins Ssf1, Nsa1, Rix1, Arx1 and Lsg1 were analyzed by SDS-PAGE and Coomassie staining (upper panel, lanes 1-5) and western blotting using the indicated antibodies (lower panel). M, molecular weight protein standard. The asterisks mark the positions of the bait proteins.

(C) 2-hybrid analysis reveals an interaction of the Rea1 MIDAS (residues 4620-4910) with Rsa4, but not with other pre-60S factors. 2-hybrid plasmids expressing the indicated *GAL4-BD* (*GAL4* DNA binding domain) and *GAL4-AD* (*GAL4* activation domain) constructs were transformed into the yeast reporter strain PJ69-4A. Transformants were spotted in 10-fold serial dilutions onto SDC-Trp-Leu (SDC) or SDC-Trp-Leu-His (SDC-His) plates. Expression of the *HIS3* marker allows growth on SDC-His plates and thus indicates a 2-hybrid interaction. Plates were incubated for 4 days at 30°C. The combination of p53 and the SV40 large T-antigen served as a positive control.

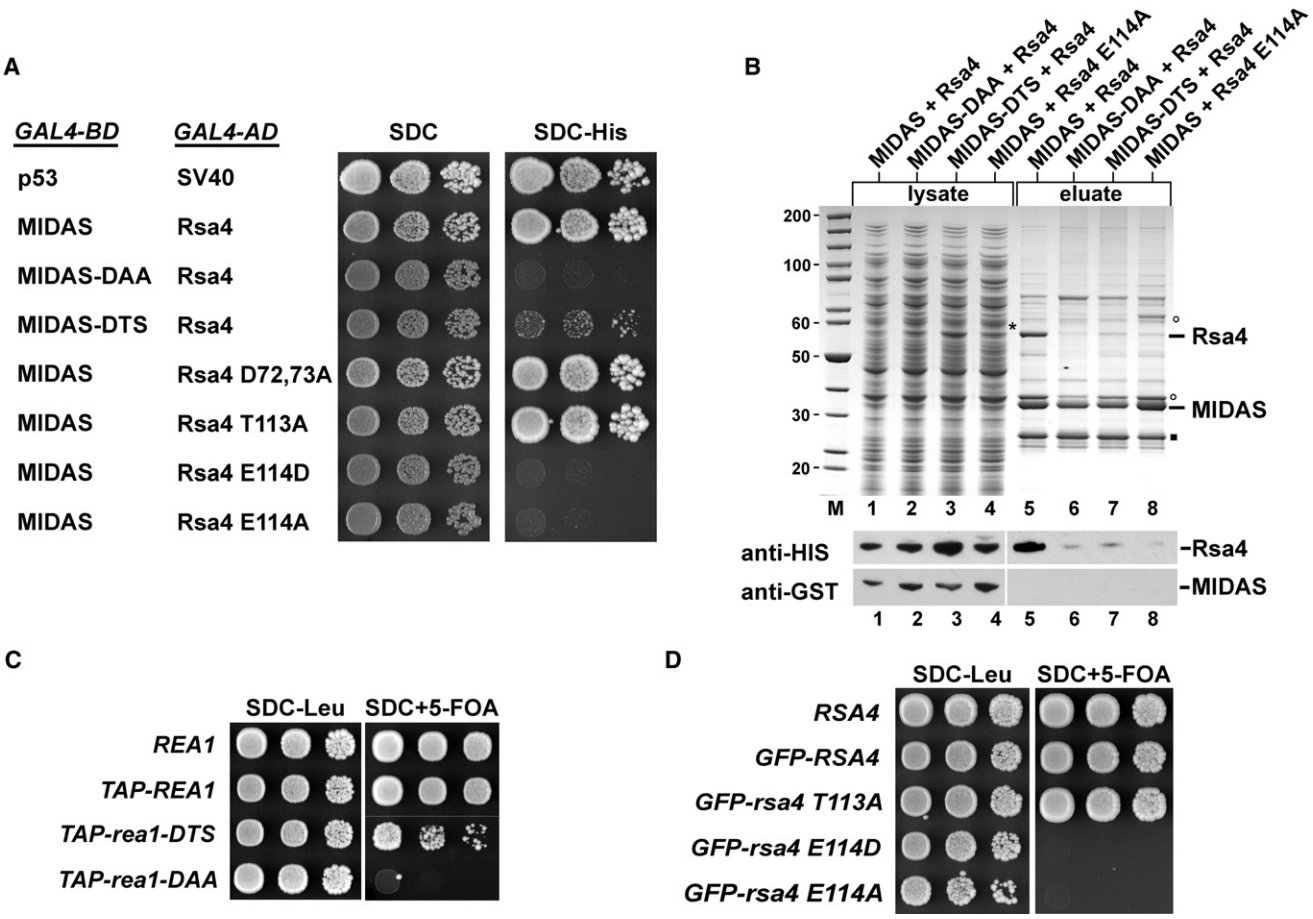

Figure 4. Physical Interaction Requires Critical Residues in the Rea1 MIDAS and Rsa4 N-Terminal Domain

(A) 2-hybrid interaction between the wild-type and mutant alleles of Rea1 MIDAS and Rsa4 N-domain. 2-hybrid plasmids expressing the indicated *GAL4-BD* and *GAL4-AD* constructs were transformed into the yeast reporter strain PJ69-4A. Transformants were spotted in 10-fold serial dilutions onto SDC-Trp-Leu (SDC) or SDC-Trp-Leu-His (SDC-His) plates and incubated at 30°C. The Rea1 MIDAS comprised residues 4620-4910, and the N-domain of Rsa4 residues 1–154.

(B) The Rea1 MIDAS and Rsa4 bind directly to each other. The GST-TEV-tagged MIDAS of Rea1 (either wild-type or the DAA and DTS mutants; residues 4608-4910) was co-expressed with HIS_6-tagged wild-type Rsa4 or the *rsa4 E114A* mutant in *E. coli* in the indicated combinations. Whole-cell lysates were prepared and the GST-MIDAS constructs were affinity-purified on GSH-beads and eluted by TEV-cleavage. Whole-cell lysates (1–4) and the corresponding eluates (5–8) were analyzed by SDS-PAGE and Coomassie staining (upper panel) or western blotting (lower panel) using anti-HIS antibodies to detect Rsa4 and anti-GST antibodies to detect the MIDAS (note that the GST antibody only reacts with the GST-MIDAS in the lysate but not in the eluate, where the GST tag was cleaved off by the TEV protease). The position of GST-MIDAS in the lysate is indicated by an asterisk, the TEV protease by a filled square and *E. coli* contaminants by open circles. Molecular weight marker (M).

(C and D) Growth analysis of the indicated *rea1* MIDAS (C) and *rsa4* mutants (D). Wild-type *REA1* and the *rea1* mutants mapping in the MIDAS domain and tagged with the TAP epitope were transformed into the *REA1* shuffle strain. Wild-type *RSA4* and the indicated *rsa4* mutants tagged with GFP were transformed into the *RSA4* shuffle strain. Transformants were spotted in 10-fold serial dilution steps onto SDC-Leu plates (to control the plating efficiency) and onto SDC+5-FOA plates (to check whether the mutations are lethal). Plates were incubated at 30°C for 3 days.

et al., 2005; Luo et al., 2007; Takagi, 2007). Consequently, we mutated the conserved DxSxS motif predicted to coordinate the MIDAS ion in Rea1 into DxTxS (MIDAS-DTS) or DxAxA (MIDAS-DAA) (Figure S3C). Whereas the single MIDAS-DTS mutant was viable although with a reduced cell growth, the MIDAS-DAA double mutant was lethal (Figure 4C). Importantly, the 2-hybrid and the biochemical interaction between these mutant forms of MIDAS and Rsa4 were significantly reduced (Figures 4A and 4B). In addition, the combination of a *rsa4* mutant allele (*rsa4-1*) with *rea1*-S4712T (MIDAS-DTS) caused a synthetic lethal phenotype (Figure S3D). Altogether these data demonstrate a strong physical and functional interaction between the Rea1 MIDAS and Rsa4.

Next, we searched for an essential acidic (aspartate or glutamate) residue in the Rsa4 N-domain that could provide the sixth coordination site of the MIDAS ion. We found that a conserved aspartic acid residue (E114) in the Rsa4 N-domain (Figure S4A) is essential for cell growth. Both, an *rsa4* E114D or E114A point mutation when introduced into the full-length protein could not rescue the lethal phenotype of the *rsa4Δ* strain (Figure 4D) and abolished the biochemical and the 2-hybrid interaction with the Rea1 MIDAS (Figures 4A and 4B). In contrast, mutating other

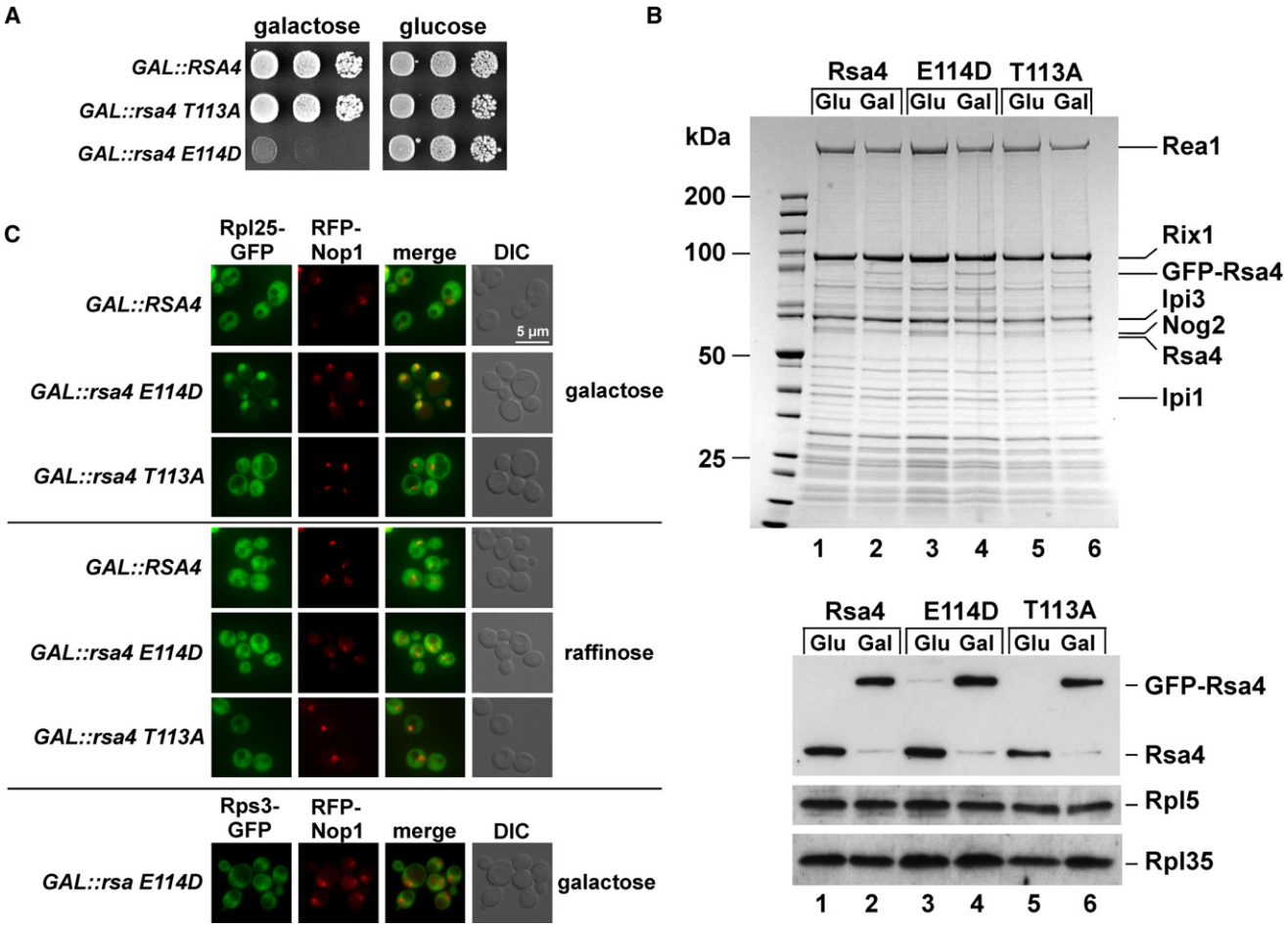

Figure 5. Mutation of the Conserved E114 in Rsa4 Generates a Dominant-Negative Phenotype and Inhibits 60S Subunit Formation

(A) The Rsa4 E114D mutation confers a dominant-negative phenotype. Wild-type *RSA4* and the indicated *rsa4 T113A* and *rsa4 E114D* mutant alleles were N-terminally GFP-tagged and expressed under the control of the inducible *GAL1* promoter in yeast. Transformants were spotted in 10-fold serial dilution steps onto SGC-Leu (galactose) and SDC-Leu (glucose) plates. Plates were incubated for 3 days at 30°C.

(B) Endogenous Rsa4 is displaced from the pre-60S subunit upon overexpression of the toxic *GAL::rsa4* E114D mutant. The yeast strain Y4294 strain was transformed with the constructs *GAL::RSA4*, *GAL::rsa4* E114D and *GAL::rsa4* T113A, respectively, which were tagged with GFP to distinguish them from endogenous Rsa4. Cells were grown for 6 h in glucose (Glu) or galactose (Gal) containing medium, before Rix1-TAP was affinity-purified and analyzed by SDS-PAGE and Coomassie staining (upper part) or western blotting (lower part) using an anti-Rsa4 antibody, which recognizes both the endogenous Rsa4 and overexpressed GFP-Rsa4. The Rpl5 and Rpl35 antibodies were used to probe for equal loading of the gel. Indicated on the right are prominent bands.

(C) Analysis of nuclear export of 60S and 40S subunits in the dominant-negative *GAL::rsa4 E114D* mutant (TAP-tagged). The indicated yeast strain (YDK11-5A) expressing either the 60S subunit reporter Rpl25-GFP or 40S subunit reporter Rps3-GFP was grown in galactose- or raffinose-containing medium at 30°C for 6 h, before the subcellular location of Rpl25-GFP and Rps3-GFP was analyzed by fluorescence microscopy. The strains also expressed mRFP-Nop1 as nucleolar marker. A merge between Rpl25-GFP or Rps3-GFP and mRFP-Nop1, as well as Nomarski (DIC) pictures are shown. The scale bar represents 5 µm.

conserved residues (T113A, D72A, D73A) did neither affect growth nor binding to Rea1 MIDAS (Figures 4A and 4D; data not shown). These findings suggest that E114 in the N-domain of Rsa4 provides the sixth coordination site for binding the MIDAS ion.

The importance of E114 in Rsa4 for the interaction with Rea1 and the overall 60S biogenesis is underscored by the observation that Rsa4 E114D overexpression under the *GAL* promoter exerts a dominant-lethal phenotype (Figures 5A and S4B). In contrast, cells overexpressing wild-type Rsa4 or the Rsa4 T113A mutation continued to grow normally in galactose-containing medium (Figures 5A and S4B). Biochemical analyses showed that overproduced Rsa4 E114D efficiently replaced the endogenous Rsa4 protein from its binding site on the pre-60S subunit without affecting significantly the overall biochemical composition (Figure 5B) and characteristic shape of the Rix1-particle (EM-analysis, data not shown). Moreover, in vivo analyses revealed that ribosome formation was inhibited upon overexpression of Rsa4 E114D. Specifically, late 7S to 5.8S rRNA processing was impaired (Figure S5) and pre-60S particles strongly accumulated in the nucleus (Figure 5C) causing a reduction of mature 60S subunits relative to 40S subunits and the appearance of "half-mer" polysomes in the cytoplasm (Figure S4C). These data suggest that Rsa4 binds to the preribosome prior

to interaction with the MIDAS domain and that the Rsa4 E114D mutant protein assembled into the Rix1-particle effectively blocks progression of the nascent pre-60S subunit and subsequent export to the cytoplasm.

Interaction between Rea1 MIDAS and Rsa4 Is Required for Their ATP-Dependent Release from the Pre-60S Particle

We next asked whether the MIDAS-Rsa4 interaction is coupled with Rea1's ATPase function. Previously, we observed that when Rix1-TAP was affinity-purified and treated with ATP, Rea1 and to a lesser extent also ribosomal 60S proteins (Rpl) were dissociated from the Rix1-Ipi1-Ipi3 complex (Nissan et al., 2004). To test whether this ATP-dependent release of Rea1 depends on the MIDAS-Rsa4 contact we affinity-purified Rix1-TAP from cells harboring either wild-type Rsa4 or mutated Rsa4 E114D in the presence of ATP. Strikingly, pre-60S particles carrying mutant Rsa4 E114D were inert toward ATP-treatment since neither pre-60S factors (e.g., Rsa4 E114D, Rea1, Nog1 and Nog2) nor 60S subunit proteins (Rpl) were released from the immobilized Rix1-Ipi1-Ipi3 complex (Figure 6A, lane 4). In contrast, these pre-60S factors and a significant amount of Rpl proteins were dissociated from the Rix1-subcomplex upon ATP incubation in the case of wild-type Rsa4 (Figure 6A, lane 3). However, incubation with the non-hydrolyzable ATP analog AMP-PNP did not promote release of the pre-60S factors and ribosomal proteins from the wild-type Rix1-particle suggesting that ATP hydrolysis is required for the dissociation step (Figure 6A, lane 5).

The in vitro assay employed so far (see Nissan et al., 2004) revealed ATP-dependent dissociation of factors and Rpl proteins from the purified Rix1-subcomplex, but did not monitor whether the released non-ribosomal factors were still associated with the ribosomal Rpl proteins (i.e., 60S subunits). To address this point, we extended our in vitro assay. The pre-60S particle was tandem affinity-purified via Rix1-TAP from wild-type cells and the final EGTA eluate was incubated with or without ATP. Subsequently, the entire reaction mixtures were analyzed by sucrose gradient centrifugation. In the mock-treated sample (-ATP), Rea1, Rsa4 and the Rix1-subcomplex significantly co-sedimented with the 60S subunit on the sucrose gradient (Figure 6B, fraction 10). However, a pool of the Rix1-subcomplex devoid of Rpl proteins was also recovered in the upper part of the sucrose gradient, which corresponds to the free Rix1-Ipi1-Ipi3 heterotrimer known to exist in yeast (Krogan et al., 2004). In the ATP-treated sample Rea1 and Rsa4 were efficiently released from the pre-60S particle and recovered in the upper part of the sucrose gradient but in different fractions. The Rix1-subcomplex was also released from the 60S subunit upon ATP-treatment, but not completely and a residual pool remained bound (Figure 6B and Figure S6; see also Discussion). In contrast, other pre-60S factors including Nog1, Nog2, Nsa2, Rlp24, Nop7 and Tif6 were not released by ATP treatment and co-sedimented with the 60S subunit (Figure 6B and data not shown). Consistent with this data, Nsa2 is still present on the Arx1-particle that evolved from the Rix1-particle during 60S subunit biogenesis (see also Figure 3B). Altogether, the data suggest that an interaction between the Rea1 MIDAS and Rsa4 is necessary for ATP-dependent dissociation of a group of preribosomal factors from the 60S subunit (i.e., Rea1, Rsa4, Rix1-subcomplex), whereas other factors present on the Rix1-particle (see above) apparently were not released. Thus, these latter factors could require other mechanisms for their removal from the evolving pre-60S particle (see also Discussion).

Finally, we investigated which morphological changes were induced by ATP-treatment of the Rix1-particle. Rix1-particles were applied to EM-grids and incubated with ATP before staining for subsequent EM analysis and image processing. Comparison and quantification of class averages of ATP-treated and untreated samples revealed that ATP caused a significant increase of tail-less (from 29% to 64%) and a corresponding decrease (from 71% to 36%) in tail-containing pre-60S particles (Figure 6C and Figure S1). Concomitantly, ATP-treatment induced a ~3-fold increase in smaller fragments that were apparently released from the Rix1-particles (Figure S1C). The analysis of the ATP-treated sample revealed that 20% of these smaller fragments clustered into classes that resembled Rea1 molecules, which were largely absent in the untreated sample (Figure 6C, Figure S1). Other fragments generated by ATP-treatment formed classes that were similar in the treated and untreated sample and could represent the dissociated Rix1-subcomplex (Figure S1; see Discussion). Incubation of Rix1-particles with AMP-PNP did neither induce major structural changes of the particles nor cause a release of Rea1 (M.D., unpublished data). In conclusion, the ATP-induced decrease of tail-containing particles together with the increase of smaller fragments, one of them being clearly Rea1, agrees well with the biochemical data and is consistent with a model of an ATP-dependent release of preribosomal factors from the Rix1-particle.

DISCUSSION

This study has uncovered a mechanochemical constellation of biogenesis factors on the surface of a distinct pre-60S particle that allows ATP-dependent remodeling of the nascent 60S subunit prior to nuclear export. Our EM data demonstrate that the AAA domain of Rea1 is fixed at the Rix1-particle, whereas the Rea1 tail is flexible with respect to the 60S moiety and can move toward a region on the pre-60S subunit where Rsa4 is located (Figure 7). Moreover, the EM data indicate that Rea1 consists of two major structural entities, a ring domain that is connected to the body possibly involving the Rix1-subcomplex and a ~15 nm long tail protruding from the AAA domain. Thus, Rea1's head domain, which harbours the six AAA protomers, could form a hexameric ring structure in analogy to the AAA domain of dynein (Roberts et al., 2009).

The Rea1 tail is intrinsically flexible and probably also hinged in respect to the preribosomal particle as suggested by the different angular mobility observed in the Rea1 molecule. This mobility of the tail enables the tail to loop back onto the preribosome as seen in some selected particles (Figure 1D and Movies S1 and S2). Currently, it is unclear whether the movement of Rea1 toward Rsa4 and/or their subsequent interaction is regulated, e.g., by a GTPase, or whether similar to the priming of the dynein heavy chain (Roberts et al., 2009) is driven by binding of ATP to the motor domain that moves the tail toward Rsa4.

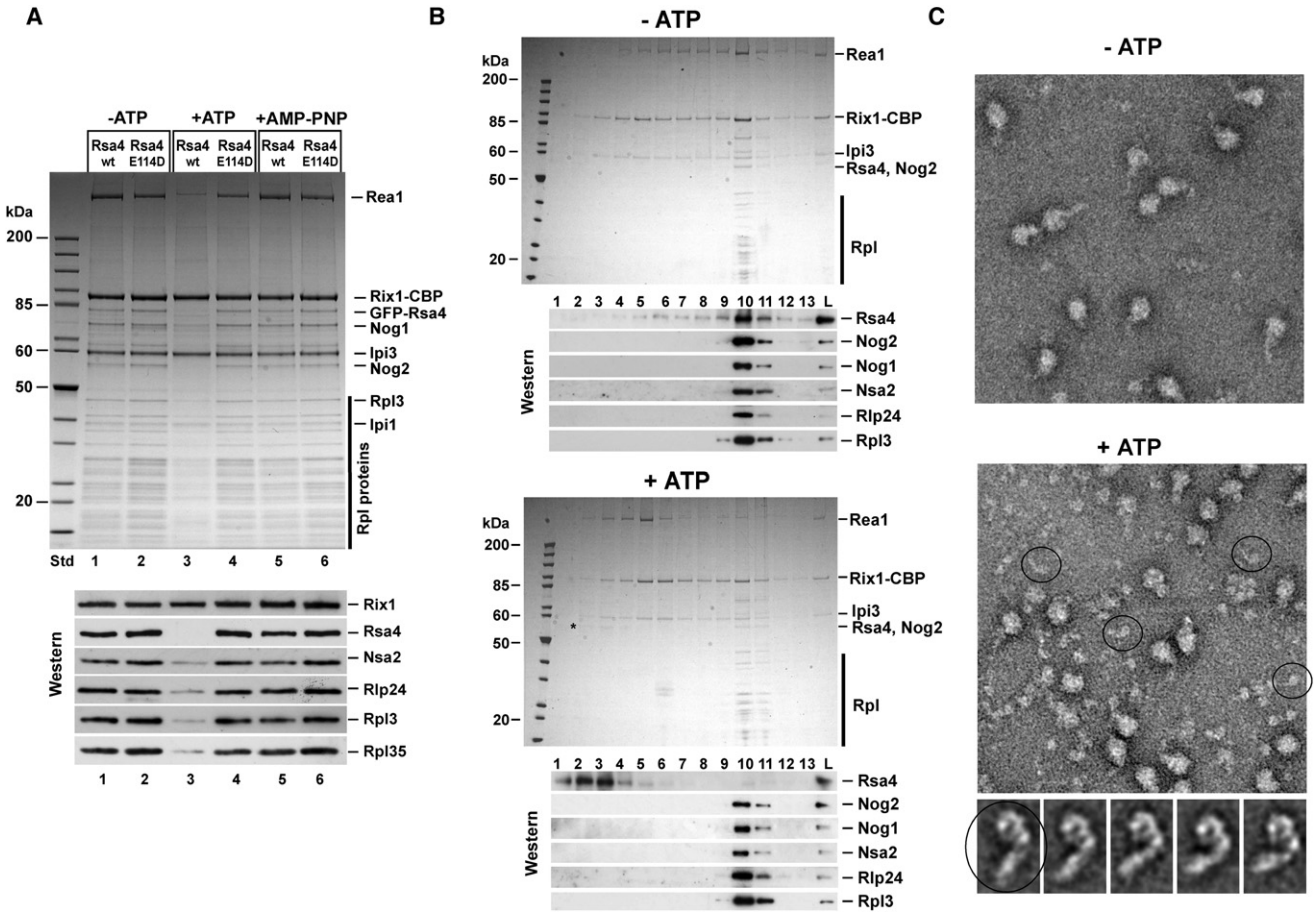

Figure 6. ATP-Dependent Release of Rsa4, Rea1, and the Rix1-Subcomplex from the Pre-60S Particle

(A) The MIDAS-Rsa4 interaction is required for ATP-dependent release of Rea1, Rsa4, and Rpl proteins from the Rix1-subcomplex. Rix1-TAP was affinity-purified from cells expressing GFP-Rsa4 (wild-type, wt) or mutant GFP-Rsa4 E114D. During TEV-cleavage and the successive purification steps 2 mM ATP, 2 mM AMP-PNP, or mock buffer (-ATP) was added. After EGTA elution from the final calmodulin beads, the Rix1-TAP preparations were analyzed by SDS-PAGE and Coomassie staining (upper part) or western blotting (lower part) using anti-CBP (to detect the Rix1-CBP bait), anti-Rsa4 (to detect GFP-Rsa4), anti-Nsa2, anti-Rlp24, anti-Rpl3, and Rpl35 antibodies.

(B) Release of non-ribosomal factors from the pre-60S particle by ATP-treatment monitored by sucrose gradient centrifugation. The Rix1-particle was tandem affinity-purified and the final EGTA eluate was incubated with 2 mM ATP for 2 hr at 16°C before loading the whole mixture on a sucrose gradient (5%–30%). After centrifugation for 15 hr at 27,000 rpm, the gradient was fractionated, and the gradient fractions 1-13 and the load fraction (L) were analyzed by SDS-PAGE and Coomassie staining (upper part) or western blotting using the indicated antibodies (lower part). The band labeled by a star indicates the ATP-released Rsa4.

(C) ATP-dependent release of Rea1 from the Rix1-particle followed by electron microscopy. Rix1-particles affinity-purified via Rix1-TAP were immobilized on EM-grids and incubated with 2 mM ATP before staining for subsequent electron microscopy. Comparison of negatively stained mock-treated (-ATP) and ATP-treated (+ATP) sample revealed an increase of tail-less and decrease of tail-containing particles as well as an increase of smaller fragments (for quantification see Figure S1C). Some of these fragments resembled Rea1 molecules (circle), which were further analyzed by alignment and classification (lower panel gallery; see Figure S1 for overview). Some of these class averages corresponding to released Rea1 showed the same projection of the globular domain but grouped into classes with different tail positions indicating intrinsic flexibility of Rea1.

Fixation of the long Rea1 molecule at two distinct sites on the preribosomal surface is finally achieved by binding of MIDAS in Rea1 to Rsa4. In this constellation, a tension force could be generated by ATP hydrolysis in the AAA-ATPase motor domain, which is vectorially transmitted into the pre-60S particle for structural rearrangement (Figure 7).

An alternative to a spring-like tension model (Figure 7) is a long-range cooperative communication between the AAA head and the MIDAS domain. In such a scenario the long Rea1 tail could couple the two functional activities by transmitting structural information between the motor head and the substrate binding site at the MIDAS domain. Thus, propagation of information between AAA head and MIDAS via the tail could coordinate Rsa4 binding with the ATPase function. This mechanism would be similar to the binding of microtubules to the dynein heavy chain. There, a conformational change in dynein's microtubule-binding domain is transmitted toward the ATPase domain via the relative sliding of two α helices within the stalk (Carter et al., 2008).

Integrins utilize a MIDAS to bind to their extracellular ligands. Our mutational analysis suggests a similar binding mechanism

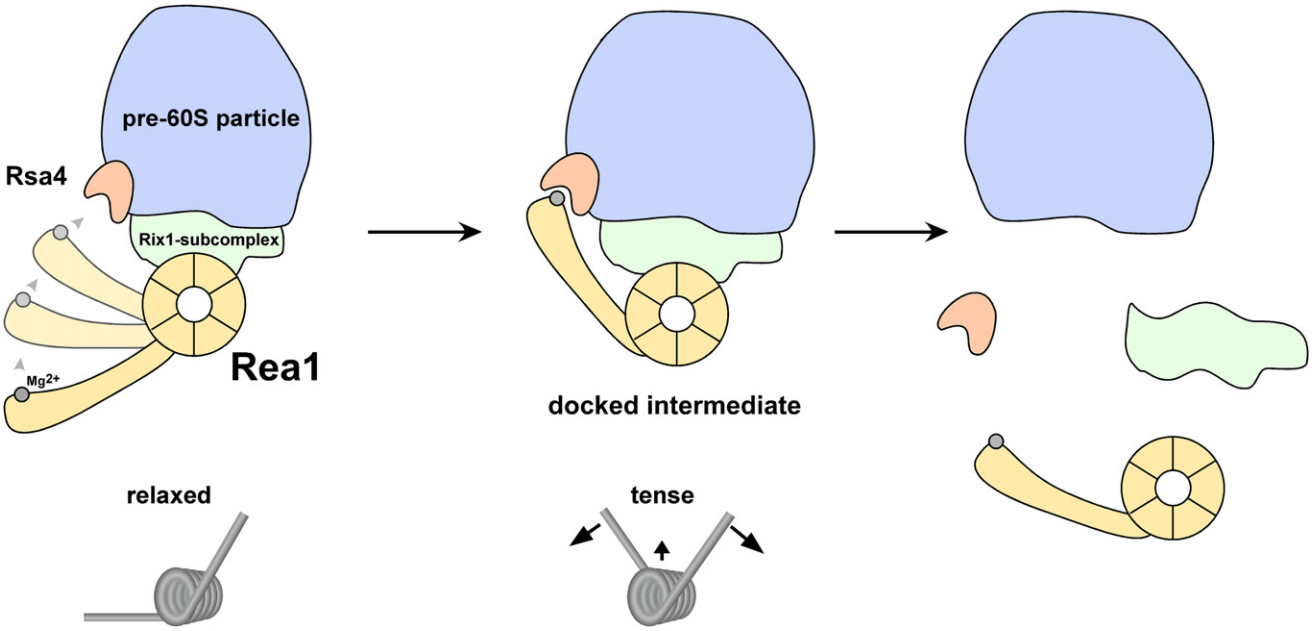

Figure 7. Model of a Mechanochemical Device on the Pre-60S Subunit to Generate Tensile Force for Removal of Pre-60S Factors

Schematic drawing of the pre-60S particle with attached Rea1 (composed of a hexameric AAA ATPase ring and a protruding tail) and Rsa4 (with a MIDAS binding site). Rsa4, Rea1 and the Rix1-subcomplex are released in an ATP-dependent manner. The tip of the flexible Rea1 tail harbours the MIDAS domain, which coordinates the MIDAS ion (Mg^{2+}). The AAA ring of Rea1 is attached via an adaptor structure (Rix1-subcomplex) to the 60S moiety, but the MIDAS tail can move up and contact the pre-60S particle at a distant site where Rsa4 is located. In a hypothetical pre-60S intermediate (middle panel), the MIDAS is docked to Rsa4 and hence tensile force generated by ATP hydrolysis in the Rea1 AAA domain can be used to pull off Rsa4, the Rix1-subcomplex and Rea1 from the pre-60S particle (right panel). The two different states of the Rea1 molecule (tail not bound and bound to Rsa4, respectively) are compared to a tensile spring in its relaxed or loaded (tense) state.

between Rea1 and Rsa4. The MIDAS domain of integrins harbors a ratchet-like α-helix that undergoes a conformational change (between open and close state) upon ligand binding. This effect is then transmitted toward a neighboring domain and finally through the entire integrin molecule into the cell (''outside-in signaling'') (Arnaout et al., 2005; Luo et al., 2007). The critical α-helix undergoing rearrangement upon ligand binding is also conserved in the Rea1 MIDAS domain. Moreover, it was shown that integrin MIDAS-ligand interactions have to resist mechanical tension and are further stabilized under tension (Craig et al., 2004; Astrof et al., 2006). In analogy, the initial contact between MIDAS and Rsa4 on the pre-60S particle could be strengthened by a pulling force generated by the Rea1 motor domain, allowing the unrestricted transmission of power onto the pre-60S particle for remodeling, which eventually leads to the dissociation of Rea1, Rsa4 and the Rix1-complex from the preribosome. After this release tension becomes reduced, which in consequence could weaken the interaction between MIDAS and Rsa4. In agreement with this speculation, Rea1 and Rsa4 released from the 60S subunit after ATP-treatment were found in different fractions of the sucrose gradient and class averages of the released Rea1 did not show an enlarged tip of the tail as would be expected if Rsa4 would remain bound.

In vitro the Rix1-subcomplex was only partially released from the pre-60S particle upon ATP treatment, whereas Rsa4 and Rea1 were dissociated very effectively. We attribute this difference to the fact that only two third of the Rix1-particles carry the Rea1 AAA ATPase (i.e., tail-containing particles). Assuming that only the concerted action between the Rea1 MIDAS and Rsa4 will lead to an ATP-dependent removal of the Rix1-subcomplex from the particle, the Rix1-subcomplex bound to tailless pre-60S subunits may not be detachable in vitro. Whether the Rix1-particles lacking Rea1 are bona fide pre-60S intermediates or some Rea1 molecules fall off during the prolonged purification procedure is not clear.

Our data are consistent with a model in which the Rix1-subcomplex is attached to the interface region of the 60S moiety, which later on during 60S biogenesis (i.e., at the level of the Arx1-particle) recruits the export factors Nmd3, Crm1 and Mex67-Mtr2 (Yao et al., 2007). Therefore, the ATP-dependent clearance of preribosomal factors from this surface could trigger the final nuclear biogenesis steps, which include structural rearrangement of pre-rRNA including 7S to 5.8S rRNA processing and unmasking of binding sites for export receptors. Thus, the generation of a tensile force by the Rea1 AAA ATPase could provoke structural maturation of a late nuclear pre-60S particle to generate the export-competent large subunit. Since ATP treatment did not release all preribosomal factors from the Rix1-particle (e.g., Nog1, Nog2, Nsa2, Rlp24, Nop7, Tif6), additional steps are needed for final maturation of the 60S subunit. One candidate factor is another AAA ATPase, Drg1, which was reported to trigger the release of a number of shuttling preribosomal factors (e.g., Nog1, Rlp24, Tif6, Arx1) from the pre-60S particles in the cytoplasm shortly after nuclear export (Pertschy et al.,

2007). Moreover, other reported release factors (e.g., Rpl10, Sqt1, Rei1, Jjj1) including GTPases (Lsg1 and Elf1) were implicated in the final dissociation and recycling of a number of pre-60S factors such as Nmd3, Arx1, Alb1 and Tif6 in the cytoplasm (for review see Henras et al., 2008; Zemp and Kutay, 2007).

In conclusion, rather than involving a cytoskeletal filament, the dynein-related Rea1 AAA ATPase and its interacting partners form a proper mechanochemical arrangement on the Rix1 pre-60S particle to exert a power stroke that can be used to release preribosomal factors and generate the export-competent 60S subunit.

EXPERIMENTAL PROCEDURES

Strains, Media, and Plasmids

Plasmids used in this study were generated using standard procedures and are listed in Table S2. Yeast *Saccharomyces cerevisiae* strains used in this study are listed in Table S3. The *Rea1/Rsa4* double shuffle strain was generated according to (Sträßer et al., 2000). Yeast genetic methods such as gene deletion or epitope tagging (TAP, HA, GFP) of genes at the genomic locus, transformation, mating and tetrad analysis were performed according to published procedures (Baßler et al., 2001; Longtine et al., 1998; Puig et al., 1998).

Protein Purification, Antibody Labeling, and Electron Microscopy

Rea1 was fused N-terminally with a TAP-tag expressed from a plasmid under control of the *GAL1* promoter in a wild-type yeast strain. Cells were grown in galactose-containing (YPG) medium to induce Rea1 overexpression. TAP-Rea1 was purified according to (Nissan et al., 2002), except that the buffers used for incubation on the calmodulin beads and the subsequent wash step contained 2 mM ATP for release of Rea1 from the preribosomal particles.

For immuno-EM, purification of Rix1-particles and antibody binding were performed as described (Nissan et al., 2002). For Ipi3-HA labeling the preribosomes were purified via Ipi3-HA-TAP, which yields the same type of particle (Nissan et al., 2004).

All negatively stained samples of Rea1 and the Rix1-particle were prepared with the sandwich technique as described (Diepholz et al., 2008). Particles were imaged under low dose using a Philips CM200 FEG electron microscope with a 2k x 2k CCD camera (TVIPS-GmbH) or using a Tecnai F30 electron microscope with a 4k x 4k Eagle camera (Table S1, for imaging conditions).

Image Processing

Particle images were selected from micrographs using 'Boxer' (Ludtke et al., 1999). Further image processing was done with IMAGIC 5 (van Heel et al., 1996). Particles were band-pass filtered and normalized in their gray value distribution. Unlabelled Rix1-particles were mass-centered, and classified following the alignment by classification strategy (Dube et al., 1993), whereas antibody-labeled Rix1-particles were aligned to a set of references. The set of references included one class average of tail-containing particles of group1 and one of group 2 (Figure 1C, S1 for grouping) and their mirror images. For labeled and unlabeled Rix1-particles alignment was followed by multivariate statistical analysis (MSA). For labeled Rix1-particles only those particles were retained in the data set, which grouped into classes resembling class averages of group 1 or group 2. Alignment and classification were repeated until classes remained stable (usually 1–2 iterations).

Finally for labeled particles, the aligned dataset was classified using a mask that focused the classification onto the periphery of the particle. This approach identified areas where additional density at the perimeter appeared frequently, but could not distinguish between small changes in the orientation of the body. However, due to preselection of particle images that belonged to group 1 or group 2 the orientational variations were relatively small.

To determine the distribution of the tail angles in the stained Rix1-particles (Figure 1D) these images were aligned to a representative set of class averages of tail containing particles, where the tails were computationally removed by a tight mask. Particle images that aligned to the same reference were sub-classified with a new mask only including the tail region. For accessing the intrinsic flexibility of Rea1 molecules (Figures 1B and 6C), only particle views that exhibited a regular ring-shaped domain were used. Class averages of these particles, including only the ring domain and the short tail-segment, were aligned relative to each other and used as references. Aligned particle images were classified using MSA focused on the ring domain (tight circular mask). Particles that grouped into the same class were sub-classified taking the whole particle into account (larger circular mask).

Miscellaneous

Reconstitution of the MIDAS-Rsa4 Interaction in *E. coli* and their subsequent affinity-purification were performed essentially as described (Gadal et al., 2001) with modifications given in the Supplemental Data. The preparation of rRNA and Northern blot analysis, and ATP treatment of the Rix1-particle are described in the Supplemental Data. Additional methods used in this study and described earlier include TAP-purification of pre-60S particles (Baßler et al., 2001; Nissan et al., 2002), sucrose gradient analysis to obtain ribosomal and polysomal profiles (Baßler et al., 2001), ribosomal export assays using the large subunit reporter Rpl25-GFP (Gadal et al., 2002) and the small subunit reporter Rps3-GFP (Milkereit et al., 2002) monitored by fluorescence microscopy according to (Baßler et al., 2006) and yeast 2-hybrid analysis (Kressler et al., 2008).

SUPPLEMENTAL DATA

Supplemental Data include Supplemental Experimental Procedures, six figures, two movies, and three tables and can be found with this article online at http://www.cell.com/supplemental/S0092-8674(09)00792-2.

ACKNOWLEDGMENTS

The excellent technical help of Martina Kallas and Claire Batisse is gratefully acknowledged. We thank Drs. M. Remacha, H. Tschochner, M. Fromont-Racine, A. W. Johnson, M. Seedorf, B. Stillman, and J. Warner for antibodies. B.B. was supported by the EU-grant '3D repertoire (LSHG-CT-2005-512028) and by the Welcome Trust (WT 087658). M.D. was supported by an E-STAR project (FP6 Marie Curie Action for Early-Stage-Training, MEST-CT-2004-504640). E.H. and J.B. are recipients of grants from the Deutsche Forschungsgemeinschaft (Hu363/9-2) and Fonds der Chemischen Industrie.

Received: October 16, 2008
Revised: May 11, 2009
Accepted: June 17, 2009
Published: September 3, 2009

REFERENCES

Arnaout, M.A., Mahalingam, B., and Xiong, J.P. (2005). Integrin structure, allostery, and bidirectional signaling. Annu. Rev. Cell Dev. Biol. *21*, 381–410.

Astrof, N.S., Salas, A., Shimaoka, M., Chen, J., and Springer, T.A. (2006). Importance of force linkage in mechanochemistry of adhesion receptors. Biochemistry *45*, 15020–15028.

Baßler, J., Grandi, P., Gadal, O., Leßmann, T., Tollervey, D., Lechner, J., and Hurt, E.C. (2001). Identification of a 60S pre-ribosomal particle that is closely linked to nuclear export. Mol. Cell *8*, 517–529.

Baßler, J., Kallas, M., and Hurt, E. (2006). The NUG1 GTPase reveals and N-terminal RNA-binding domain that is essential for association with 60 S pre-ribosomal particles. J. Biol. Chem. *281*, 24737–24744.

Carter, A.P., Garbarino, J.E., Wilson-Kubalek, E.M., Shipley, W.E., Cho, C., Milligan, R.A., Vale, R.D., and Gibbons, I.R. (2008). Structure and functional role of dynein's microtubule-binding domain. Science *322*, 1691–1695.

Chantha, S.C., and Matton, D.P. (2006). Underexpression of the plant NOTCH-LESS gene, encoding a WD-repeat protein, causes pleitropic phenotype during plant development. Planta *225*, 1107–1120.

Craig, D., Gao, M., Schulten, K., and Vogel, V. (2004). Structural insights into how the MIDAS ion stabilizes integrin binding to an RGD peptide under force. Structure *12*, 2049–2058.

Diepholz, M., Venzke, D., Prinz, S., Batisse, C., Flörchinger, B., Rössle, M., Svergun, D.I., Böttcher, B., and Féthière, J. (2008). A different conformation for the EGC stator sub-complex in solution and in the assembled yeast V-ATPase. Structure *16*, 1789–1798.

Dube, P., Tavares, P., Lurz, R., and van Heel, M. (1993). The portal protein of bacteriophage SPP1: a DNA pump with 13-fold symmetry. EMBO J. *12*, 1303–1309.

Erzberger, J.P., and Berger, J.M. (2006). Evolutionary relationships and structural mechanisms of AAA+ proteins. Annu. Rev. Biophys. Biomol. Struct. *35*, 93–114.

Fromont-Racine, M., Senger, B., Saveanu, C., and Fasiolo, F. (2003). Ribosome assembly in eukaryotes. Gene *313*, 17–42.

Gadal, O., Strauß, D., Kessl, J., Trumpower, B., Tollervey, D., and Hurt, E. (2001). Nuclear export of 60S ribosomal subunits depends on Xpo1p and requires a NES-containing factor Nmd3p that associates with the large subunit protein Rpl10p. Mol. Cell. Biol. *21*, 3405–3415.

Gadal, O., Strauss, D., Petfalski, E., Gleizes, P.E., Gas, N., Tollervey, D., and Hurt, E. (2002). Rlp7p is associated with 60S preribosomes, restricted to the granular component of the nucleolus, and required for pre-rRNA processing. J. Cell Biol. *157*, 941–951.

Galani, K., Nissan, T.A., Petfalski, E., Tollervey, D., and Hurt, E. (2004). Rea1, a Dynein-related Nuclear AAA-ATPase, Is Involved in Late rRNA Processing and Nuclear Export of 60 S Subunits. J. Biol. Chem. *279*, 55411–55418.

Garbarino, J.E., and Gibbons, I.R. (2002). Expression and genomic analysis of midasin, a novel and highly conserved AAA protein distantly related to dynein. BMC Genomics *3*, 18–28.

Granneman, S., and Baserga, S.J. (2004). Ribosome biogenesis: of knobs and RNA processing. Exp. Cell Res. *296*, 43–50.

Henras, A.K., Soudet, J., Gerus, M., Lebaron, S., Caizergues-Ferrer, M., Mougin, A., and Henry, Y. (2008). The post-transcriptional steps of eukaryotic ribosome biogenesis. Cell. Mol. Life Sci. *65*, 2334–2359.

Kressler, D., Roser, D., Pertschy, B., and Hurt, E. (2008). The AAA ATPase Rix7 powers progression of ribosome biogenesis by stripping Nsa1 from pre-60S particles. J. Cell Biol. *181*, 935–944.

Krogan, N.J., Peng, W.T., Cagney, G., Robinson, M.D., Haw, R., Zhong, G., Guo, X., Zhang, X., Canadien, V., Richards, D.P., et al. (2004). High-definition macromolecular composition of yeast RNA-processing complexes. Mol. Cell *13*, 225–239.

Longtine, M.S., McKenzie, A., Demarini, D.J., Shah, N.G., Wach, A., Brachat, A., Philippsen, P., and Pringle, J.R. (1998). Additional modules for versatile and economical PCR-based gene deletion and modification in Saccharomyces cerevisiae. Yeast *10*, 953–961.

Ludtke, S.J., Baldwin, P.R., and Chiu, W. (1999). EMAN: semiautomated software for high-resolution single-particle reconstructions. J. Struct. Biol. *128*, 82–97.

Luo, B.H., Carman, C.V., and Springer, T.A. (2007). Structural basis of integrin regulation and signaling. Annu. Rev. Immunol. *25*, 619–647.

Milkereit, P., Strauß, D., Baßler, J., Gadal, O., Kühn, H., Schütz, S., Gas, N., Lechner, J., Hurt, E., and Tschochner, H. (2002). A Noc-complex specifically involved in the formation and nuclear export of ribosomal 40S subunits. J. Biol. Chem. *278*, 4072–4081.

Nissan, T.A., Baßler, J., Petfalski, E., Tollervey, D., and Hurt, E.C. (2002). 60S pre-ribosome formation viewed from assembly in the nucleolus until export to the cytoplasm. EMBO J. *21*, 5539–5547.

Nissan, T.A., Galani, K., Maco, B., Tollervey, D., Aebi, U., and Hurt, E. (2004). A pre-ribosome with a tadpole-like structure functions in ATP-dependent maturation of 60S subunits. Mol. Cell *15*, 295–301.

Pertschy, B., Saveanu, C., Zisser, G., Lebreton, A., Tengg, M., Jacquier, A., Liebminger, E., Nobis, B., Kappel, L., van der Klei, I., et al. (2007). Cytoplasmic recycling of 60S preribosomal factors depends on the AAA protein Drg1. Mol. Cell. Biol. *27*, 6581–6592.

Puig, O., Rutz, B., Luukkonen, B.G., Kandels-Lewis, S., Bragado-Nilsson, E., and Seraphin, B. (1998). New constructs and strategies for efficient PCR-based gene manipulations in yeast. Yeast *14*, 1139–1146.

Roberts, A.J., Numata, N., Walker, M.L., Kato, Y.S., Malkova, B., Kon, T., Ohkura, R., Arisaka, F., Knight, P.J., Sutoh, K., et al. (2009). AAA+ Ring and linker swing mechanism in the dynein motor. Cell *136*, 485–495.

Spahn, C.M., Beckmann, R., Eswar, N., Penczek, P.A., Sali, A., Blobel, G., and Frank, J. (2001). Structure of the 80S ribosome from Saccharomyces cerevisiae–tRNA-ribosome and subunit-subunit interactions. Cell *107*, 373–386.

Sträßer, K., Baßler, J., and Hurt, E.C. (2000). Binding of the Mex67p/Mtr2p heterodimer to FXFG, GLFG, and FG repeat nucleoporins is essential for nuclear mRNA export. J. Cell Biol. *150*, 695–706.

Takagi, J. (2007). Structural basis for ligand recognition by integrins. Curr. Opin. Cell Biol. *19*, 557–564.

Tschochner, H., and Hurt, E. (2003). Pre-ribosomes on the road from the nucleolus to the cytoplasm. Trends Cell Biol. *13*, 255–263.

Vale, R.D. (2000). AAA proteins: lords of the ring. J. Cell Biol. *150*, 13–19.

van Heel, M., Harauz, G., Orlova, E.V., Schmidt, R., and Schatz, M. (1996). A new generation of the IMAGIC image processing system. J. Struct. Biol. *116*, 17–24.

Yao, W., Roser, D., Köhler, A., Bradatsch, B., Baßler, J., and Hurt, E. (2007). Nuclear export of ribosomal 60S subunits by the general mRNA export receptor Mex67-Mtr2. Mol. Cell *26*, 51–62.

Zemp, I., and Kutay, U. (2007). Nuclear export and cytoplasmic maturation of ribosomal subunits. FEBS Lett. *581*, 2783–2793.

Cell, Volume *138*

Supplemental Data

Mechanochemical Removal of Ribosome Biogenesis Factors from Nascent 60S Ribosomal Subunits

Cornelia Ulbrich, Meikel Diepholz, Jochen Baßler, Dieter Kressler, Brigitte Pertschy, Kyriaki Galani, Bettina Böttcher, and Ed Hurt

SUPPLEMENTAL EXPERIMENTAL PROCEDURES

Reconstitution of the MIDAS-Rsa4 Interaction in *E. coli*

E. coli strain Rosetta Star was co-transformed with pPROEX GST-TEV-*REA1*-MIDAS and pT7 HIS-*RSA4* or the respective mutant combination. Cells were cultured in 1 l minimal medium at 37°C to an OD_{600} of 0.5 and shifted to 16°C before induction with 0.2 mM IPTG for 2 h. Cell pellets were lysed in 10 ml buffer (150 mM NaCl, 50 mM Tris-HCl pH 7.5, 5 mM $MgCl_2$, 0.1 % Tween-20, 10% glycerol) by sonification and centrifuged (14000 rpm, 15 min). GST-TEV-MIDAS was purified from the supernatant with Protino Glutathione Agarose 4B (Macherey-Nagel). After two washing steps with 10 ml buffer, GST-tagged proteins were eluted by TEV-cleavage for 1 h at 16°C. Eluted proteins were analysed by SDS-PAGE and Coomassie staining or Western blotting using anti-Penta•His (Qiagen) and anti-GST (Biomol Upstate) antibodies.

Antibodies

Antibodies used for the Western analysis were used in the following dilutions: α-Rsa4 1:10.000 (de la Cruz et al., 2005), α-Nog2 1:20.000, α-Rlp24 1:15.000 and α-Nog1 1:30.000 (Saveanu et al., 2003), α-Noc3 1:500 (Milkereit et al., 2001), α-Ytm1 1:100 (Miles et al., 2005), α-Nmd3 1:10.000 (gift by Arlen Johnson), α-Nsa2 1:10.000 (Lebreton et al., 2006), α-Tif6 1:10.000 (Senger et al., 2001), α-Rpl35 1:35.000 (Frey et al., 2001), α-Rpl5 1:10.000 (Deshmukh et al., 1995), α-Nop7 1:50.000 (Du and Stillman, 2002), α-Rpl3 1:20.000 (Vilardell and Warner, 1997).

Northern blotting

Strains *GAL::*GFP-*RSA4, GAL::*GFP-*rsa4 E114D* were pre-grown in SRC-Trp medium to OD_{600nm} 0.2 before adding raffinose and galactose respectively to concentration 2% at time point zero. Samples were taken after various time points. RNA preparations were performed from 40 OD_{600} units per time point using the mechanical disruption protocol of the RNeasy Mini Kit (Qiagen). 3µg RNA each were loaded onto a 1.5% 20 cm long MOPS-agarose gel and separated at 60V for 10 hrs in MOPS buffer as described in the manual for the RNeasy Mini Kit. The RNA was transferred over night onto a Hybond N nylon membrane (Amersham) and afterwards crosslinked to the membrane by UV. Hybridization was done over night at 42°C in 500 mM $NaPO_4$ buffer, pH 7.2, 7% SDS, 1 mM EDTA using 5'-^{32}P labeled oligonucleotides with the following sequences: A2-A3, 5'-TGTTACCTCTGGGCCC-3'; D-A2, 5'GACTCTCCATCTCTTGTCTTCTTG3'; E-C2, 5'-GGCCAGCAATTTCAAGTTA-3'; 25S, 5'-CTCCGCTTATTGATATGC-3'; 18S, 5'-CATGGCTTAATCTTTGAGAC-3'; and 5.8S, 5'-GCGTTCTTCATCGATGC-3'. The membranes were washed three times for 20 minutes at 42°C in 40 mM $NaPO_4$ buffer, pH 7.2, 1% SDS, and radioactivity was detected by exposing X-ray films. Membranes were regenerated by washing 3 times for 20 minutes at 42°C in 1% SDS.

Purification of Rix1-particles in the presence of ATP

Strains Rix1-TAP *GAL::GFP-RSA4, GAL::GFP-rsa4 E114D* were pre-grown in SRC-Trp and then shifted to YPG for 6hrs at 30°C. Rix1 particles were purified in the presence of 10mM $MgCl_2$ according to Nissan et al. (2004). With the exception that 2mM of ATP were added together with the TEV protease and were present in all subsequent steps except the EGTA elution. As control identical purifications were performed without addition of ATP. Shown are the final EGTA eluates.

Analysis of the ATP-treated Rix1-particle on sucrose gradients

Rix1-particles were purified in the presence of 10mM $MgCl_2$ according to Nissan et al. (2004). After EGTA elution 10mM $MgCl_2$ and 2mM ATP were added and the purified particles were incubated for 2 hrs at 16°C. The reactions mix was loaded onto a 5-30% sucrose gradient in 1X TAP buffer (100 mM NaCl, 1.5 mM MgCl2, 0.15% NP40, 50 mM Tris-HCl pH7.5). The gradients were centrifuged for 15 hrs with 27,000 rpm at 4°C (Beckman, SW40). Finally, gradients were fractionated, TCA-precipitated and fractions were analysed by SDS-PAGE (SDS 4-12% polyacrylamid gradient gel) and Coomassie staining or Western blotting. The amount of Rix1 in the sucrose gradient fractions was quantified by the 'Quantity One Software' (BIORad).

Table S1. Compilation of sample preparation and imaging conditions for the represented data

Sample	Electron Microscope	Magni-fication	Pixel-Size/Å	# Micro graphs	# selected Particles
Rea1 molecule	CM200 FEG	27,500	5.2	80	9091
Rix1-particle Rea1-HA + AB	CM200 FEG	27,500	5.2	64	1497
Rix1-particle, Rix1-HA + AB	CM200 FEG	27,500	5.2	100	1555
Rix1-particle Ipi3-HA-TAP+AB	F30	20,500	5.0	18	1544
Rix1-particle, Rpl3-HA +AB	CM200 FEG	27,500	5.2	32	1479
Rix1-particle Rpl5-HA + AB	CM200 FEG	27,500	5.2	50	1529
Rix1-particle, HA-Rsa4 +AB	CM200 FEG	27,500	5.2	64	1839
Rix1-particle no label + AB	CM200 FEG	27,500	5.2	50	1787
Rix1-particle Rpl3-HA	CM200 FEG	27,500	5.2	50	2005
Rix1-particle	CM200 FEG	27,500	5.2	190	8619
Rix1-particle mock treated	F30	20,500	5.0	20	5389 big 2258 small
Rix1-particle + 2 mM ATP	F30	31,000	3.7	25	5341 big 6014 small

F30: FEI Tecnai F30 electron microscope with field emission gun operating at 300 kV, Eagle 4kx4k CCD camera: data collected automatically with Serial EM under low dose conditions using the montage option; defocus range 1.2 +/- 0.3 μm

CM200 FEG: Philips CM200 FEG field emission gun electron microscope operating at 200 kV, TVIPS GmbH 2kx2k CCD camera: data collected manually under low dose conditions; defocus range 1.5+/- 0.3 μm.

NS: negatively stained sample according to following protocol: sample was incubated for 1 min on glow discharged grid, washed 3 times with water and 3 times with 2% uranyl acetate; the last washing step was incubated for 5 min before removal

SW: negatively stain sample sandwiched between two layers of carbon as outlined before (Diepholz et al. 2008)

AB: antibody against HA; Rix1-particle: pre-60S subunit affinity-purified by Rix1-TAP as bait, additionally modified subunits are given.

Table S2. Plasmids used in this study

Name	Relevant information	Reference
pRS316-*RSA4*	CEN, *URA3*, *RSA4*	This study
pRS314-*RSA4*	CEN, *TRP1*, *RSA4*	This study
pRS314-*rsa4-1*	CEN, *TRP1*, *rsa4-1*	This study
pRS314-*rsa4 D72AD73A*	CEN, *TRP1*, *rsa4 D72A,D73A*	This study
pGFP-*RSA4*	YCplac22, CEN, *TRP1*, yEGFP-*RSA4* T*ADH1*,	This study
pGFP-*rsa4 T113A*	YCplac22, CEN, *TRP1*, yEGFP-*rsa4 T113A* T*ADH1*	This study
pGFP-*rsa4 E114D*	YCplac22, CEN, *TRP1*, yEGFP-*rsa4 E114D* T*ADH1*	This study
pGFP-*rsa4 E114A*	YCplac22, CEN, *TRP1*, yEGFP-*rsa4 E114A* T*ADH1*	This study
pGalGFP-*RSA4*	YCplac22, CEN, *TRP1*, P*GAL1* yEGFP-*RSA4* T*ADH1*	This study
pGalGFP-*rsa4 T113A*	YCplac22, CEN, *TRP1*, P*GAL1* yEGFP-*rsa4 T113A*T*ADH1*	This study
pGalGFP-*rsa4 E114D*	YCplac22, CEN, *TRP1*, P*GAL1* yEGFP-*rsa4 E114D* T*ADH1*	This study
pGalGFP-*rsa4 E114A*	YCplac22, CEN, *TRP1*, P*GAL1* yEGFP-*rsa4 E114A* T*ADH1*	This study
pGalTAP-*RSA4*	YCplac111, CEN, *LEU2*, P*GAL1* NTAP+2xFlag-*RSA4* T*ADH1*	This study
pGalTAP-*rsa4 T113A*	YCplac111, CEN, *LEU2*, P*GAL1* NTAP+2xFlag-rsa4 *T113A* T*ADH1*	This study
pGalTAP-*rsa4 E114D*	YCplac111, CEN, *LEU2*, P*GAL1* NTAP+2xFlag-rsa4 *E114D* T*ADH1*	This study
pHA-*RSA4*	YCplac111, CEN, *LEU2*, 2xHA-*RSA4* T*ADH1*	This study
YCG-*YLR106c*	CEN, *URA3*, *REA1*	Euroscarf, Germany
pRS415-*REA1*	CEN, *LEU2*, *REA1*	Galani et al., 2004
pRS415-*rea1-7*	CEN, *LEU2*, *rea1-7ts*	Galani et al., 2004
pRS415-*rea1-21*	CEN, *LEU2*, *rea1-21ts*	Galani et al., 2004
pTAP-*REA1*	CEN, *LEU2*, NTAP+2xFlag-*REA1*	This study
pTAP-*rea1-DAA*	CEN, *LEU2*, NTAP+2xFlag *rea1 S4712A,S4714A*	This study
pTAP-*rea1-DTS*	CEN, *LEU2*, NTAP+2xFlag *rea1 S4712T*	This study
pRS314-RFP-*NOP1-RPL25*-GFP	CEN, *TRP1*, P*NOP1* mRFP-*NOP1-RPL25*-yEGFP large ribosomal subunit export reporter	This study
pRS314-RFP-*NOP1-RPS3*-GFP	CEN, *TRP1*, P*NOP1* mRFP-*NOP1-RPS3*-yEGFP small ribosomal subunit export reporter	This study
pRS315-*RIX1*-TAP	CEN, *LEU2*, *RIX1*-TAP	This study
pGBKT7-*rea1MIDAS*	CEN, TRP1, 2µ, G4BD-c-myc-*rea1MIDAS*aa4622-4910	This study
pGBKT7-*rea1MIDAS-DAA*	CEN, TRP1, 2µ, G4BD-c-myc-*rea1MIDAS S4712A,S4714A* aa4622-4910	This study
pGBKT7-*rea1MIDAS-DTS*	CEN, TRP1, 2µ, G4BD-c-myc- *rea1MIDAS S4712T* aa4622-4910	This study
pGADT7-*RSA4*	CEN, LEU2, 2µ, G4AD-HA-*RSA4*	This study
pGADT7-*rsa4N1-154*	CEN, LEU2, 2µ, G4AD-HA-*rsa4N aa1-154*	This study
pGADT7-*rsa4N20-128*	CEN, LEU2, 2µ, G4AD-HA-*rsa4N aa20-128*	This study
pGADT7-*rsa4 D72A,D73A*	CEN, LEU2, 2µ, G4AD-HA-*rsa4 D72A,D73A aa1-154*	This study
pGADT7-*rsa4 T113A*	CEN, LEU2, 2µ, G4AD-HA-*rsa4 T113A aa1-154*	This study
pGADT7-*rsa4 E114D*	CEN, LEU2, 2µ, G4AD-HA-*rsa4 E114D aa1-154*	This study
pGADT7-*rsa4 E114A*	CEN, LEU2, 2µ, G4AD-HA-*rsa4 E114A aa1-154*	This study
pACTII-*NOG2*	CEN, LEU2, 2µ, G4AD-HA-*NOG2*	This study
pACTII-*NUG1*	CEN, LEU2, 2µ, G4AD-HA-*NUG1*	Bassler et al., 2006
pACTII-*NOG1*	CEN, LEU2, 2µ, G4AD-HA-*NOG1*	Lebreton et al., 2006
pACTII-*NSA2*	CEN, LEU2, 2µ, G4AD-HA-*NSA2*	Lebreton et al., 2006
pACTII-*IPI3*	CEN, LEU2, 2µ, G4AD-HA-*IPI3*	This study
pACTII-*IPI1*	CEN, LEU2, 2µ, G4AD-HA-*IPI1*	This study

pACTII-*RIX1*	CEN, LEU2, 2µ, G4AD-HA-*RIX1*	This study
pVA3-1	aa 72-390 of murine p53 expressed from $pAS1_{CYH2}$; 2µ, *TRP1*, P*ADH1*, N-terminal G4BD	Clontech
pTD1-1	aa 87-708 of SV40 large T-antigen expressed from pACT2; 2µ, *LEU2*, P*ADH1*, N-terminal G4AD	Clontech
pT7 HIS-*RSA4*	pET9D, Kan, HIS6-*RSA4*	This study
pT7 HIS-*rsa4* E114A	pET9D, Kan, HIS6-*rsa4* E114A	This study
pPROEX GST-TEV-*REA1*-MIDAS	pPROEX HTb HIS-TEV-GST-TEV-*REA1-MIDAS*, Amp	This study
pROEX GST-TEV-*REA1*-MIDAS-DTS	pPROEX HTb HIS-TEV-GST-TEV-rea*1*-MIDAS-DTS, Amp	This study
pROEX GST-TEV-*REA1*-MIDAS-DAA	pPROEX HTb HIS-TEV-GST-TEV-rea*A1*-MIDAS-DAA, Amp	This study
pFA6a-kanMX6	for genomic deletion disruption	Longtine et al., 1998
pFA6a-HIS3MX6	for genomic deletion disruption	Longtine et al., 1998
pFA6a-natNT2	for genomic deletion disruption	Janke et al., 2004
pFA6a-3xHA-TAP-T.*CYC1*-natNT2	3xHA+TAP tag; for genomic C-terminal tagging	This study
pFA6a-3xHA-HIS3	3xHA tag; for genomic C-terminal tagging	Longtine et al., 1998
pBS1479	TAP tag; for genomic C-terminal tagging	Puig et al., 1998

Table S3. Yeast Strains used in this study

Name	Genotype	Reference
Ssf1-TAP (Y3425)	DS1-2b *MAT*α *SSF1*-TAP::TRP1	Yao et al., 2007
Nsa1-TAP (Y4159)	DS1-2b *MAT*α *NSA1*-TAP::TRP1	Kressler et al., 2008
Arx1-TAP (Y2151)	DS1-2b *MAT*α *ARX1*-TAP::TRP1	Nissan et al., 2002
Lsg1-TAP (Y2165)	DS1-2b *MAT*α *LSG1*-TAP::TRP1	Nissan et al., 2002
Rix1-TAP (Y2152)	DS1-2b *MAT*α *RIX1*-TAP::TRP1	Nissan et al., 2002
Rix1-TAP Rpl3-HA (Y3943)	DS1-2b *MAT*α *RIX1*-TAP::TRP1 *RPL3*-3xHA::HIS3	this study
Rix1-TAP Rpl5-HA (Y3944)	DS1-2b *MAT*α *RIX1*-TAP::TRP1 *RPL5*-3xHA::HIS3	this study
Rix1-HA-TAP (Y4213)	DS1-2b *MAT*α RIX1-3xHA-CBP-TEV-ptA2::natNT2	this study
Ipi31-HA-TAP (Y4520)	DS1-2b *MAT*α *Ipi3*-3xHA-CBP-TEV-ptA2::natNT2	this study
Rix1-TAP Rea1-HA	DS1-2b *MAT*α *RIX1*-TAP::TRP1 *Rea1*-3xHA::HIS3	this study
Rix1-TAP HA-Rsa4 (Y4270)	DS1-2b *MAT*α *RIX1*-TAP::TRP1 *rsa4*::kanMX4 YCplac111-P.Rsa4-HA-*RSA4*-T.ADH1	this study
Rea1-TAP (Y2484)	DS1-2b *MAT*α *REA1*-TAP::TRP1	this study
Rea1 shuffle (Y4512)	W303 *MAT***a** *rea1*::kanMX6 YCG-*YLR106c*	this study
Rsa4 shuffle (Y3978)	W303 *MAT***a** *rsa4*::kanMX6 pRS316-*RSA4*	this study
Rea1-Rsa4 double shuffle (Y3982)	W303 *MAT***a** *rea1*::kanMX6 *rsa4*::HIS3MX6 YCG-*YLR106c* pRS316-*RSA4*	this study
Rix1 shuffle (Y4294)	BY4743 *MAT***a** *rix1*::kanMX4 *trp1*::natNT2	this study
haploid WT white YDK11-5A	W303 *MAT*α *ade3*::kanMX4	Kressler et al., 1999
Y2H strain PJ69-4A	*MAT***a**, trp1-901, leu2-3,112, ura3-52, his3-200, gal4, gal80, GAL2-ADE2, *LYS2*::GAL1-HIS3, *met2*::GAL7-lacz	James et al., 1996

*strains used in this study are either derived from W303 (MATa/MATα ade2-1/ade2-1 his3-11,15/ his3-11,15 leu2-3,112/leu2-3,112 trp1-1/trp1-1 ura3-1/ura3-1 can1-100/can1-100) or from BY4743 (Euroscarf,Germany) or from DS1-2b (FY23xFY86; MATα his3-Δ200 leu2-Δ1 trp1-Δ63 ura3-52)

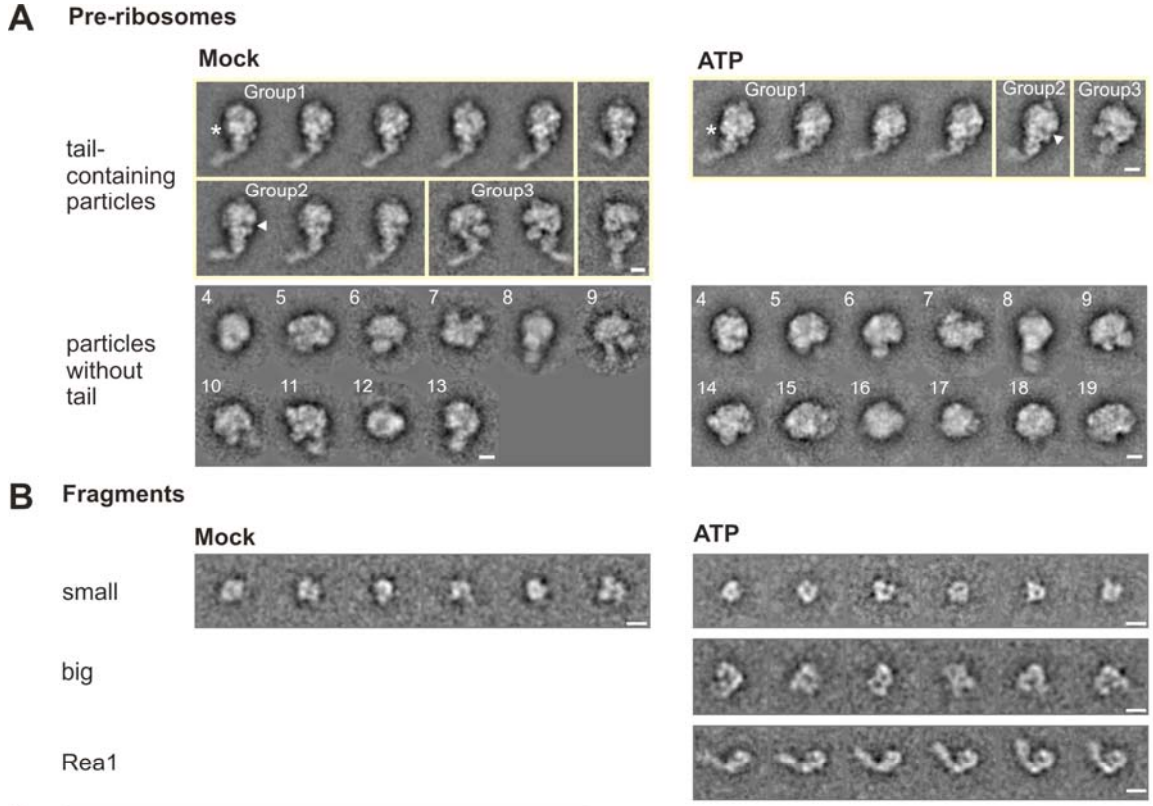

C

	mock		ATP	
	total	percent	total	percent
Pre-ribosomes	**5389**	100%	**5341**	100%
With Tail	**3825**	71%	**1920**	36%
No Tail	**1564**	29%	**3421**	64%
Fragments	**2258**	100%	**6014**	266%

	mock		ATP	
	total	percent	total	percent
Fragments	**2258**	100%	**6014**	100%
Small	**2237**	99%	**4044**	67%
Big	**15**	1%	**772**	13%
Rea1 shape	**6**	0%	**1198**	20%
With Tail	**3825**	100%	**1920**	100%
Group 1	**1990**	52%	**1503**	78%
Group 2 (Hole)	**908**	24%	**144**	8%
Group 3 (Helmet)	**413**	11%	**61**	3%
Other	**514**	13%	**212**	11%

	mock		ATP	
	total	percent	total	percent
No tail	**1564**	100%	**3421**	100%
Group 4	**81**	5%	**344**	10%
Group 5	**58**	4%	**259**	8%
Group 6	**84**	5%	**248**	7%
Group 7	**62**	4%	**98**	3%
Group 8	**35**	2%	**180**	5%
Group 9	**34**	2%	**147**	4%
Group 10	**123**	8%	-	-
Group 11	**115**	7%	-	-
Group 12	**123**	8%	-	-
Group 13	**82**	5%	-	-
Group 14	-	-	**224**	7%
Group 15	-	-	**111**	3%
Group 16	-	-	**97**	3%
Group 17	-	-	**68**	2%
Group 18	-	-	**141**	4%
Group 19	-	-	**86**	3%
Other	**767**	49%	**1418**	41%

Figure S1. EM class averages and statistical analysis of mock-treated and ATP-treated Rix1-particles

ATP treated and mock-treated Rix1-particle preparations showed larger pre-ribosomal particles and smaller fragments. Pre-ribosomal particles and fragments were analyzed separately by alignment and classification.

(A) Typical class averages of tail-containing pre-60S particles (upper panel). These particles occur in only few different views, which can be grouped by the appearance of the body. Class averages belonging to the same group are framed by a yellow line. Groups 1-3 account for more than 85% of all tail-containing particles. Typical for group 1 is a patch of high density (*)

above the attachment site. Group 2 shows an apparent indention in the middle of the particle opposite to the side of the tail (arrow head). Group 3 has a characteristic more segmented appearance of the body. The relative amount of Rix1-particles in the three groups is different in ATP-treated and mock-treated sample (see (C) for statistics). ATP-treatment reduces predominantly particles in group 2 and 3. Typical class averages of tail-less pre-60S particles (lower panel). For ATP-treated and mock-treated samples the class averages are much more variable than for tail-containing particles. We show a selection of the most frequent views (see (C) for statistics).

(B) Typical class averages of the smaller fragments. Mock-treated and untreated samples show a background of smaller fragments, which are not pre-ribosomal particles. In the mock-treated samples, projections of smaller fragments have a comparable diameter of 10-12 nm (upper panel, left). Similar projections are also found in the ATP-treated samples (upper panel, right). In addition, ATP-treated samples also show elongated particles that resemble the Rea1 molecule (lower panel, right) and larger fragments (middle panel, right), which are both absent in the mock-treated sample.

(C) Statistics of the distribution of particles in the mock-treated and ATP-treated Rix1-particles. The number of pre-60S subunits with and without tail was estimated by counting the particles that clustered into the respective classes. For the overall distribution of particles, we set the total number of pre-60S particles in each sample and the relative amount of fragments per ribosomal particle in the mock-treated sample to 100%. The relative distributions in the analysis of ‘fragments’, ‘tail particles’ and ‘particles without tail’ are given in respect to the absolute number of particles of the respective species (‘fragments’, ‘with tail ’, ‘no tail’). This statistical analysis reveals an ATP-dependent decrease in tail-containing particles together with an increase in smaller fragments and a change in the composition of tail-containing particles and smaller fragments.

A

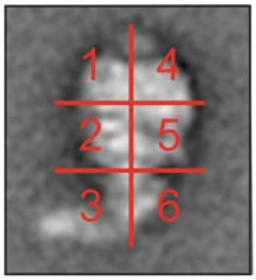

Rea1-HA	285
10 (4 %)	7 (2 %)
8 (3 %)	15 (5 %)
59 (21 %)	15 (5 %)

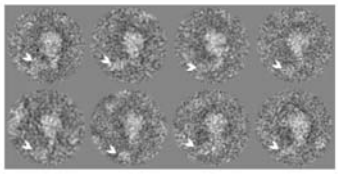

Rpl3-HA	387
248 (64 %)	31 (8 %)
14 (4 %)	15 (4 %)
10 (3 %)	16 (4 %)

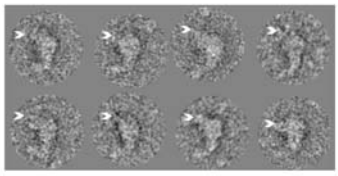

Rpl5-HA	324
3 (1%)	7 (2%)
3(1 %)	43 (13%)
10 (3 %)	27 (8 %)

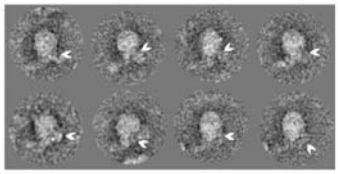

Rix1-HA	386
12 (3 %)	8 (2 %)
16 (4 %)	11 (3 %)
21 (5 %)	75 (19 %)

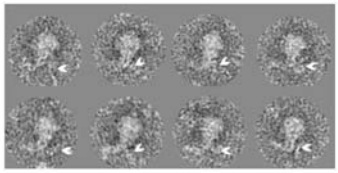

Ipi3-HA	407
8 (2 %)	14 (3 %)
6 (1 %)	97 (24 %)
14 (3 %)	99 (24 %)

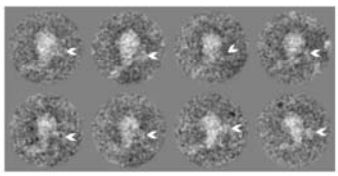

HA-Rsa4	469
25 (5 %)	13 (3 %)
78 (17 %)	18 (4 %)
16 (3 %)	7 (1%)

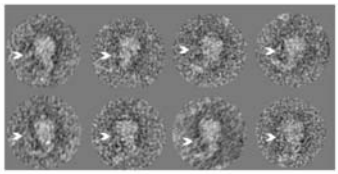

B

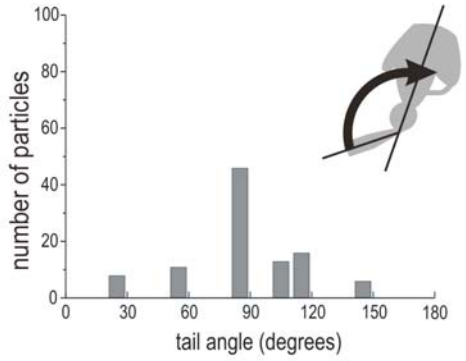

Figure S2: Statistical analysis of localization of ribosomal and pre-ribosomal proteins by antibody labeling and distribution of tail movement in Rix1-particles

(A) Statistical analysis of antibody labeling. A typical projection of the Rix1-particle was divided into six equally sized segments (upper panel). For the different labeling experiments, we counted densities connected to the periphery of the Rix1-particles in the different segments. The results are summarized in the tables below the graph, which have the same layout as the grid used for the segmentation. The segment with the highest occupancy for each labeling experiment is highlighted in grey. The absolute numbers of counted particles are given in the upper right corner of each table. Galleries of typical raw images of labeled Rix1-particles are shown for the different experiments on the right. The additional density in the periphery is indicated by an arrow head.

(B) Histogram of the tail angles of Rea1 in the Rix1-particle. A subset of particles with the same orientation of the body (group2, see Figure S1A) and the largest mobility of the tail was selected. Angles were measured between the tail and the long axis of the Rix1-particle, as indicated in the scheme above. The histogram shows that the most frequent tail position of approximately one third of all particles is 90° to the long axis of the Rix1-particle.

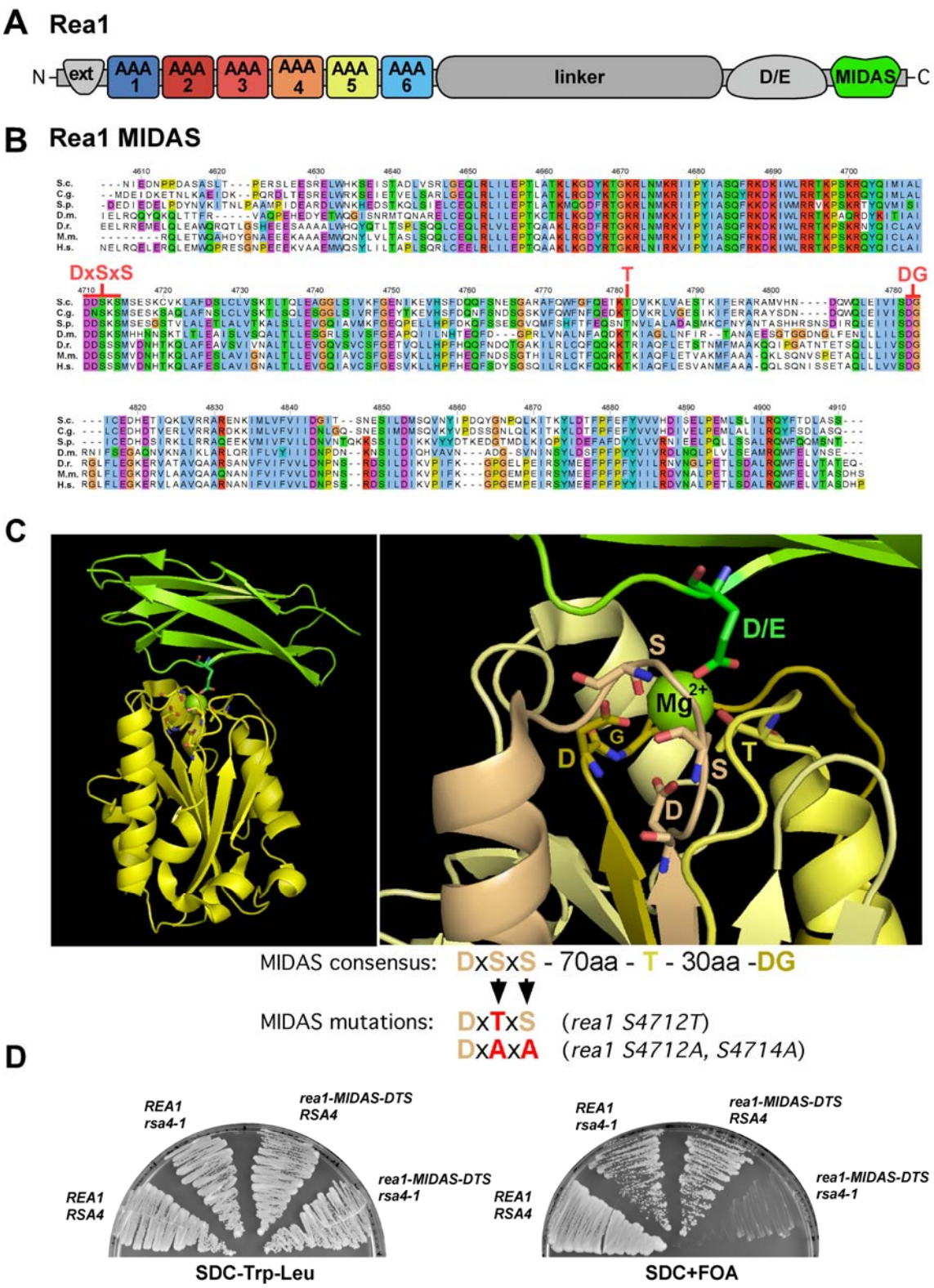

Figure S3. Rea1 MIDAS mutants and their genetic interaction with *rsa4-1*

(A) Domain organization of the Rea1 AAA ATPase according to (Garbarino and Gibbons, 2002). (B) Sequence alignment of the Rea1 MIDAS domain from *Saccharomyces cerevisiae*

(S.c.) with its different homologues from *Candida glabrata* (C.g.), *Schizosaccharomyces pombe* (S.p.), *Drosophila melanogaster* (D.m.), *Danio rerio* (D.r.), *Mus musculus* (M.m.) and *Homo sapiens* (H.s.) by ClustalW2 (http://www.ebi.ac.uk/Tools/clustalw2/index.html?) and displayed with Jalview. Indicated above the alignment are the conserved residues that bind the MIDAS ion.

(C) X-ray structure (pdb number 1T0P) of the αL-β2-integrin MIDAS fold (yellow) with ICAM ligand (green) and the MIDAS ion (Mg^{2+}, green sphere). Overview of the crystal structure (left) and a zoom into the area of the fold, in which the MIDAS ion is coordinated. Shown in the structure are the five residues (D, S, S, T, D), which coordinate the Mg^{2+}. Below the structure the MIDAS consensus and the Rea1 MIDAS mutations generated in this study are indicated.

(D) Analysis of synthetic lethal interactions between the *rsa4-1* mutant (Q12P, K355R, D423N, F436L; generated by a PCR-based random mutagenesis) combined with the *rea1-S4712T* (MIDAS-DTS; see also Figure 4C) mutant. The *Rea1/Rsa4* double shuffle strain was transformed with plasmids that carry the indicated wild-type and mutant alleles. Transformants were streaked out on a SDC+5-FOA plate and incubated at 30°C for three days. No growth indicates synthetic lethality. For the plating control, cells were also grown on SDC–Trp-Leu plates.

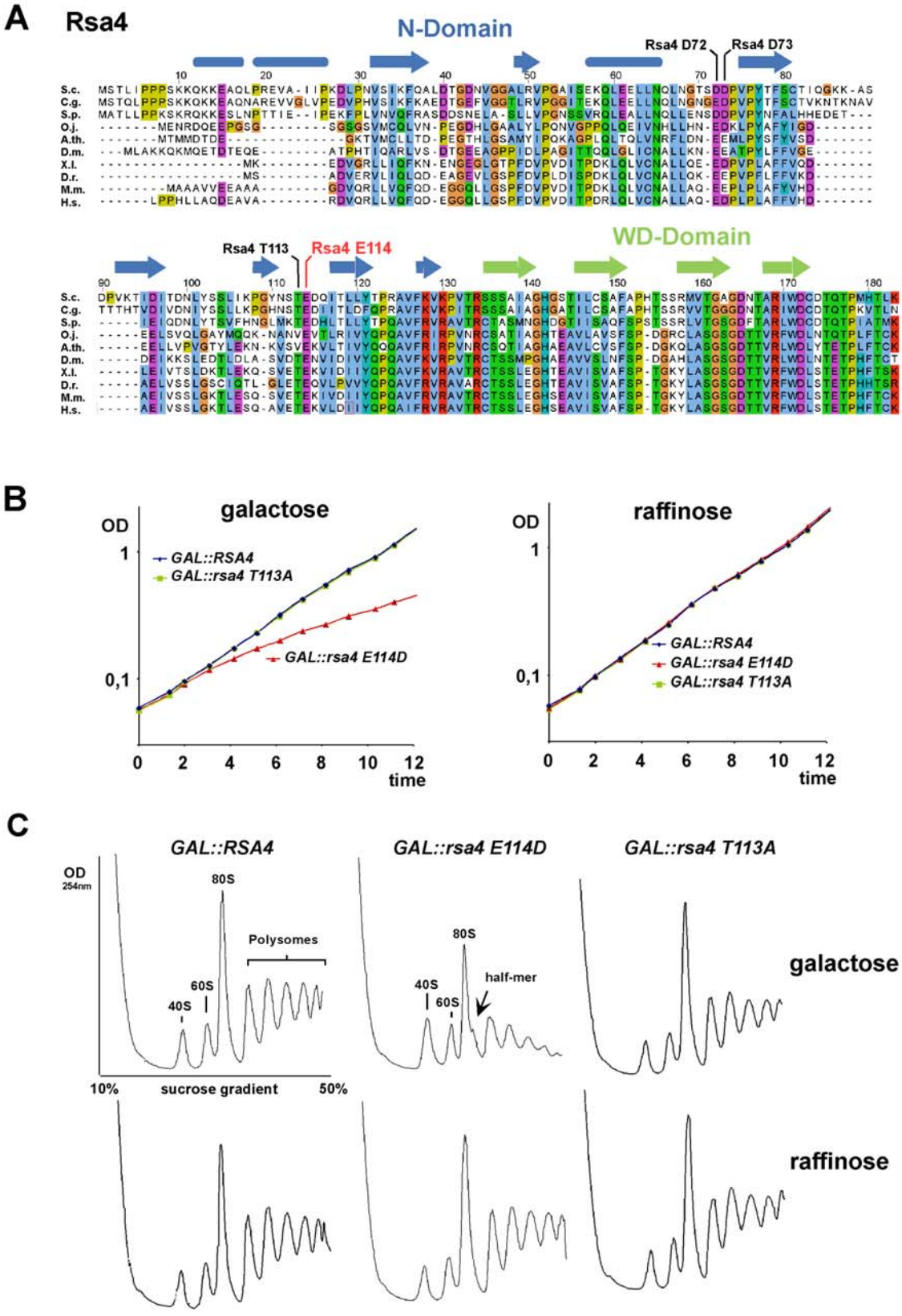
A
Rsa4
N-Domain
Rsa4 D72
Rsa4 D73
WD-Domain
Rsa4 T113
Rsa4 E114
B
galactose
raffinose
OD
GAL::RSA4
GAL::rsa4 T113A
GAL::rsa4 E114D
time
C
GAL::RSA4
GAL::rsa4 E114D
GAL::rsa4 T113A
OD 254nm
80S
60S
40S
Polysomes
half-mer
10%
sucrose gradient
50%
galactose
raffinose

Figure S4. Characterization of the dominant-negative *GAL::rsa4 E114D* mutant.

(A) Sequence alignment of the N-terminal domain (N-Domain) plus a short sequence of the β-propeller C-domain (WD-Domain) of Rsa4 and its different orthologues. *Saccharomyces cerevisiae* (S.c.), *Candida glabrata* (C.g.), *Schizosaccharomyces pombe* (S.p.), *Oryza sativa Japonica* (O.j.), *Arabidopsis thaliana* (A.t.), *Drosophila melanogaster* (D.m.), *Xenopus laevis* (X.l.), *Danio rerio* (D.r.), *Mus musculus* (M.m.) and *Homo sapiens* (H.s.). Indicated above the alignment are the conserved residues E114, T113, D72 and D73 mutated in this study in yeast Rsa4, and a secondary structure prediction (α-helical bars; β-sheet arrows).

B) Growth curve of the dominant-negative *GAL::*GFP-*rsa4 E114D* mutant. Strains *GAL::* GFP-*RSA4, GAL::* GFP-*rsa4 E114D GAL::* GFP-*rsa4 T113A* were pre-grown in SRC-Trp medium to OD_{600nm} 0.2 before adding raffinose and galactose respectively to concentration 2% at time point zero. OD_{600nm} was measured to follow cell growth.

(C) Analysis of polysome profiles of the dominant-negative *GAL::*TAP-*rsa4 E114D* mutant. The indicated strains expressing *GAL::* TAP-*RSA4*, *GAL::* TAP-*rsa4 E114D* or *GAL::* TAP-*rsa4 T113A* were grown in SGC-Leu (galactose) or SRC-Leu (raffinose) medium at 30°C for 6 hrs, before whole cell lysates were analyzed by sedimentation centrifugation on sucrose density gradients (OD_{254nm}). 40S, 60S and 80S ribosomes, polysomes and “half-mer” polysomes are indicated.

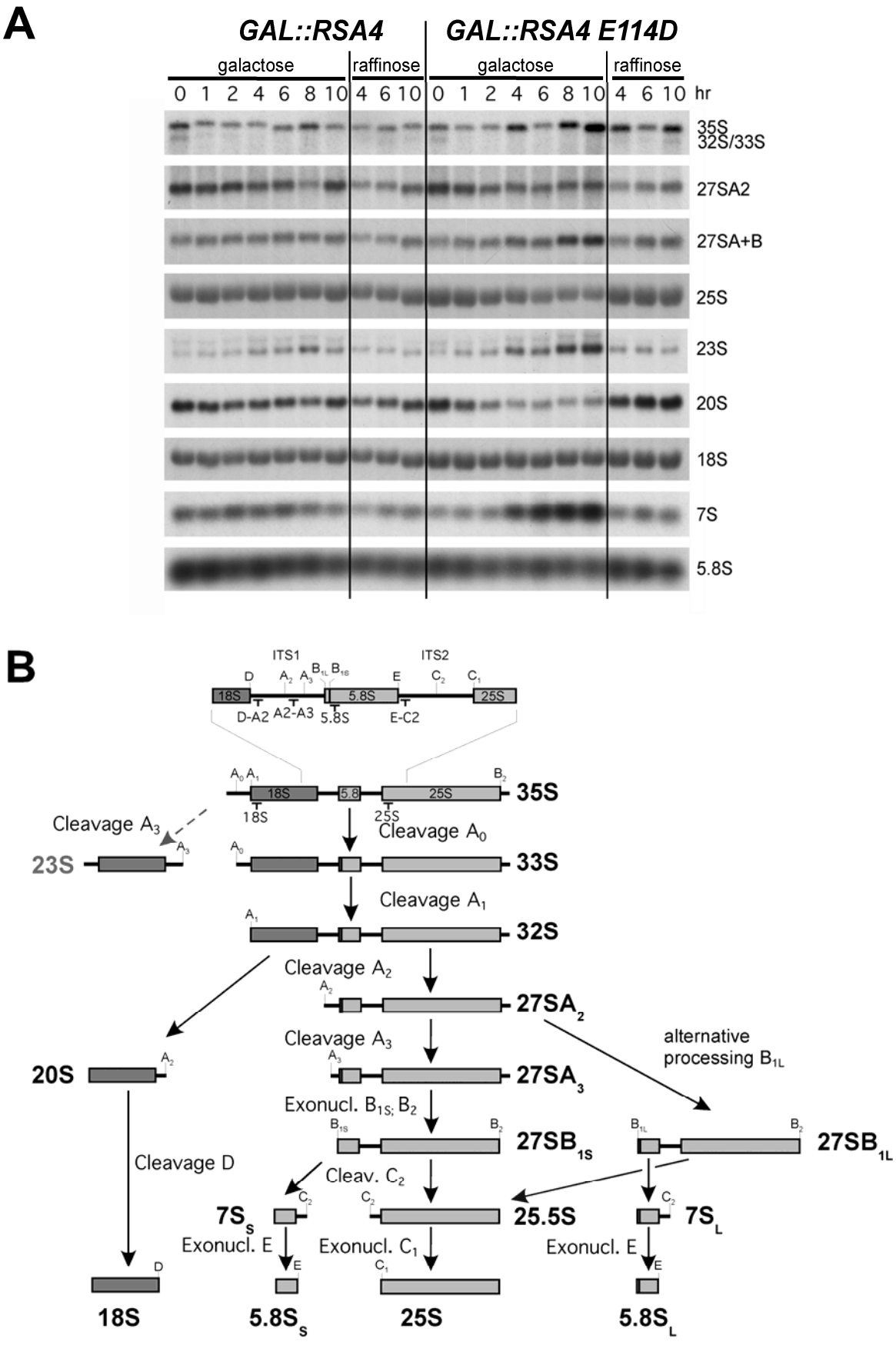
A
GAL::RSA4
GAL::RSA4 E114D
galactose
raffinose
galactose
raffinose
0 1 2 4 6 8 10 4 6 10 0 1 2 4 6 8 10 4 6 10 hr
35S
32S/33S
27SA2
27SA+B
25S
23S
20S
18S
7S
5.8S
B
ITS1
ITS2
D
A2
A3
B1L
B1S
E
C2
C1
18S
5.8S
25S
D-A2
A2-A3
5.8S
E-C2
A0 A1
B2
35S
Cleavage A3
Cleavage A0
23S
33S
Cleavage A1
32S
Cleavage A2
27SA2
Cleavage A3
27SA3
alternative processing B1L
20S
Exonucl. B1S, B2
27SB1S
27SB1L
Cleavage D
Cleav. C2
7SS
25.5S
7SL
Exonucl. E
Exonucl. C1
Exonucl. E
18S
5.8SS
25S
5.8SL

Figure S5. Pre-rRNA processing in the dominant-negative *GAL::rsa4 E114D* mutant

(A) Over-expression of the Rsa4 E114D protein impairs 7S pre-rRNA processing. The expression of wild-type Rsa4 and Rsa4 E114D was induced by galactose and RNA was isolated after 0, 2, 4, 6, 8 and 10 hours of induction. rRNA processing intermediates were detected by Northern blotting. Probes used for the shown autoradiographs were D-A2 (for 35S, 32/33S, and 20S pre-rRNAs), A2-A3 (for 27SA2 and 23S pre-rRNAs), E-C2 (for 27S and 7S pre-rRNAs) and 18S, 25S and 5.8S for the respective mature rRNA species.

(B) Scheme of the rRNA processing pathway. The binding sites of the probes used for detection are indicated. In the course of rRNA processing, the 35S pre-rRNA undergoes a series of endonucleolytic processing events at sites A_0, A_1 and A_2 that lead to the separation into the 20S and $27SA_2$ pre-rRNAs. Defects in processing at these sites lead to premature cleavage at A_3, generating the aberrant 23S rRNA. The 20S pre-rRNA is converted into the mature 18S rRNA by an endonucleolytic cleavage. Endo- and exonucleolytic processing of the $27SA_2$ pre-rRNA generates the two alternative 5' ends of the 5.8S rRNA. Finally, the 27SB pre-rRNA is cleaved at site C_2 into a 25.5S and a 7S precursor which are both exonucleolytically processed to yield the mature 25S and 5.8S rRNAs (for further details of rRNA processing, see Henras et al., 2008).

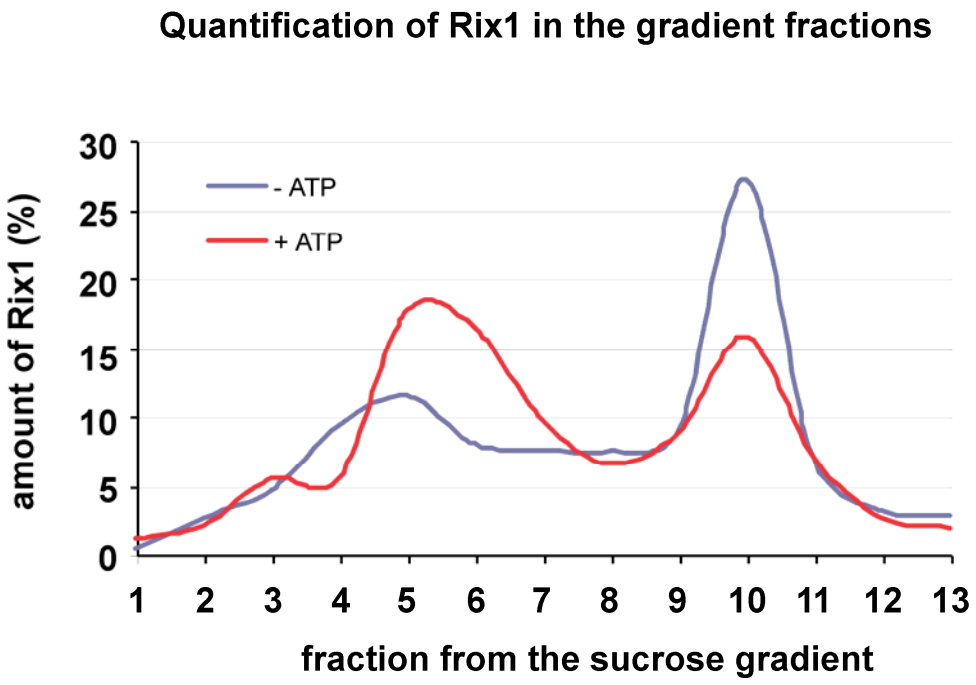

Figure S6. Quantification of ATP-induced Rix1 release from the pre-60S particle

The amount of Coomassie-stained Rix1 protein present in each of the sucrose gradient fractions 1-13 (shown in Figure 6B) was quantified by the 'Quantity One Software' (BIORad). The % signal intensity of Rix1 in a given fraction was compared to the total Rix1 signal present in all sucrose gradient fractions (100%). These values (amount of Rix1 in %) were then plotted against the fraction number 1-13. The blue graph shows the amount of Rix1 without ATP, and the red graph with ATP treatment.

Supplemental References

Baßler, J., Kallas, M., and Hurt, E. (2006). The NUG1 GTPase reveals and N-terminal RNA-binding domain that is essential for association with 60 S pre-ribosomal particles. J Biol Chem 281, 24737-24744.

De la Cruz, J., Sanz-Martinez, E., and Remacha, M. (2005). The essential WD-repeat protein Rsa4p is required for rRNA processing and intra-nuclear transport of 60S ribosomal subunits. Nucleic Acids Res 33, 5728-5739.

Deshmukh, M., Stark, J., Yeh, L.C., Lee, J.C., and Woolford, J.L., Jr. (1995). Multiple regions of yeast ribosomal protein L1 are important for its interaction with 5 S rRNA and assembly into ribosomes. J Biol Chem 270, 30148-30156.

Du, Y.C., and Stillman, B. (2002). Yph1p, an ORC-interacting protein: potential links between cell proliferation control, DNA replication, and ribosome biogenesis. Cell 109, 835-848.

Frey, S., Pool, M., and Seedorf, M. (2001). Scp160p, an RNA-binding, polysome-associated protein, localizes to the endoplasmic reticulum of Saccharomyces cerevisiae in a microtubule-dependent manner. JBiolChem 276, 15905-15912.

Galani, K., Nissan, T.A., Petfalski, E., Tollervey, D., and Hurt, E. (2004). Rea1, a Dynein-related Nuclear AAA-ATPase, Is Involved in Late rRNA Processing and Nuclear Export of 60 S Subunits. J Biol Chem 279, 55411-55418.

James, P., Halladay, J., and Craig, E.A. (1996). Genomic libraries and a host strain designed for highly efficient two-hybrid selection in yeast. Genetics 144, 1425-1436.

Janke, C., Magiera, M.M., Rathfelder, N., Taxis, C., Reber, S., Maekawa, H., Moreno-Borchart, A., Doenges, G., Schwob, E., Schiebel, E.*, et al.* (2004). A versatile toolbox for PCR-based tagging of yeast genes: new fluorescent proteins, more markers and promoter substitution cassettes. Yeast 21, 947-962.

Kressler, D., Doere, M., Rojo, M., and Linder, P. (1999). Synthetic lethality with conditional dbp6 alleles identifies Rsa1p, a nucleoplasmic protein involved in the assembly of 60S ribosomal subunits. Mol Cell Biol 19, 8633-8645.

Kressler, D., Roser, D., Pertschy, B., and Hurt, E. (2008). The AAA ATPase Rix7 powers progression of ribosome biogenesis by stripping Nsa1 from pre-60S particles. J Cell Biol 181, 935-944.

Lebreton, A., Saveanu, C., Decourty, L., Jacquier, A., and Fromont-Racine, M. (2006). Nsa2 is an unstable, conserved factor required for the maturation of 27 SB pre-rRNAs. J Biol Chem 281, 27099-27108.

Longtine, M.S., McKenzie, A., Demarini, D.J., Shah, N.G., Wach, A., Brachat, A., Philippsen, P., and Pringle, J.R. (1998). Additional modules for versatile and economical PCR-based gene deletion and modification in Saccharomyces cerevisiae. Yeast 10, 953-961.

Miles, T.D., Jakovljevic, J., Horsey, E.W., Harnpicharnchai, P., Tang, L., and Woolford, J.L., Jr. (2005). Ytm1, Nop7, and Erb1 form a complex necessary for maturation of yeast 66S preribosomes. Mol Cell Biol 25, 10419-10432.

Milkereit, P., Gadal, O., Podtelejnikov, A., Trumtel, S., Gas, N., Petfalski, E., Tollervey, D., Mann, M., Hurt, E., and Tschochner, H. (2001). Maturation of Pre-Ribosomes Requires Noc-Proteins and is Coupled to Transport from the Nucleolus to the Nucleoplasm. Cell 105, 499-509.

Nissan, T.A., Baßler, J., Petfalski, E., Tollervey, D., and Hurt, E.C. (2002). 60S pre-ribosome formation viewed from assembly in the nucleolus until export to the cytoplasm. EMBO J 21, 5539-5547.

Puig, O., Rutz, B., Luukkonen, B.G., Kandels-Lewis, S., Bragado-Nilsson, E., and Seraphin, B. (1998). New constructs and strategies for efficient PCR-based gene manipulations in yeast. Yeast 14, 1139-1146.

Saveanu, C., Namane, A., Gleizes, P.E., Lebreton, A., Rousselle, J.C., Noaillac-Depeyre, J., Gas, N., Jacquier, A., and Fromont-Racine, M. (2003). Sequential protein association with nascent 60S ribosomal particles. Mol Cell Biol 23, 4449-4460.

Senger, B., Lafontaine, D.L.J., Graindorge, J.-S., Gadal, O., Camasses, A., Sanni, A., GarnierJ.-M., Breitenbach, M., Hurt, E.C., and Fasiolo, F. (2001). The nucle(ol)ar Tif6p and Efl1p, a novel EF-2 like GTPase, are required for a late cytoplasmic step of ribosome synthesis. Mol Cell 8, 1363-1373.

Vilardell, J., and Warner, J.R. (1997). Ribosomal protein L32 of Saccharomyces cerevisiae influences both the splicing of its own transcript and the processing of rRNA. Mol Cell Biol *17*, 1959-1965.

Yao, W., Roser, D., Köhler, A., Bradatsch, B., Baßler, J., and Hurt, E. (2007). Nuclear export of ribosomal 60S subunits by the general mRNA export receptor Mex67-Mtr2. Mol Cell 26, 51-62.

the patients with spermatogenic failure, Y chromosome anomalies, or sex reversal examined by Lange et al.), it is a clear drawback to the Y chromosome's mechanism of self-preservation. Indeed, every form of refuge really does have its price.

REFERENCES

Aitken, R.J., and Marshall Graves, J.A. (2002). Nature *415*, 963.

Guedes, A.D., Bianco, B., Lipay, M.V., Brunoni, D., de Lourdes Chauffaille, M., and Verreschi, I.T. (2006). Am. J. Med. Genet. A. *140A*, 1871–1875.

Jacobs, P., Dalton, P., James, R., Mosse, K., Power, M., Robinson, D., and Skuse, D. (1997). Ann. Hum. Genet. *61*, 471–483.

Lahn, B.T., Pearson, N.M., and Jegalian, K. (2001). Nat. Rev. Genet. *2*, 207–216.

Lange, J., Skaletsky, H., van Daalen, S.K.M., Embry, S.L., Korver, C.M., Brown, L.G., Oates, R.D., Silber, S., Repping, S., and Page, D.C. (2009). Cell, this issue.

McClintock, B. (1941). Genetics *26*, 234–282.

Page, S.L., and Shaffer, L.G. (1998). Chromosome Res. *6*, 115–122.

Skaletsky, H., Kuroda-Kawaguchi, T., Minx, P.J., Cordum, H.S., Hillier, L., Brown, L.G., Repping, S., Pyntikova, T., Ali, J., Bieri, T., et al. (2003). Nature *423*, 825–837.

Wilson, M.A., and Makova, K.D. (2009). PLoS Genet. *5*, e1000568. 10.1371/journal.pgen.1000568.

The Rea1 Tadpole Loses Its Tail

Jason Talkish[1] and John L. Woolford, Jr.[1,*]
[1]Department of Biological Science, Carnegie Mellon University, Pittsburgh, PA 15213, USA
*Correspondence: jw17@andrew.cmu.edu

DOI 10.1016/j.cell.2009.08.019

More than 170 assembly factors aid the construction and maturation of yeast ribosomes. After these factors' functions are completed, they must be released from preribosomes. In this issue, Ulbrich et al. (2009) describe a mechanochemical process through which the AAA ATPase Rea1 induces release of an assembly protein complex from preribosomes.

Ribosomes, the ubiquitous factories that produce proteins from mRNAs, are essential for growth, proliferation, and adaptation of cells. In eukaryotes, assembly of these complex ribonucleoprotein particles (RNPs) begins in the nucleolus with the association of a subset of ribosomal proteins (r-proteins) and *trans*-acting assembly factors with the nascent ribosomal RNA (rRNA) to form the 90S pre-rRNP, the single precursor to both the 40S and 60S mature subunits. The assembly factors are transient actors—they are released once their role is completed. But do they just know when to let go or are they actively removed from the maturing subunits? In this issue, Ulbrich et al. (2009) provide the most detailed study to date to answer this question. They discover a mechanochemical process for release of assembly factors and suggest that release is an integral part of ribosomal subunit maturation.

Beginning with the 90S precursor, the pre-rRNP undergoes a series of pre-rRNA processing and assembly steps while transiting from the nucleolus through the nucleoplasm to the cytoplasm to form mature 40S and 60S functional subunits (Henras et al., 2008). The two ribosomal subunits contain intricate structural cores of rRNA decorated on their surfaces with r-proteins. Studies of bacterial ribosome assembly in vitro revealed that ribosomal subunit assembly is cooperative and hierarchical. Ribosomal RNA and bound r-proteins undergo multiple structural rearrangements induced by binding of additional r-proteins to enable successive assembly steps (reviewed in Nomura, 1990). However, binding of r-proteins to rRNA is not sufficient to drive assembly forward.

Genetic and proteomic analysis in yeast has identified >170 proteins present in pre-rRNPs, but not mature ribosomes, that are required for ribosome assembly in vivo. These assembly factors, largely conserved from yeast to humans, include AAA ATPases, GTPases, RNA-dependent ATPases/helicases, kinases, nucleases, scaffolding proteins, and RNA-binding proteins. At least nine of these proteins, including GTPases and ATPases, release other factors, reduce the complexity of pre-rRNPs, and power the progression of subunit maturation (Figure 1; reviewed in Henras et al., 2008; Zemp and Kutay, 2007).

Although we now have a great deal of insight into what mature ribosomal subunits look like, understanding the mechanism of ribosome assembly in detail requires learning the precise functions of each assembly factor. Several key questions immediately come to mind: At which point in the assembly pathway does each factor associate with pre-rRNPs? Where is each factor located in preribosomes? When does each factor function? Upon which molecules does each factor act? When, how, and why do assembly factors exit from pre-rRNPs?

In their new study, Ulbrich and coworkers use an elegant combination of electron microscopy, site-directed mutagenesis, and assays of factor release from preribosomes to answer these questions about the AAA ATPase Rea1. These analyses enable them to work out how Rea1 operates in ribosome biogenesis.

Rea1 is the largest protein in yeast, 550 kDa, and is related to the motor protein dynein. It contains six AAA ATPase protomers at its N terminus, followed by a long linker region, a negatively charged domain, and a C-terminal MIDAS (metal ion-dependent adhesion site) protein-protein interaction motif. Rea1 has been found in late, nucleoplasmic pre-60S particles. Rea1 can also be isolated from preribosomes in a salt-stable complex with the assembly factors Rix1, Ipi1, and Ipi3, indicating intimate interactions among these molecules (Galani et al., 2004). Importantly, the ability to purify preribosomes containing the Rea1 protein enabled demonstration of ATP-dependent dissociation of Rea1 and the Rix1-Ipi1-Ipi3 subcomplex from preribosomes (Nissan et al., 2004).

To build a more detailed mechanism for how Rea1 functions, Ulbrich et al. used negative staining and cryoelectron microscopy of the purified protein to investigate the structure of Rea1. Rea1 contains a ring (presumably the six ATPase protomers) connected to a flexibly hinged tail. Analysis of preribosomal particles by immunoelectron microscopy revealed a "tadpole"-like structure. The "head" of the tadpole contains r-proteins, and Rea1 comprises the tail. The AAA domains of Rea1 are located near the central protuberance of the preribosome body, and the C-terminal MIDAS domain is located at the end of Rea1's tail. The Rix1-Ip1-Ipi3 subcomplex is sandwiched between Rea1 and the pre-60S particle.

Whereas the ATPase domain is anchored to the preribosomal particle, Rea1's tail shows more heterogeneity in its localization. In some pre-60S particles, the tip of Rea1's tail appears to contact the body of the pre-60S particle, which is suggestive of a second, perhaps more transient interaction. Ulbrich et al. used structural and biochemical assays to identify an assembly factor, Rsa4, that may be a potential Rea1 interactor located on the pre-rRNP surface. Importantly, the authors show that the interaction of Rsa4 with Rea1 is needed for ribosome biogenesis and that it requires the MIDAS domain of Rea1 both in vitro and in vivo. Disrupting the Rea1-Rsa4 interaction prevents removal of Rea1 and the Rix1-Ipi1-Ipi3 complex from preribosomes. All of their data to date suggest a scenario in which the tail of Rea1 contacts Rsa4 and, upon ATP hydrolysis, peels it off of the pre-60S subunit. This is coupled to the release of Rea1 itself and the Rix1 subcomplex.

There are several reasons why assembly factors must be disassembled from preribosomes. Certainly recycling of these proteins is an efficient plan. Yeast produce just enough of each factor to feed the ribosome assembly pipeline for a few minutes under conditions of rapid growth. Also, there is a limit to the size of a particle that can squeeze through nuclear pores, so most factors must be removed prior to export of the largely mature ribosomal subunits. Release of assembly factors may be coupled with rearrangements of pre-rRNP structures necessary for subsequent steps in the biogenesis of ribosomal subunits. Finally, factor release may serve as a timing/quality control mechanism, signaling successful completion of a maturation step. Prior to their release, bound assembly factors may prevent premature binding of export or translation factors. For example, the release of Rea1 and the Rix1 subcomplex from preribosomes, just before nuclear export of the particles, may enable subsequent binding of the Mex67 export factor to 5S rRNA in the central protuberance of the ribosome (Yao et al., 2007). In *rea1* or *rsa4* yeast mutants where this release is blocked, there is no nuclear export of nascent ribosomes.

The authors present several models for how Rea1 could displace Rsa4 and the Rix1 complex. The "spring-like tension" model posits that binding of both the AAA domain and the tip of the flexible Rea1 tail to two different sites on the preribosome, followed by ATP hydrolysis, creates tension that translates into displacement of proteins bound to Rea1. Alternatively, the "long-range cooperative communication" model proposes that one or more conformational changes in Rea1 are transmitted from one end of the molecule to the other. For example, binding of the Rea1 tail to the preribosome might alter the conformation of an α helix in the MIDAS domain, which then is somehow coupled with forces created by the AAA motor domain, to initiate changes in the preribosome. The challenge now is to design appropriate experiments to test these models, perhaps by obtaining higher-resolution structures of the Rea1 motor protein, which will inform yeast mutagenesis studies. Clearly ribosome

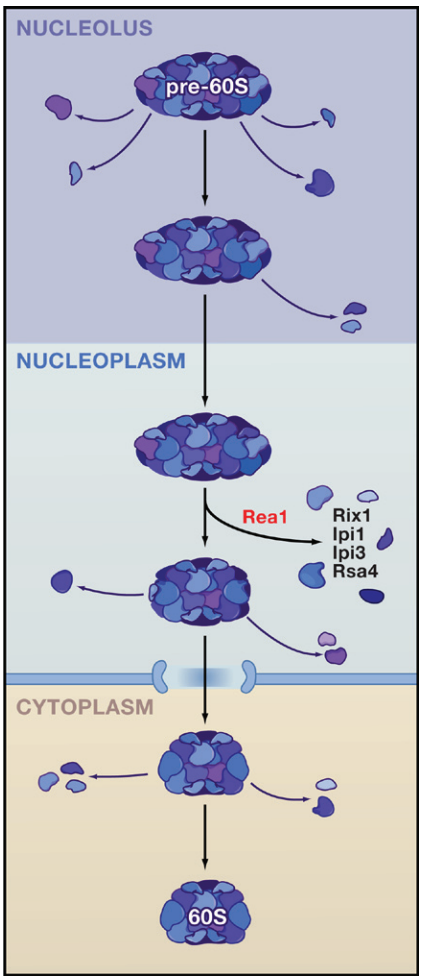

Figure 1. Giving Assembly Factors the Old "Heave Ho"

Proteins associated with preribosomal particles that are required for ribosome assembly are released by other factors as the preribosomes become mature ribosomal subunits during transit from the nucleolus through the nucleoplasm to the cytoplasm. Release of assembly factors is essential for the ribosome biogenesis pathway and may help to drive the maturation of ribosomal subunits. Rea1, a ribosome-associated factor related to dynein, removes the Rix1-Ipi1-Ipi3 assembly complex in the nucleoplasm. Rea1 associates with pre-60S particles through an interaction with the Rix1 complex. It also makes a second contact to the particle through an interaction between its C-terminal MIDAS domain and the Rsa4 assembly factor. Rea1 translates this two-point attachment and the hydrolysis of ATP into a mechanochemical process that removes Rsa4, the Rix1 complex, and itself from pre-60S particles.

biogenesis proceeds by means more complex than changes in conformation induced by r-protein binding. The process requires large inputs of energy generated by ATPases and GTPases.

It seems unlikely that the immense, energy-consuming enzyme Rea1 functions only to release a handful of assembly factors. It will be exciting to discover how Rea1-mediated remodeling is coupled with pre-rRNA processing. One will also want to discover whether and how release is regulated. Does one of the GTPases in the Rix1 particle activate Rea1? Does Rea1 contact any other preribosomal molecules? Are other assembly factors, in addition to Rsa4 and the Rix subcomplex, released by Rea1? Of course, once these questions are answered, the when, how, and why of the release of the remaining 150+ assembly factors from preribosomes await discovery.

REFERENCES

Galani, K., Nissan, T.A., Petfalski, E., Tollervey, D., and Hurt, E. (2004). J. Biol. Chem. *279*, 55411–55418.

Henras, A.K., Soudet, J., Gerus, M., Lebaron, S., Caizergues-Ferrer, M., Mougin, A., and Henry, Y. (2008). Cell. Mol. Life Sci. *65*, 2334–2359.

Nissan, T.A., Galani, K., Maco, B., Tollervey, D., Aebi, M., and Hurt, E. (2004). Mol. Cell *15*, 295–301.

Nomura, M. (1990). The Ribosome. W.E. Hill, A. Dahlberg, R.A. Garrett, P.B. Moore, D. Schlessinger, and J.R. Warner, eds. (Washington, D.C.: American Society for Microbiology), pp. 3–55.

Ulbrich, C., Diepholz, M., Bassler, J., Kressler, D., Pertschy, B., Galani, K., Böttcher, B., and Hurt, E. (2009). Cell, this issue.

Yao, W., Roser, D., Kohler, A., Bradatsch, B., Bassler, J., and Hurt, E. (2007). Mol. Cell *26*, 51–62.

Zemp, I., and Kutay, U. (2007). FEBS Lett. *581*, 2783–2793.

IKKε: A Bridge between Obesity and Inflammation

Jerrold M. Olefsky[1,*]

[1]Department of Medicine, University of California, San Diego, La Jolla, CA 92093, USA

*Correspondence: jolefsky@ucsd.edu

DOI 10.1016/j.cell.2009.08.018

Obesity leads to tissue inflammation and insulin resistance, which are features of metabolic diseases such as type 2 diabetes. Chiang et al. (2009) now show that the IκB kinase IKKε is an important link between obesity and inflammation and may be a new therapeutic target for treating obesity-related metabolic diseases.

Insulin resistance involves a decreased ability of tissues to respond to insulin and is a key metabolic abnormality in most patients with type 2 diabetes (Olefsky and Courtney, 2005). Although there can be genetic or other causes of insulin resistance, the predominant cause is obesity. The prevalence of obesity is increasing at an alarming rate in all age groups worldwide, and the obesity epidemic is driving the increased incidence of type 2 diabetes. Obesity leads to an increase in tissue inflammation, particularly within adipose (fat) tissue (Figure 1) (Schenk et al., 2008; Shoelson et al., 2007; Hotamsiligil and Erbay, 2008). It was Xu et al. (2003) and Weisberg et al. (2003) who first reported that large numbers of macrophages accumulate in fat depots in obese mice and humans. Tissue macrophages recruited to adipose tissue in obese animals exhibit increased expression of a broad array of genes encoding inflammatory pathway components. These macrophages secrete proinflammatory cytokines (TNF-α, IL1-β, IL-6, etc.) that work in a paracrine, and possibly endocrine, fashion leading to defects in insulin signaling and systemic insulin resistance. Blocking the function of these macrophages results in a glucose-tolerant, insulin-sensitive phenotype (Schenk et al., 2008; Shoelson et al., 2007; Solinas et al., 2007; Hotamsiligil and Erbay, 2008). Other insulin target tissues can also participate in the chronic inflammatory state. In the liver, the specialized resident macrophages or Kupffer cells show activation of proinflammatory pathways in response to obesity. In skeletal muscle, there is increased accumulation of proinflammatory macrophages within the intramuscular adipose depots that develop in obesity (Varma et al., 2009). Changes in the mixture of adipokines released from adipose tissue, as well as ectopic lipid deposition in liver and muscle, can also contribute to decreased insulin sensitivity. In this issue of *Cell*, Chiang et al. (2009) now show that the protein kinase IKKε is a crucial bridge between obesity and inflammation.

IKKε is a member of the IκB kinase family, and its expression is induced by activation of the inflammatory NF-κB signaling pathway. The function of IKKε is incompletely understood, although it

Molecular Cell
Article

The AAA-ATPase Rea1 Drives Removal of Biogenesis Factors during Multiple Stages of 60S Ribosome Assembly

Jochen Baßler,[1,*] Martina Kallas,[1] Brigitte Pertschy,[2] Cornelia Ulbrich,[1] Matthias Thoms,[1] and Ed Hurt[1,*]
[1]Biochemie-Zentrum der Universität Heidelberg, Im Neuenheimer Feld 328, 69120 Heidelberg, Germany
[2]Institut für Molekulare Biowissenschaften, Karl-Franzens Universität Graz, Universitätsplatz 2, A-8010 Graz, Austria
*Correspondence: jochen.bassler@bzh.uni-heidelberg.de (J.B.), ed.hurt@bzh.uni-heidelberg.de (E.H.)
DOI 10.1016/j.molcel.2010.05.024

SUMMARY

The AAA$^+$-ATPase Rea1 removes the ribosome biogenesis factor Rsa4 from pre-60S ribosomal subunits in the nucleoplasm to drive nuclear export of the subunit. To do this, Rea1 utilizes a MIDAS domain to bind a conserved motif in Rsa4. Here, we show that the Rea1 MIDAS domain binds another pre-60S factor, Ytm1, via a related motif. In vivo Rea1 contacts Ytm1 before it contacts Rsa4, and its interaction with Ytm1 coincides with the exit of early pre-60S particles from the nucleolus to the nucleoplasm. In vitro, Rea1's ATPase activity triggers removal of the conserved nucleolar Ytm1-Erb1-Nop7 subcomplex from isolated early pre-60S particle. We suggest that the Rea1 AAA$^+$-ATPase functions at successive maturation steps to remove ribosomal factors at critical transition points, first driving the exit of early pre-60S particles from the nucleolus and then driving late pre-60S particles from the nucleus.

INTRODUCTION

Ribosomes consisting of ribosomal RNA (rRNA) and ribosomal proteins (r proteins) are the machines that synthesize all cellular proteins. In eukaryotes, the two ribosomal subunits (60S and 40S) are first assembled in the nucleolus, a territory of the nucleus specialized for ribosome production, before export to the cytoplasm. During ribosome synthesis ~200 nonribosomal factors and ~100 small nucleolar RNAs (snoRNAs) transiently work on the evolving ribosomal subunits to facilitate their assembly and maturation (Fromont-Racine et al., 2003; Henras et al., 2008; Tschochner and Hurt, 2003). Ribosome biogenesis requires extensive regulation and coordination to meet the cellular demands for continuous ribosome production, which is essential for all actively dividing cells. Accordingly, the misregulation of signaling pathways in cancer cells stimulates ribosome biogenesis, and, conversely, defects in ribosome assembly can cause inherited human diseases collectively called ribosomopathies (Freed et al., 2010; Ganapathi and Shimamura, 2008; Narla and Ebert, 2010). This all indicates that a detailed mechanistic understanding of ribosome biogenesis could aid in designing new strategies for cancer therapy or curing ribosomopathies.

In the past, ribosome biogenesis was extensively studied in yeast by numerous integrative approaches (reviewed in Fromont-Racine et al., 2003; Granneman and Baserga, 2004; Henras et al., 2008; Kressler et al., 2009; Strunk and Karbstein, 2009; Tschochner and Hurt, 2003). To date, there are fewer investigations of ribosome assembly in higher eukaryotes, but nevertheless they suggest that the mechanism of ribosome formation and the participating biogenesis factors have been conserved during evolution (Grimm et al., 2006; Hölzel et al., 2005, 2007; Rohrmoser et al., 2007; Thomas and Kutay, 2003; Trotta et al., 2003; Zemp et al., 2009). The emerging consensus from all of these studies is that nonribosomal factors act sequentially with distinct recruitment and displacement during the interdependent steps of ribosome formation (reviewed in Fromont-Racine et al., 2003; Henras et al., 2008; Tschochner and Hurt, 2003).

Among the myriad of *trans*-acting factors are energy-consuming enzymes like GTPases, DExD/H-box ATPases, kinases, and AAA$^+$-ATPases. In particular, the AAA$^+$-ATPases Rix7, Rea1, and Drg1 were shown to be involved in 60S subunit biogenesis by providing the energy for ATP-hydrolysis-driven removal of biogenesis factors (Kressler et al., 2009). In their cases, putative substrate proteins associated with different pre-60S particles could be identified (Kressler et al., 2008; Pertschy et al., 2007; Ulbrich et al., 2009).

The first mechanistic insight for the Rea1 AAA$^+$-ATPase was obtained by demonstrating how this enzyme stimulates the removal of ribosome biogenesis factors from the evolving 60S subunit (Ulbrich et al., 2009). Rea1 consists of a hexameric AAA-motor head domain and a long flexible tail that carries a MIDAS domain (*m*etal *i*on-*d*ependent *a*dhesion *s*ite) at the carboxy-terminal end (Garbarino and Gibbons, 2002; Ulbrich et al., 2009). Electron microscopy revealed that Rea1 contacts the pre-60S particle at two discrete sites on the pre-60S particle. Its AAA-motor head is fixed in close vicinity to the adaptor Rix1-Ipi3-Ipi1 subcomplex, whereas the MIDAS domain at the tip of the tail contacts the pre-ribosome at a second site where the pre-60S factor Rsa4 is located (Ulbrich et al., 2009). It is possible that such a constellation of biogenesis factors on the pre-60S particle could generate a pulling force upon ATP hydrolysis to release Rsa4, the Rix1-Ipi3-Ipi1 subcomplex, and Rea1 from the pre-60S particle, preparing it for nuclear export (Ulbrich et al., 2009).

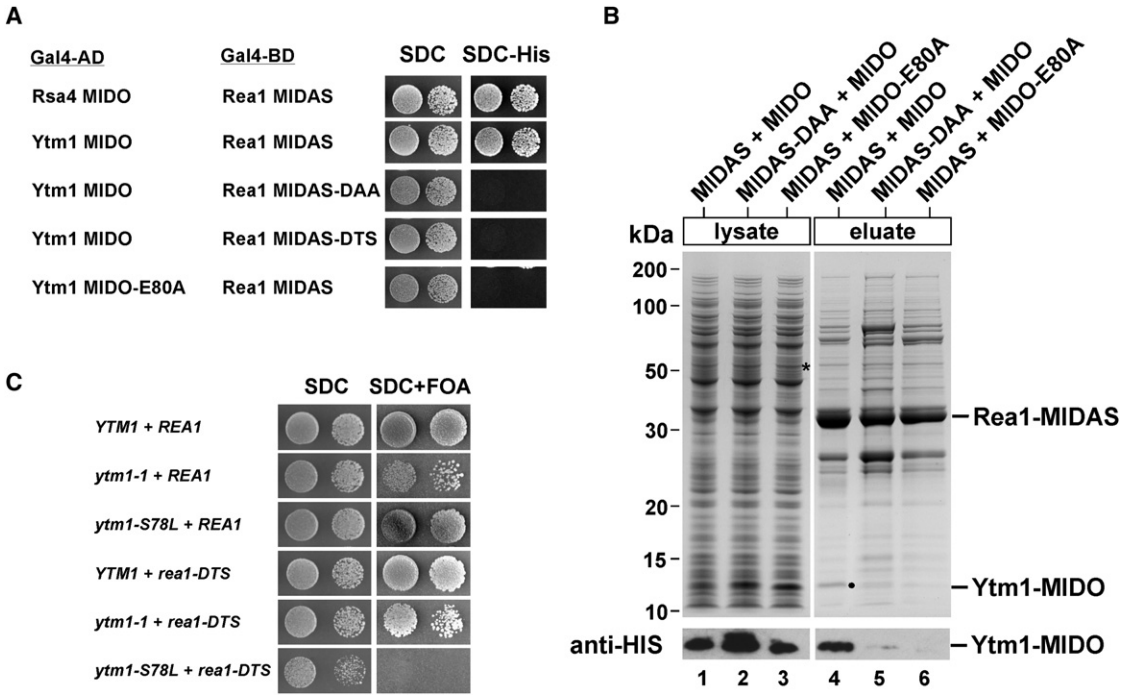

Figure 1. The MIDO of Ytm1 Interacts with Rea1's MIDAS In Vivo and In Vitro

(A) Yeast two-hybrid interaction between wild-type and mutant alleles of Rea1-MIDAS and Ytm1-MIDO. Yeast two-hybrid plasmids expressing the indicated *GAL4-BD* (*GAL4* DNA-binding domain) and *GAL4-AD* (*GAL4* activation domain) fusion proteins were transformed into the yeast reporter strain PJ69-4A. Transformants were spotted in 10-fold serial dilutions onto SDC-Trp-Leu (SDC) or SDC-Trp-Leu-His (SDC-His) and incubated at 30°C for 4 days. The Rea1-MIDAS comprises residues 4622–4910; the MIDO of Rsa4, residues 1–154; and the MIDO of Ytm1, residues 1–92. Growth on SDC-His plate indicates a two-hybrid interaction.

(B) Rea1-MIDAS and Ytm1-MIDO bind directly to each other. The GST-TEV-tagged MIDAS of Rea1 (wild-type or DAA mutant; residues 4608–4910) was coexpressed with His_6-Ytm1-MIDO (1–92 aa) or the His_6-Ytm1-MIDO E80A mutant in *E. coli* in the indicated combinations. The GST-MIDAS fusion proteins were affinity purified on GSH beads and eluted by TEV cleavage. Supernatants and eluates were analyzed by SDS-PAGE and Coomassie staining (top) and western blotting (bottom) using anti-HIS antibodies to detect Ytm1 in eluates and total cell lysates. Protein bands above GST-MIDAS are *E. coli* contaminants.

(C) The *ytm1-MIDO* mutant S78L is genetically linked to the *rea1-DTS* mutant. The YTM1Δ/REA1Δ double-shuffle strain was transformed with wild-type and the indicated mutant alleles of *YTM1* and *REA1*, respectively. Transformants were spotted in 10-fold serial dilutions onto SDC-Trp-Leu (SDC) or SDC+FOA to test for synthetic lethality. Plates were incubated at 30°C for 2 (SDC) or 4 days (SDC+FOA).

A sequence analysis of Ytm1 MIDO is shown in Figure S1.

Bioinformatic analysis indicated that another pre-60S factor in yeast, Ytm1, carries an N-terminal domain that is homologous to the Rsa4 N-terminal domain (Nal et al., 2002), which was previously shown to bind the Rea1 MIDAS (Ulbrich et al., 2009). Here, we demonstrate that Ytm1 is capable of binding to the Rea1 MIDAS and that this contact is essential for an earlier step during 60S subunit biogenesis. In vitro studies indicated that the Ytm1-Rea1 interaction is required for removal of several nucleolar factors from the early pre-60S particle. Thus, Rea1 induces the release of the Ytm1-Erb1-Nop7 subcomplex from the nascent 60S subunit and consequently enables this early pre-60S intermediate to exit from the nucleolus. Later on during 60S biogenesis, Rea1 functions again on the Rix1 particle to mediate removal of Rsa4 and the Rix1-Ipi3-Ipi1 subcomplex (Ulbrich et al., 2009).

RESULTS

MIDO Domains in Ytm1 and Rsa4 Bind to the Rea1 MIDAS

The conserved yeast pre-60S biogenesis factors Rsa4 and Ytm1 (in higher eukaryotes, termed Nle and WDR12, respectively) both consist of an amino-terminal extension (~90–150 residues) with significant homology (Figure S1 available online) (Nal et al., 2002) and a C-terminal β propeller (WD40) domain. Because the Rsa4 N domain binds to the Rea1 MIDAS (Ulbrich et al., 2009), we tested for an analogous interaction between the Ytm1 N domain and the Rea1 MIDAS. Yeast two-hybrid and in vitro binding assays demonstrated that amino acids 1–92 of Ytm1 (Figure S1) are sufficient for binding the intact, but not mutated, Rea1 MIDAS, which is predicted to be impaired in MIDAS ion coordination (Figures 1A and 1B).

Previously, we identified a conserved glutamate in the Rsa4 N domain (E114) to be essential for the interaction with the Rea1 MIDAS (Ulbrich et al., 2009). Sequence alignment indicated that this essential E114 in Rsa4 corresponds to the highly conserved E80 in the N-terminal extension of Ytm1 (Figure S1). Consistently, mutation of E80 > A in Ytm1 (*ytm1 E80A)* rendered the protein nonfunctional because it could not complement the lethal phenotype of the *ytm1Δ* strain (Figure S2A). Moreover, Ytm1 E80A could not bind to the Rea1 MIDAS in the two-hybrid and in the in vitro reconstitution assay (Figures 1A and 1B). Thus, Ytm1 and Rsa4 bind to the Rea1 MIDAS by a similar mechanism

involving a conserved glutamate within the *M*IDAS *i*nteracting *do*main (MIDO) to coordinate the MIDAS ion. Altogether, these findings suggest that Rea1 in concert with Ytm1 could play a so far uncharacterized role in 60S biogenesis.

Genetic Interaction between *YTM1 MIDO* and *REA1 MIDAS*

To determine whether Ytm1 and Rea1 are functionally linked during ribosome biogenesis, we tested for genetic interactions between these two factors. However, the *ytm1-1* allele, which carries two point mutations in the C-terminal β propeller known to impair binding of Ytm1 to the nascent 60S subunit (via Erb1 and Nop7) (Miles et al., 2005; Tang et al., 2008), showed no genetic linkage to the *rea1-DTS* (MIDAS) mutation (Figure 1C). Hence, we developed a genetic screen to identify *ytm1* mutations, which exhibit a genetic (i.e., synthetic lethal) interaction with *rea1-DTS* (see Experimental Procedures). The *ytm1 S78L* mutant, isolated from this screen, was viable in the presence of the intact *REA1* but synthetic lethal when combined with the *rea1-DTS* allele (Figure 1C). Of note, the S78L mutation lies close to the critical E80 residue in Ytm1 that is essential for the interaction with the Rea1 MIDAS (Figure S1). In contrast, *ytm1 S78L* was not genetically linked to the *rsa4-1* mutation (data not shown), which was also synthetic lethal with *rea1-DTS* (Ulbrich et al., 2009). Thus, Ytm1 and Rsa4 are physically and functionally linked to the MIDAS domain of Rea1 via their amino-terminal MIDO motifs, but the functions of Rsa4 and Ytm1 appear to be independent from each other. Consistent with this notion, Ytm1 is associated with early nucleolar pre-60S particles (e.g., the Nsa1-TAP particle) (Miles et al., 2005; Ulbrich et al., 2009), whereas Rsa4 is part of a later pre-60S (Rix1) particle in the nucleoplasm (de la Cruz et al., 2005; Ulbrich et al., 2009).

GAL::ytm1 E80A Exerts a Dominant-Lethal Phenotype with Defects in Early 60S Subunit Biogenesis

To clarify the in vivo requirement for the Ytm1-Rea1 interaction for 60S biogenesis, we placed the *ytm1 E80A* allele under the control of the inducible *GAL* promoter for overexpression studies in yeast. Like in the case of *GAL::rsa4 E114D* (Ulbrich et al., 2009), overproduction of *GAL::ytm1 E80A* in galactose-containing medium was toxic to the cells (Figure 2A). Induction of the dominant-negative Ytm1 E80A caused a robust 60S biogenesis defect with a reduction of free 60S subunits (Figure S2D) and accumulation of the 60S reporter Rpl25-GFP within the nucleolus (Figure 2C). In contrast, the localization of the 40S reporter Rps3-GFP was not affected (data not shown). Northern blot analysis of the rRNA processing in the Ytm1 E80A mutant revealed increased levels of early 27S pre-rRNA processing intermediates (Figure 2B, lanes 6–10), consistent with the existence of stalled nucleolar particles. In contrast, overproduction of the dominant Rsa4 E114D mutant induced a later pre-rRNA processing defect, as displayed by the accumulation of 7S pre-rRNA (Figure 2B, lanes 16–20), and pre-60S particles were shown to accumulate in the nucleoplasm (Ulbrich et al., 2009). The appearance of 27S pre-rRNAs in the Rsa4 E114D mutant could be due to trapping of Rea1 in the nucleoplasm (e.g., on Rix1 particles), which, in a feedback mechanism, could affect earlier 60S biogenesis steps that also require Rea1 (see below). Moreover, both Ytm1 E80A and Rsa4 E114D showed a temporal later increase of 23S and 35S rRNAs, which is likely due to secondary effects. As Ytm1 copurifies with pre-60S particles containing 27S pre-rRNAs (Miles et al., 2005), whereas Rsa4 is associated with pre-60S particles containing 7S and 25S rRNA (Ulbrich et al., 2009; see below), we conclude that an interaction between Ytm1 and Rea1 is required for a nucleolar step during 60S subunit formation, which occurs prior to the nucleoplasmic Rsa4-Rea1 interaction.

Nucleolar Relocation of the Rix1-Defined Pre-60S Particle upon Ytm1 E80A Overexpression

To identify biogenesis factors whose dynamic association with nascent pre-60S subunits depends on a productive Ytm1-Rea1 interaction, we sought to test the intracellular location of early, intermediate, and late pre-60S factors upon *GAL::ytm1 E80A* induction. Wild-type Ytm1-GFP and mutant Ytm1 E80A-GFP did not differ in their subcellular localization (Figure S2C). However, GFP-tagged Rea1, Rix1, Ipi1, and Ipi3 were significantly shifted from a nucleoplasmic to a nucleolar location upon overexpression of Ytm1 E80A (Figures 3 and S4). Other factors tested (e.g., nucleolar Erb1, Nop7, and Has1 or nucleoplasmic Rsa4 and Arx1) remained unaffected in their steady-state localizations (Figure S3). Thus, overexpression of dominant Ytm1 E80A caused the redistribution of Rea1 and the Rix1-Ipi3-Ipi1 subcomplex from the nucleoplasm to the nucleolus.

Dominant-Negative Ytm1 E80A or *Rea1* Depletion Shift the Nucleoplasmic Rix1 Particle to an Early Nucleolar Pre-60S Intermediate

Next, we investigated the protein and the RNA composition of the pre-60S (Rix1) particle carrying Rea1 and the Rix1 subcomplex upon overexpression of toxic Ytm1 E80A. Rix1-TAP particles, affinity purified from *GAL::ytm1 E80A* cells, co-enriched the dominant Ytm1 E80A mutant protein and numerous early pre-60S factors (e.g., Rrp5, Noc1, Noc2, Noc3, Spb1, Erb1, Nop4, Nop2, Spb4, Nop12, Has1, and Fpr4) as well as 27S pre-rRNAs. Typical Rix1 particle protein factors (e.g., Rea1, Rsa4, Nog2, Arx1, and Alb1), as well as Rix1-associated rRNA intermediates like 25S, 7S, and 5.8S rRNAs, were significantly depleted (Figures 4A, 4B, and S4A). On the other hand, 27S rRNAs were significantly increased in the Rix1-TAP particle derived from the dominant *ytm1 E80A* mutant. Affinity purification of dominant-negative Ytm1 E80A-TAP itself yielded a similar set of co-enriched early pre-60S factors when compared to affinity-purified wild-type Ytm1-TAP, but some differences were observed (e.g., Dbp10 and Drs1 were reduced, but Spb4 was increased in the Ytm1 E80A-TAP purification; Figure S2B). These data show that impairment of the Ytm1-Rea1 interaction shifts the Rix1 pre-60S particle toward an earlier intermediate. This earlier intermediate largely resembles the nucleolar Ytm1-TAP particle in protein composition but, in addition, carries the Rix1-Ipi3-Ipi1 subcomplex and a residual pool of Rea1 that is normally absent from the wild-type Ytm1-TAP particle (Figure S2B).

Because these data indicated that Rea1 collaborates with Ytm1 in early pre-60S biogenesis, we next depleted Rea1 to test whether 60S formation becomes arrested at a similar step as in the Ytm1 E80A mutant, upstream of the Rea1-Rsa4 contact. Rix1-TAP affinity purifications were performed using extracts

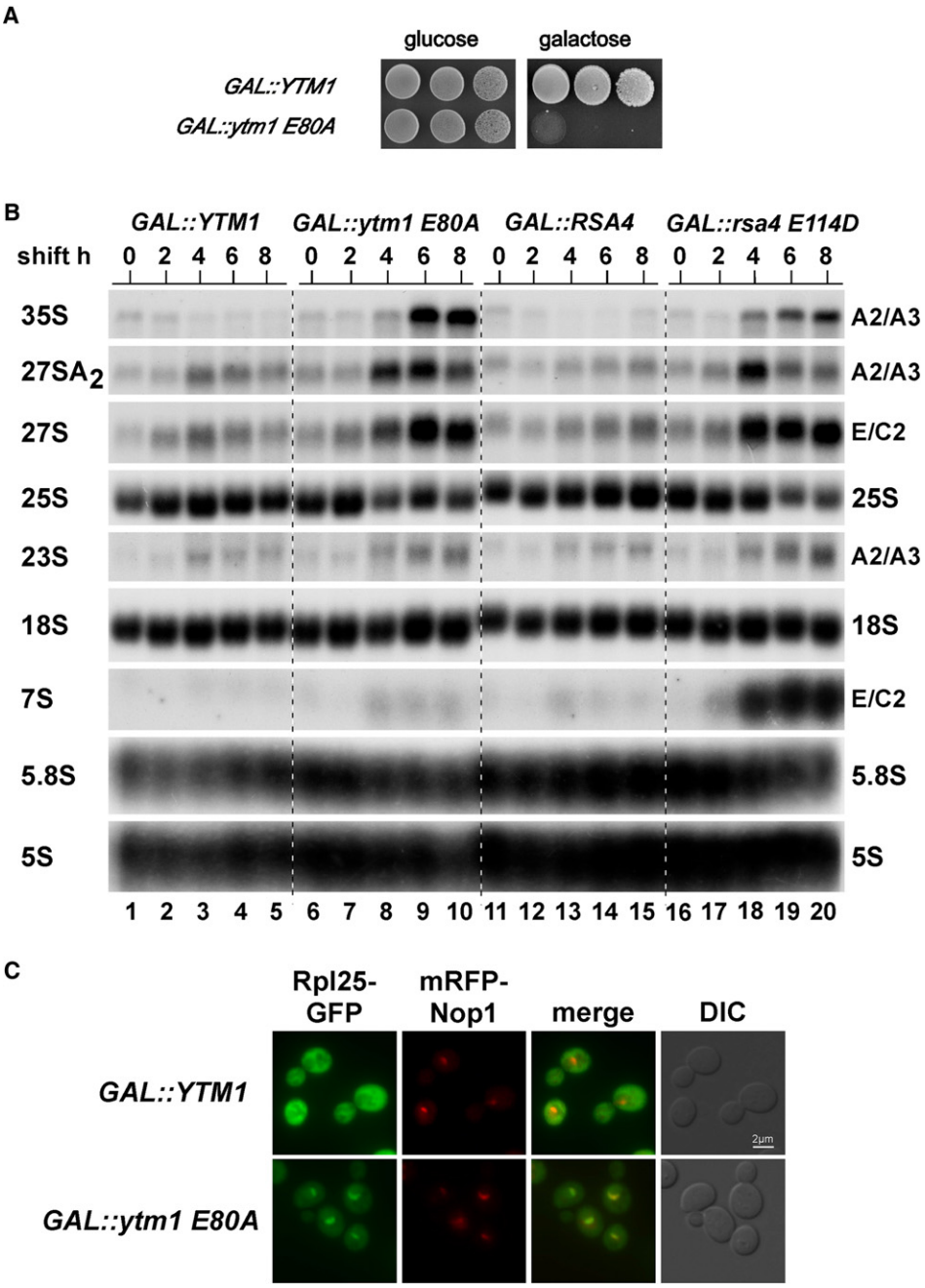

Figure 2. Dominant-Lethal Ytm1 E80A Inhibits Formation of 60S Subunits

(A) The *ytm1 E80A* mutant causes a dominant-negative growth phenotype. Wild-type *YTM1* and the indicated *ytm1 E80A* mutant allele were overexpressed under the control of the inducible *GAL1* promoter in a wild-type yeast strain. Transformants were spotted in 10-fold serial dilutions on SDC-Leu (glucose) and SGC-Leu (galactose) plates. Glucose plates were incubated for 2 days and galactose plates for 7 days at 30°C.

(B) Overexpression of the Ytm1 E80A protein blocks 27S to 7S pre-rRNA processing. Cells were grown in SRC-Leu (time point 0) before expression of *YTM1*, *ytm1 E80A*, *RSA4*, *rsa4 E114D* was induced by transferring cells into SGC-Leu. Total RNA was isolated after 0, 2, 4, 6, and 8 hr of induction and analyzed by northern blot. Probes used for the shown autoradiographs are indicated aside. Panels for 35S, $27SA_2$, and 23S rRNA show detection from the same exposure time.

(C) Analysis of 60S ribosomal export in the dominant-negative *GAL::ytm1 E80A* mutant. Wild-type yeast strain, harboring plasmids pRS314-RFP-*NOP1*-*RPL25*-GFP and YCplac111-GAL::*YTM1* wild-type or *ytm1 E80A*, was grown (30°C) in raffinose-containing medium before cells were shifted to galactose medium to induce overexpression of Ytm1 and Ytm1 E80A, respectively. The subcellular location of the Rpl25-GFP (reporter for 60S export) and mRFP-Nop1 (nucleolar marker) were analyzed by fluorescence microscopy after 5 hr shift. Single and merged pictures of Rpl25-GFP and mRFP-Nop1 as well as Nomarski (DIC) pictures, are shown. Scale bar, 2 μm.

For further characterization of the *ytm1 E80A* mutant, see Figure S2.

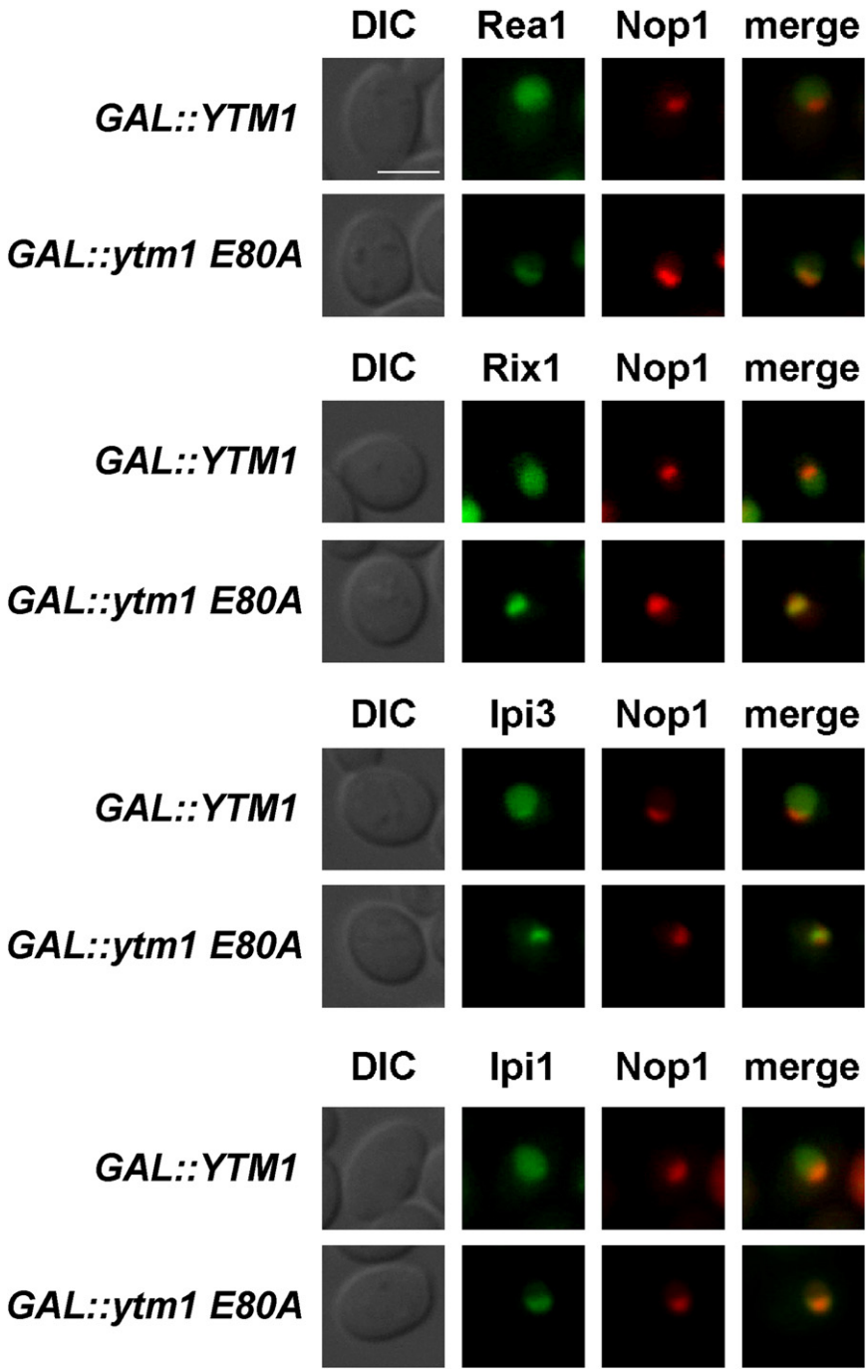

Figure 3. GFP-Rea1 and the Rix1-Ipi3-Ipi1 Subcomplex Become Mislocalized upon Overexpression of Dominant-Negative Ytm1 E80A

Yeast strains carrying chromosomal GFP fusion proteins (P_{Rea1}::GFP-Rea1, Rix1-GFP, Ipi3-GFP, and Ipi1-GFP) were transformed with pRS314 mRFP-Nop1 (nucleolar marker) and YCplac111-*GAL::YTM1* or YCplac111-*GAL::ytm1-E80A*. Transformants were grown in SRC-Leu-Trp medium (raffinose) and shifted to SGC-Leu-Trp (galactose) medium for 6 hr to induce overexpression of Ytm1 or Ytm1-E80A. Subcellular location of GFP fusion proteins was determined by fluorescence microscopy. Nomarski (DIC), GFP, RFP, and merge pictures are shown. Scale bar, 2μm. Figure S3 shows the localization of additional 60S biogenesis factors upon Ytm1 E80A overexpression.

from *GAL::REA1* cells grown in either galactose (Rea1 expression) or glucose-containing medium (Rea1 depletion). In the presence of Rea1, the Rix1 particle exhibited the typical composition of associated factors, including Rea1, Rsa4, and the Rix1-Ipi3-Ipi1 subcomplex. When *REA1* expression was repressed, the Rix1 particle no longer contained Rea1 or Rsa4 but was co-enriched in Ytm1 and other early pre-60S factors (e.g., Erb1, Spb1, Nop2, Noc2, Noc3, and Spb4), as well as early 27S pre-rRNAs (Figures 4C and S4B). Moreover, pre-60S factors and pre-rRNAs typically found in late nucleoplasmic or cytoplasmic nascent 60S subunits (e.g., Arx1, Tif6, and 7S rRNA) were depleted from this unusual Rix1 particle. However, unlike in the Ytm1 E80A mutant, Noc1, Rrp5, and $27SA_2$ were not co-enriched when Rix1-TAP was affinity purified from Rea1-depleted cells (Figures 4 and S4B). Consistent with Rea1 playing a dual role together with either Ytm1 or Rsa4, respectively, its depletion leads to the accumulation of 27S and 7S pre-rRNAs (Figure S4C). Thus, both the expression of toxic Ytm1 E80A and the depletion of Rea1 shift the Rix1 pre-60S particle to an earlier stage containing nucleolar but lacking nucleoplasmic biogenesis factors.

In Vitro Assay for Rea1-Dependent Removal of the Ytm1-Erb1-Nop7 Subcomplex from the Pre-60S Particle

In vitro Rea1 can mediate ATP-dependent release of Rsa4 and the Rix1-Ipi3-Ipi1 subcomplex from Rix1-purified pre-60S particles (Ulbrich et al., 2009). To test in vitro whether Rea1 can induce the release of Ytm1 from pre-60S subunits, we incubated the Ytm1-TAP particle (Figure S2B) with purified Rea1 and ATP. Subsequently, the reaction was separated on a sucrose gradient and analyzed by SDS-PAGE and Coomassie staining or western blotting to monitor the release of biogenesis factors from the pre-60S subunit. However, neither Ytm1 nor other biogenesis factors were found to dissociate from this pre-60S particle (Figures 5A and 5B).

We speculated that the purified Ytm1 particle is not suitable for releasing Ytm1 in vitro. Therefore, we tested a Rix1-TAP particle, isolated from the Rea1-depleted cells, that yielded a pre-60S

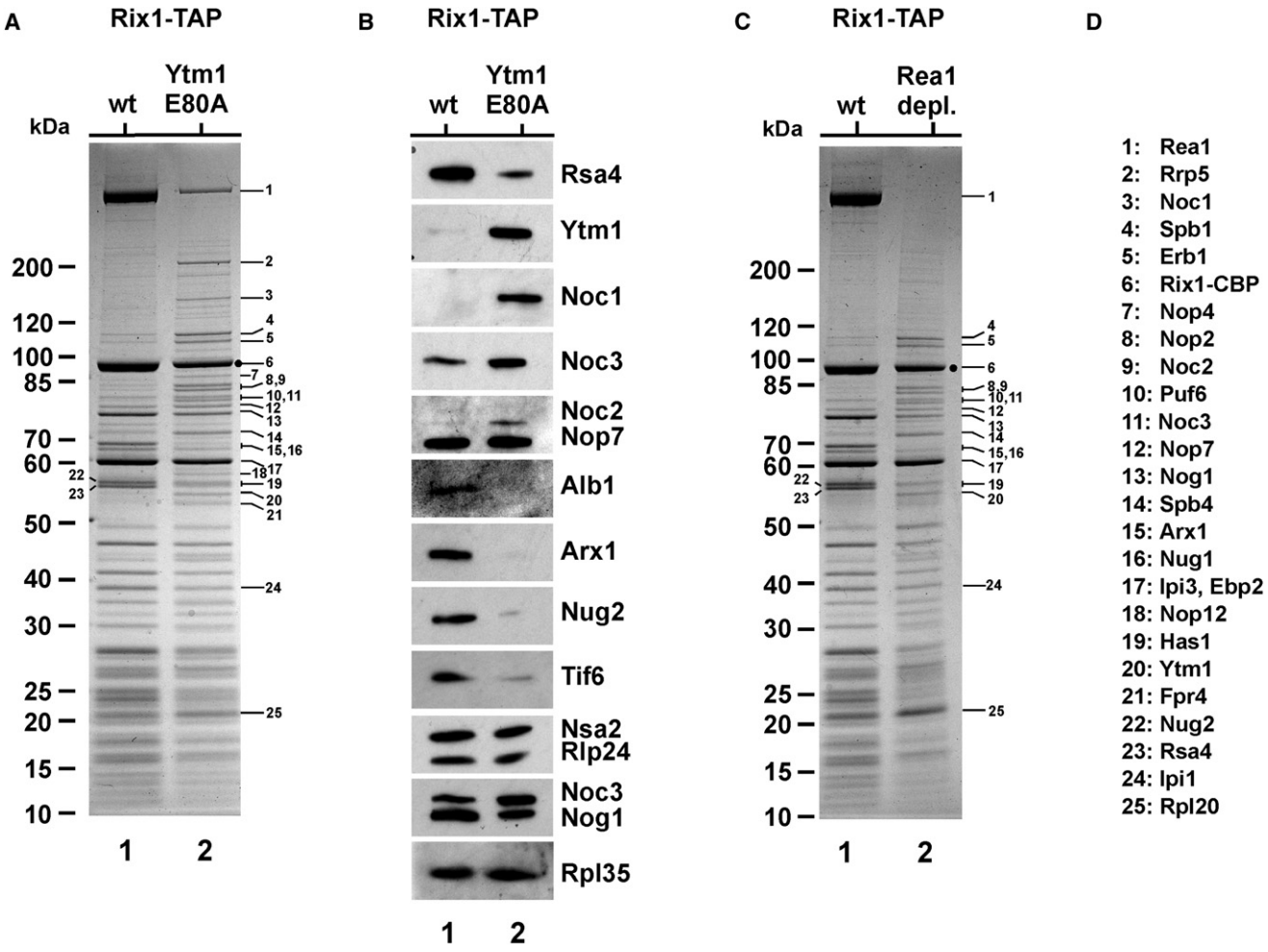

Figure 4. Rix1-TAP Co-Enriches a Nucleolar Pre-60S Particle upon Overexpression of Ytm1 E80A or Rea1 Depletion

(A and B) Yeast strain Rix1-TAP was transformed with YCplac111-*GAL::YTM1* or YCplac111-*GAL::ytm1 E80A*. Transformants were grown in SRC-Leu medium (raffinose) and shifted to YPG (galactose) medium for 6 hr to induce overexpression of Ytm1 or Ytm1 E80A. Subsequently, TAP purifications were performed, and final EGTA eluates were analyzed by 4%–12% gradient SDS-PAGE and Coomassie staining (A) and western blotting (B) using the indicated antibodies. Molecular weight marker (M) is indicated. Labeled protein bands were identified by mass spectrometry (see D for band assignation).

(C) Yeast strain Rix1-TAP with *GAL::HA-REA1* was grown in YPG (galactose) and shifted to YPD (glucose) for 16 hr to deplete for Rea1. Subsequently, Rix1-TAP purification was performed, and the final EGTA eluate were analyzed by 4%–12% gradient SDS-PAGE and Coomassie staining (Rea1 depl., lane 2). This eluate was compared to a Rix1-TAP purification when Rea1 was overexpressed (grown in YPG, "wt" lane 1). Molecular weight marker (M) is indicated, and labeled protein bands were identified by mass spectrometry (see D for band assignation).

(D) Band assignation.

The rRNA content of the purified particles, as well as the rRNA processing defect of a *Gal::REA1* strain, is shown in Figure S4.

particle harboring the Rix1 subcomplex, Ytm1, and the other early pre-60S factors but devoid of Rea1 (see Figure 4C, lane 2). Strikingly, when this pre-60S particle was incubated with purified Rea1, an ATP-dependent release of Ytm1, Erb1, and, to a lesser extent, Nop7 from the pre-60S particle was observed (Figures 5C and 5D). In contrast, other biogenesis factors, including Rlp24 and Nsa2, remained bound to this in vitro matured pre-60S particle. Further in vitro tests showed that ATP or Rea1 alone, or addition of Rea1 with a nonhydrolyzable ATP analog (AMP-PNP), did not induce the release of Ytm1 from the pre-60S particle (Figure 6B and data not shown). Moreover, the mutant Ytm1 E80A protein, when assembled onto the pre-60S particle, was not removed in vitro from this particle even in the presence of Rea1 and ATP (Figure 6C). These data indicate that the interaction between Rea1 and the Ytm1-MIDO is required for an ATP-hydrolysis-dependent removal of the Ytm1-Erb1-Nop7 subcomplex from an early pre-60S particle.

DISCUSSION

This study has revealed that the conserved Ytm1-Erb1-Nop7 subcomplex associated with a nucleolar pre-60S particle is a target of the Rea1 AAA^{+}-ATPase. Thus, Rea1 performs a so

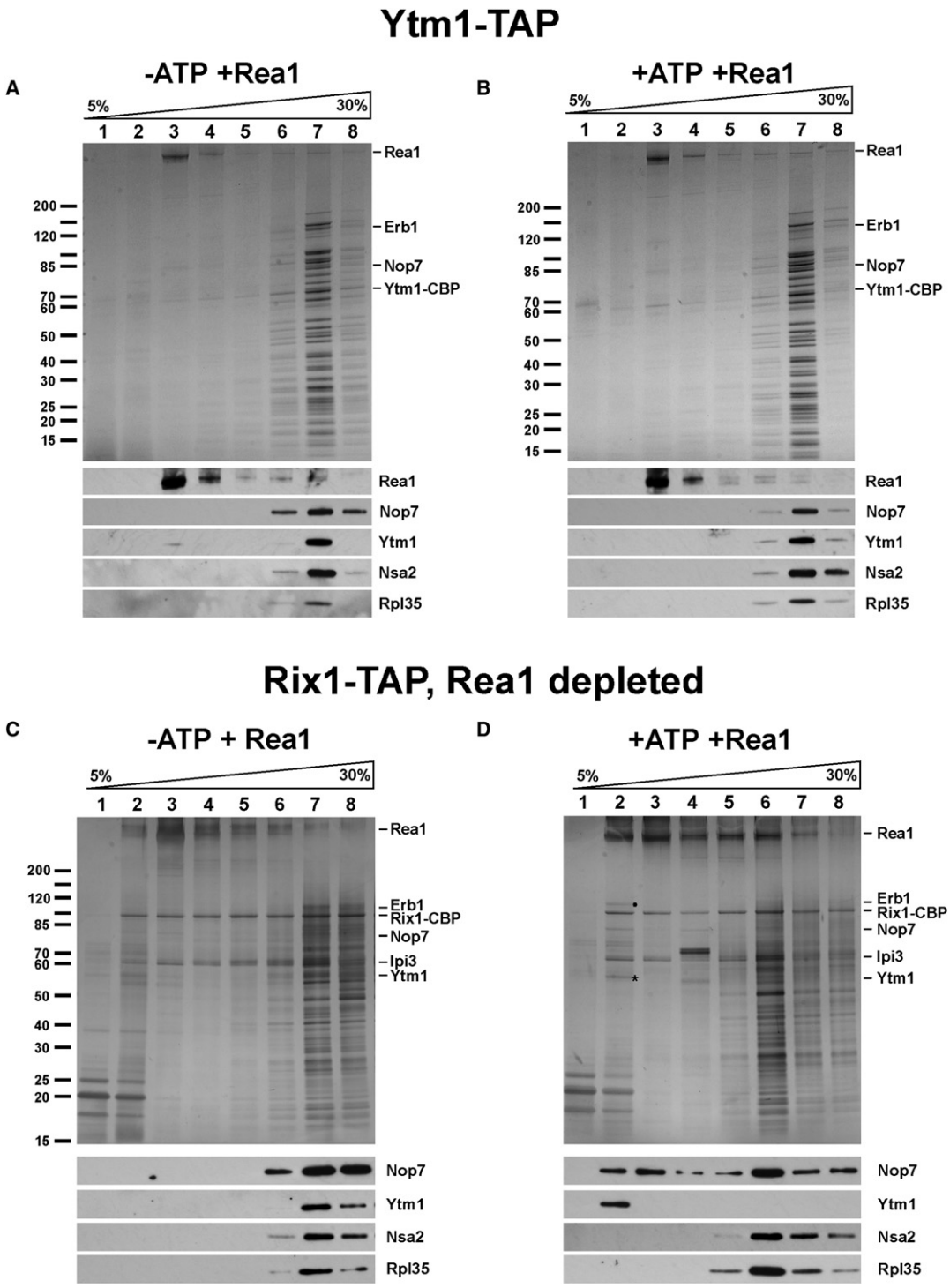

Figure 5. Rea1 Extracts Ytm1-Erb1-Nop7 from the Purified Pre-60S Ribosomal Particle In Vitro

(A and B) The Ytm1-TAP particle was affinity purified, mixed with purified Rea1, and incubated for 45 min at 23°C with ± 4 mM ATP. Subsequently, the mixture was loaded on a 5%–30% sucrose gradient and centrifuged for 16 hr at 27.000 rpm. Gradient fractions 1–8 were analyzed by SDS-PAGE and Coomassie staining (top) or western blotting using the indicated antibodies (bottom).

(C and D) The Rix1-TAP particle was affinity purified from Rea1-depleted cells (see Figure 4C), mixed with purified Rea1, and incubated for 45 min at 23°C with ± 4 mM ATP. Subsequently, the mixture was loaded on a 5%–30% sucrose gradient and centrifuged for 16 hr at 27.000 rpm as described in (A) and (B). Gradient fractions 1–8 were analyzed by SDS-PAGE and silver staining (top) or western blotting using the indicated antibodies (bottom). Bands released by ATP treatment were Erb1 (●) and Ytm1 (*), which were identified by mass spectroscopy.

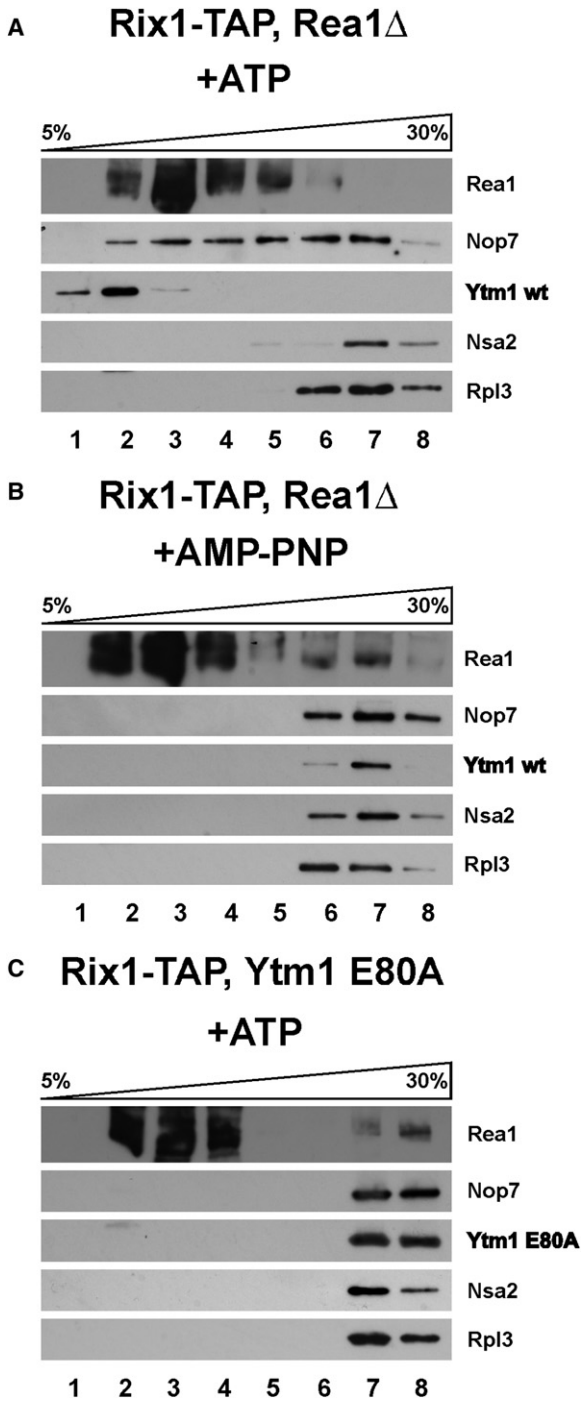

Figure 6. The Release of Ytm1 Depends on the Ytm1-Rea1 Interaction and ATP Hydrolysis

(A–C) The Rix1-TAP particle was affinity purified from Rea1-depleted cells (A and B) (see Figure 4C) or from Ytm1-E80A-induced cells (C) (see Figure 4A), mixed with purified Rea1, and incubated for 45 min at 23°C with 4 mM ATP or AMP-PNP, respectively. Subsequently, the mixture was loaded on a 5%–30% sucrose gradient and centrifuged for 16 hr at 27.000 rpm. Gradient fractions 1–8 were analyzed by western blotting using the indicated antibodies.

far unrecognized role during early pre-60S subunit biogenesis in the nucleolus. Taken together, the data from this and previous work (Ulbrich et al., 2009) demonstrate that the MIDO of Ytm1 and Rsa4 interact directly but sequentially with the Rea1 MIDAS during 60S subunit biogenesis. Abrogation of the Rea1-Ytm1 interaction by the dominant-lethal Ytm1 E80A mutation causes an early block during 60S biogenesis at the transition from the nucleolus to the nucleoplasm. In contrast, impairing the Rea1-Rsa4 interaction by the dominant Rsa4 E114D mutation inhibited export of the pre-60S particle from the nucleoplasm to the cytoplasm (Ulbrich et al., 2009). Because Ytm1 is recruited first to pre-60S particles in the nucleolus, it is possible that the binding site occupied by Ytm1 overlaps with the binding site to which Rsa4 is subsequently recruited. Hence, the Ytm1-Erb1-Nop7 subcomplex may block premature recruitment of Rsa4 to the nucleolar pre-60S particle. Alternatively, Rsa4 binding to pre-60S particles may require a distinct pre-rRNA processing step (e.g., 27S→25S, 7S) that depends directly or indirectly on the Ytm1-Erb1-Nop7 subcomplex. How Rea1 promotes the release of its substrates from the pre-60S particles remains to be determined. As suggested previously for the Rea1-dependent Rsa4 release, Rea1 may act as a mechanochemical enzyme and, due to the presence of its long and flexible tail domain, could exert a tensile force affecting distantly located factors on the surface of the pre-60S particle (for discussion, see Ulbrich et al., 2009). However, other mechanisms are also imaginable, such as nucleotide-dependent conformational changes within Rea1 that may apply tension to bound proteins, thereby allowing Rea1 to dissociate protein-protein interactions (Vale, 2000). In addition, the Rea1 ATPase activity may not only be used to release factors, but also to remodel the structure of the pre-60S particle, such as the restructuring of pre-rRNA for subsequent processing steps (e.g., 27S→7S, 25S and 7S→5.8S).

A pre-60S particle carrying both Ytm1 and the Rix1 subcomplex has not been reported. However, it is possible that this hypothetical biogenesis intermediate is short lived but could be significantly accumulated upon Rea1 repression or induction of the dominant Ytm1 E80A mutant. Of note, only this mutant intermediate, but not the wild-type Ytm1-TAP particle, was competent for in vitro release of Ytm1-Erb1-Nop7. This finding indicates that the wild-type Ytm1-TAP particle may not yet be "ready" for this step, perhaps because it still requires a structural rearrangement (e.g., rRNA processing) or recruitment of additional *trans*-acting factors (e.g., the Rix1-Ipi3-Ipi1 subcomplex). Of interest, the Rix1 pre-60S particle purified from the Ytm1 E80A background is largely depleted of Rea1. This could indicate that a functional Ytm1 is required to recruit Rea1 to nucleolar pre-60S particles.

Our in vitro data further indicated that both a productive Rea1-Ytm1 interaction and ATP hydrolysis are necessary to release the Ytm1-Erb1-Nop7 subcomplex from the pre-ribosomal particle. Whereas Ytm1 and Erb1 were efficiently dissociated, Nop7 was only partially released. This finding is consistent with other biochemical data, which indicate that a pool of Nop7 remains associated with late nucleoplasmic pre-60S particles that are devoid of Ytm1 and Erb1 (Kressler et al., 2008; Nissan et al., 2002). Therefore, this residual pool of Nop7 may be removed

later from the evolving pre-60S subunit by other biogenesis factors. In vivo removal of Ytm1-Erb1-Nop7 may also be affected by additional mechanisms, as it was reported that addition of phosphatase inhibitors to cell lysates caused a dissociation of the Ytm1-Erb1-Nop7 subcomplex from pre-60S particles (Miles et al., 2005). This observation suggests that phosphorylation and/or dephosphorylation may be also involved in factor removal from the early pre-60S particle.

In vivo, the transition of the pre-60S particle from the nucleolus to the nucleoplasm is not only accompanied with the release of Ytm1 and Erb1, but also with the release of additional nucleolar factors, including Spb1, Nop2, Noc2, Noc3, Nop4, Puf6, Spb4, Nop12, Has1, and Fpr4. It remains to be determined whether the removal of the Ytm1-Erb1-Nop7 subcomplex by Rea1 could pave the way for the subsequent dissociation of other early pre-60S factors in vivo, an event concomitant with the release of the nascent pre-60S particle from the nucleolus to the nucleoplasm. However, additional mechanisms may exist for the removal of factors, such as displacement by "downstream" factors such as Arx1, Rsa4, or Nog2/Nug2 upon transition of the particle into the nucleoplasm or removal of Nsa1 from an early pre-60S particle by the Rix7 AAA^+ ATPase (Gadal et al., 2001; Kressler et al., 2008).

Because Rea1 and its targets, Ytm1 and Rsa4, are conserved from yeast to human, it is likely that the Rea1-driven 60S biogenesis steps occur in all eukaryotes. Consistent with this notion, the human nucleolar PeBoW complex composed of Pes1 (Nop7), Bop1 (Erb1), and WDR12 (Ytm1) is essential for cell proliferation and processing of rRNA in mammalian cells (Davies et al., 2008; DeLaBarre and Brunger, 2005; Grimm et al., 2006; Hölzel et al., 2007; Hölzel et al., 2005; Rohrmoser et al., 2007). Thus, future studies regarding the structure and function of the conserved Rea1 and its binding partners could contribute to general understanding of eukaryotic ribosome biogenesis and its link to other cellular processes and diseases.

EXPERIMENTAL PROCEDURES

Strains, Media, and Plasmids

Plasmids and yeast *Saccharomyces cerevisiae* strains used in this study are listed in Tables S1 and S2. Yeast double-shuffle strains were generated as described (Strässer et al., 2000). Yeast genetic methods such as gene deletion or GFP tagging of genes at the genomic locus (Longtine et al., 1998; Puig et al., 1998), transformation, mating, and tetrad analysis were performed according to published procedures.

Screen for *ytm1* Mutants that Are Synthetic Lethal with *rea1-DTS*

A library of *ytm1* mutant alleles was generated by incubating plasmid pRS314-*YTM1* in hydroxylamine buffer (1 M hydroxylamine, 400 mM NaOH, 20 mM Na_3PO_4, and 5 mM EDTA) for 20 hr at 50°C. The DNA was precipitated with 80% ethanol and transformed into the screening strain, *ytm1::natNT2*, *rea1::kanMX6*, *his3*, *trp1*, *leu2*, *ura3*, *ade2*, *ade3* harboring plasmids p*CEN6*-ADE3-HIS3-YTM1*, pRS416-*REA1* (*URA3*), and YC-plac111-TAP-*rea1-DTS* (*LEU2*). Transformants were selected on SDC-Trp-Leu-Ura. Colonies that carry a lethal *ytm1* mutant depend on the presence of the plasmid p*CEN6*-ADE3-HIS3-YTM1*. In contrast, transformants with viable *ytm1* alleles can lose this plasmid, which can be identified by a red-white sectoring phenotype (yeast cells that are *ade2* exhibit a red color, whereas *ade2 ade3* cells are white). Importantly, plasmid p*CEN6*-ADE3-HIS3-YTM1* carries a mutated *cen6** that enables enhanced plasmid loss under nonselective conditions. White colonies were picked and further grown on SDC-Trp-Leu plates to allow for loss of pRS416-*REA1* before plating the cells on SDC+5-FOA. No growth on 5-FOA-containing plates indicated synthetic lethality of the *ytm1* allele in combination with the *rea1-DTS* allele. Plasmids carrying this type of mutated *ytm1* alleles were re-isolated and re-transformed into the corresponding tester strains to confirm the synthetic lethal phenotype.

Rix1-TAP Purification from Cell Lysates Containing Overexpressed Ytm1 E80A or Lacking Rea1

The Rix1-TAP strain was transformed with the plasmid encoding *GAL::ytm1-E80A* or *GAL::YTM1*. Pre-cultures were grown in 2l SRC-Leu to prevent plasmid loss to an OD of 2.0, followed by shifting cells to galactose medium (YPG) for 6 hr.

To deplete Rea1 from Rix1-TAP cells, the endogenous *REA1* promoter was replaced by the inducible *GAL* promoter. Rix1-TAP *GAL1::REA1* cells were grown in YPG medium before shifting cells into 2l YPD medium for 16 hr to deplete for Rea1. Finally, cells were harvested and lysed, and TAP purification was performed (Nissan et al., 2002) to isolate the Rix1-containing particle.

In Vitro Release of the Ytm1-Erb1-Nop7 Subcomplex from the Pre-60S Particle

The nucleolar pre-60S particle was affinity purified via Rix1-TAP from Rea1-depleted cells (see above). For isolation of Rea1, Rea1 was overexpressed in yeast from plasmid p*GAL::ProtA-TEV-CBP-FLAG-REA1* by shifting a 1 l pre-culture (SRC-Leu) grown to OD 1.0 into 2l YPG medium for 6 hr at 30°C and subsequent tandem affinity purification of TAP-Rea1. The eluted pre-60S particle (10 mM Tris [pH 8.0], 5 mM EGTA, and 15 mM $MgCl_2$) was mixed with or without purified Rea1 before addition of 4 mM ATP and incubation for 45 min at 23°C. This 600 µl reaction mixture was loaded on a 5%–30% sucrose gradient and centrifuged using an SW40 rotor for 16 hr at 27.000 rpm and 4°C. Gradient fractions were collected, precipitated by TCA, and analyzed by SDS-PAGE and Coomassie staining or western blotting using the indicated antibodies according to Ulbrich et al. (2009).

Miscellaneous

Additional methods used in this study and described earlier include TAP purification of pre-60S particles (Bassler et al., 2001; Nissan et al., 2002), purification of TAP-Rea1 (Ulbrich et al., 2009), sucrose gradient analysis to obtain ribosomal and polysomal profiles (Bassler et al., 2001), ribosomal export assays using the large subunit reporter Rpl25-GFP (Gadal et al., 2002) monitored by fluorescence microscopy according to Bassler et al. (2006), and yeast two-hybrid analysis (Kressler et al., 2008). Preparation of rRNA, northern blot analysis (including sequences of probes D-A2, A2-A3, E-C2, 18S, 25S, and 5.8S), western blot analysis, and expression of recombinant proteins in *E. coli* and their subsequent affinity purification were performed as described (Ulbrich et al., 2009). The sequence of the 5S northern blotting probe is GGTCACCCA CTACACTACTCGG.

SUPPLEMENTAL INFORMATION

Supplemental Information includes four figures and two tables and can be found with this article online at doi:10.1016/j.molcel.2010.05.024.

ACKNOWLEDGMENTS

We thank Drs. J. de la Cruz, H. Tschochner, M. Fromont-Racine, A.W. Johnson, M. Seedorf, B. Stillman, and J.L. Woolford for antibodies. We are grateful to Dr. E. Thomson and Dr. D. Kressler for fruitful discussion on the project and yeast strains Nog1-GFP and Erb1-GFP; Dr. K. Galani for strain Rix1-TAP, *GAL1::Rea1*; Dr. T. Nissan for Nop7-GFP and Has1-GFP strains; and W. Chang for Rea1Δ, Ytm1Δ double deletion strain. E.H. and J.B. are recipients of grants from the Deutsche Forschungsgemeinschaft (Hu363/9-2 and Gottfried Wilhelm Leibniz Program) and Fonds der Chemischen Industrie. B.P. was supported by the Austrian Science Fund (FWF; Hertha Firnberg grant T404-B12).

Received: December 14, 2009
Revised: March 17, 2010
Accepted: April 21, 2010
Published: June 10, 2010

REFERENCES

Bassler, J., Grandi, P., Gadal, O., Lessmann, T., Petfalski, E., Tollervey, D., Lechner, J., and Hurt, E. (2001). Identification of a 60S preribosomal particle that is closely linked to nuclear export. Mol. Cell *8*, 517–529.

Bassler, J., Kallas, M., and Hurt, E. (2006). The NUG1 GTPase reveals and N-terminal RNA-binding domain that is essential for association with 60 S pre-ribosomal particles. J. Biol. Chem. *281*, 24737–24744.

Davies, J.M., Brunger, A.T., and Weis, W.I. (2008). Improved structures of full-length p97, an AAA ATPase: implications for mechanisms of nucleotide-dependent conformational change. Structure *16*, 715–726.

de la Cruz, J., Sanz-Martínez, E., and Remacha, M. (2005). The essential WD-repeat protein Rsa4p is required for rRNA processing and intra-nuclear transport of 60S ribosomal subunits. Nucleic Acids Res. *33*, 5728–5739.

DeLaBarre, B., and Brunger, A.T. (2005). Nucleotide dependent motion and mechanism of action of p97/VCP. J. Mol. Biol. *347*, 437–452.

Freed, E.F., Bleichert, F., Dutca, L.M., and Baserga, S.J. (2010). When ribosomes go bad: diseases of ribosome biogenesis. Mol. Biosyst. *6*, 481–493.

Fromont-Racine, M., Senger, B., Saveanu, C., and Fasiolo, F. (2003). Ribosome assembly in eukaryotes. Gene *313*, 17–42.

Gadal, O., Strauss, D., Braspenning, J., Hoepfner, D., Petfalski, E., Philippsen, P., Tollervey, D., and Hurt, E.C. (2001). A nuclear AAA-type ATPase (Rix7p) is required for biogenesis and nuclear export of 60S ribosomal subunits. EMBO J. *20*, 3695–3704.

Gadal, O., Strauss, D., Petfalski, E., Gleizes, P.E., Gas, N., Tollervey, D., and Hurt, E. (2002). Rlp7p is associated with 60S preribosomes, restricted to the granular component of the nucleolus, and required for pre-rRNA processing. J. Cell Biol. *157*, 941–951.

Ganapathi, K.A., and Shimamura, A. (2008). Ribosomal dysfunction and inherited marrow failure. Br. J. Haematol. *141*, 376–387.

Garbarino, J.E., and Gibbons, I.R. (2002). Expression and genomic analysis of midasin, a novel and highly conserved AAA protein distantly related to dynein. BMC Genomics *3*, 18–28.

Granneman, S., and Baserga, S.J. (2004). Ribosome biogenesis: of knobs and RNA processing. Exp. Cell Res. *296*, 43–50.

Grimm, T., Hölzel, M., Rohrmoser, M., Harasim, T., Malamoussi, A., Gruber-Eber, A., Kremmer, E., and Eick, D. (2006). Dominant-negative Pes1 mutants inhibit ribosomal RNA processing and cell proliferation via incorporation into the PeBoW-complex. Nucleic Acids Res. *34*, 3030–3043.

Henras, A.K., Soudet, J., Gérus, M., Lebaron, S., Caizergues-Ferrer, M., Mougin, A., and Henry, Y. (2008). The post-transcriptional steps of eukaryotic ribosome biogenesis. Cell. Mol. Life Sci. *65*, 2334–2359.

Hölzel, M., Rohrmoser, M., Schlee, M., Grimm, T., Harasim, T., Malamoussi, A., Gruber-Eber, A., Kremmer, E., Hiddemann, W., Bornkamm, G.W., and Eick, D. (2005). Mammalian WDR12 is a novel member of the Pes1-Bop1 complex and is required for ribosome biogenesis and cell proliferation. J. Cell Biol. *170*, 367–378.

Hölzel, M., Grimm, T., Rohrmoser, M., Malamoussi, A., Harasim, T., Gruber-Eber, A., Kremmer, E., and Eick, D. (2007). The BRCT domain of mammalian Pes1 is crucial for nucleolar localization and rRNA processing. Nucleic Acids Res. *35*, 789–800.

Kressler, D., Roser, D., Pertschy, B., and Hurt, E. (2008). The AAA ATPase Rix7 powers progression of ribosome biogenesis by stripping Nsa1 from pre-60S particles. J. Cell Biol. *181*, 935–944.

Kressler, D., Hurt, E., and Bassler, J. (2009). Driving ribosome assembly. Biochim. Biophys. Acta *1803*, 673–683.

Longtine, M.S., McKenzie, A., III, Demarini, D.J., Shah, N.G., Wach, A., Brachat, A., Philippsen, P., and Pringle, J.R. (1998). Additional modules for versatile and economical PCR-based gene deletion and modification in Saccharomyces cerevisiae. Yeast *10*, 953–961.

Miles, T.D., Jakovljevic, J., Horsey, E.W., Harnpicharnchai, P., Tang, L., and Woolford, J.L., Jr. (2005). Ytm1, Nop7, and Erb1 form a complex necessary for maturation of yeast 66S preribosomes. Mol. Cell. Biol. *25*, 10419–10432.

Nal, B., Mohr, E., Silva, M.I., Tagett, R., Navarro, C., Carroll, P., Depetris, D., Verthuy, C., Jordan, B.R., and Ferrier, P. (2002). Wdr12, a mouse gene encoding a novel WD-Repeat Protein with a notchless-like amino-terminal domain. Genomics *79*, 77–86.

Narla, A., and Ebert, B.L. (2010). Ribosomopathies: human disorders of ribosome dysfunction. Blood *115*, 3196–3205.

Nissan, T.A., Bassler, J., Petfalski, E., Tollervey, D., and Hurt, E.C. (2002). 60S pre-ribosome formation viewed from assembly in the nucleolus until export to the cytoplasm. EMBO J. *21*, 5539–5547.

Pertschy, B., Saveanu, C., Zisser, G., Lebreton, A., Tengg, M., Jacquier, A., Liebminger, E., Nobis, B., Kappel, L., van der Klei, I., et al. (2007). Cytoplasmic recycling of 60S preribosomal factors depends on the AAA protein Drg1. Mol. Cell. Biol. *27*, 6581–6592.

Puig, O., Rutz, B., Luukkonen, B.G., Kandels-Lewis, S., Bragado-Nilsson, E., and Séraphin, B. (1998). New constructs and strategies for efficient PCR-based gene manipulations in yeast. Yeast *14*, 1139–1146.

Rohrmoser, M., Hölzel, M., Grimm, T., Malamoussi, A., Harasim, T., Orban, M., Pfisterer, I., Gruber-Eber, A., Kremmer, E., and Eick, D. (2007). Interdependence of Pes1, Bop1, and WDR12 controls nucleolar localization and assembly of the PeBoW complex required for maturation of the 60S ribosomal subunit. Mol. Cell. Biol. *27*, 3682–3694.

Strässer, K., Bassler, J., and Hurt, E.C. (2000). Binding of the Mex67p/Mtr2p heterodimer to FXFG, GLFG, and FG repeat nucleoporins is essential for nuclear mRNA export. J. Cell Biol. *150*, 695–706.

Strunk, B.S., and Karbstein, K. (2009). Powering through ribosome assembly. RNA *15*, 2083–2104.

Tang, L., Sahasranaman, A., Jakovljevic, J., Schleifman, E., and Woolford, J.L., Jr. (2008). Interactions among Ytm1, Erb1, and Nop7 required for assembly of the Nop7-subcomplex in yeast preribosomes. Mol. Biol. Cell *19*, 2844–2856.

Thomas, F., and Kutay, U. (2003). Biogenesis and nuclear export of ribosomal subunits in higher eukaryotes depend on the CRM1 export pathway. J. Cell Sci. *116*, 2409–2419.

Trotta, C.R., Lund, E., Kahan, L., Johnson, A.W., and Dahlberg, J.E. (2003). Coordinated nuclear export of 60S ribosomal subunits and NMD3 in vertebrates. EMBO J. *22*, 2841–2851.

Tschochner, H., and Hurt, E. (2003). Pre-ribosomes on the road from the nucleolus to the cytoplasm. Trends Cell Biol. *13*, 255–263.

Ulbrich, C., Diepholz, M., Bassler, J., Kressler, D., Pertschy, B., Galani, K., Böttcher, B., and Hurt, E. (2009). Mechanochemical removal of ribosome biogenesis factors from nascent 60S ribosomal subunits. Cell *138*, 911–922.

Vale, R.D. (2000). AAA proteins: Lords of the ring. J. Cell Biol. *150*, F13–F19.

Zemp, I., Wild, T., O'Donohue, M.F., Wandrey, F., Widmann, B., Gleizes, P.E., and Kutay, U. (2009). Distinct cytoplasmic maturation steps of 40S ribosomal subunit precursors require hRio2. J. Cell Biol. *185*, 1167–1180.

Molecular Cell, *Volume 38*

Supplemental Information

The AAA-ATPase Rea1 Drives Removal of Biogenesis Factors during Multiple Stages of 60S Ribosome Assembly

Jochen Baßler, Martina Kallas, Brigitte Pertschy, Cornelia Ulbrich, Matthias Thoms, and Ed Hurt

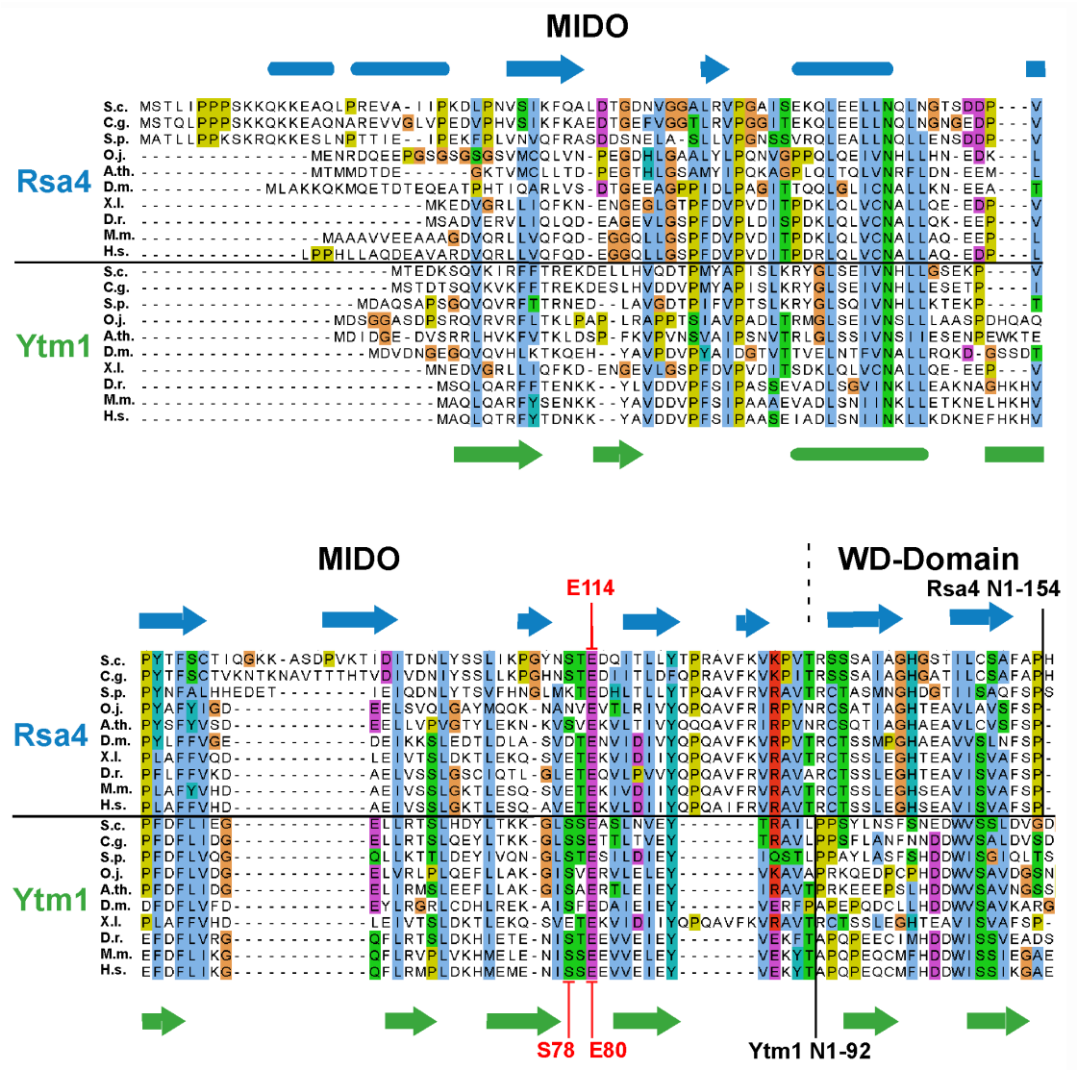

Figure S1. Ytm1 and Rsa4 share a homologous MIDO domain (related to Figure 1)

Amino acid sequence alignment of the MIDO domains of Rsa4 (upper) and Ytm1 (lower) from *Saccharomyces cerevisiae* (S.c.) with its different homologues from *Candida glabrata* (C.g.), *Schizosaccharomyces pombe* (S.p.), *Oryza sativa Japonica* (O.j.), *Arabidopsis thaliana* (A.th.), *Drosophila melanogaster* (D.m.), *Xenopus laevis* (X.l.), *Danio rerio* (D.r.), *Mus musculus* (M.m.) and *Homo sapiens* (H.s.) using the ClustalW2 program (http://www.ebi.ac.uk/Tools/clustalw2/index.html) and displayed by *Jalview*. Secondary structure predictions of the *S. cerevisiae* proteins are indicated for Rsa4 in blue on the top, and for Ytm1 in green at bottom of the alignment (α-helical as thick line; β-sheet as arrow). Indicated in the alignment are also the conserved residues Rsa4 E114, Ytm1 S78 and Ytm1 E80, which are critical for interaction with the Rea1 MIDAS.

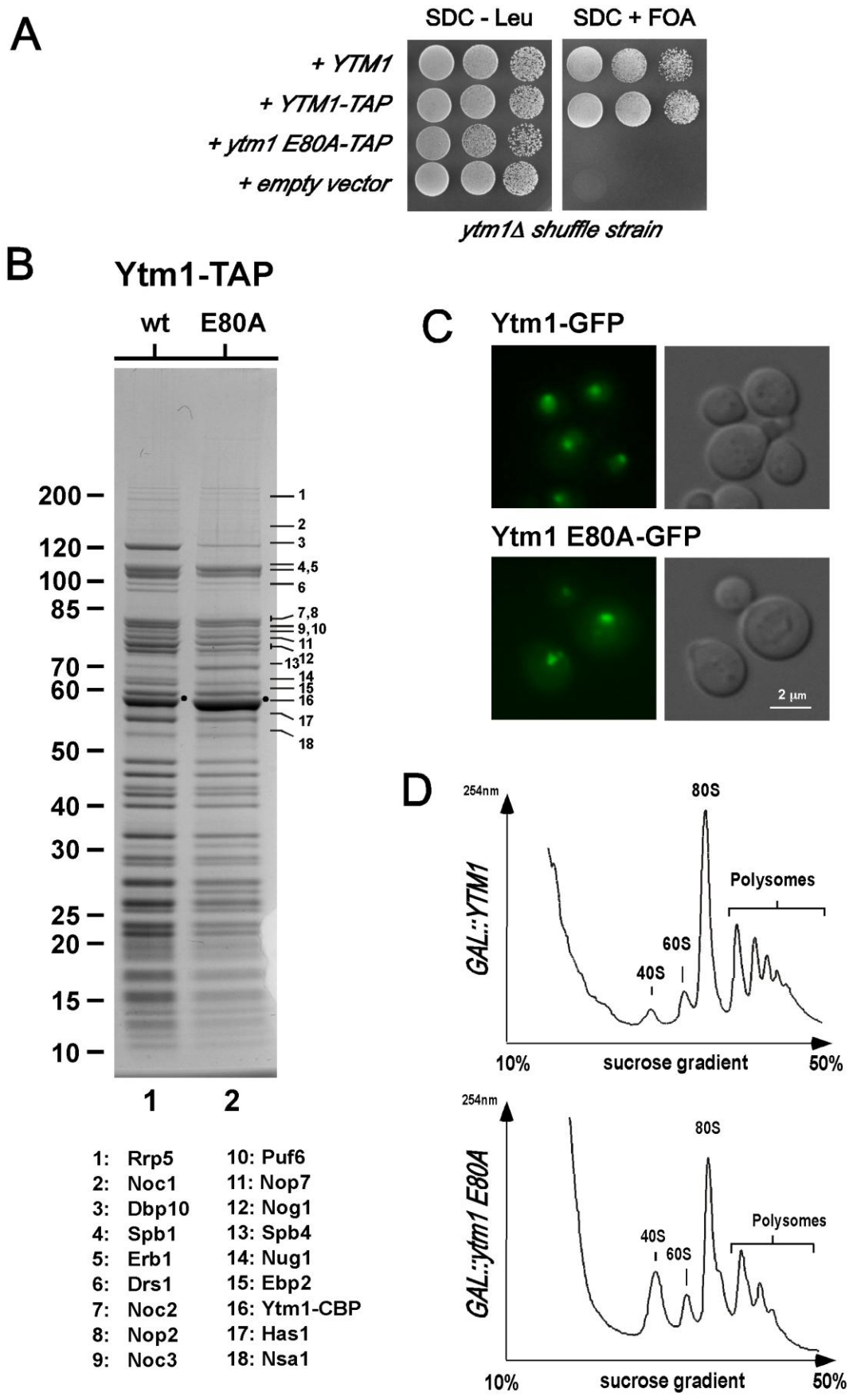

Figure S2. The dominant Ytm1 E80A protein is still associated with pre-60S particles (related to Figure 2)

Figure S2. The dominant Ytm1 E80A protein is still associated with pre-60S particles (related to Figure 2)

(A) The *ytm1 E80A* mutant exhibits a lethal phenotype. Plasmids pRS315 encoding for *YTM1*, *YTM1*-TAP, *ytm1 E80A*-TAP or empty plasmid were transformed into the *YTM1*Δ shuffle strain and spotted in 10-fold serial dilution steps onto SDC-Leu plates (to control for plating efficiency) and onto SDC+FOA plates (to check for viability). Plates were incubated at 30ºC for 2 days (SDC-Leu) or 3 days (SDC+FOA).

(B) Ytm1 and Ytm1 E80A are associated with similar pre-60S particles. Wild-type yeast strain was transformed with pRS315-*YTM1*-TAP or pRS315-*ytm1* E80A-TAP. Cells were grown in SDC-Leu, lysed and Ytm1-TAP proteins were affinity-purified. Eluates were analyzed by 4-12% SDS-PAGE and Coomassie staining. Molecular marker and bait proteins are indicated. The labelled non-ribosomal factors were identified by mass spectroscopy and listed.

(C) Ytm1 E80A localize to the nucleolus. Wild-type yeast strain was transformed with plasmids pRS315-*YTM1*-eGFP or pRS315-*ytm1*-E80A-eGFP to express Ytm1-eGFP from the endogenous *YTM1* promoter. Logarithmically growing cells were analyzed by fluorescence microscopy (Ytm1-GFP, Ytm1 E80A-GFP) and by Nomarski optics (DIC). Scale bar 2µm.

(D) Dominant-negative Ytm1 E80A causes a reduction of 60S subunits. Analysis of polysome profiles of the dominant-negative GAL::*ytm1 E80A* mutant. The wild-type strain expressing *GAL::YTM1* or *GAL::ytm1 E80A* was grown in SRC-Leu (raffinose) medium and shifted into SGC-Leu (galactose) medium at 30°C for 6 hrs. Whole cell lysate was analyzed by sedimentation centrifugation on a 10-50% sucrose density gradient (OD_{254nm}). 40S and 60S subunits, 80S ribosomes and polysomes are indicated.

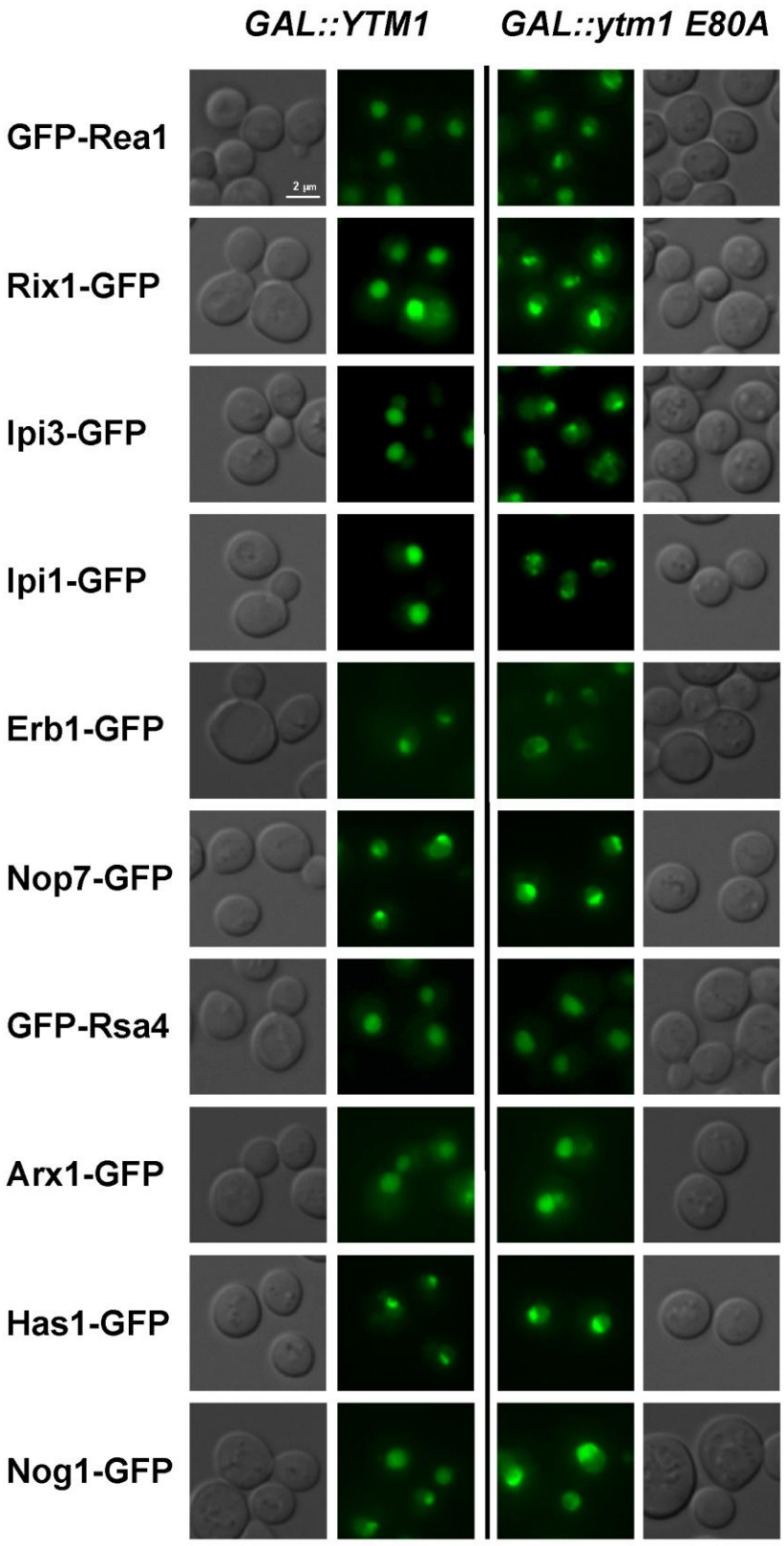

Figure S3. Dominant-negative Ytm1 E80A causes a redistribution of Rea1 and the Rix1-Ipi3-Ipi1 subcomplex from the nucleoplasm to the nucleolus (related to Figure 3)

Figure S3. Dominant-negative Ytm1 E80A causes a redistribution of Rea1 and the Rix1-Ipi3-Ipi1 subcomplex from the nucleoplasm to the nucleolus (related to Figure 3)

Yeast cells expressing the indicated chromosomally integrated GFP fusion proteins under the control of the endogenous promoters were transformed with YCplac111-*GAL::YTM1* or YCplac111-*GAL::ytm1-E80A*. Transformants were grown in SRC-Leu medium (raffinose) and shifted to SGC-Leu (galactose) medium for 6 hrs to induce overexpression of Ytm1 or Ytm1 E80A. Logarithmically growing cells were analyzed by fluorescence microscopy for GFP and by Nomarski optics. Scale bar 2 µm.

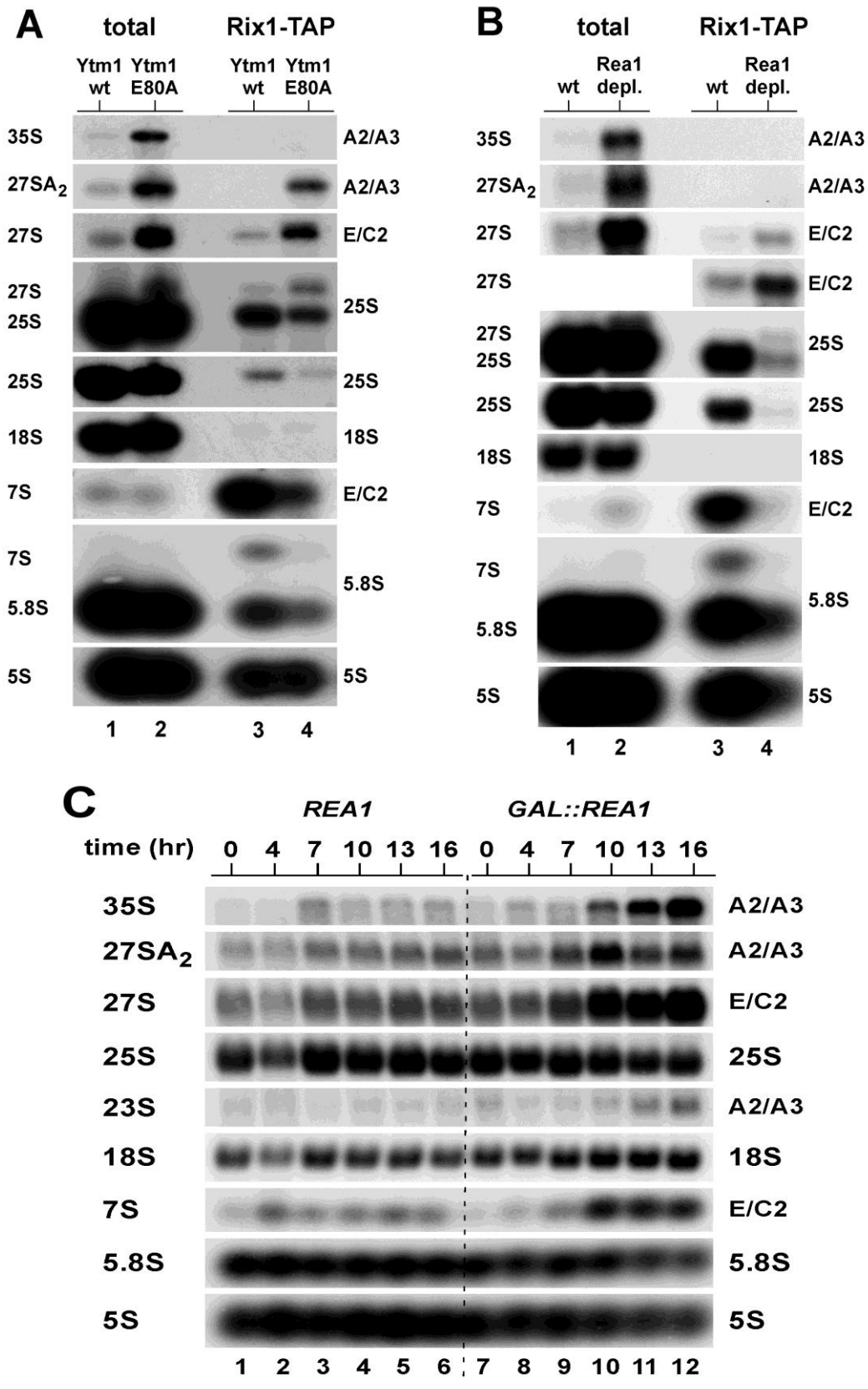

Figure S4. Rix1-TAP co-enriches 27S rRNA upon overexpression of Ytm1 E80A or Rea1 depletion (related to Figure 4)

Figure S4. Rix1-TAP co-enriches 27S rRNA upon overexpression of Ytm1 E80A or Rea1 depletion (related to Figure 4)

(A) Yeast strain Rix1-TAP was transformed with YCplac111-*GAL::YTM1* or YCplac111-*GAL::ytm1 E80A*. Transformants were grown in SRC-Leu medium (raffinose) and shifted to YPG (galactose) medium for 6 hrs to induce overexpression of Ytm1 or Ytm1 E80A. **(B)** Yeast strain Rix1-TAP with *GAL::HA-Rea1* was grown in YPG (galactose) and shifted to YPD (glucose) for 16 hrs to deplete for Rea1. Subsequently, TAP-purifications were performed and RNA was extracted from final EGTA eluates and analyzed by Northern blot analysis **(A, B)**. RNA present in the total lysate (lane 1,2) and in the TAP-preparations (lane 3, 4) were compared by using the probes indicated aside of the shown autoradiographs. Panels for 35S, $27SA_2$ and 23S rRNA show detection from the same exposure time. Please note that that the total RNA recovery from the Rix1-TAP preparation derived from Rea1-depleted cells was reduced when compared to the Rix1-particle isolated from non-depleted cells (as judged from the amount of 5S rRNA). Nevertheless, increased amounts of 27S rRNA and decreased 7S rRNA levels are observed in the Rix1-particle isolated from Rea1-depleted cells.

(C) Depletion of Rea1 results in accumulation of 27S and 7S rRNA. The *Gal::REA1 RIX1-TAP* yeast strain was trans-formed with empty plasmid pRS315 (*GAL::REA1*) or complemented with pRS415-*REA1* (*REA1*). Both strains were grown in SGC-Leu (time point 0) before shift to SDC-Leu to repress *GAL::Rea1* expression. Aliquots were taken after the indicated time points (hrs) and Northern blot analysis was performed. (Panels for 35S, $27SA_2$ and 23S rRNA show detection from the same exposure time.)

Binding sites of the probes used for detection see Ulbrich et al., 2009. Details of rRNA processing, see Henras et al., 2008.

Table S1. Plasmids

Name	Relevant information	Reference
pRS416-*YTM1*	*CEN*, *URA3*, *YTM1*	Euroscarf
pRS314-*YTM1*	*CEN*, *TRP1*, *YTM1*	This study
pRS314-*ytm1-1*	*CEN*, *TRP1*, *ytm1-1 (E19G, G398N, S442N)*	This study
pRS314-*ytm1-S78L*	*CEN*, *TRP1*, *ytm1-S78L*	This study
pRS315-*YTM1*	*CEN*, *LEU2*, *YTM1*	This study
pRS315-*YTM1*-TAP	*CEN*, *LEU2*, *YTM1-TAP*	This study
pRS315-*ytm1 E80A*-TAP	*CEN*, *LEU2*, *ytm1-E80A-TAP*	This study
pRS315-*YTM1*-eGFP	*CEN*, *LEU2*, *YTM1-TAP*	This study
pRS315-*ytm1*-E80A-eGFP	*CEN*, *LEU2*, *ytm1-E80A-TAP*	This study
YCplac111-P_{Gal1}::*YTM1*	*CEN*, *LEU2*, *GAL1*::*YTM1* T_{ADH1}	This study
YCplac111-P_{Gal1}::*ytm1 E80A*	*CEN*, *LEU2*, *GAL1*::*ytm1 E80A* T_{ADH1}	This study
pCEN6*-HIS3-ADE3-YTM1	*CEN6**, HIS3, ADE3, YTM1	This study
pPROEX GST-TEV-*REA1*-MIDAS	pPROEX HTb HIS-TEV-GST-TEV-*REA1-MIDAS*, Amp	(Ulbrich et al., 2009)
pROEX GST-TEV-*REA1*-MIDAS-DAA	pPROEX HTb HIS-TEV-GST-TEV-rea*A1*-MIDAS-DAA, Amp	(Ulbrich et al., 2009)
pT7 HIS-*YTM1-N*	pET9D, Kan, HIS6-*YTM1-N* aa1-92	This study
pT7 HIS-*YTM1-N E80A*	pET9D, Kan, HIS6-*ytm1-N E80A* aa1-92	This study
YCG-*YLR106c*	*CEN*, *URA3*, *REA1*	Euroscarf, Germany
pRS415-*REA1*	*CEN*, *LEU2*, *REA1*	(Galani et al., 2004)
pRS415-*REA1*	*CEN, LEU2, REA1*	(Galani et al., 2004)
YCplac111-TAP-*REA1*	*CEN*, *LEU2*, NTAP+2xFlag-*REA1*	(Ulbrich et al., 2009)
YCplac111-TAP-*rea1 DTS*	*CEN*, *LEU2*, NTAP+2xFlag-*rea1 DTS*	(Ulbrich et al., 2009)
YCplac111-P_{Gal1}::TAP-*REA1*	CEN, *LEU2*, *GAL1*:: NTAP+2xFlag-*REA1*	This study
pRS314-RFP-*NOP1-RPL25*-eGFP	*CEN*, *TRP1*, NOP1::mRFP-*NOP1 - RPL25*-GFP – large ribosomal subunit export reporter	(Ulbrich et al., 2009)
pGBKT7-*rea1MIDAS*	*CEN*, *TRP1*, 2µ, G4BD-c-myc-*rea1MIDAS* aa4622-4910	(Ulbrich et al., 2009)
pGBKT7-*rea1MIDAS-DAA*	*CEN*, *TRP1*, 2µ, G4BD-c-myc-*rea1-MIDAS-S4712A-S4714A,* aa4622-4910	(Ulbrich et al., 2009)
pGADT7-*ytm1-MIDO*	*CEN*, *LEU2*, 2µ, G4AD-HA-*ytm1, 1-92aa*	This study
pGADT7-*ytm1-MIDO-E80A*	*CEN*, *LEU2*, 2µ, G4AD-HA-*ytm1-E80A, 1-92aa*	This study
pGADT7-*RSA4-MIDO*	*CEN*, *LEU2*, 2µ, G4AD-HA-*RSA4, 1-154aa*	(Ulbrich et al., 2009)
pRS316-*RSA4*	*CEN*, *URA3*, *RSA4*	(Ulbrich et al., 2009)
pRS314-*RSA4*	*CEN*, *TRP1*, *RSA4*	(Ulbrich et al., 2009)
pRS314-*rsa4-1*	*CEN*, *TRP1*, *rsa4-1*	(Ulbrich et al., 2009)
pFA6a-HIS3MX6	Cassette for genomic deletion disruption	(Longtine et al., 1998)
pFA6a-GFP(S65T)-HIS3MX6	Cassette for C-terminal GFP tagging	(Longtine et al., 1998)
pFA6a-TRP1-P_{GAL1}-3HA	Cassette for N-terminal HA tagging with *GAL1* promoter	(Longtine et al., 1998)
pFA6a-hphNTI	Cassette for genomic deletion disruption	(Janke et al., 2004)
pFA6a-natNT2-PREA1-GFP(S65T)	Cassette for N-terminal GFP tagging with *REA1* promoter	This study
pFA6a-natNT2-PRSA4-GFP(S65T)	Cassette for N-terminal GFP tagging with *RSA4* promoter	This study

Table S2. Yeast Strains

Name	Genotype	Reference
FYa (Y3949)	*MAT**a**, his3-Δ200 leu2-Δ1 trp1-Δ63 ura3-52*	This study
DS1-2b (Y2197)	*MATα, his3-Δ200 leu2-Δ1 trp1-Δ63 ura3-52*	
Y2H strain PJ69-4A	*MAT**a**, trp1-901, leu2-3,112, ura3-52, his3-200, gal4, gal80, P_{GAL2}::ADE2, LYS2::* P_{Gal1}::*HIS3, met2::P_{GAL7}-lacz*	(James et al., 1996)
Rix1-GFP (Y3691)	*MATα, his3-11,15, leu2, trp1, ura3, RIX1-GFP::TRP1*	(Nissan et al., 2002)
Ipi3-GFP (Y3690)	*MATa, ade2, ade3, his3, leu2, trp1, ura3, IPI3-GFP::TRP1*	(Galani et al., 2004)
Ipi1-GFP (Y3690)	*MATα, his3, leu2, trp1, ura3-1, IPI1-GFP::TRP1*	(Galani et al., 2004)
GFP-Rea1 (Y3989)	*MATα, ade2-1, ura3-1, his3-11.15, leu2-3.112, trp1-1, can1-100, ade3::kanMX4, natNT2-P_{Rea1}-GFP(S65T)-REA1*	This study
GFP-Rsa4 (Y3991)	*MATa, ade2-1, ura3-1, his3-11.15, leu2-3.112, trp1-1, can1-100, ade3::kanMX4, natNT2-P_{Rsa4}-GFP(S65T)-RSA4*	This study
Nop7-GFP (Y2944)	*MATα, his3, leu2, trp1, ura3-1, NOP7-GFP::HIS3*	(Nissan et al., 2002)
Erb1-GFP (Y4341)	*MATa, ade2-1, ura3-1, his3-11.15, leu2-3.112, trp1-1, can1-100, ade3::kanMX4, rix7::kanMX6, ERB1-GFP(S65T)::natNT2; pHT4467Δ-RIX7*	This study
Has1-GFP (Y2943)	*MATα, his3, leu2, trp1, ura3-1, Has1-GFP::HIS3*	This study
Arx1-GFP (Y2168)	*MATα, his3, leu2, trp1, ura3-1, ARX1-GFP::HIS3*	(Nissan et al., 2002)
Nog1-GFP (Y4337)	*MATa, ade2-1, ura3-1, his3-11.15, leu2-3.112, trp1-1, can1-100, ade3::kanMX4, rix7::kanMX6, NOG1-GFP(S65T)::natNT2; pHT4467Δ-RIX7*	This study
Rix1-TAP (Y2152)	*MATα, his3-Δ200, leu2-Δ1, trp1-Δ63, ura3-52, RIX1-TAP::TRP1*	(Nissan et al., 2002)
Rix1-TAP, P_{Gal1}::HA-Rea1 (Y3698)	*MATα, ade2-1, ura3-52, leu2-3,112, can1-100, TRP1:: GAL1::HA-REA1, RIX1-TAP:: HIS3*	This study
Ytm1Δ (Y4295)	*MAT**a**, ytm1::hphNT1A, ade3::KanMX, ade2-1,ura3-1, his3-11.15, leu2-3.112, trp1-1, can1-100. pRS416-YTM1*	This study
Ytm1Δ (Y4292)	*MATα, ytm1::hphNT1A, ade3::KanMX, ade2-1,ura3-1, his3-11.15, leu2-3.112, trp1-1, can1-100. pRS416-YTM1*	This study
Ytm1Δ Rea1Δ (Y4502)	*MAT**a**, ytm1::hphNT1, rea1::HIS3, his3, trp1, leu2, ura3, ade2. pRS416-REA1, pRS416-YTM1*	This study
Ytm1 Rea1 - SL screening strain (Y4259)	*MATα, ade2-1, ade3::KanMX4, ura3-1, his3-11.15, leu2-3,112, trp1-1, rea1::KanMX, ytm1::natNT2, pRS416-REA1,* pTAP-*rea1-DTS*, pCEN6*-HIS3-ADE3-YTM1	This study

Supplemental References

Galani, K., Nissan, T.A., Petfalski, E., Tollervey, D., and Hurt, E. (2004). Rea1, a Dynein-related Nuclear AAA-ATPase, Is Involved in Late rRNA Processing and Nuclear Export of 60 S Subunits. J Biol Chem *279*, 55411-55418.

James, P., Halladay, J., and Craig, E.A. (1996). Genomic libraries and a host strain designed for highly efficient two-hybrid selection in yeast. Genetics *144*, 1425-1436.

Janke, C., Magiera, M.M., Rathfelder, N., Taxis, C., Reber, S., Maekawa, H., Moreno-Borchart, A., Doenges, G., Schwob, E., Schiebel, E., and Knop, M. (2004). A versatile toolbox for PCR-based tagging of yeast genes: new fluorescent proteins, more markers and promoter substitution cassettes. Yeast *21*, 947-962.

Longtine, M.S., McKenzie, A., Demarini, D.J., Shah, N.G., Wach, A., Brachat, A., Philippsen, P., and Pringle, J.R. (1998). Additional modules for versatile and economical PCR-based gene deletion and modification in Saccharomyces cerevisiae. Yeast *10*, 953-961.